IV.5.b July 9, 2014 LLAC

Narrative of Event: This event was a small RG event (around 5:00) and potential lower LA Canyon event. The NMED 110 sampler was triggered in lower LA Canyon, that its flow was observed at BDD at around 4:00 as indicated on the graph. Consistent with other events the lower LA Canyon high flow preceded the RG peak discharge. No sampling was initiated at the BDD Intake on this date.

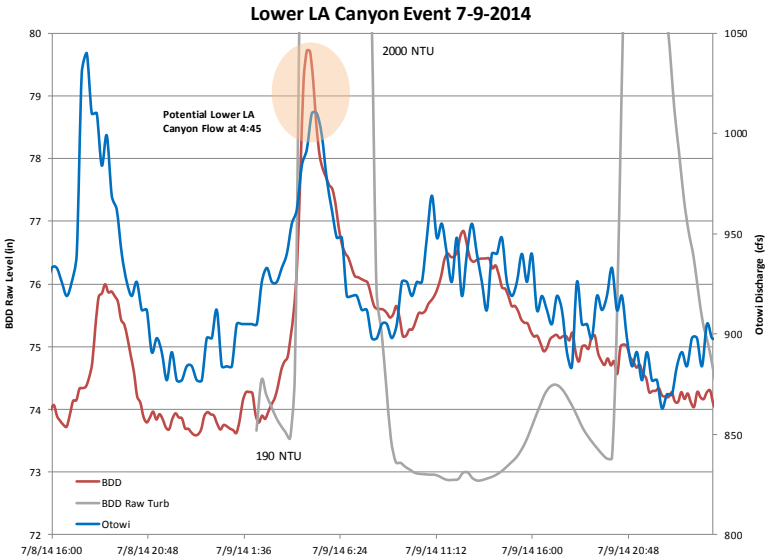

Station	Max Discharge (cfs)	Time
Otowi	1010	5:03
E050.1	-	-
E060.1	-	-
E109.9	>5	-
BDD	na	4:45

The potential lower LAC flows on this date was confirmed by the BDD raw water turbidimeter, where rise in the river turbidity could be observed.

Week of 7-6-14 Weather Information - Los Alamos											
2014	Temp. (°F)			Humidity (%)			Wind (mph)			Precip. (in)	Events
Jul	high	avg	low	high	avg	low	high	avg	high	sum	
6	88	74	59	63	36	12	13	4	24	0	
7	86	74	63	56	38	17	16	6	25	0	Rain
8	82	70	58	83	46	25	23	5	30	0.06	Rain
9	74	64	54	100	67	36	14	6	-	0.54	Rain
10	81	70	59	73	52	25	15	6	22	0.01	Rain
11	82	72	63	68	48	28	20	5	28	0	Rain
12	84	71	58	79	49	22	12	3	24	0	

Week of 7-6-14 Weather Information - Santa Fe											
2014	Temp. (°F)			Humidity (%)			Wind (mph)			Precip. (in)	Events
Jul	high	avg	low	high	avg	low	high	avg	high	sum	
6	91	74	57	77	41	15	22	8	37	0	Thunderstorm
7	91	74	57	67	46	19	26	6	38	0.35	Rain , Thunderstorm
8	86	72	57	72	50	28	22	10	36	0.26	Rain , Thunderstorm
9	84	70	59	87	60	26	21	14	31	0.08	Rain , Thunderstorm
10	87	74	62	72	41	23	17	6	28	0	
11	90	74	62	75	47	22	20	6	25	0.01	Rain , Thunderstorm
12	89	71	55	90	46	25	17	6	25	0	Thunderstorm

IV.5.c July 10-11, 2014 LLAC

Narrative of Event: This event was a potential lower LA Canyon event. The NMED 110 sampler was triggered in lower LA Canyon, and its flow was observed at BDD at around 7:30 (7/10) and 15:30 (7/11) as indicated on the graph. Consistent with other events, the lower LA Canyon high flow preceded the RG peak/higher discharge. No sampling was initiated at the BDD Intake on this date.

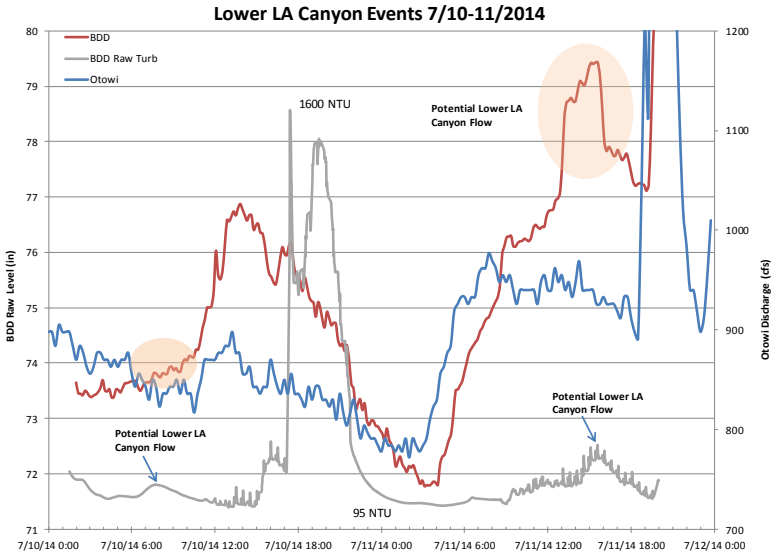

Station	Max Discharge (cfs)	Time
Otowi	970	7:30 (7/11)
E050.1	-	-
E060.1	-	-
E109.9	>5	-
BDD	na	13:00 (7/10) 15:00 (7/11)

The potential lower LAC flows on these two days were confirmed by the BDD raw water turbidimeter, where rise in the river turbidity could be observed.

Week of 7-6-14 Weather Information - Los Alamos

2014	Temp. (°F)			Humidity (%)			Wind (mph)			Precip. (in)	Events
Jul	high	avg	low	high	avg	low	high	avg	high	sum	
6	88	74	59	63	36	12	13	4	24	0	
7	86	74	63	56	38	17	16	6	25	0	Rain
8	82	70	58	83	46	25	23	5	30	0.06	Rain
9	74	64	54	100	67	36	14	6	-	0.54	Rain
10	81	70	59	73	52	25	15	6	22	0.01	Rain
11	82	72	63	68	48	28	20	5	28	0	Rain
12	84	71	58	79	49	22	12	3	24	0	

Week of 7-6-14 Weather Information - Santa Fe

2014	Temp. (°F)			Humidity (%)			Wind (mph)			Precip. (in)	Events
Jul	high	avg	low	high	avg	low	high	avg	high	sum	
6	91	74	57	77	41	15	22	8	37	0	Thunderstorm
7	91	74	57	67	46	19	26	6	38	0.35	Rain , Thunderstorm
8	86	72	57	72	50	28	22	10	36	0.26	Rain , Thunderstorm
9	84	70	59	87	60	26	21	14	31	0.08	Rain , Thunderstorm
10	87	74	62	72	41	23	17	6	28	0	
11	90	74	62	75	47	22	20	6	25	0.01	Rain , Thunderstorm
12	89	71	55	90	46	25	17	6	25	0	Thunderstorm

IV.5.d July 15, 2014 RG

Narrative of Event: This event was a river storm event. Sampling was initiated by BDD operator due to increased value of the turbidity in the river. The NMED 110 sampler was triggered in lower LA Canyon and its flow was observed at BDD at around 22:43 as indicated on the graph.

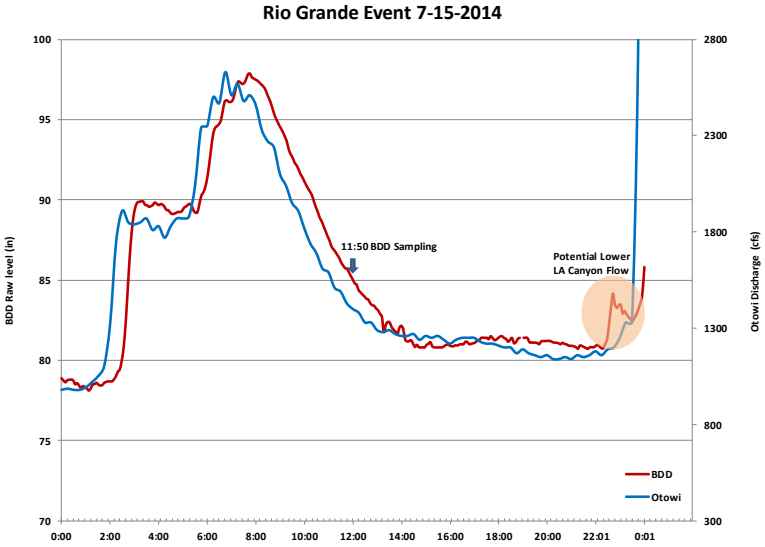

Station	Max Discharge (cfs)	Time
Otowi	2600	7:00
E050.1	-	-
E060.1	-	-
E109.9	>5	22:43
BDD	na	7:45

The SSC measured at BDD was 14,630 mg/L (11:51) consistent with the USGS value of 11,600 mg/L (14:00) at Otowi Gage.

Sampling & Analyses Information			
Bottle #	**Sampler BDD2**	**Time**	**Otowi Discharge (cfs)**
1-6	sampler failure	6:00	2040
7	Dioxins/Furans	11:25	1610
8	Perchlorate	11:25	1610
9	TOC	11:25	1610
10	PCBs	11:25	1610
11	Cyanide	11:25	1610
12	sampled	11:25	1610
Bottle #	**Sampler BDD3**	**Time**	**Otowi Discharge (cfs)**
1	SSC	11:50	1590
2	GS-IsoU/Pu/Am241	11:50	1590
3	GS-IsoU/Pu/Am241	11:50	1590
4	GS-IsoU/Pu/Am241	11:50	1590
5	GS-IsoU/Pu/Am241	11:50	1590
6	Sr 90	11:50	1590
7	Ra 226/228	11:50	1590
8	Gross a-b	11:50	1590
9	Metals	11:50	1590

Week of 7-13-14 Weather Information - Los Alamos

2014	Temp. (°F)			Humidity (%)			Wind (mph)			Precip. (in)	Events
Jul	high	avg	low	high	avg	low	high	avg	low	sum	
13	77	70	62	66	52	35	16	4	22	0	Rain
14	81	69	57	93	54	26	24	8	30	0	Rain
15	72	63	54	100	81	55	15	8	26	1.22	Rain
16	70	62	55	97	69	46	23	7	37	0.29	Rain
17	77	66	56	84	61	32	15	5	29	0	Rain
18	80	68	57	99	62	29	28	7	41	0	
19	77	70	62	77	55	32	20	8	37	0.09	Rain

Week of 7-13-14 Weather Information - Santa Fe

2014	Temp. (°F)			Humidity (%)			Wind (mph)			Precip. (in)	Events
Jul	high	avg	low	high	avg	low	high	avg	high	sum	
13	82	70	57	78	54	30	15	6	16	0.14	Rain , Thunderstorm
14	87	73	60	86	58	26	33	12	44	0.05	Rain , Thunderstorm
15	75	66	57	97	74	42	21	9	29	0.22	Rain , Thunderstorm
16	81	68	57	93	70	42	24	14	34	0.21	Rain , Thunderstorm
17	84	70	57	81	56	23	26	8	38	0	Rain , Thunderstorm
18	89	74	60	86	56	18	17	9	20	0	
19	90	76	63	70	43	14	23	9	32	0	

IV.5.e July 16, 2014 LAC & RG

Narrative of Event: This was a Rio Grande and LA Canyon event which occurred at different times. Sampling was triggered by E050.1 flow. The NMED 110 sampler was also triggered in lower LA Canyon and its flow was observed at BDD at around 22:40 as indicated on the graph.

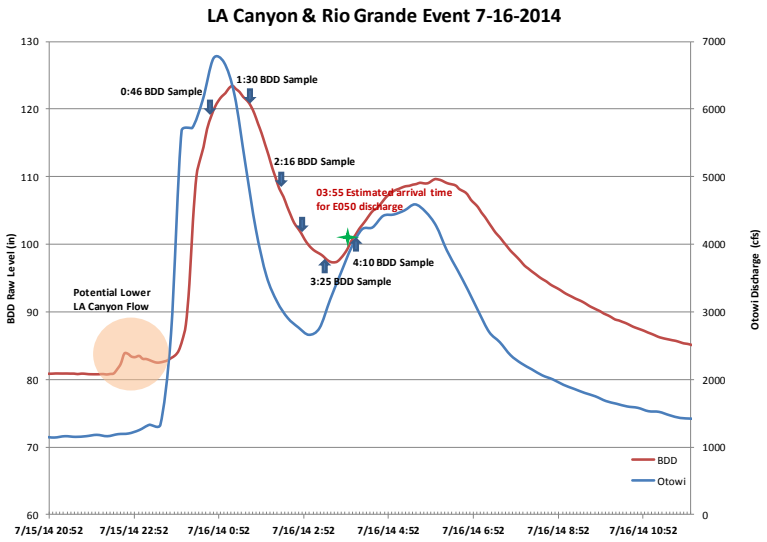

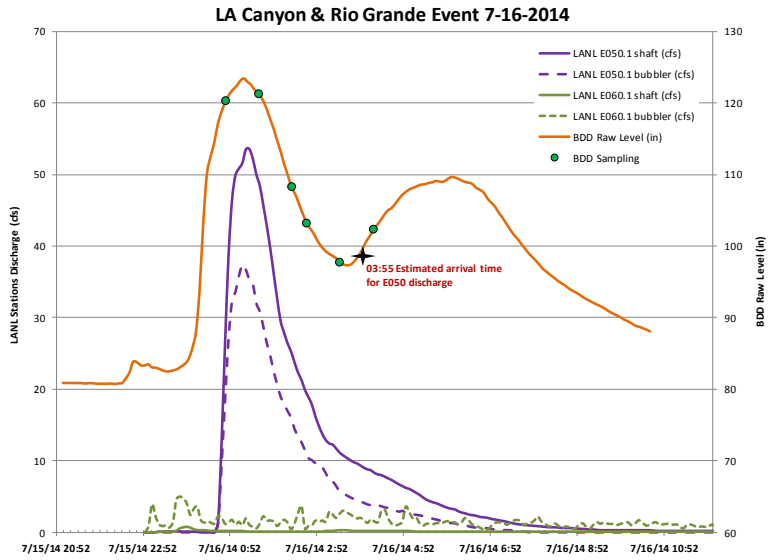

Station	Max Discharge (cfs)	Time
Otowi	6750	0:45
E050.1	63	1:18
E060.1	-	-
E109.9	>5	22:40
BDD	na	1:30

Sampling & Analyses Information			
Bottle #	Sampler BDD2	Time	Otowi Discharge (cfs)
1-3	sampled	0:47	5720
2-12	sampler failure	2:47	5720
Bottle #	Sampler BDD3	Time	Otowi Discharge (cfs)
1	Perchlorate	0:46	5720
2	SSC Hall Environ	0:46	5720
3	PCBs	0:46	5720
4-8	sampler failure	0:46	5720
9	GS-IsoU/Pu/Am241	1:31	6690
10	GS-IsoU/Pu/Am241	1:31	6690
11	SSC	1:31	6690
12	Metals/Gross a-b	1:31	6690
13	Ra 226/228	1:31	6690
14	GS-IsoU/Pu/Am241	1:31	6690
15	GS-IsoU/Pu/Am241	1:31	6690
16	Sr 90	1:31	6690
17	GS-IsoU/Pu/Am241	2:16	4220
18	GS-IsoU/Pu/Am241	2:16	4220
19	GS-IsoU/Pu/Am241	2:16	4220
20	Ra 226/228	2:16	4220
21	SSC	2:16	4220
22	Sr 90	2:16	4220
23	GS-IsoU/Pu/Am241	2:16	4220
24	Gross a-b	2:16	4220
Bottle #	Sampler BDD4	Time	Otowi Discharge (cfs)
1-4	sampled	2:40	3150
5	Sr 90	2:40	3150
6-7	sampled	2:40	3150
8	Metals	2:40	3150
9	Gross a-b	3:25	2660
10	Ra 226/228	3:25	2660
11	SSC	3:25	2660
12	GS-IsoU/Pu/Am241	3:25	2660
13	GS-IsoU/Pu/Am241	3:25	2660
14	GS-IsoU/Pu/Am241	3:25	2660
15	GS-IsoU/Pu/Am241	3:25	2660
16	Metals	3:25	2660
17	GS-IsoU/Pu/Am241	4:10	3570
18	GS-IsoU/Pu/Am241	4:10	3570
19	Ra 226/228	4:10	3570
20	Metals/GS-IsoU/Pu/Am241	4:10	3570
21	GS-IsoU/Pu/Am241	4:10	3570
22	SSC	4:10	3570
23	Gross a-b	4:10	3570
24	Sr 90	4:10	3570

Week of 7-13-14 Weather Information - Los Alamos											
2014	Temp. (°F)			Humidity (%)			Wind (mph)			Precip. (in)	Events
Jul	high	avg	low	high	avg	low	high	avg	low	sum	
13	77	70	62	66	52	35	16	4	22	0	Rain
14	81	69	57	93	54	26	24	8	30	0	Rain
15	72	63	54	100	81	55	15	8	26	1.22	Rain
16	70	62	55	97	69	46	23	7	37	0.29	Rain
17	77	66	56	84	61	32	15	5	29	0	Rain
18	80	68	57	99	62	29	28	7	41	0	
19	77	70	62	77	55	32	20	8	37	0.09	Rain

The BDD sampling covered the RG storm event only, and therefore, the SSC peak appears to be in response to the RG storm event.

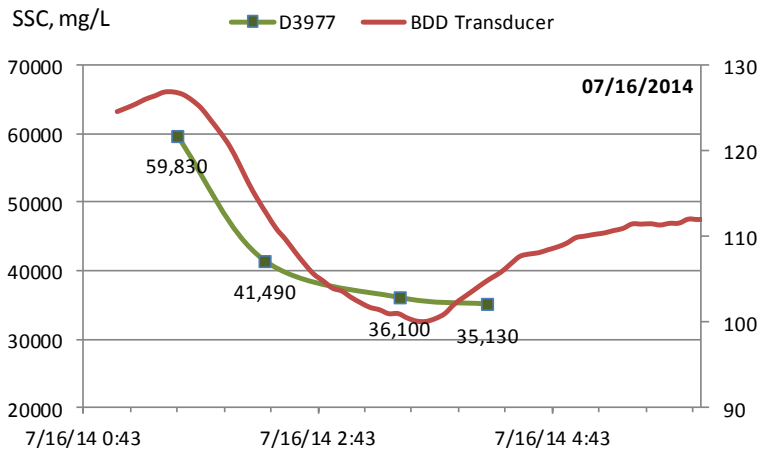

IV.5.f July 24, 2014 RG

Narrative of Event: This was a small RG storm event. Sampling was initiated by BDD operator due to increased value of turbidity.

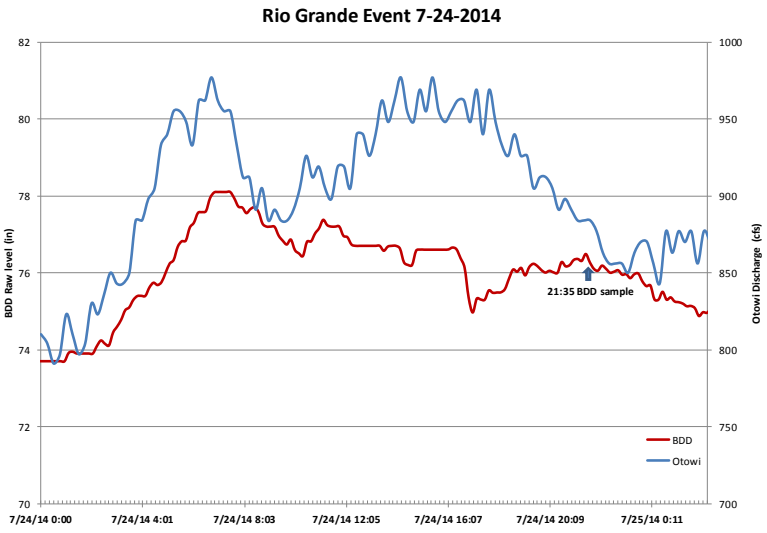

Station	Max Discharge (cfs)	Time
Otowi	977	6:45
E050.1 av	-	-
E060.1	-	-
BDD	na	7:10

Sampling & Analyses Information			
Bottle #	Sampler BDD2	Time	Otowi Discharge (cfs)
1	SSC (BDD lab)	21:35	900
2	GS-IsoU/Pu/Am241	21:35	900
3	GS-IsoU/Pu/Am241	21:35	900
4	GS-IsoU/Pu/Am241	23:35	856
5	GS-IsoU/Pu/Am241	23:35	856
6	SSC (BDD lab)	23:35	856
7-12	sampled	1:35	863

The SSC measured during this event were 1,442 mg/L (21:35) and 857 mg/L (23:35) most probably due to the small increase in the RG discharge.

Week of 7-20-14 Weather Information - Santa Fe											
2014	Temp. (°F)			Humidity (%)			Wind (mph)			Precip. (in)	Events
Jul	high	avg	low	high	avg	low	high	avg	low	sum	
20	95	74	57	72	42	17	16	8	23	0.13	Rain , Thunderstorm
21	93	78	64	66	38	17	14	7	20	0.01	Rain
22	93	78	62	67	41	16	23	9	41	0.06	Rain , Thunderstorm
23	84	72	60	78	59	33	17	8	24	0.43	Rain , Thunderstorm
24	89	74	61	67	40	18	16	6	22	0	
25	93	77	61	58	34	17	17	5	24	0	Thunderstorm
26	96	80	64	56	34	13	18	9	30	0	

IV.5.g July 29, 2014 LAC & RG

Narrative of Event: This was a Rio Grande and LA/P Canyons event. Sampling was triggered by flow through E050.1. There was a very limited flow at E060.1. The NMED 110 sampler was triggered in the lower LA Canyon and its flow was observed at BDD at around 15:50 as marked on the graph.

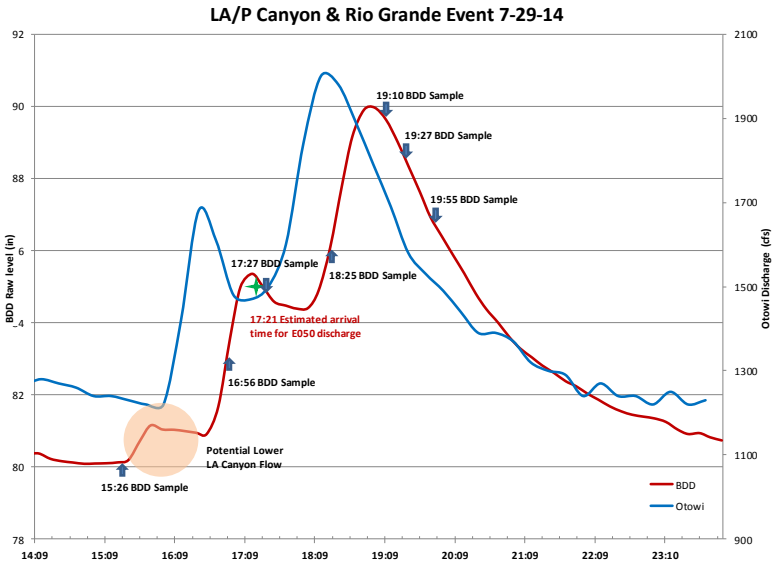

Station	Max Discharge (cfs)	Time
Otowi	1680/2000	16:30/18:15
E050.1 av	78	14:50
E060.1 av	1.7	17:30
E109.9	>5	15:50
BDD	na	17:16/19:00

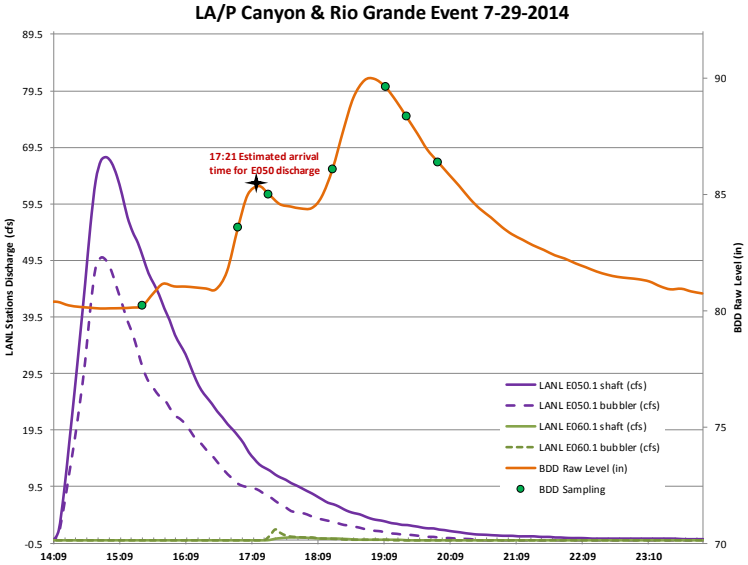

Week of 7-27-14 Weather Information - Los Alamos											
2014	Temp. (°F)			Humidity (%)			Wind (mph)			Precip. (in)	Events
Jul	high	avg	low	high	avg	low	high	avg	low	sum	
27	83	72	61	83	47	29	17	10	24	0.08	Rain
28	75	66	58	77	62	38	17	9	25	0	
29	70	64	57	100	84	58	13	5	-	0.2	Rain
30	75	67	59	86	65	38	17	6	28	0.01	Rain
31	71	62	54	100	86	55	17	10	41	0.85	Fog , Rain
Aug	high	avg	low	high	avg	low	high	avg	high	sum	
1	68	60	53	100	80	51	16	5	22	0.25	Rain
2	69	62	55	100	70	48	14	6	21	0.02	

Sampling & Analyses Information			
Bottle #	**Sampler BDD2**	**Time**	**Otowi Discharge (cfs)**
1-2	sampled	15:27	1240
3	Cyanide	15:27	1240
4	PCBs	17:27	1480
5	Dioxins/Furans	17:27	1480
6	Perchlorate/TOC	17:27	1480
7	PCBs	19:27	1790
8	Perchlorate/TOC	19:27	1790
9	Dioxins/Furans	19:27	1790
10-12	sampled	20:27	1490
Bottle #	**Sampler BDD3**	**Time**	**Otowi Discharge (cfs)**
1	SSC	15:26	1240
2	GS-IsoU/Pu/Am241	15:26	1240
3	GS-IsoU/Pu/Am241	15:26	1240
4	GS-IsoU/Pu/Am241	15:26	1240
5	GS-IsoU/Pu/Am241	15:26	1240
6	Sr 90	15:26	1240
7	Ra	15:26	1240
8	Gross a-b/Metals	15:26	1240
9-16	sampled	16:11	1220
17	SSC	16:56	1680
18	GS-IsoU/Pu/Am241	16:56	1680
19	GS-IsoU/Pu/Am241	16:56	1680
20	GS-IsoU/Pu/Am241	16:56	1680
21	GS-IsoU/Pu/Am241	16:56	1680
22	Sr 90	16:56	1680
23	Ra	16:56	1680
24	Gross a-b/Metals	16:56	1680
Bottle #	**Sampler BDD4**	**Time**	**Otowi Discharge (cfs)**
1-8	sampled	17:40	1470
9	SSC	18:25	1840
10	GS-IsoU/Pu/Am241	18:25	1840
11	GS-IsoU/Pu/Am241	18:25	1840
12	GS-IsoU/Pu/Am241	18:25	1840
13	GS-IsoU/Pu/Am241	18:25	1840
14	Sr 90	18:25	1840
15	Ra	18:25	1840
16	Gross a-b/Metals	18:25	1840
17	SSC	19:10	1980
18	GS-IsoU/Pu/Am241	19:10	1980
19	GS-IsoU/Pu/Am241	19:10	1980
20	GS-IsoU/Pu/Am241	19:10	1980
21	GS-IsoU/Pu/Am241	19:10	1980
22	Sr 90	19:10	1980
23	Ra	19:10	1980
24	Gross a-b/Metals	19:10	1980
Bottle #	**Sampler BDD5**	**Time**	**Otowi Discharge (cfs)**
1	SSC	19:55	1580
2	GS-IsoU/Pu/Am241	19:55	1580
3	GS-IsoU/Pu/Am241	19:55	1580
4	GS-IsoU/Pu/Am241	19:55	1580
5	GS-IsoU/Pu/Am241	19:55	1580
6	Sr 90	19:55	1580
7	Ra	19:55	1580
8	Gross a-b/Metals	19:55	1580
9-24	sampled	20:40	1490

From the graph below, we can conclude that the lower LAC flow was not sufficient to increase the river SSC upon its arrival at BDD. The SSC peak appears to be as a result of the RG storm event with an hour delay.

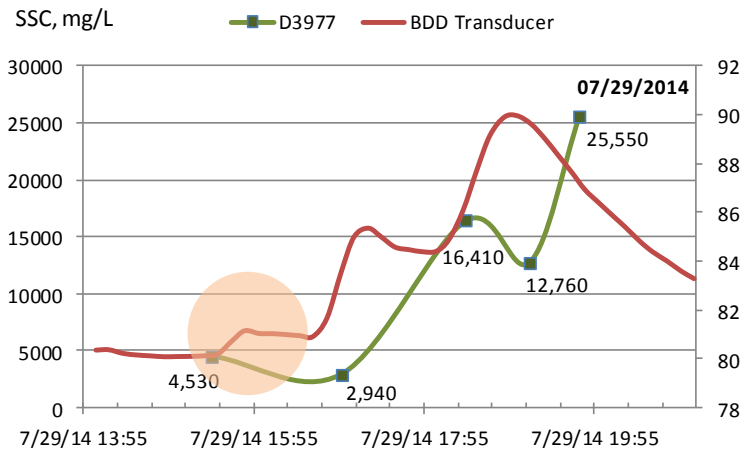

IV.5.h July 31 - August 1, 2014 LAC & RG

Narrative of Event: This was a Rio Grande and LA/P Canyons event. Sampling was triggered by flow through E050.1. Both canyons flowed during this storm event, but peak discharges for each occurred at different times. The NMED 110 sampler was also triggered in lower LA Canyon and its flow was observed at BDD from 2:30 until 6:00 on 8/1/2014 as indicated on the graph.

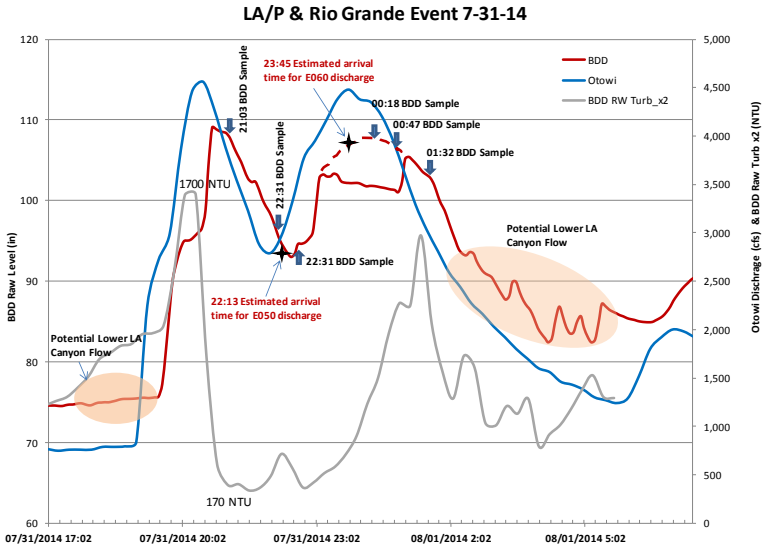

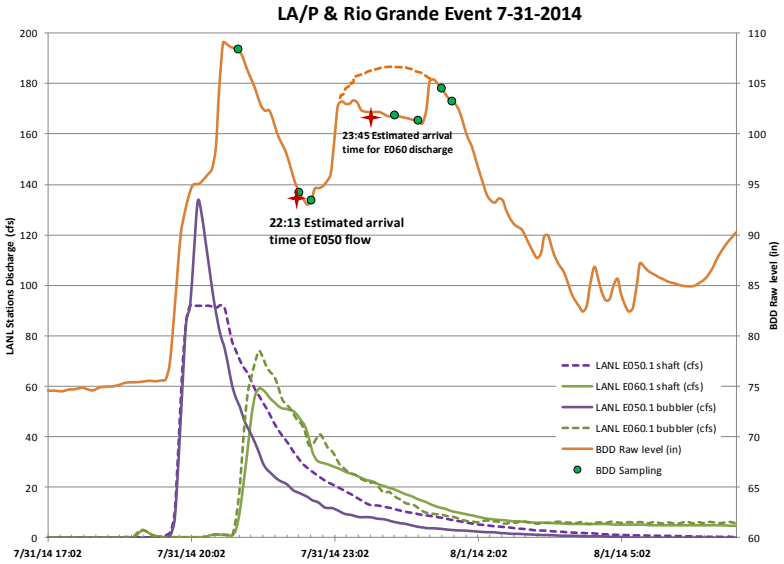

Week of 7-27-14 Weather Information - Los Alamos											
2014	Temp. (°F)			Humidity (%)			Wind (mph)			Precip. (in)	Events
Jul	high	avg	low	high	avg	low	high	avg	low	sum	
27	83	72	61	83	47	29	17	10	24	0.08	Rain
28	75	66	58	77	62	38	17	9	25	0	
29	70	64	57	100	84	58	13	5	-	0.2	Rain
30	75	67	59	86	65	38	17	6	28	0.01	Rain
31	71	62	54	100	86	55	17	10	41	0.85	Fog , Rain
Aug	high	avg	low	high	avg	low	high	avg	high	sum	
1	68	60	53	100	80	51	16	5	22	0.25	Rain
2	69	62	55	100	70	48	14	6	21	0.02	

Station	Max Discharge (cfs)	Time
Otowi	4560/4480	20:30/23:45
E050.1	220	20:05
E060.1	81	21:15
E109.9	>5	2:30-6:00
BDD	na	20:53/00:34

Sampling & Analyses Information			
Bottle #	Sampler BDD2	Time	Otowi Discharge (cfs)
1-3	sampled	20:08	2990
4	PCBs	22:18	2880
5	GS-IsoU/Pu/Am241	22:18	2880
6	GS-IsoU/Pu/Am241	22:18	2880
7	PCBs	0:18	4480
8	Dioxins/Furans	0:18	4480
9	Perchlorate	0:18	4480
10	TOC	1:18	3950
11	Cyanide	1:18	3950
Bottle #	Sampler BDD3	Time	Otowi Discharge (cfs)
1-8	sampled	20:10	2990
9	SSC	21:03	4560
10	GS-IsoU/Pu/Am241	21:03	4560
11	GS-IsoU/Pu/Am241	21:03	4560
12	GS-IsoU/Pu/Am241	21:03	4560
13	GS-IsoU/Pu/Am241	21:03	4560
14	Ra226/228	21:03	4560
15	Sr 90	21:03	4560
16	Gross a-b/Metals	21:03	4560
Bottle #	Sampler BDD4	Time	Otowi Discharge (cfs)
1	SSC	22:31	2790
2	Sr 90	22:31	2790
3	GS-IsoU/Pu/Am241	22:31	2790
4	GS-IsoU/Pu/Am241	22:31	2790
5	Gross a-b/Metals	22:31	2790
Bottle #	Sampler BDD5	Time	Otowi Discharge (cfs)
1	SSC	0:47	4350
2	GS-IsoU/Pu/Am241	0:47	4350
3	GS-IsoU/Pu/Am241	0:47	4350
4	GS-IsoU/Pu/Am241	0:47	4350
5	GS-IsoU/Pu/Am241	0:47	4350
6	Ra226/228	0:47	4350
7	Sr 90	0:47	4350
8	Gross a-b/Metals	0:47	4350
9	SSC	1:32	3620
10	GS-IsoU/Pu/Am241	1:32	3620
11	GS-IsoU/Pu/Am241	1:32	3620
12	GS-IsoU/Pu/Am241	1:32	3620
13	GS-IsoU/Pu/Am241	1:32	3620
14	Ra226/228	1:32	3620
15	Sr 90	1:32	3620
16	Gross a-b/Metals	1:32	3620

The BDD raw water turbidimeter confirmed two flows from the lower LAC, one on 7/31 at about 18:00 and another on 8/1 from 2:00 to 5:00. The SSC values were very high but it is difficult to determine whether their values were due to RG or LA Canyon storm event. The SSC peaks due to the RG are usually observed with a time lag, therefore, we may interpret the high SSC of 55,000 mg/L to be the result of the lower LA Canyon flow.

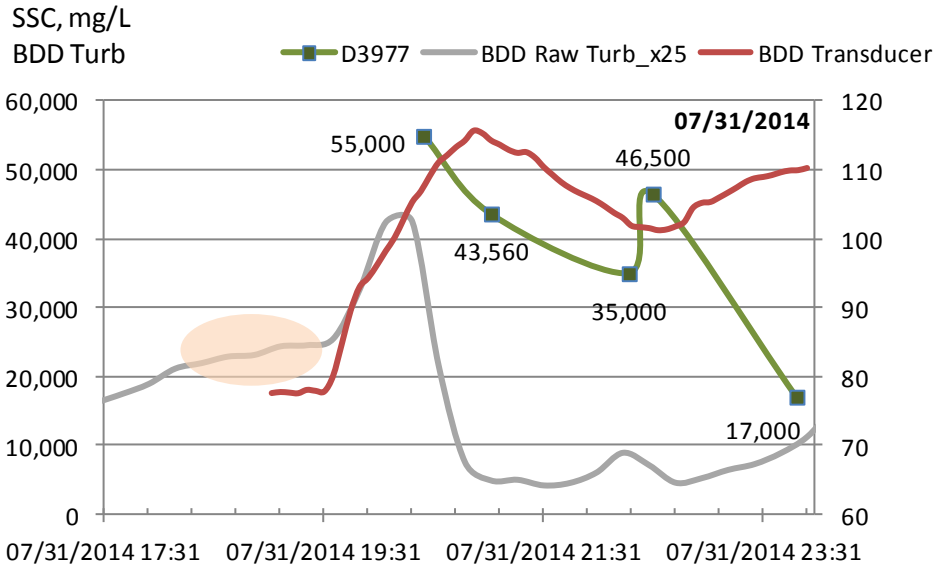

IV.5.i August 4, 2014 RG

Narrative of Event: This was a Rio Grande and potentially lower LA Canyon storm event. Sampling was initiated by BDD operator at 16:58 due to increased value of turbidity. The NMED 110 sampler was triggered in the lower LA Canyon, but its flow could not be observed at BDD due to malfunction of BDD transducer on that date.

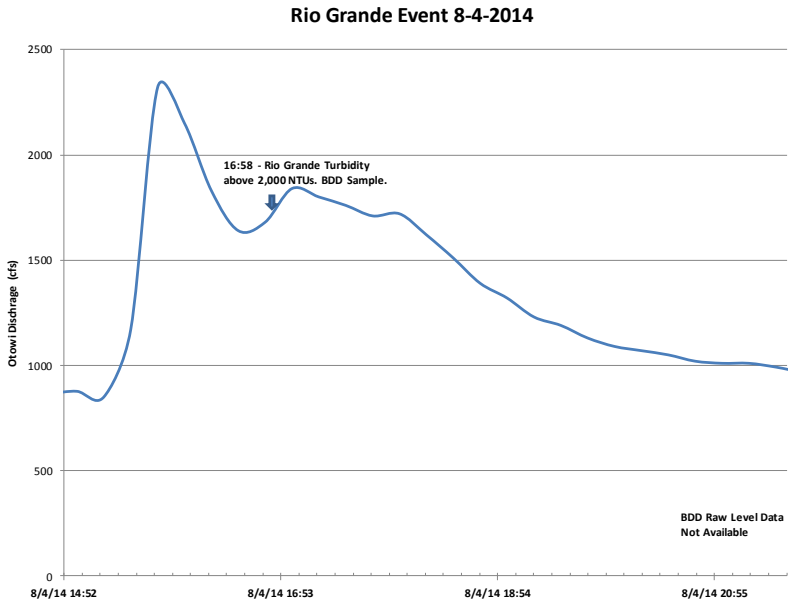

Station	Max Discharge (cfs)	Time
Otowi	2320	15:45
E050.1	-	-
E060.1	-	-
BDD*	na	na

*BDD transducer was not in working order for this event.

Sampling & Analyses Information			
Bottle #	**Sampler BDD2**	**Time**	**Otowi Discharge (cfs)**
1	SSC	16:58	1830
2	GS-IsoU/Pu/Am241	16:58	1830
3	GS-IsoU/Pu/Am241	16:58	1830
4-12	sampled	23:35	1620
Bottle #	**Sampler BDD5**	**Time**	**Otowi Discharge (cfs)**
1	GS-IsoU/Pu/Am241	16:56	1830

The SSC measured at 16:58 was 88,620 mg/L, which could have been the result of the RG storm event and concurrent LA Canyon event.

Week of 8-3-14 Weather Information - Santa Fe											
2014	Temp. (°F)			Humidity (%)			Wind (mph)			Precip. (in)	Events
Aug	high	avg	low	high	avg	low	high	avg	low	sum	
3	78	66	55	83	55	37	14	8	21	0	
4	78	68	60	90	77	45	17	9	-	1.26	Rain , Thunderstorm
5	82	68	55	93	63	29	14	6	-	0	
6	86	70	55	87	54	18	8	4	-	0	
7	80	68	57	87	58	30	25	5	33	0	Rain
8	84	67	50	93	54	17	13	6	18	0	
9	84	70	55	80	45	18	24	5	36	0	Rain , Thunderstorm

IV.5.j August 26-27, 2014 RG

Narrative of Event: This was a Rio Grande and potentially lower LA Canyon storm event. Sampling was initiated by BDD operator at 22:50 due to increased value of turbidity in the river. The NMED 110 sampler was triggered in lower LAC and its flow was observed at BDD at 23:47 and at 1:23 (8/27) as indicated on the graph.

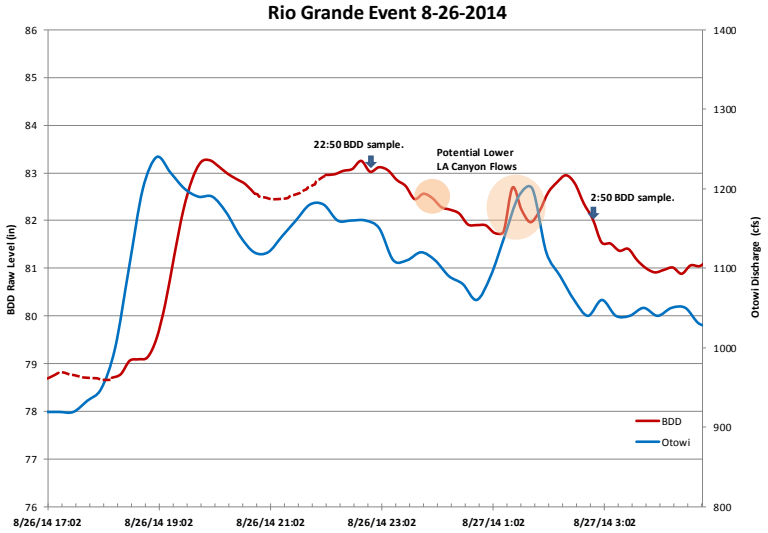

Station	Max Discharge (cfs)	Time
Otowi	1240/1200	19:00/1:45
E050.1	-	-
E060.1	-	-
E109.9	>5	23:47/1:23
BDD	na	19:57/2:21

The measured SSC were 16,158 mg/L at 22:49, and 5,729 mg/L at 2:50. The RG and LAC events were concurrent, so we cannot distinguish between SSC increase caused by the RG and LAC flows.

Sampling & Analyses Information			
Bottle #	**Sampler BDD2**	**Time**	**Otowi Discharge (cfs)**
1	Perchlorate	22:50	1180
2	PCBs/TOC	22:50	1180
3	Cyanide	22:50	1180
4	Dioxins/Furans	0:50	1110
5-6	sampled	0:50	1110
7	GS-IsoU/Pu/Am241	2:50	1090
8	GS-IsoU/Pu/Am241	2:50	1090
9	SSC	2:50	1090
10-12	sampled	3:50	1040
Bottle #	**Sampler BDD3**	**Time**	**Otowi Discharge (cfs)**
1	SSC	22:49	1180
2	GS-IsoU/Pu/Am241	22:49	1180
3	GS-IsoU/Pu/Am241	22:49	1180
4	GS-IsoU/Pu/Am241	22:49	1180
5	GS-IsoU/Pu/Am241	22:49	1180
6	Sr 90	22:49	1180
7	Ra 226/228	22:49	1180
8	Gross a-b/Metals	22:49	1180
9-24	sampled	23:34	1160

Week of 8-24-14 Weather Information - Los Alamos											
2014	**Temp. (°F)**			**Humidity (%)**			**Wind (mph)**			**Precip. (in)**	**Events**
Aug	high	avg	low	high	avg	low	high	avg	high	sum	
24	78	68	58	57	39	24	16	5	24	0	
25	80	70	60	65	36	23	21	6	32	0	
26	73	64	56	100	68	38	15	6	21	0.11	Rain
27	70	62	54	100	73	33	14	4	-	0.23	Rain
28	72	61	50	66	46	30	14	4	18	0	
29	75	64	54	58	37	23	13	7	20	0	
30	81	70	58	47	30	16	16	7	25	0	

Week of 8-24-14 Weather Information - Santa Fe											
2014	**Temp. (°F)**			**Humidity (%)**			**Wind (mph)**			**Precip. (in)**	**Events**
Aug	high	avg	low	high	avg	low	high	avg	high	sum	
24	84	66	50	83	44	19	13	5	20	0	
25	87	70	55	63	39	18	22	5	30	0	
26	79	66	55	90	66	39	15	6	22	0.22	Rain , Thunderstorm
27	77	64	55	97	72	30	13	6	17	0.16	Rain , Thunderstorm
28	78	62	48	80	51	27	10	5	-	0	
29	80	65	50	80	44	20	14	5	-	0	
30	86	68	53	66	37	17	13	5	23	0	

IV.5.k August 27, 2014 LLAC

Narrative of Event: This was a potential lower LA Canyon event. The NMED 110 sampler was triggered in lower LA Canyon and its flow was observed at BDD throughout the day as indicated on the graph. Samples were not collected at BDD intake, because there was no real time communication between BDD and NMED 110 sampler.

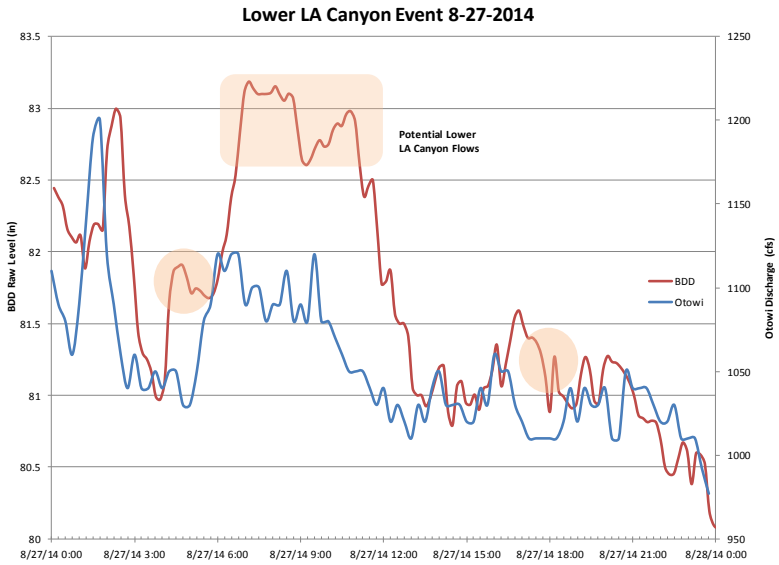

Week of 8-24-14 Weather Information - Los Alamos											
2014	Temp. (°F)			Humidity (%)			Wind (mph)			Precip. (in)	Events
Aug	high	avg	low	high	avg	low	high	avg	high	sum	
24	78	68	58	57	39	24	16	5	24	0	
25	80	70	60	65	36	23	21	6	32	0	
26	73	64	56	100	68	38	15	6	21	0.11	Rain
27	70	62	54	100	73	33	14	4	-	0.23	Rain
28	72	61	50	66	46	30	14	4	18	0	
29	75	64	54	58	37	23	13	7	20	0	
30	81	70	58	47	30	16	16	7	25	0	

IV.5.l September 5-6, 2014 RG

Narrative of Event: This was a Rio Grande and potentially lower LA Canyon storm event. Sampling was initiated by BDD operator at 19:57 due to increased value of turbidity. The BDD transducer data was compared to Otowi Gage discharge data. Some flows in lower LAC occurred concurrently with the RG storm flow, but a couple of flows from lower LAC arrived at BDD sometime before the large RG storm flow on 9-5-2014.

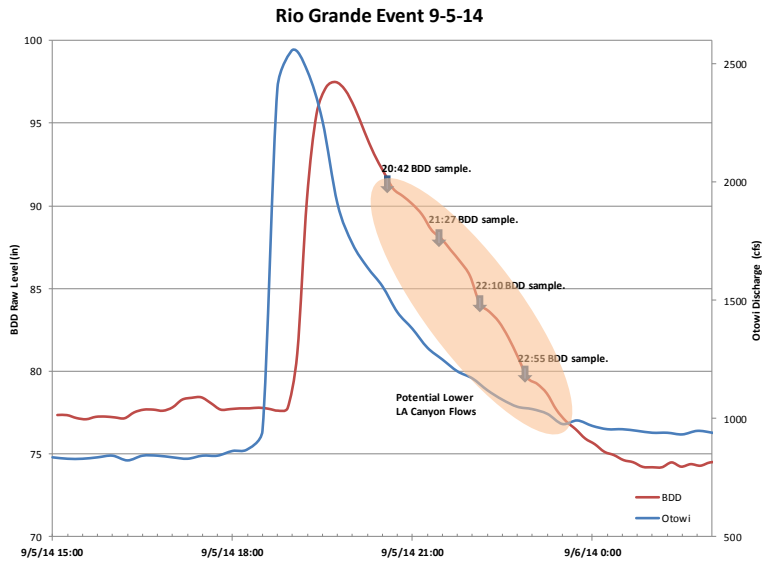

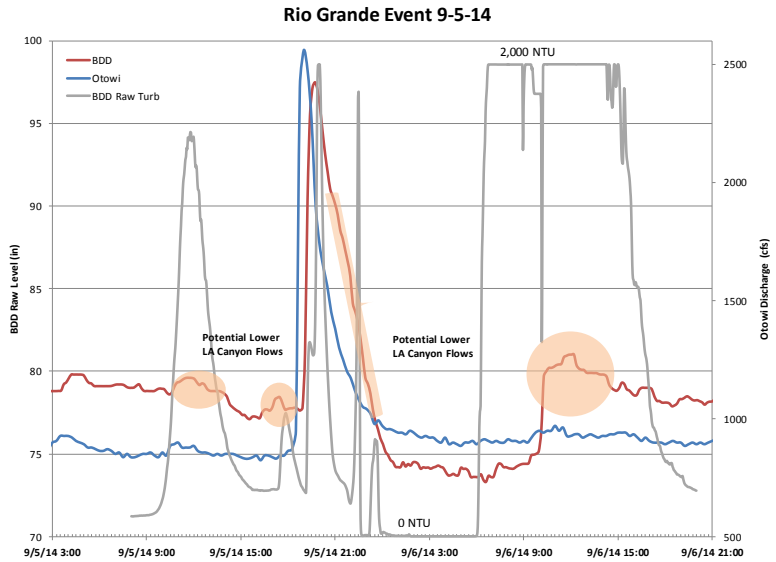

Not only that suspected LLAC flows were confirmed by the BDD raw water turbidimeter, but additional LLAC flows were discovered. Turbidities peaks occurred at 11:50 (9/5), 17:50 (9/5), 19:56 (9/5), 22:30 (9/5), 23:40 (9/5), from 6:00 to 17:00 (9/6).

Station	Max Discharge (cfs)	Time
Otowi	2560	19:00
E050.1	-	-
E060.1	-	-
BDD	na	19:40

Sampling & Analyses Information			
Bottle #	**Sampler BDD2**	**Time**	**Otowi Discharge (cfs)**
1-12	sampler failure	19:57	2470
Bottle #	**Sampler BDD3**	**Time**	**Otowi Discharge (cfs)**
1-8	sampler failure	19:57	2470
9	SSC	20:42	1740
10	GS-IsoU/Pu/Am241	20:42	1740
11	GS-IsoU/Pu/Am241	20:42	1740
12	GS-IsoU/Pu/Am241	20:42	1740
13	GS-IsoU/Pu/Am241	20:42	1740
14	Sr 90	20:42	1740
15	Ra 226/228	20:42	1740
16	Gross a-b/Metals	20:42	1740
17	SSC	21:27	1450
18	GS-IsoU/Pu/Am241	21:27	1450
19	GS-IsoU/Pu/Am241	21:27	1450
20	GS-IsoU/Pu/Am241	21:27	1450
21	GS-IsoU/Pu/Am241	21:27	1450
22	Sr 90	21:27	1450
23	Ra 226/228	21:27	1450
24	Gross a-b/Metals	21:27	1450
Bottle #	**Sampler BDD4**	**Time**	**Otowi Discharge (cfs)**
1	SSC	22:10	1250
2	GS-IsoU/Pu/Am241	22:10	1250
3	GS-IsoU/Pu/Am241	22:10	1250
4	GS-IsoU/Pu/Am241	22:10	1250
5	Ra 226/228	22:10	1250
6	Sr 90	22:10	1250
7	PCBs	22:10	1250
8	Gross a-b/Metals	22:10	1250
9	SSC	22:55	1100
10	GS-IsoU/Pu/Am241	22:55	1100
11	GS-IsoU/Pu/Am241	22:55	1100
12	GS-IsoU/Pu/Am241	22:55	1100
13	GS-IsoU/Pu/Am241	22:55	1100
14	Sr 90	22:55	1100
15	Ra 226/228	22:55	1100
16	Gross a-b/Metals	22:55	1100

Week of 9-1-14 Weather Information - Los Alamos											
2014	Temp. (°F)			Humidity (%)			Wind (mph)			Precip. (in)	Events
Sep	high	avg	low	high	avg	low	high	avg	high	sum	
1	82	74	65	33	23	15	21	12	28	0	
2	83	71	59	34	21	13	17	5	23	0	
3	84	74	64	35	22	13	15	7	25	0	
4	81	71	61	60	40	16	21	7	32	0	
5	75	66	56	89	62	34	15	5	23	0.22	Rain
6	71	62	53	98	74	45	16	9	23	0.06	

Week of 9-1-14 Weather Information - Santa Fe											
2014	Temp. (°F)			Humidity (%)			Wind (mph)			Precip. (in)	Events
Sep	high	avg	low	high	avg	low	high	avg	high	sum	
1	89	70	51	61	27	12	18	7	30	0	
2	89	73	57	37	23	11	15	9	24	0	
3	90	72	55	51	26	10	13	5	21	0	
4	87	72	59	62	41	17	26	10	36	0	Rain , Thunderstorm
5	80	68	57	84	56	35	18	8	26	0	Thunderstorm
6	77	65	55	84	64	38	22	10	26	0	

The graph below contains additional information for the SSC at Otowi gage as measured by USGS. Except for the last value of the SSC at BDD, all measurements agree very well with the Otowi SSC. However, there were multiple identified flows from LLAC, so it is not possible to distinguish between the LLAC and the RG flows.

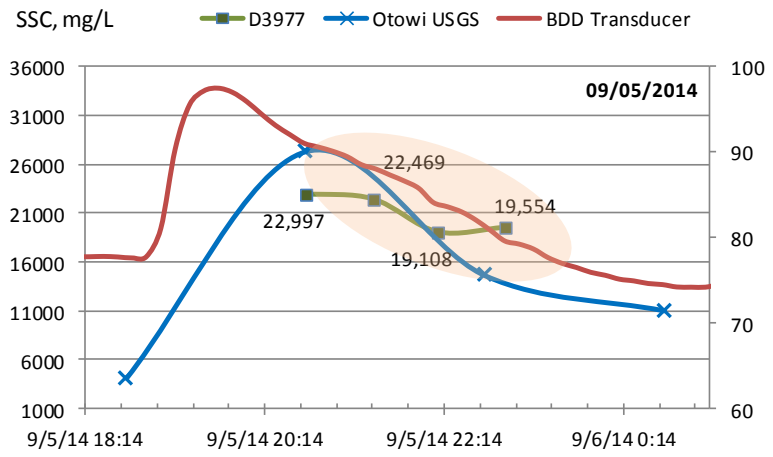

IV.5.m September 22-23, 2014 RG

Narrative of Event: This was a Rio Grande and potentially lower LA Canyon storm event. Sampling was initiated by BDD operator at 23:12 due to increased value of turbidity in the river. The BDD transducer data was compared to Otowi Gage data and flows in lower LA Canyon flows were interpreted to have occurred concurrent with the river event throughout the day as indicated on the graph.

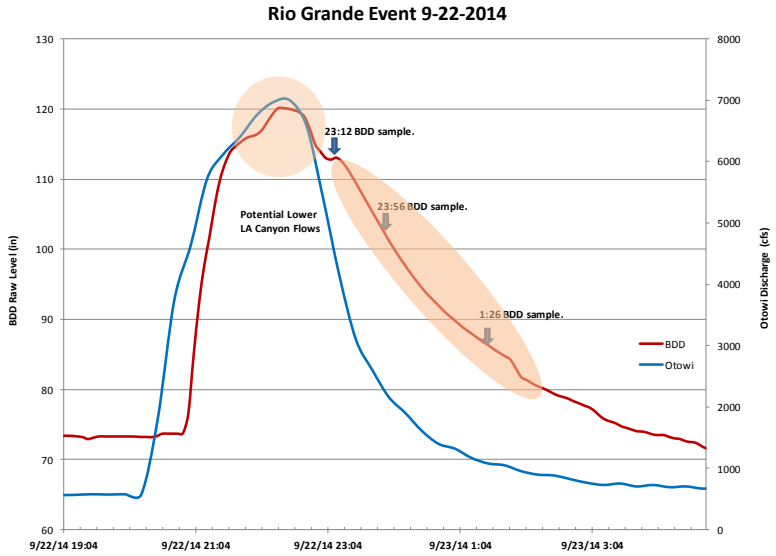

Station	Max Discharge (cfs)	Time
Otowi	7,000	22:30
E050.1	-	-
E060.1	-	-
BDD	na	22:45

Since the two storm events occurred almost at the same time, we can only draw the conclusion that the high SSCs were due to both events.

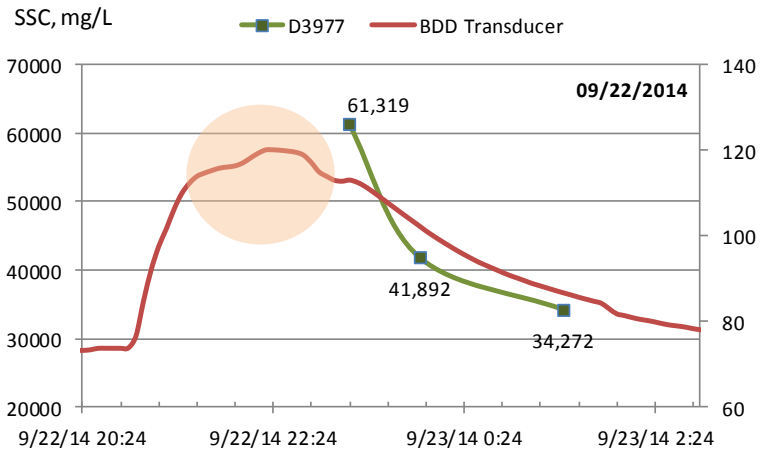

Sampling & Analyses Information			
Bottle #	**Sampler BDD2**	**Time**	**Otowi Discharge (cfs)**
1-3	sampler failure	21:43	6130
4	Particle size (Hall)	23:43	3100
5	PCBs	23:43	3100
6	Perchlorate	23:43	3100
7-12	sampler failure	1:43	
Bottle #	**Sampler BDD3**	**Time**	**Otowi Discharge (cfs)**
1-16	sampler failure	19:57	578
17	SSC	23:12	5420
18	GS-IsoU/Pu/Am241	23:12	5420
19	GS-IsoU/Pu/Am241	23:12	5420
20	GS-IsoU/Pu/Am241	23:12	5420
21	GS-IsoU/Pu/Am241	23:12	5420
22	Sr 90	23:12	5420
23	Ra 226/228	23:12	5420
24	Gross a-b/Metals	23:12	5420
Bottle #	**Sampler BDD4**	**Time**	**Otowi Discharge (cfs)**
1	SSC	23:56	2600
2	GS-IsoU/Pu/Am241	23:56	2600
3	GS-IsoU/Pu/Am241	23:56	2600
4	GS-IsoU/Pu/Am241	23:56	2600
5	GS-IsoU/Pu/Am241	23:56	2600
6	Sr 90	23:56	2600
7	Ra 226/228	23:56	2600
8	Gross a-b/Metals	23:56	2600
9	sampler failure	0:41	1800
10	Cyanide	0:41	1800
11-16	sampled	0:41	1800
17	SSC	1:26	1320
18	GS-IsoU/Pu/Am241	1:26	1320
19	GS-IsoU/Pu/Am241	1:26	1320
20	GS-IsoU/Pu/Am241	1:26	1320
21	GS-IsoU/Pu/Am241	1:26	1320
22	Sr 90	1:26	1320
23	sampled	1:26	1320
24	Gross a-b/Metals	1:26	1320

Week of 9-21-14 Weather Information - Los Alamos											
2014	Temp. (°F)			Humidity (%)			Wind (mph)			Precip. (in)	Events
Sep	high	avg	low	high	avg	low	high	avg	high	sum	
21	76	67	58	86	59	27	21	11	26	0	
22	70	63	56	100	81	52	16	10	24	0.01	Rain
23	74	64	53	100	64	26	10	5	-	0	Fog
24	78	66	55	71	36	19	17	5	24	0	
25	79	68	57	75	54	21	15	6	22	0	
26	75	64	52	93	62	35	16	7	22	0	
27	71	62	54	80	59	37	17	9	26	0	

Week of 9-22-14 Weather Information - Santa Fe											
2014	Temp. (°F)			Humidity (%)			Wind (mph)			Precip. (in)	Events
Sep	high	avg	low	high	avg	low	high	avg	high	sum	
21	82	68	55	87	55	26	23	14	34	0	Rain
22	75	68	60	87	71	44	20	10	25	0.04	Rain , Thunderstorm
23	81	70	59	93	71	30	15	4	22	0	
24	82	66	50	83	48	20	20	9	31	0	
25	81	66	52	86	55	26	18	7	28	0	
26	77	62	48	90	65	33	12	7	20	0	

V. RIO GRANDE HYDROLOGIC PARAMETERS

V.1 Rio Grande Discharge and SSC

BDD does not measure the discharge at the intake. At times when discharge at the BDD is needed the discharge documented by USGS at the Otowi Gage# USGS 08313000 "Rio Grande at Otowi Bridge, NM" is used for reference purposes and as an estimate for the flow at the BDD. The purpose of this section is to look into certain parameters that were measured during the surface water monitoring, graph them and compare with known parameters of the Rio Grande.

BDD measured the suspended sediment concentration (SSC) during storm events. The descriptive statistics of this data is offered in Attachment 4. The time plot on Figure 16 depicts the SSC for seven years of monitoring effort. The data includes only the results from the test ASTM: D3977-97 method. The time plot indicates an increase in SSC since 2011, but the box plots of the SSC (Figure 17) indicate a decrease in the median values from 2010 until 2012 and then an increase until 2014.

Figure 16. Time plot of SSC at BDD.

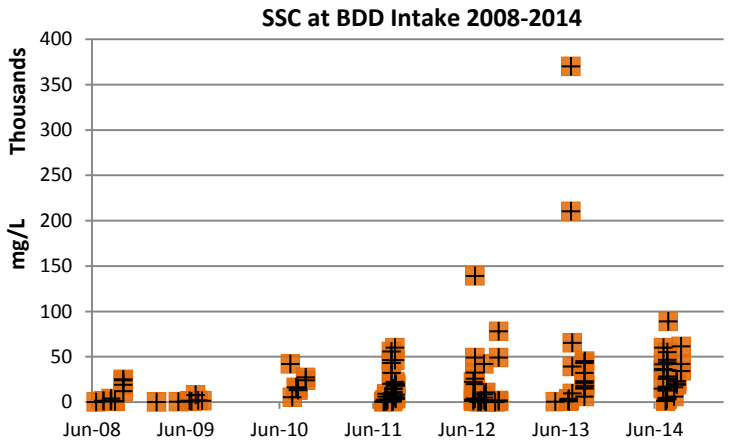

Figure 17. SSC annual boxplots 2008-2014.

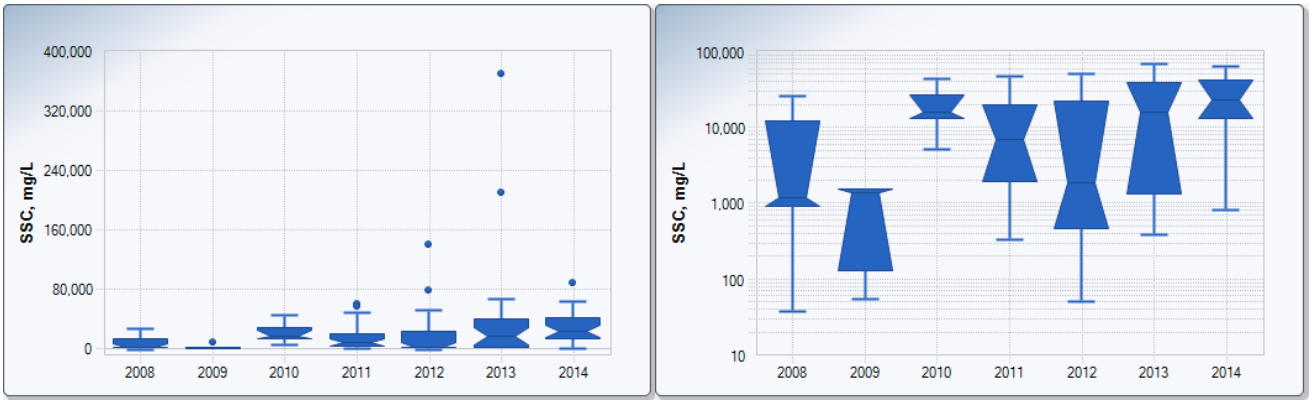

The USGS at the Otowi Gage measures the discharge and SSC of the RG. The SSC is measured once a day by collecting a surface water sample using autosampler and more often when a storm event occurs in the RG. In addition, USGS collects a sample of the cross section on a regular basis at the Otowi Gage in order to measure the total SSC. Consequently, the USGS "corrects" the measured SSC to the total SSC of the cross section of the gage station. All posted SSC field measurements on the USGS web site are the "corrected" total SSC. On average, the total SSC is 1.6 times greater than the measured SSC at the Otowi Gage (Nordin, 1965).

The USGS parameters of discharge and SSC were plotted together with the BDD SSC measured at the intake and the NMED SSC measured upgradient from the Otowi Bridge (by an autosampler). The graphs were labeled with the major LA storm events and their maximum discharge at the lower LA Canyon (former LANL gage station E109.9).

The USGS SSC measured at the Otowi gage does not always capture the highest SSC for a particular day since it is taken at a preset time. When there is no river storm event, the USGS SSC represents well the daily river conditions.

Figure 18. 2010 hydrologic parameters of Rio Grande.

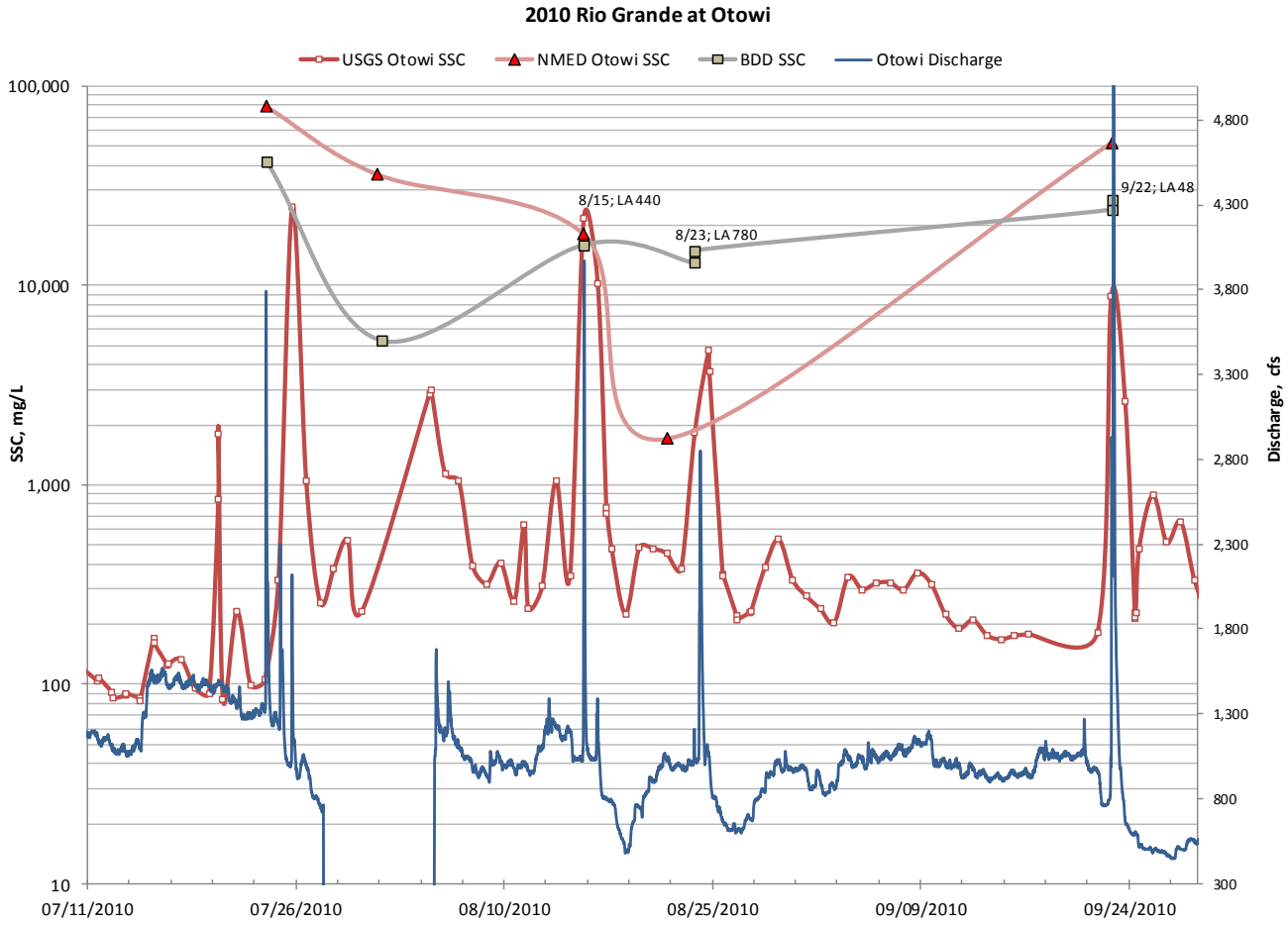

The 2010 graph presented on Figure 18 indicates that for most river storm events, the SSC increases as the flow increases, although the effect may take up to three days to express. Qualitatively, during the summer season, as the RG discharge peaks, we should expect a peak in the SSC with a certain time delay and of different magnitude for each storm event.

One date that deserves mentioning on Figure 18 is 8/23/2010. River storm event did not occur until 8/24/2010, and the RG flow on 8/23/2010 (18:00) was 1,210 cfs with SSC of 1,840 mg/L. Strong LAC storm event occurred on 8/23/2010 between 15:00 and 19:00, with maximum (estimated) flow of 780 cfs. BDD SSC on 8/23/2010 at 17:59 was measured to be 15,000 mg/L. It appears that the storm flow which occurred at LAC and entered the RG increased the SSC at BDD from 1,840 to 15,000 mg/L.

The process of graphing the RG parameters at Otowi Gage and the BDD was repeated for all monitoring years. 2011 was the season when monitoring data was abundant and the picture below shows dates with great SSC agreement between Otowi and BDD, see 7/22, 8/24, 8/26. For dates when there was a small or no RG event, such as 7/28, 8/3, 9/1, 9/4, 9/7 the BDD measured SSC is much greater than the SSC at Otowi, clearly an indication of the arrival of high sediment flow from LA Canyon at the time of sampling.

Figure 19. 2011 hydrologic parameters of Rio Grande.

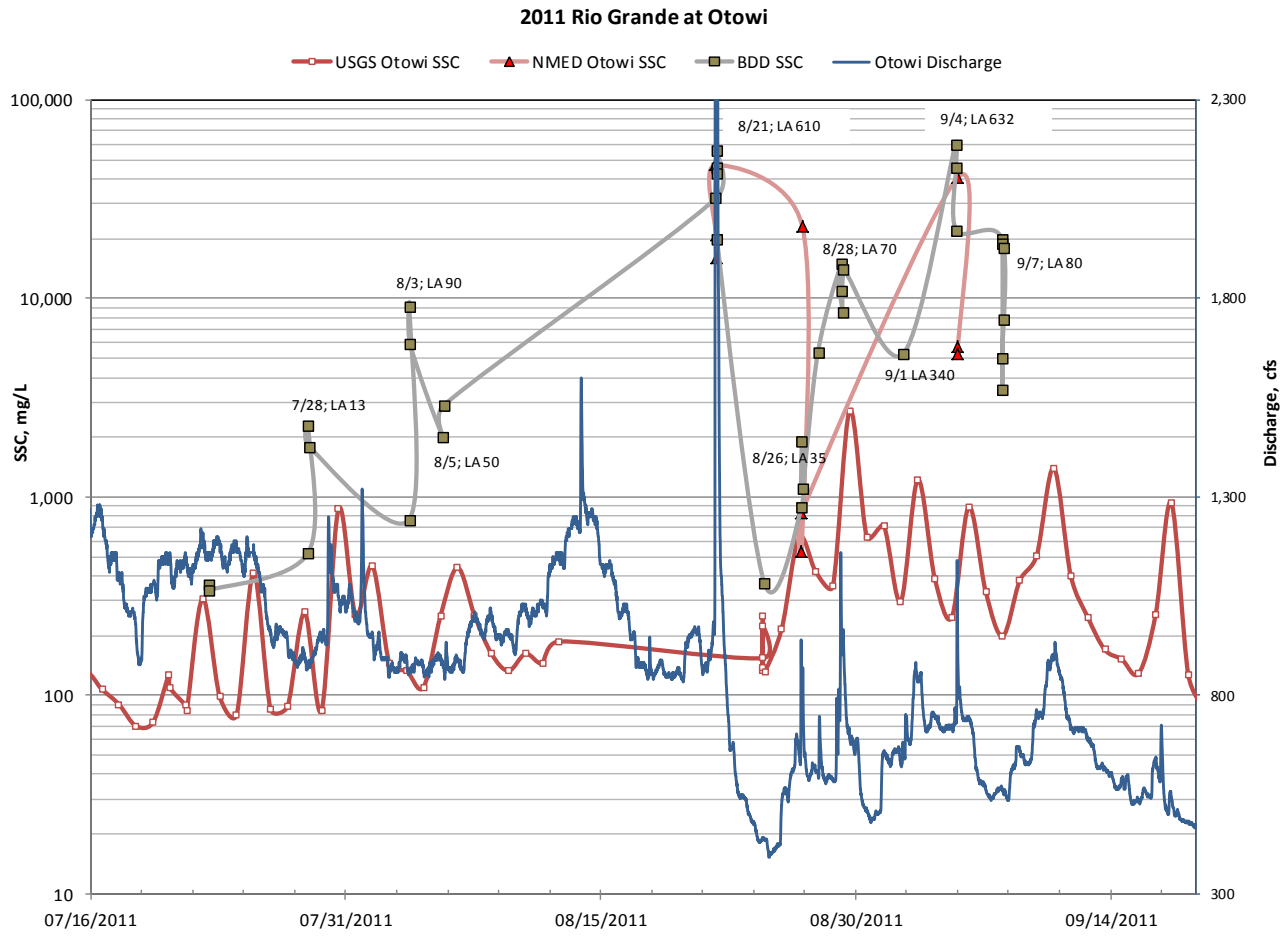

The 2011 BDD sampling strategy was to sample as many LA Canyon events as possible with a trigger being the lower LA Canyon flow (E109.9), and as a result BDD sampling was able to capture many LA Canyon flows. This fact was confirmed by the SSC values measured at BDD which were greater that the Otowi Gage SSC. The interesting fact is that even when LA Canyon flow was not great it was still "detected" at BDD through its higher SSC, such as the dates 7/28, 8/3, 8/5, 8/27, and 9/7. The SSC values of base flow sampling on 7/22 and 8/24, match very well with the Otowi Gage SSC values.

Figure 20. 2012 hydrologic parameters of Rio Grande.

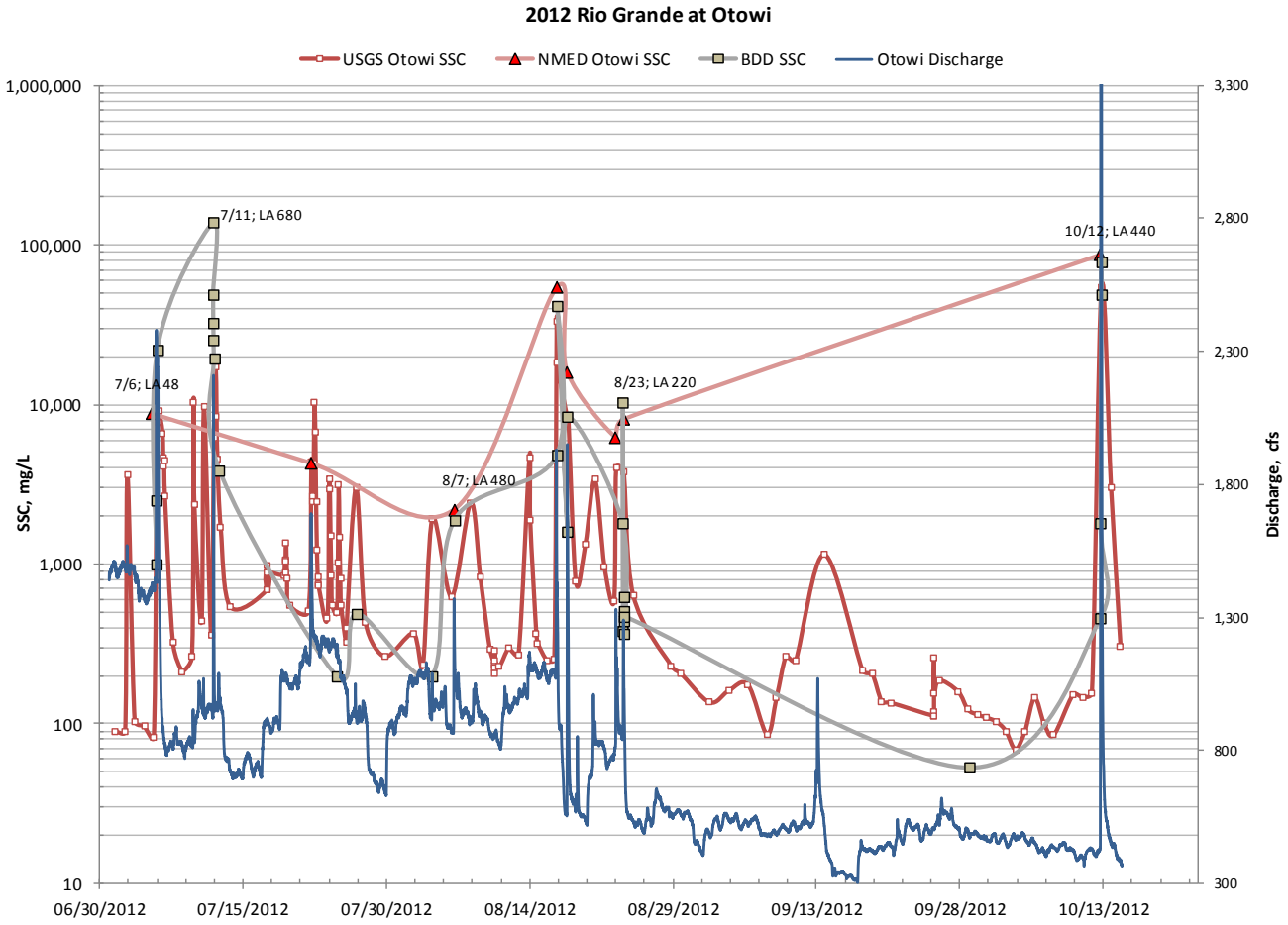

In 2012, the BDD SSC was in good agreement with SSC data from Otowi Gage collected by USGS and NMED. On 7/11/2012 there was strong LACW storm run off, so the SSC at the BDD was many times higher which was an indication of LAC arriving at BDD.

Figure 21. 2013 hydrologic parameters of Rio Grande.

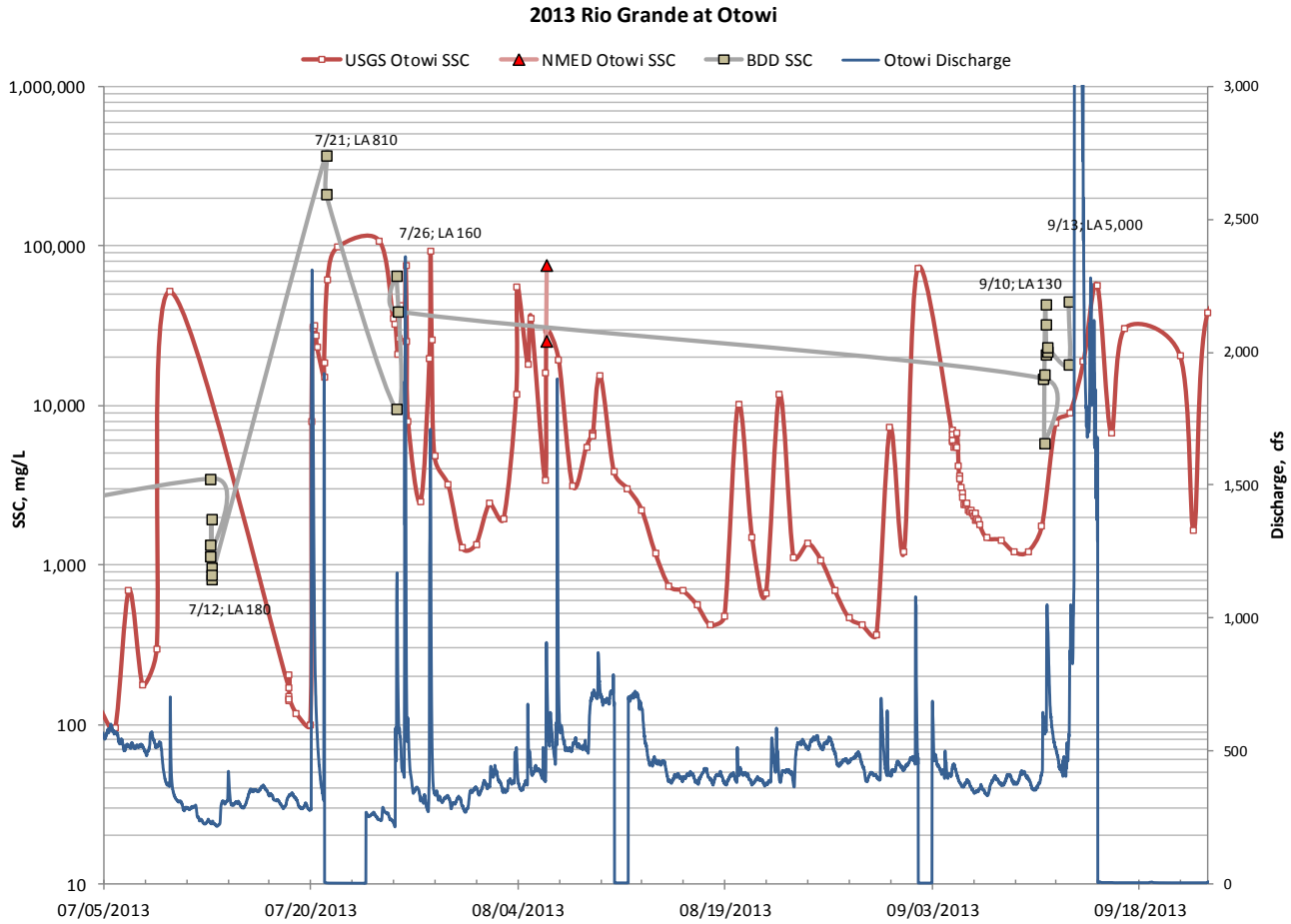

The highest SSCs measured at BDD were during 7/21/2013 and 9/10/2013 when the LACW experienced large storm flows.

Figure 22. 2014 hydrologic parameters of Rio Grande.

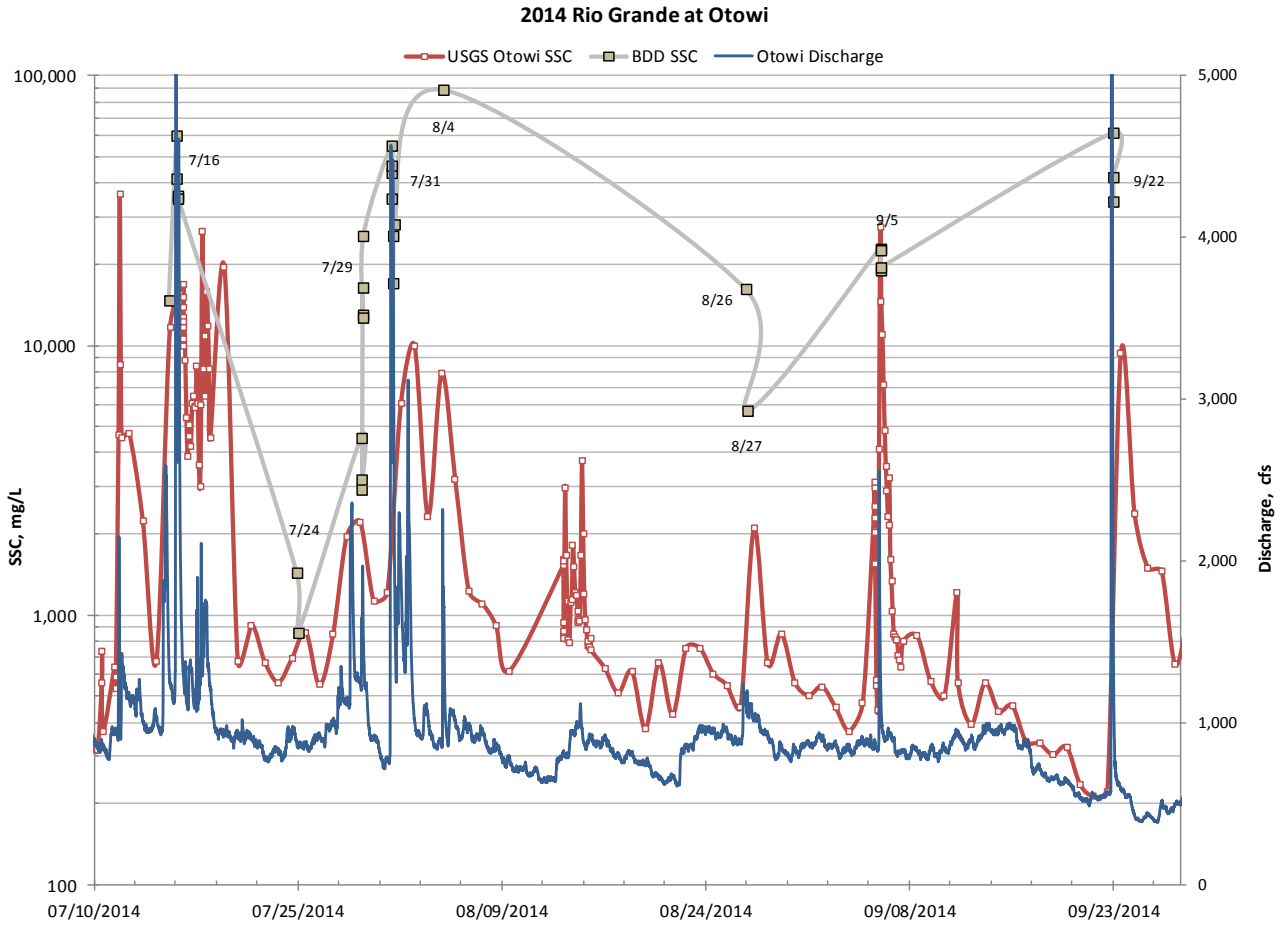

The high SSC for 7/16/2014, 7/29/2014, 8/4/2014, 8/26-27/2014, and 9/22/2014 may be interpreted as a result of high flows from the lower LAC, however, its flow cannot be verified since that part of the canyon was not monitored.

V.2 BDD Intake Turbidity and TSS, 2011-2014

The water quality of the river at the Intake is an important factor monitored all year by the parameters of turbidity and the total suspended solids (TSS) or the suspended sediment concentration (SSC) analyses. The original BDD NPDES permit required that the facility monitors turbidity daily, and TSS weekly. The river was usually sampled early in the morning during base flow conditions.

The result of this monitoring is presented on Figure 23. In general, qualitative terms, the TSS trends the turbidity. The highest turbidity and TSS values were observed during the storm season, from July until September of each year.

Figure 23. Turbidity and TSS at BDD Intake, 2011-2014

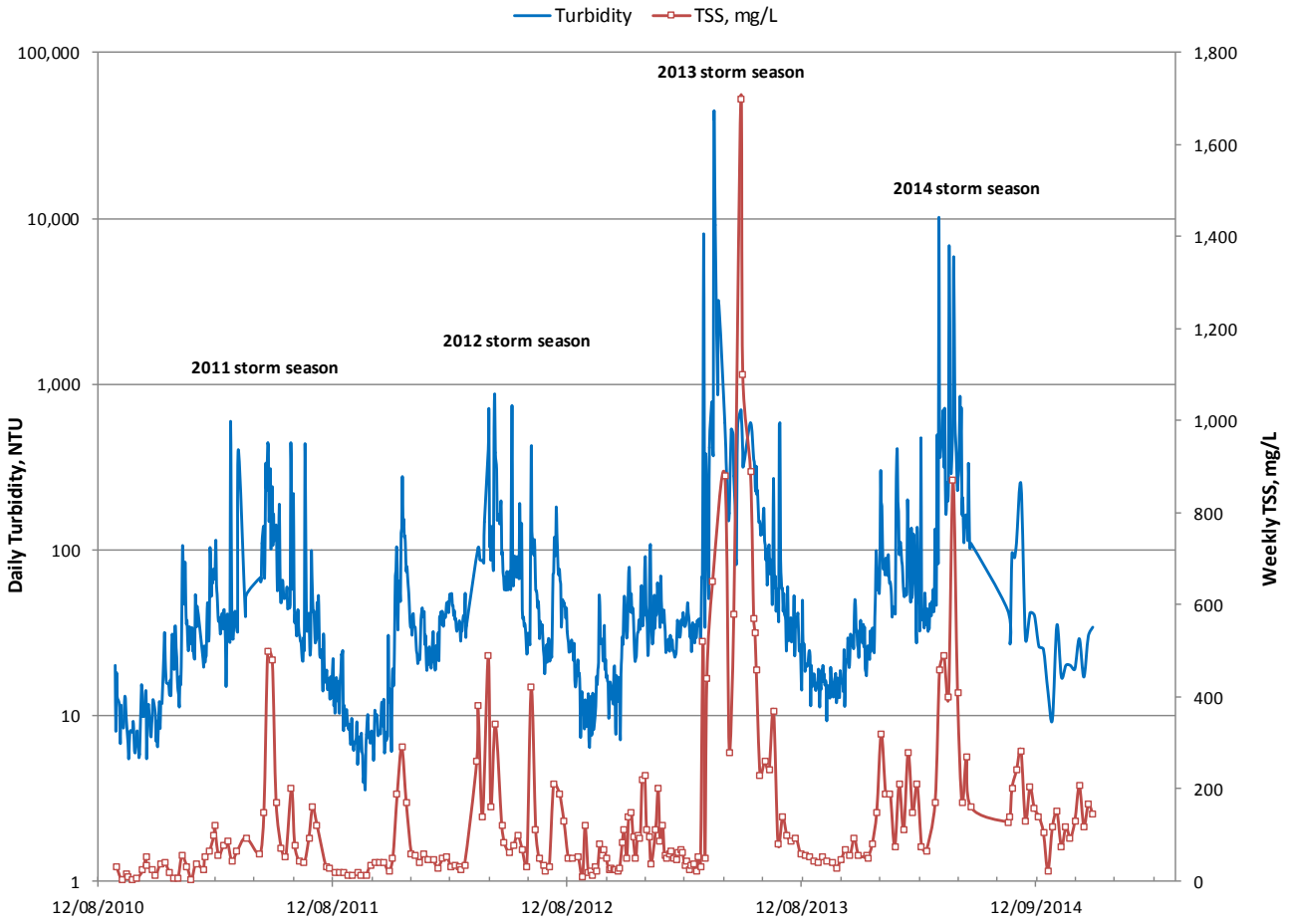

In order to explore further the quantitative dependence of these two parameters, we plotted the TSS vs turbidity as collected pursuant to the NPDES permit. Establishing a relationship between the two parameters is very important for surface water monitoring. Turbidity is a field parameter that could be measured continuously while the TSS could only be measured at the laboratory. If a good correlation between these two is found then the turbidity measurement could be used as a surrogate for measuring water quality including contaminants which have the property to adhere to sediment and soils and transport downstream through those means.

Figure 24 indicated that there is a great correlation between the TSS and turbidity of the Rio Grande with coefficient of determination of 0.83. Therefore, for constituents that transport by suspended sediment, this correlation may be used to predict their concentration by simply measuring the turbidity of the surface water.

Figure 24. TSS vs turbidity at BDD, 2011-2014.

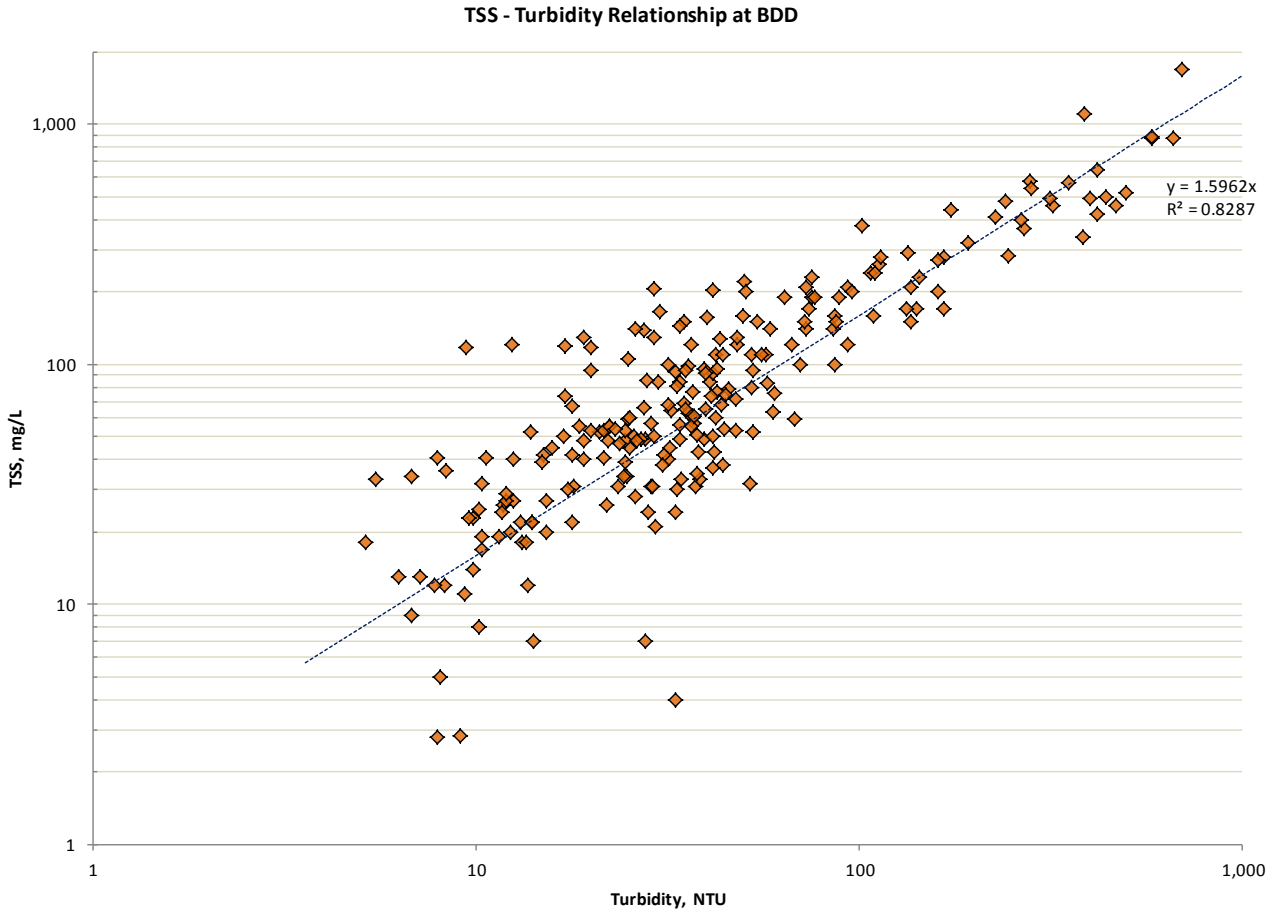

At least a couple of studies have shown that the SSC method performs better than the TSS method in describing the solid content of natural surface waters. Both studies have found that as the percent sand in the collected sample increases the inaccuracy in TSS results in comparison to the SSC results increases greatly. In general terms, USGS does not recommend the TSS method for natural waters such as the Rio Grande.

Table 18 indicates that at times the course fraction in the RG may reach 56%. However, the collected data from particle size analysis was during storm events, and, therefore we can assume that for base flow conditions, the percent course fraction (sand particles mostly) would be much less than the coarse fraction in samples collected during storm conditions. Therefore, Figure 24 is a good representation of the correlation, TSS (or SSC) vs. turbidity, since most of the data was collected during base flow conditions.

Figure 25. BDD TSS vs Otowi Gage SSC.

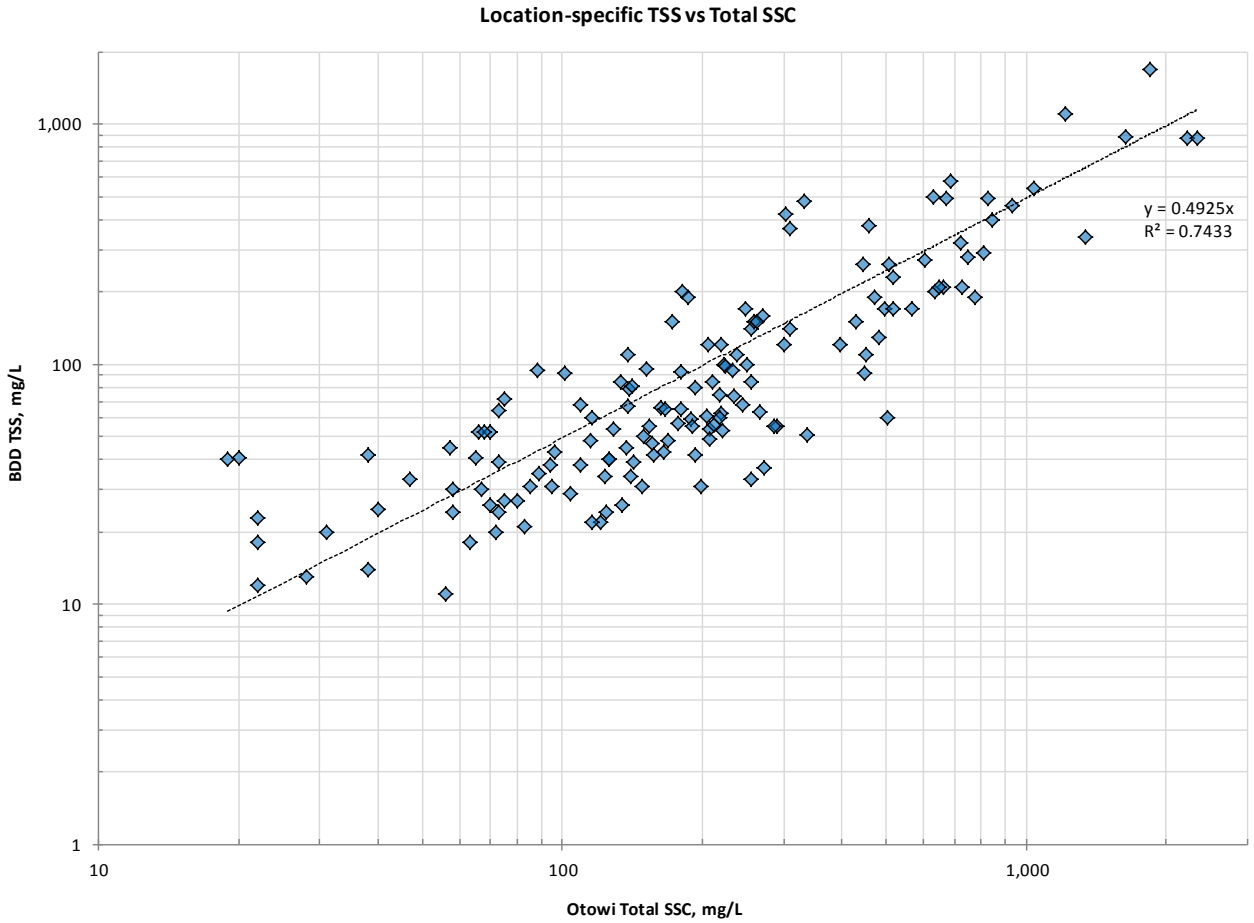

The procedure for collecting TSS sample at the diversion included a grab sample, which was usually collected from a specifically prescribed location at the diversion. As such the sample is not representative of the average TSS in the cross sectional area, but the average value of the top few feet from the surface of the water. On the other hand, USGS at Otowi Gage "corrects" the SSC results to make them representative of the total SSC along the cross section of the Otowi Gage. In order to investigate how these two parameters differ, we plotted the BDD TSS vs the Otowi Gage Total SSC as published on USGS web site. The coefficient of determination between these parameters in Figure 25 is strong and the fitting equation indicates a factor of 2 in favor of the total SSC measured at Otowi Gage. Similar dependence with similar factor (1.6) was obtained from Table 1 of (Nordin, 1965) between the measured SSC and the computed total SSC using the modified Einstein procedure.

V.3 Particle Size Analysis

The data for the particle size was divided into coarse fraction (greater than 62 µm) and fine fraction (equal or less than 62 µm). BDD data was summarized in Table 18. The particle size data was used to evaluate discharges of fine and coarse fraction suspended sediments. The discharges are presented in Table 16.

Table 16. BDD suspended sediment discharges.

Date	Time	SSC g/l	Fine Fraction %	Coarse Fraction %	Otowi Flow cfs	Coarse Discharge tons/day	Fines Discharge tons/day	Comments
07/22/2011	23:30	0.36	79	21	1,180	218	821	B
07/22/2011	23:34	0.34	75	25	1,180	245	736	B
07/28/2011	18:40	0.52	91	9	870	100	1,007	LA 13
08/03/2011	17:40	0.77	89	11	858	178	1,439	LA 90
08/21/2011	18:59	(56.00)	89	11	870	(13,112)		RG; LA 610
08/24/2011	15:01	0.37	75	25	440	100	299	B
08/26/2011	19:43	0.89	76	24	940	491	1,556	RG
08/27/2011	19:01	(5.40)	90	10	611	(807)		LA 60
09/01/2011	19:38	(5.30)	92	9	682	(752)		LA 340
09/04/2011	21:24	(60.00)	86	14	764	(15,701)		LA 682
07/11/2012	20:34	(39.00)	87	13	234	(2,903)		LA 680
08/23/2012	18:08	(10.00)	91	9	846	(1,863)		LA 220
05/21/2013	14:13	0.40	44	56	1,130	619	487	B
07/12/2013	16:38	(3.48)	96	4	240	(82)		LA 180
09/11/2013	1:38	(15.00)	85	15	625	(3,440)		LA 120
09/12/2013	21:16	(31.00)	92	8	500	(3,034)		LA 450
07/15/2014	11:51	(2.04)	82	18	1,610Q			RG
07/16/2014	0:46	4.90	97	3	5,720	2,057	66,515	RG
09/22/2014	23:43	(53.79)	100	0	3,100Q			RG
Mean w/o ()		1.07	85	15	1,540	501	9107	

B - baseflow

LA ## - Los Alamos Canyon max flow, cfs

RG - river event occurring for that date

Q - quality problem identified; data was not used in analysis

Fine Fraction - less than 62-63 µm

Coarse Fraction - equal to or greater than 62-63 µm

Mean w/o () - the average of events marked without parenthesis only, except for Fine and Coarse Fraction %

The table included two types of sampled events, one when only river events occurred and the other when LA Canyon and RG storm event occurred within close time frame. The "comments" field marks the LA Canyon maximum flow if a storm event occurred in the lower LA Canyon. It is easy to observe that the measured BDD SSC for the dates when there was an event in the lower LA Canyon was much higher than at times when only river events occurred.

For example, on 7/11/2012 when the RG flow was at 234 cfs, the measured BDD SSC was 39,000 mg/l due to strong LAC flow, while on 7/22/2011 when the river was at baseflow of 1,180 cfs, the measured BDD SSC was only 340 mg/l due to absence of LAC flow. Therefore, there is a strong relationship between the measured SSC at the diversion and the strength of the LA Canyon storm

events. It appears that the SSC is a measure of the contribution from the LA Canyon during storm events in that canyon.

The fine and coarse discharges at BDD were calculated (Table 16) and later plotted as a function of the Otowi flow (Figure 30). The discharges when the LA Canyon flow was more than 10% of the RG flow were placed in parenthesis. A couple of dates were identified with quality problems, 7/15/2014 and 9/22/2014, and the data for those dates was not considered in the analysis.

The particle size data from the lower LA Canyon (E109.9) was summarized in a similar table, Table 17. The data in the parenthesis was considered to be outliers and not used to calculate means. The fine and coarse instantaneous discharges were calculated and later plotted as a function of the LAC flow (Figure 29.)

Table 17. E109.9 suspended sediment discharges.

Date	Time	SSC, g/l	Fine Fraction %	Coarse Fraction %	LA Flow cfs	Coarse Discharge tons/day	Fine Discharge tons/day	Total Discharge tons/day
07/05/2012	19:34	302	82	18	48	6,384	29,082	35,466
07/05/2012	19:54	264	85	15	48	4,650	26,353	31,003
07/05/2012	20:50	192	87	13	48	2,931	19,616	22,548
07/24/2012	16:16	340	86	14	25	2,911	17,884	20,796
07/24/2012	16:32	248	88	12	25	1,820	13,348	15,169
08/07/2012	16:26	454	72	28	480	149,284	383,873	533,157
08/07/2012	16:30	420	76	24	480	118,375	374,854	493,229
08/23/2012	16:00	360	73	27	220	52,317	141,451	193,768
08/23/2012	17:00	236	80	20	150	17,322	69,287	86,609
08/24/2012	14:00	215	77	23	153	18,510	61,970	80,480
08/24/2012	15:00	113	85	15	40	1,659	9,400	11,059
08/24/2012	15:45	85	89	11	10	229	1,851	2,080
10/12/2012	16:45	138	81	19	200	12,830	54,696	67,525
07/20/2013	19:57	830	67	33	810	542,794	1,102,036	1,644,830
07/25/2013	23:04	162	85	15	100	5,945	33,689	39,634
07/26/2013	17:14	68	89	11	160	2,928	23,691	26,619
07/26/2013	17:42	63	87	13	150	3,006	20,114	23,120
08/03/2013	15:30	522	72	28	950	339,711	873,543	1,213,255
08/03/2013	18:34	141	93	7	50	1,207	16,041	17,248
08/05/2013	18:14	181	83	17	(600)			
08/09/2013	15:40	310	78	22	270	45,051	159,727	204,778
08/09/2013	15:56	256	82	18	170	19,165	87,309	106,475
09/12/2013	15:53	92	99	1	(80)			
09/12/2013	16:49	25	99.6	0.4	(190)			
09/12/2013	17:29	57	93	7	(50)			
Mean w/o ()		243.0	83.5	16.5	218.4	64,240	167,610	231,850

The influence of the different tributaries to LA Canyon flow is the most important factor in the SSC results of this table. Events originating from Guaje Canyon are known to contribute larger amounts of SSC to the lower LA Canyon flow than flows originating from the upper and middle LA Canyon

or Pueblo Canyon. Certain events are a combination of the different canyons' contributions. For example, an LAC event with 48 cfs on 7/5/2012 measured 302,000 mg/l while an LAC event with 160 cfs on 7/26/2013 measured only 63,000 mg/l of suspended sediment. The contributions from the different LAC tributaries was not investigated in this report.

In Table 18, the BDD particle size was compared to the lower LA Canyon and the Otowi Gage from (Nordin, 1965). The BDD fine and coarse fractions mentioned below take into account all measured values, while the BDD coarse[2] eliminated the values for dates when there was a strong lower LAC flow. Any events for which the maximum flow in the lower LAC was 10 percent or higher in relation to the RG flow is considered a LAC event that may have a strong influence on the BDD concentrations.

Table 18. BDD particle size statistics.

Fraction Type	Obs	Min	Max	Mean	Median	SD	95%ile	Skewness	Kurtosis	CV	Distribution
BDD Fine	17	44	97	84.3	89.0	12.45	96.2	-2.29	6.65	0.15	Non-Para
BDD Coarse	17	3	56	15.7	11.0	12.45	31.2	2.29	6.65	0.79	Log-Normal
BDD Coarse[2]	7	9	56	24.4	24.0	15.43	46.7	1.61	3.53	0.63	Log-Normal
Otowi Fine USGS	18	5	91	35.4	30.5	22.81	69.8	0.84	0.56	0.64	Normal
Otowi Coarse USGS	18	9	95	64.6	69.5	22.81	93.3	-0.84	0.56	0.35	Normal
109.9 Fine	25	67	99.6	83.5	85.0	8.16	97.8	0.03	-0.14	0.10	Normal
109.9 Coarse	25	0.4	33	16.5	15.0	8.16	28.0	-0.03	-0.14	0.50	Normal

One observation that needs mentioning is the difference in range and the mean of the fine fraction between the BDD and Otowi Gage. The BDD fine fractions were at very higher percent in comparison to the Otowi Gage values. Such result is expected considering the fact that storm water sampling does not sample a representative column of the cross section and therefore it is expected to be biased toward fine fractions.

A comparison of the particle size at BDD and LAC, indicated that the composition of the storm water at E109.9 and the BDD appears to be similar in its descriptive statistics. The statistical program ProUCL was used to graph box plots for these data sets and the results are presented in the following figures.

Figure 26. Otowi and BDD box plots fine fraction.

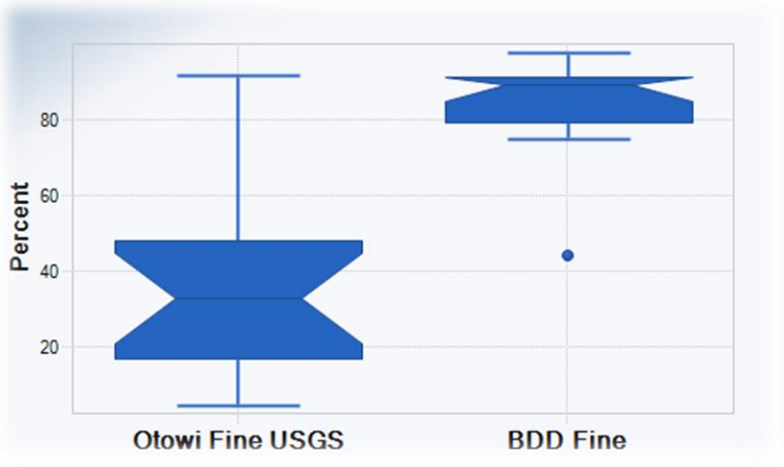

Figure 27. Otowi and BDD box plots coarse fraction.

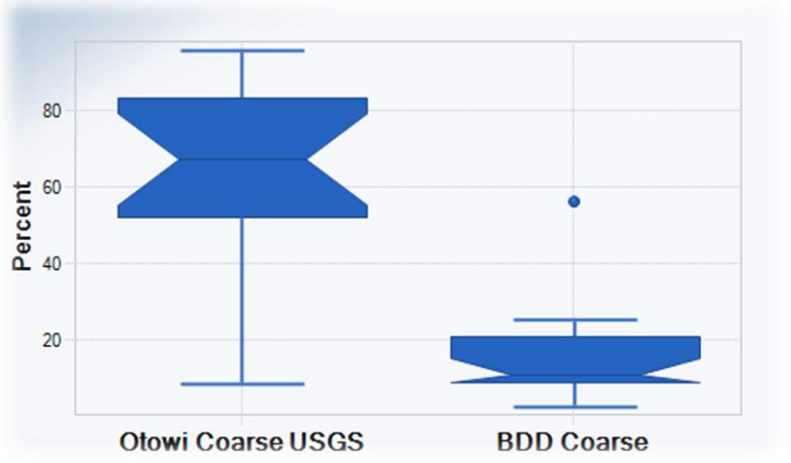

Figure 28. BDD and E109.9 box plots coarse fraction.

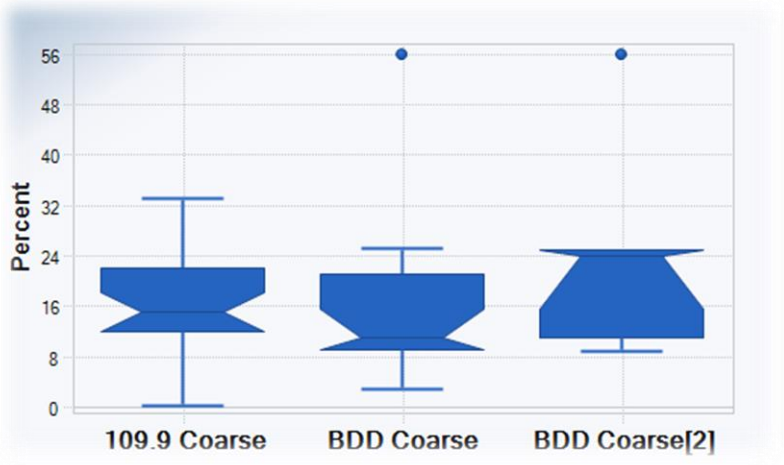

V.4 Transport Rates

Of the transport relations, the transport rate was explored in this section. Considering the viewpoint that the transport rate of bed material[3] is governed solely by the ability of the flow to move the material (meaning functional relation exists between the transport rate and the flow), the coarse fraction discharge was calculated for E109.9 and BDD and plotted as a function of the corresponding flow.

Figure 29. E109.9 coarse discharge vs flow.

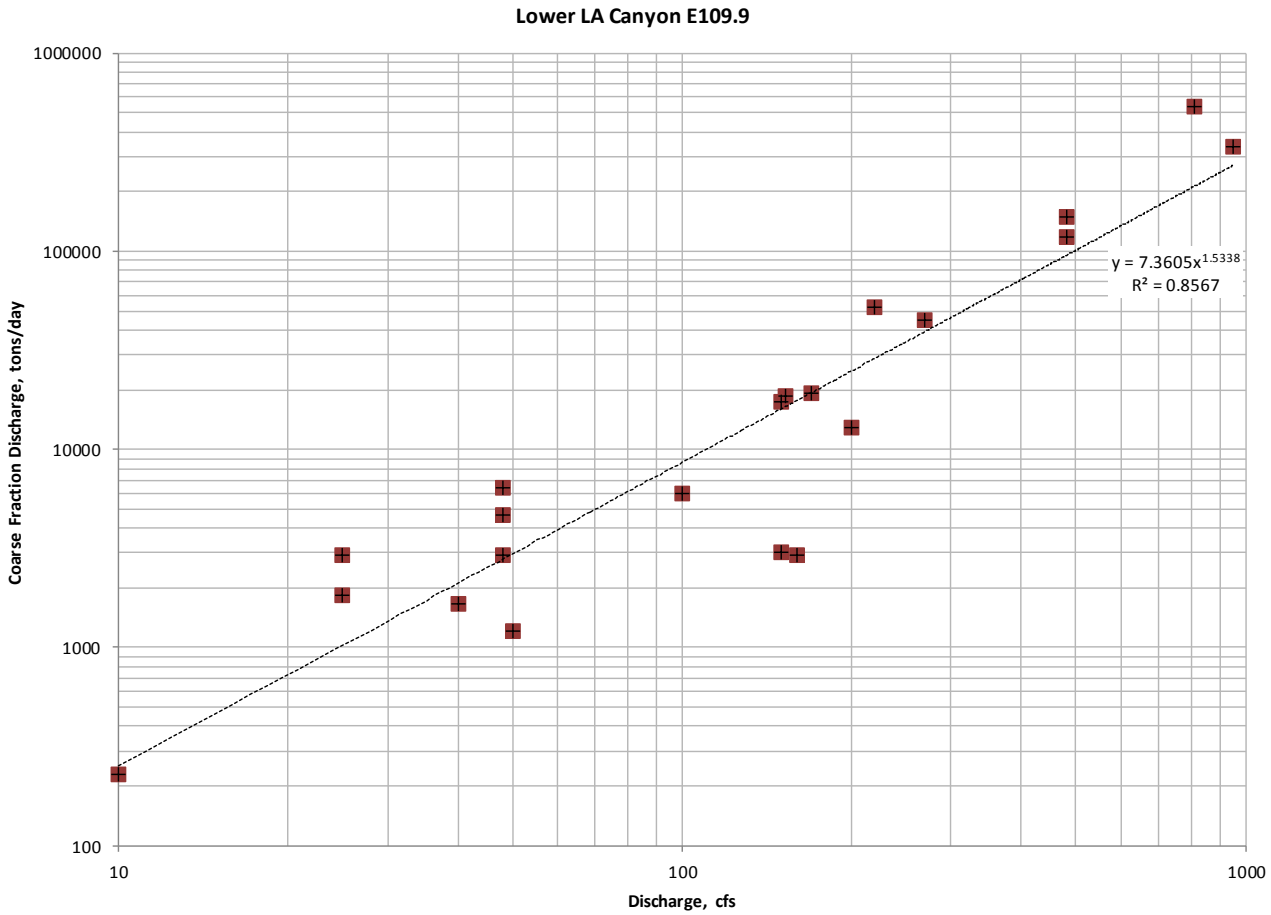

As in the previous sections, the coefficient of determination, R^2, calculated automatically by the graphing program shall be used as a measure of "correlation" between the two plotted variables. The correlation between these two parameters (Figure 29) at E109.9 was very strong while at BDD (Figure 30), there was no reasonable correlation.

For BDD Intake, we plotted the coarse discharge vs flow using all data in Table 16. On the same graph, we also plotted the USGS best fit applied to Otowi Gage bed material discharge as published

[3] For the purposes of this section bed-material and coarse fraction would be considered equivalent.

in (Nordin, 1965). The BDD coarse fraction discharges were fit to a straight line as shown on the plot in order to compare it to the USGS published work. The parameters of the equations (coefficient and exponent) were not compatible. However, BDD coarse discharge included the influence of the LA watershed in terms of high SSC values for a number of dates during which the transport properties in the RG were changed in irregular and unpredictable manner.

Figure 30. Coarse discharge at BDD vs Otowi flow.

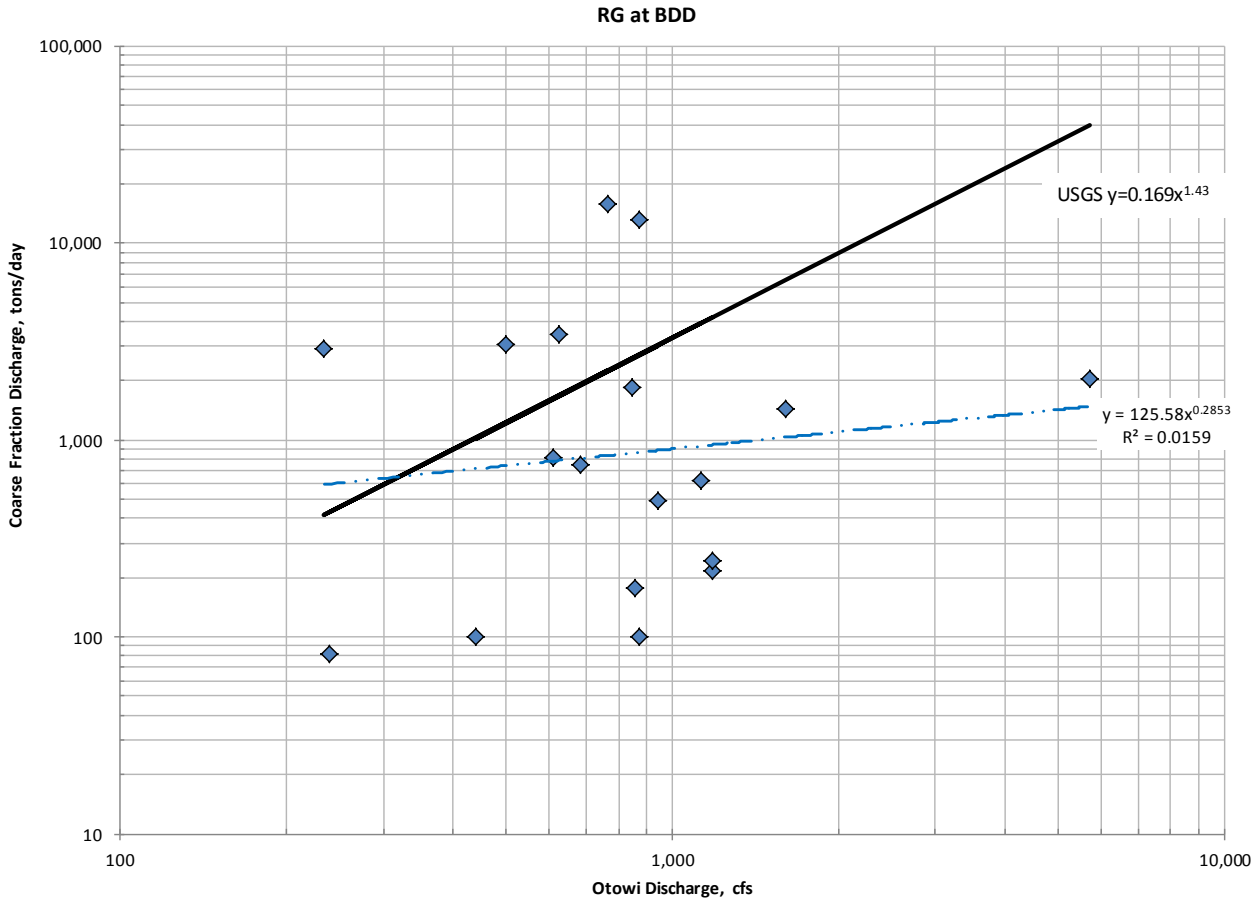

In order to explore that influence, we re-plotted the transport rate at BDD in Figure 31 by excluding the dates of strong LA Canyon flows. Although, the available data was very limited, the re-plotted data showed much stronger correlation between the coarse discharge and RG flow. The exponent of the fitted model of the re-plotted data was of similar order and quite close to the Otowi USGS study (1965). The coefficient in front of the exponent was much smaller, but the reduced value of the BDD data is clearly due to the measured point SSC, not the total SSC. In Section V.2, we found that the correlation between the point SSC (TSS) and total SSC was a factor of 2, which makes the best fit in Figure 31 even closer to the quoted reference: $Q_{\text{coarse fraction at BDD}}=0.12*(Q_{\text{Otowi}})^{1.211}$.

Figure 31. Revised RG at BDD coarse discharge vs flow.

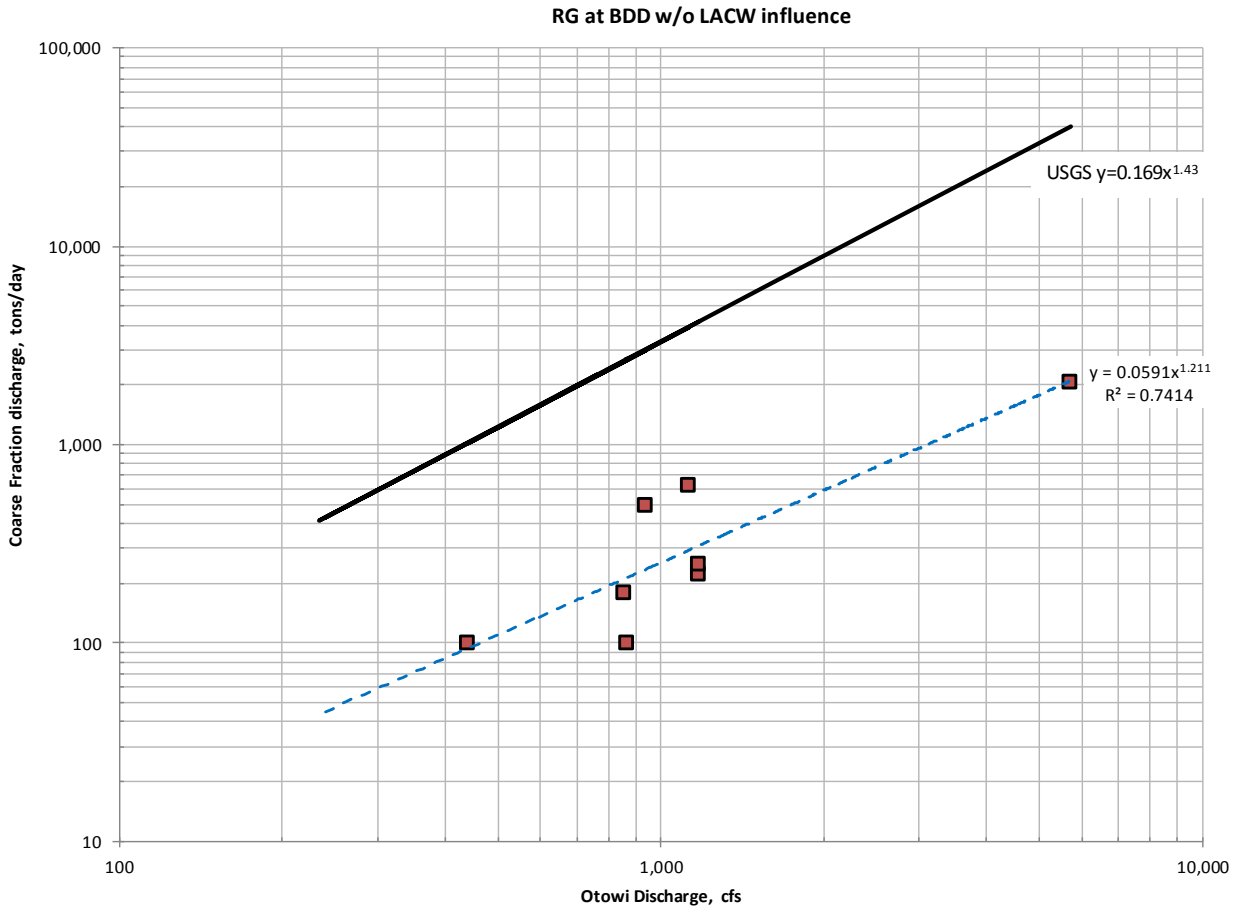

The agreement between the BDD data and the USGS Otowi study provides confidence in the obtained results. In addition, the results show that the LAC watershed influence during storm events plays a critical role on the measured concentrations at the diversion, and it changes temporarily the RG transport rates depending on the strength of each LA storm event and RG flow conditions (base vs. storm flow).

VI. RIO GRANDE SEDIMENT BACKGROUND STUDY

BDD staff obtained Rio Grande sediment data from the Intellus database and calculated Rio Grande sediment background upper tolerance limits (RG UTL av). These values would serve as a guide when comparing storm water results at the BDD for radionuclides or other LA/P watershed constituents of concern. It is well known fact that there is global fallout background, and, therefore multiple radionuclides may be normally found in surface water or river sediments at certain background levels specific to the area. The calculated RG UTL av values would provide a level at which one would be able to distinguish between radionuclide due to global fallout and elevated levels arriving to BDD

Intake from upgradient sources such as LA/P watershed. Table 19 and Table 20 present the RG UTL av and list for comparison purposes the Pajarito Plateau UTL as determined by the reference below.

Table 19. Radionuclides RG UTLs

pCi/g	Pu 239/240	Pu 238	Am 241	Sr 90	Cs 137	U 238	U 234	U 235
RG UTL av	0.014	0.008	0.018	0.76	0.50	1.28	1.43	0.083
PP UTL[4]	0.068	0.006	0.040	1.04	0.90	2.29	2.59	0.200
pCi/g	**Ra 226**	**Ra 228**	**K 40**	**Gross α**	**Gross β**	**Gross γ**		
RG UTL av	1.32	1.67	28.47	18.64	31.5	11.78		
PP UTL[4]	2.59	2.33	36.80					

Table 20. Metals RG UTLs

mg/kg	Al	As	Ba	Be	B	Cd	Cr	Co	Cu	Fe	Pb
RG UTL av	9,067	4.80	284	0.603	8.54	0.833	11.87	8.04	11.71	16,189	9.74
PP UTL[4]	15,400	3.98	127	1.310	-	0.400	10.50	4.73	11.20	13,800	19.70
mg/kg	**Hg**	**Mo**	**Ni**	**Se**	**Ag**	**Sr**	**Tl**	**Sb**	**U**	**V**	**Zn**
RG UTL av	0.0284	2.35	9.80	0.87	0.52	100.6	0.114	NA	3.70	35.2	56.2
PP UTL[4]	0.1000	-	9.38	0.30	1.00	-	0.730	0.83	2.22/6.99	19.7	60.2

The BDD sediment background study is described in Appendix 5. The used data, sampling locations, statistical methods, and used references are presented in that appendix as well.

VII. Storm Water Analytical Results

VII.1 BDD Intake Contaminants Analytical Results

The BDD data collected by different entities could be located in online database, Intellus at www.intellusnmdata.com. The amount of the available data is very large. However, for the purposes of this report, BDD staff sorted the data to make it more user-friendly and presented the collected data in Appendix 4.

VII.2 BDD Analytical Data

Attachment 4 of this report contains the descriptive statistics of collected data at the BDD from 2011 to 2014 for radionuclides, metals, total PCBs, SSC, perchlorate, and dioxins/furans in terms of 2,3,7,8-TCDD TEQs. The attachment separates the results for filtered and unfiltered samples.

In this section we will present the results from the four years of monitoring in a visual form (graphs and box plots) and note any exceedances from the RG UTLs and NMWQCC standards for surface water (20.6.4 NMAC) as listed in Table 21. During the 2014, the samples for radionuclides analytical testing (with the exception of gross alpha and gross beta) were filtered by the analytical laboratory due to the lack of communication between LANL and their contract laboratory. Those samples were

[4] Pajarito Plato UTL: Values were reported in (Ryti, September 22, 1998)

filtered by the laboratory through a 5μm sieve and were marked in this report and in Attachment 4 by BDD as "Filtered x10" or "10F". This type of data is not especially marked in the Intellus database as a third type of data, but it is qualified as "F" (filtered) which according to standard procedure must be samples that are filtered through a 0.45 μm sieve. As a result of the filtering of the samples, BDD does not have unfiltered storm water results for the 2014 season, except for limited amount of unfiltered storm water data collected by NMED/DOE OB.

Table 21. NMWQCC surface water standards and screening criteria.

NMWQCC Surface Water Standards								
Analytical Suite	Analyte Code	Analyte Name	Field Prep	Acute Aquatic	Human Health Persistent	Lifestock Watering	Wildlife Habitat	Screening Criteria
METALS	Al	Aluminum	F	658	n/a	n/a	n/a	
METALS	Sb	Antimony	F	n/a	640	n/a	n/a	
METALS	As	Arsenic	F	340	9	200	n/a	
METALS	B	Boron	F	n/a	n/a	5,000	n/a	
METALS	Cd	Cadmium	F	0.59	n/a	50	n/a	
METALS	Cr	Chromium	F	n/a	n/a	1,000	n/a	
METALS	Cr(III)	Chromium(III)	F	210	n/a	n/a	n/a	
METALS	Co	Cobalt	F	n/a	n/a	1,000	n/a	
METALS	Cu	Copper	F	4	n/a	500	n/a	
METALS	Pb	Lead	F	17	n/a	100	n/a	
METALS	Mn	Manganese	F	1,999	n/a	n/a	n/a	
METALS	Hg	Mercury	F	1.4	n/a	n/a	n/a	
METALS	Hg	Mercury	UF	n/a	n/a	10	0.77	
METALS	Ni	Nickel	F	170	4,600	n/a	n/a	
METALS	Se	Selenium	F	n/a	4,200	50	n/a	
METALS	Se	Selenium	UF	20	n/a	n/a	5	
METALS	Ag	Silver	F	0.4	n/a	n/a	n/a	
METALS	Tl	Thallium	F	n/a	0.47	n/a	n/a	
METALS	V	Vanadium	F	n/a	n/a	100	n/a	
METALS	Zn	Zinc	F	54	26,000	25,000	n/a	
WET_CHEM	CN(TOTAL)	Cyanide(Total)	UF	22	140	n/a	5.2	
PCB_CONG	1336-36-3	Total PCBs	UF	n/a	0.00064	n/a	0.014	
DIOX/FUR	n/a	Dioxin (TEQ)	UF	n/a	0.000000051	n/a	n/a	
RAD	GROSSA	Gross alpha	UF	n/a	n/a	15	n/a	
RAD	Ra-226+228	Radium-226 & 228	UF	n/a	n/a	30	n/a	
RAD	Am-241	Americium-241	UF					1.9
RAD	Cs-137	Cesium-137	UF					6.4
RAD	Pu-238	Plutonium-238	UF					1.5
RAD	Pu-239/240	Plutonium-239/240	UF					1.5
RAD	Sr-90	Strontium-90	UF					3.5
RAD	H-3	Tritium	UF					4,000
All units are ug/L except for RAD, which are pCi/L								
F=filtered and UF=unfiltered								

VII.2.a Annual Plots and Trends for Radionuclides in Storm Water

The time and box plots presented here compare how the concentrations of the radionuclides at BDD changed for each season during the monitoring period and how the unfiltered and filtered results compared.

Figure 32. Time plot for Pu-239/240.

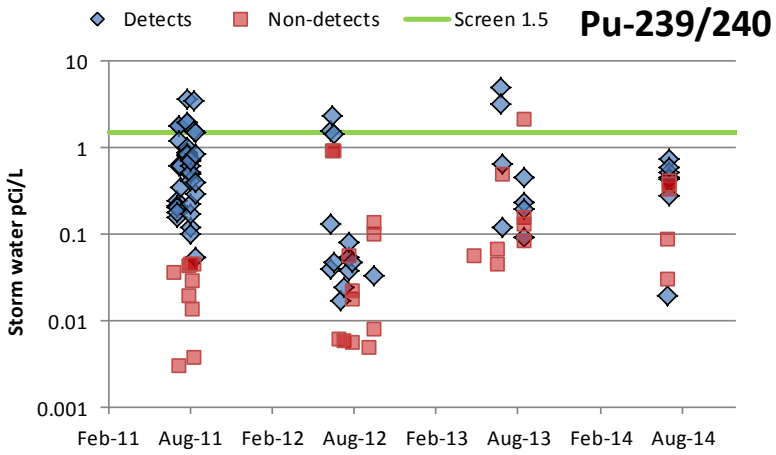

The graph for Pu-239/240 showed that there were exceedances of the NMWQCC screening value (1.5 pCi/L) in 2011, 2012, and 2013. The time plot also indicates that the quality of the data was not satisfactory for 2012 and 2013 because the non-detect values were very high. The detection limits of non-detects were in the range of 0 – 2.15 pCi/L. There was only one detected value from the filtered samples on 9/7/2011 of 0.0077 pCi/L, indicative of the metal's low solubility and preferential transport via suspended sediment.

Figure 33. Time plot for Pu-238.

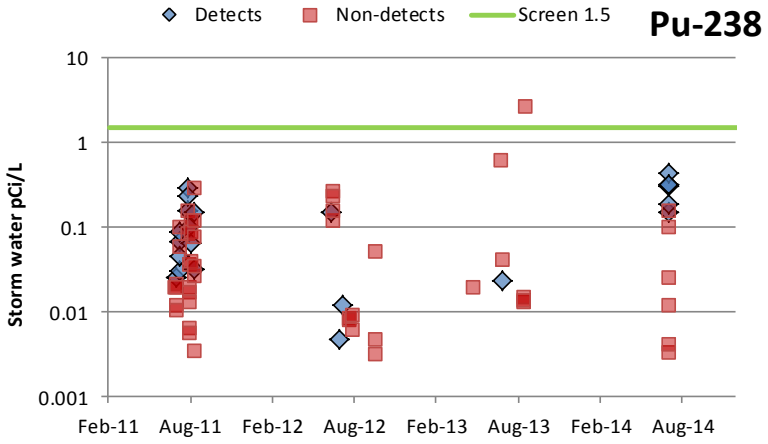

The graph for Pu-238 showed that there were no exceedances of the NMWQCC screening value (1.5 pCi/L). The time plot also indicates that the quality of the data was not satisfactory for 2013 because the non-detect values were very high. The detection limits of non-detects were in the range of

0 – 2.69 pCi/L. There were two detected values from the filtered samples on 9/7/2011 of 0.0091 pCi/L and 0.014 pCi/L, indicative of the metal's low solubility and preferential transport via suspended sediment.

Figure 34. Time plot for Am-241.

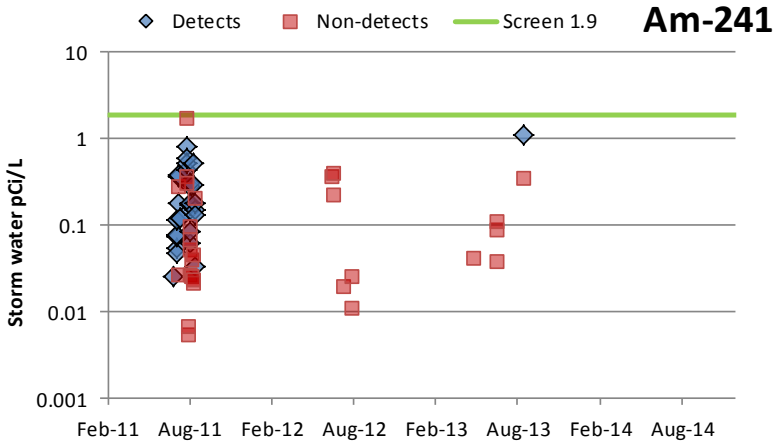

The graph for Am-241 showed that there were no exceedances of the NMWQCC screening value (1.9 pCi/L). The time plot also indicates that the quality of the data was not satisfactory for 2011, 2012, and 2013 because the non-detect values were very high. The detection limits of non-detects were in the range of negative values to 1.73 pCi/L. There were only two detected values from the filtered samples on 9/7/2011 of 0.016 pCi/L and 0.021 pCi/L, indicative of the metal's low solubility and preferential transport via suspended sediment.

Figure 35. Time plot for Cs-137.

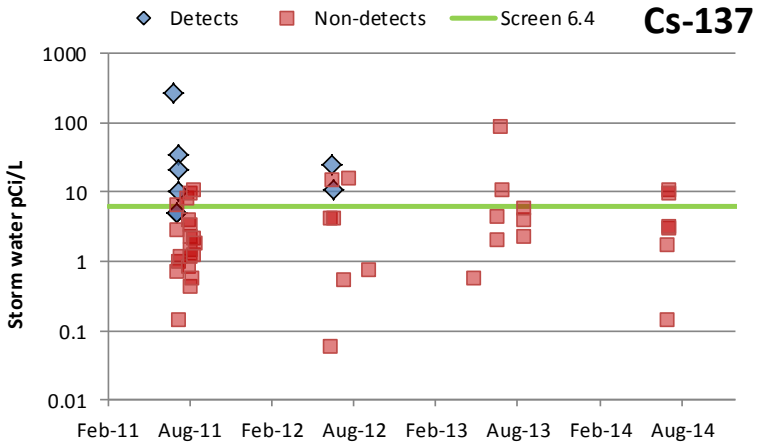

The graph for Cs-137 showed that there were exceedances of the NMWQCC screening value (6.4 pCi/L) in 2011 and 2012. The time plot also indicates that the quality of the data was not satisfactory for the entire monitoring period because the non-detect values were very high. The detection limits of non-detects were in the range of negative values – 90 pCi/L. There was only one detected

value from the filtered samples on 9/12/2013 of 7.97 pCi/L, indicative of the metal's low solubility and preferential transport via suspended sediment.

Figure 36. Time plot for Sr-90, unfiltered.

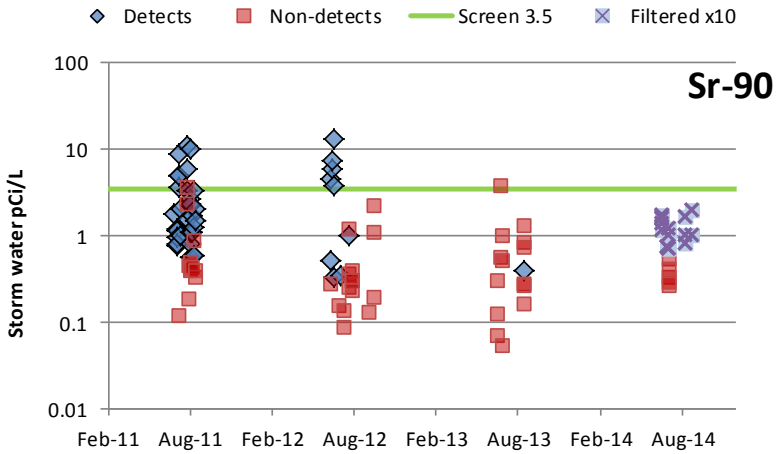

The graph for Sr-90 showed that there were exceedances of the NMWQCC screening value (3.5 pCi/L) in 2011 and 2012. The time plot also indicates that the quality of the data was not satisfactory for 2011, 2012, and 2013 because the non-detect values were very high. The detection limits of non-detects were in the range of negative values to 3.8 pCi/L. The results marked with "Filtered x10" represent the samples that were filtered in the laboratory through a 5µm sieve. The most stable state of radioactive strontium is soluble in water. In the environment, chemical reactions can change the water-soluble stable and radioactive strontium compounds into insoluble forms and vice versa. To investigate its property, we plotted the detected values from the non-filtered and filtered samples on Figure 37.

Figure 37. Time plot for Sr-90, unfiltered and filtered.

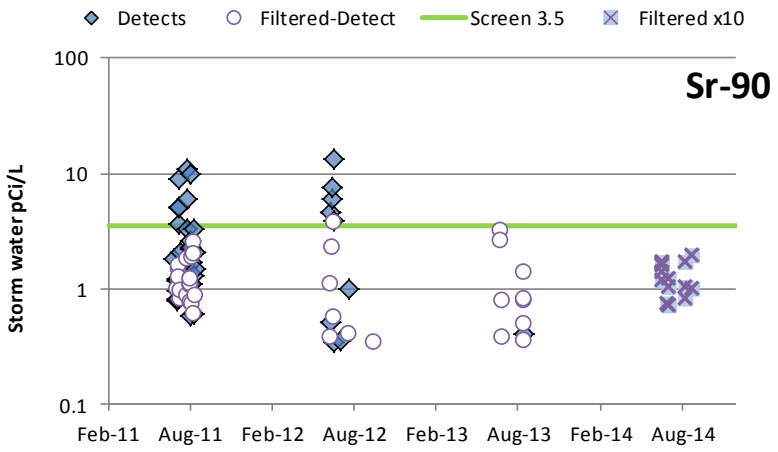

The data indicates that the Sr-90 compound(s) in the RG is very soluble. The filtered results are less than the unfiltered but still of only slightly reduced magnitude. Because of that, we have a couple of exceedances of the NNWQCC screening value for filtered results in 2012 and 2013.

The following figure compares in detail the overall distribution of all detected Sr-90 results from the unfiltered and filtered samples. Although the unfiltered results contain many more outliers than the filtered (Figure 38), the shape of the boxes is very similar although offset by a constant. Note that identified outliers were not presented on boxplots with log-scale.

Figure 38. Box plot comparing all unfiltered and filtered Sr-90 results.

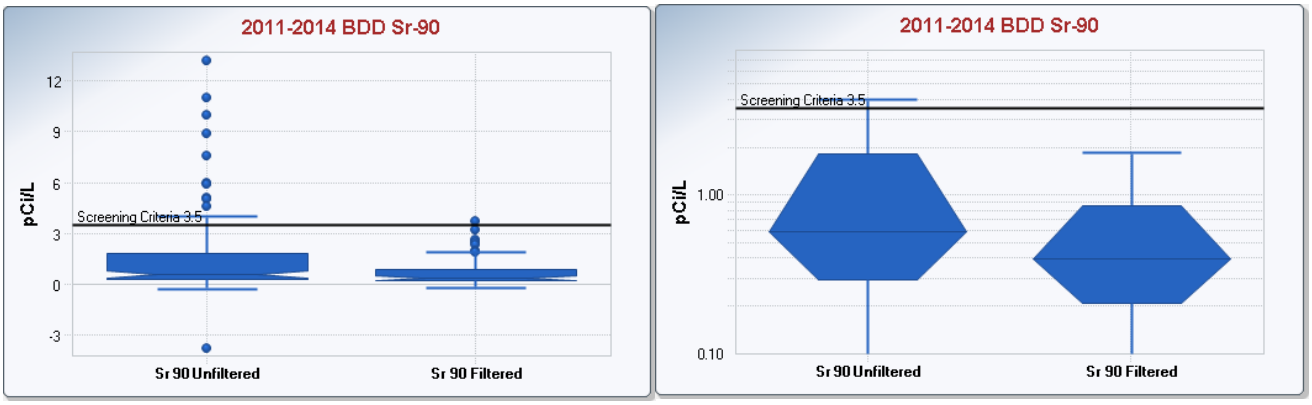

Figure 39. Time plot for Ra-226.

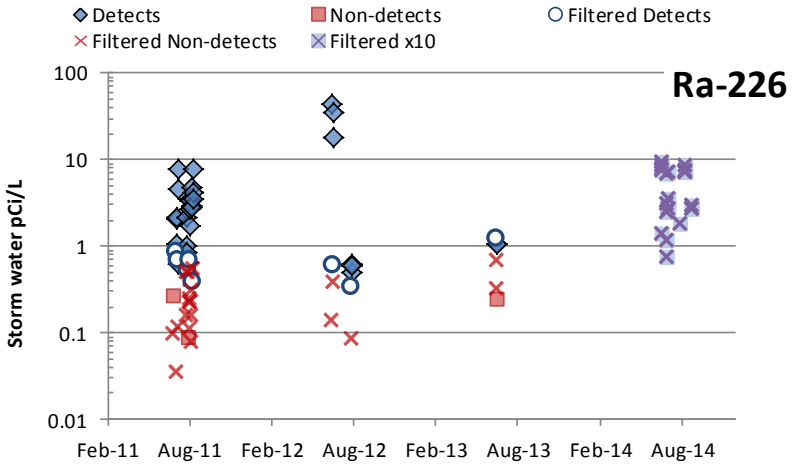

Figure 39 compares the Ra-226 results from the unfiltered and filtered samples. Most of the filtered results are of one order of magnitude less that the unfiltered results, indicative of the metal's low solubility and preferential transport via suspended sediment. There are no NMWQCC standards for Ra-226. The plot indicates that the quality of the analytical data for filtered samples is not satisfactory because less matrix interferences are expected for filtered samples. The graph included the 2014 results from samples that were filtered through a 5µm sieve. Those results were in the same range as the results in 2011, which implies that the Las Conchas fire did not contribute to higher concentrations of Ra-226.

Figure 40. Time plot for Ra-228.

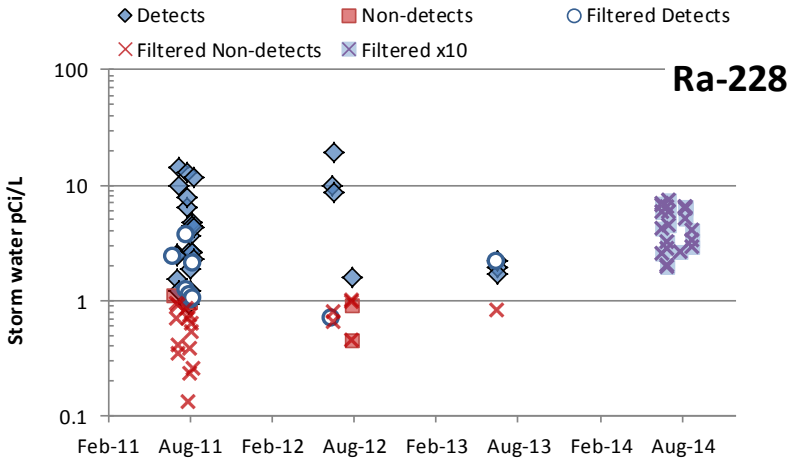

Figure 40 compares the Ra-228 results from unfiltered and filtered samples. Most filtered results are of one order of magnitude less that the unfiltered, indicative of the metal's low solubility and preferential transport via suspended sediment. However, it appears that Ra-228 is more soluble in comparison to Ra-226 because the Ra-228 results from filtered samples were of much higher concentration relative to that of Ra-228 unfiltered. There are no NMWQCC standards for Ra-228. The plot indicates that the quality of the analytical data for filtered samples is not satisfactory because less matrix interferences are expected for filtered samples. There is a NMWQCC standard of 30 ug/L for the sum of unfiltered Ra-226 and Ra-228, which was exceeded once, on 7/11/2012, mainly due to the large values of Ra-228 of 44 pCi/L and 36 pCi/L.

Figure 41. Box plots comparing all Ra-226 and Ra-228 results.

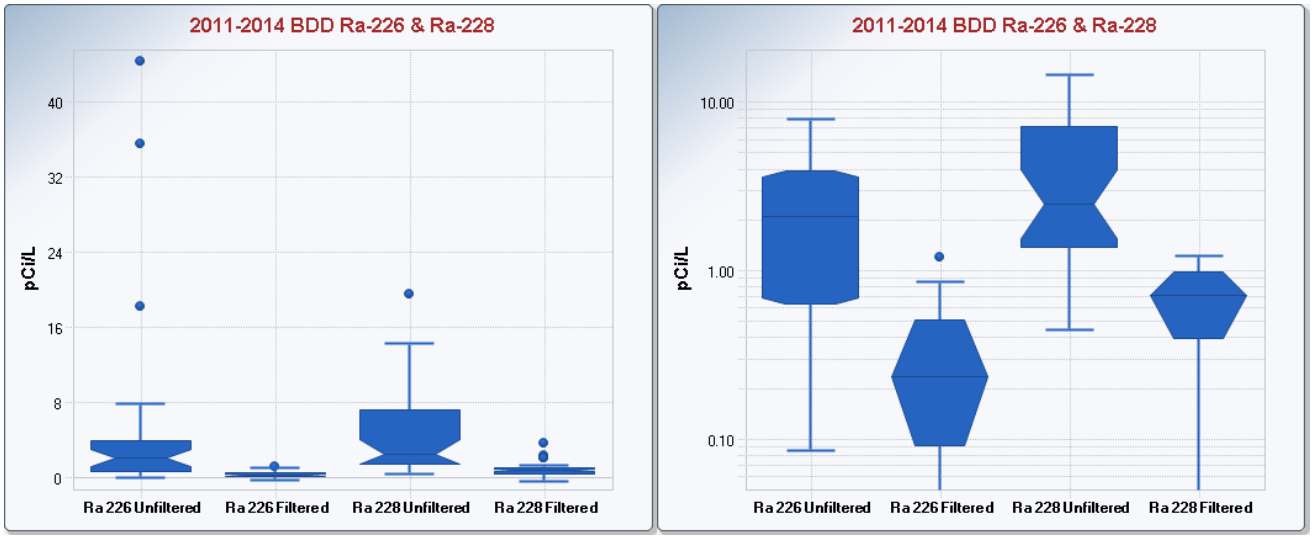

The visual representation of Radium detects by boxplots confirms that even though the values for unfiltered Ra-226 and Ra-228 are compatible in magnitude the filtered Ra-228 are greater than the filtered Ra-226 indicative of its higher water solubility.

Figure 42. Histogram of Ra-228/Ra-226 ratio in storm water and background sediment.

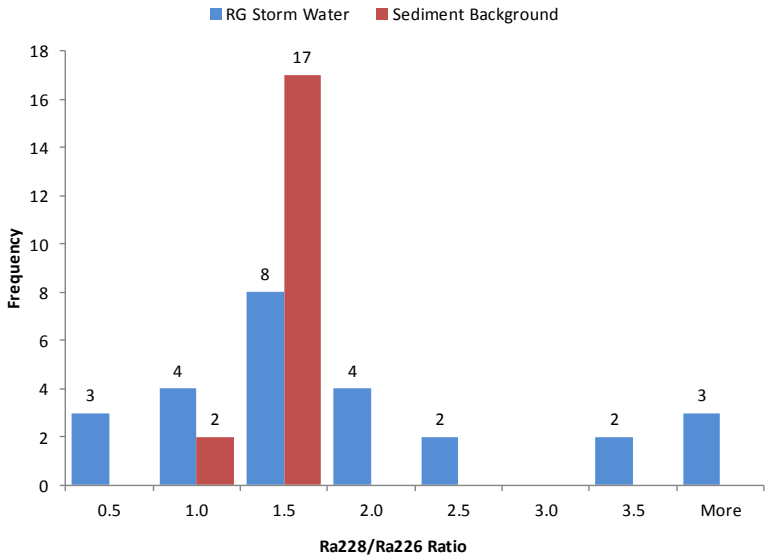

A histogram of the Ra-228 and Ra-226 ratio was plotted together with the ratio of these radionuclides found in background sediment along the RG (from Appendix 5 RG sediment background results). A similar ratio between the sediment and surface water may indicate that this sediment is the likely source of the surface water (Szabo Z, 1997), whereas likely anthropogenic sources of radium, such as phosphate-bearing fertilizers, tend to contain much more Ra-226 than Ra-228.

The histogram of the ratio of radium storm water indicates that there are potential anthropological sources of radium isotopes since ratios greater or smaller than 1.5 (Ra-228/Ra-226 of 1.5 appears to be typical for sediment) were frequently detected. For ratios less than 1.5, the potential sources might be fertilizers used in agricultural communities upgradient from BDD, but for ratios greater than 1.5, no suggested sources were found.

Figure 43. Time plot for U-234, U235, and U-238.

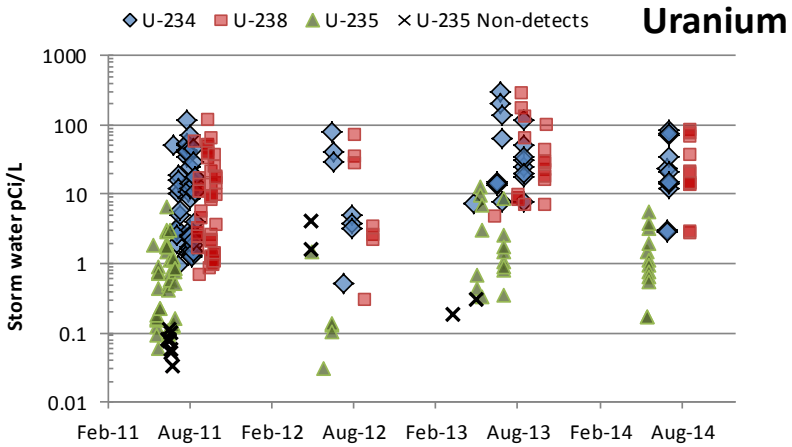

The time plot in Figure 43, presents the annual detected results of uranium isotopes of interest, U-234, U-235, and U-238, time offset for U-235 and U-238 for presentation purpose. All results from unfiltered and filtered samples for U-234 and U-238 were detects, but only a few samples tested for U-235 were non-detects. There are no NMWQCC standards for uranium isotopes. Figure 44 represents the annual distributions of each uranium isotope. Note that identified outliers were not presented on boxplots with log-scale.

Figure 44. Box plots for annual U-234, U-235, and U-238, unfiltered.

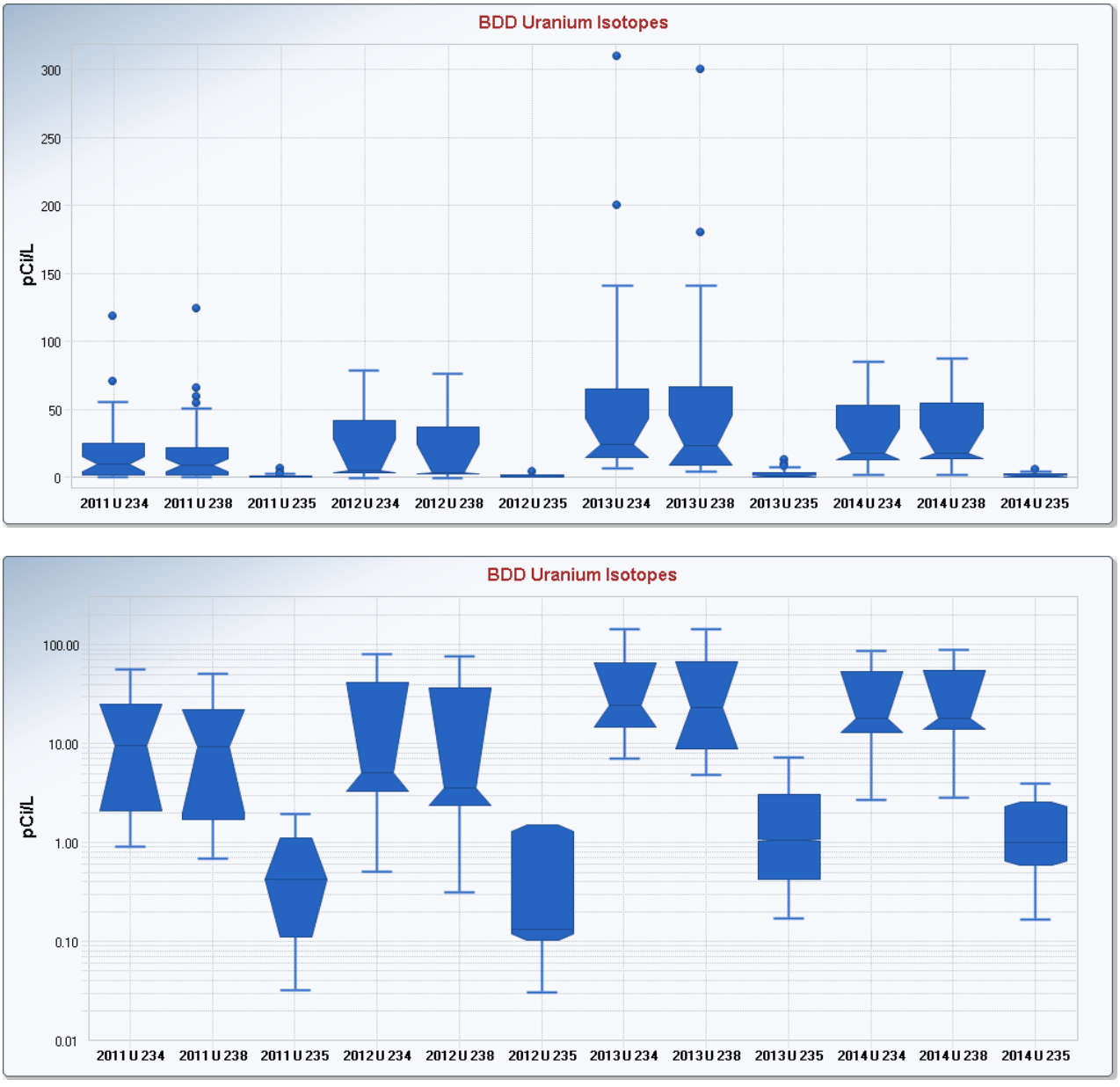

It is noteworthy to mention that the shapes of U-234 and U-238 in 2011, 2012, and 2014 are very similar, and each box of U-238 is slightly below the box of U-234, but the shapes for the same isotopes in 2013 differ in shape between each other, and the range for U-238 for the same year is wider

than U-234. All corresponding values of the distributions, percentiles and central tendencies, were higher in 2013 and 2014 than in 2011, which suggest sources for these isotopes to be upgradient from Otowi Bridge not in the LACW.

The following figures compare the results for unfiltered and filtered samples. For all isotopes the results for filtered samples were less than the unfiltered ones indicative of transport via suspended sediment.

Figure 45. Box plots comparing unfiltered and "standard" filtered U-234, U-235, and U-238 results.

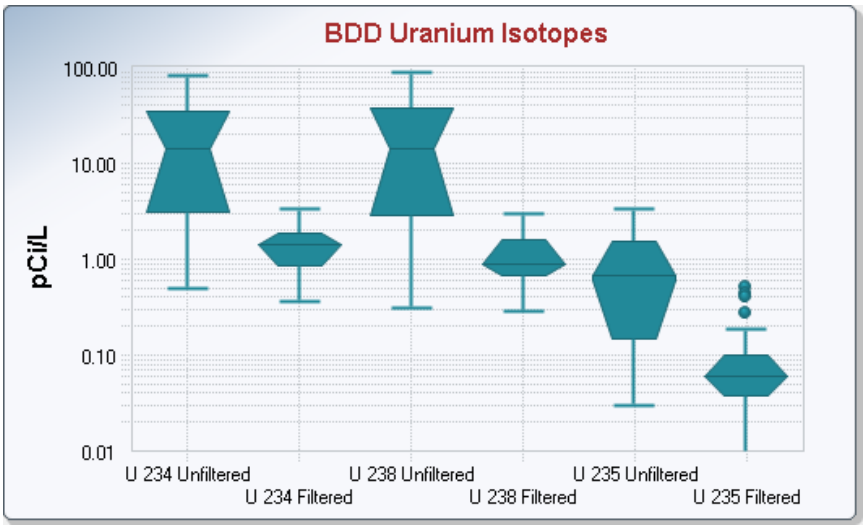

The shape of the U-238 distribution is preserved during filtration but not the shape of U-234, which is expected because the radioactive decay may leave U-234 in a more soluble state than its parent.

Figure 46. Box plots comparing all filtered results for U-234, U-235, and U-238.

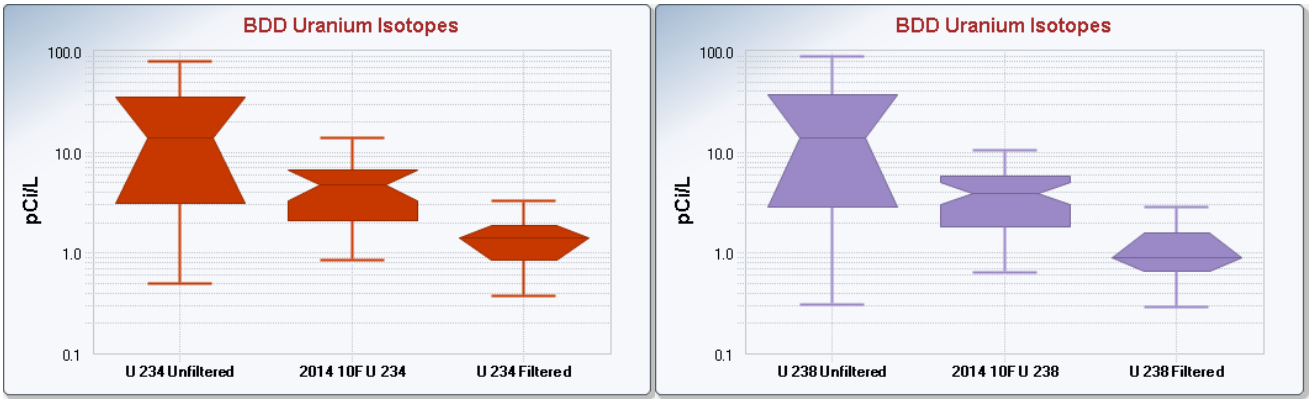

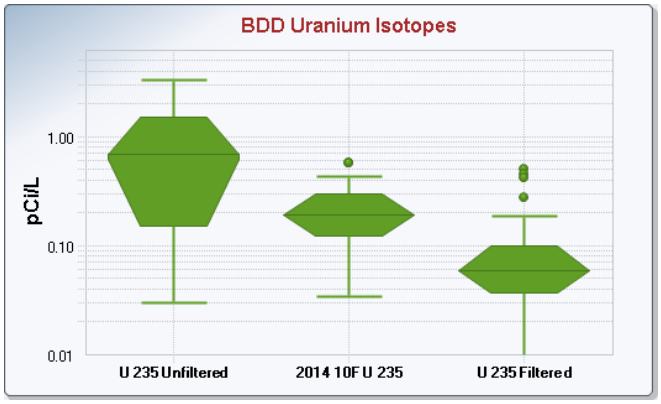

Figure 46 compared all results for the three uranium isotopes, from unfiltered samples, 10F filtered samples and standard filtered samples. The "standard filtered samples" were samples that were filtered through 0.45 µm sieve, while the "10F" were samples that were filtered through a 5µm sieve. The reduced concentrations with reduced particle size are consistent with all isotopes.

Figure 47. Histogram of U-234/U-238 ratio.

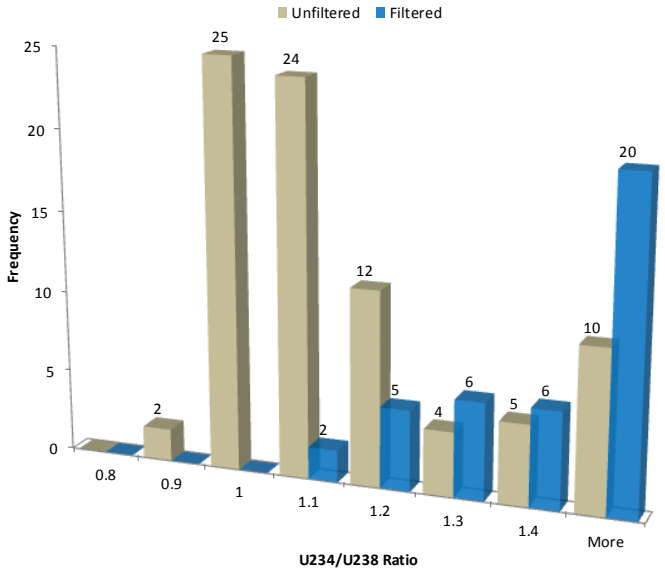

The U-234/U-238 ratio of unfiltered and filtered samples was explored by creating a histogram of the values. The unfiltered samples were clustered around 1 and 1.1 which is an expected result, but the filtered samples ratio shifts to higher values, which confirms higher solubility of U-234 in comparison to U-238.

Figure 48. Histogram of U-234/U-238 ratio in storm water, background sediment, and groundwater.

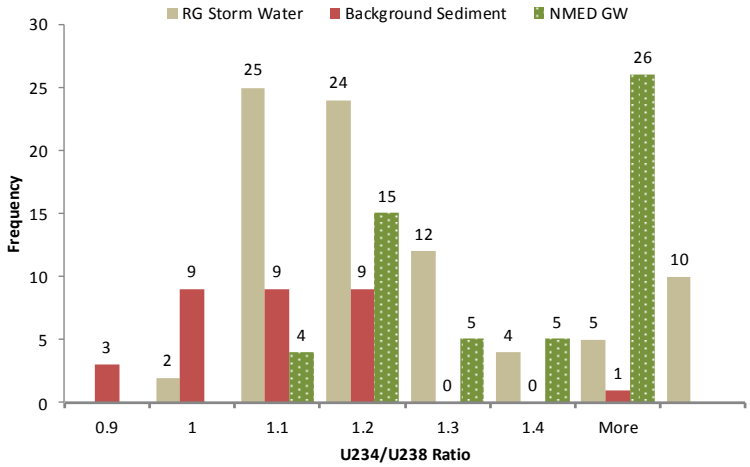

The U-234/U-238 ratio was further explored and compared to the RG sediment background values (from Appendix 5 study) and to the NMED studies of the groundwater in the Espanola basin from 1995 and 2012 (LA-UR-13-25923). The storm water ratios are shifted to higher ratio range in comparison to the sediment ratio which suggests that at least part of this sediment is the most probable source of the storm water but not all. The ratios of greater than 1.3 may indicate a contribution from the LACW, since uranium was discharged in that watershed. The groundwater ratios are shifted toward higher than 1.2 values which is very similar behavior as the filtered samples. It appears that the uranium isotopes in surface water are being stabilized and show similar ratio to the sediments that "produced" them.

Figure 49. Histogram of U-238/U-235 ratio.

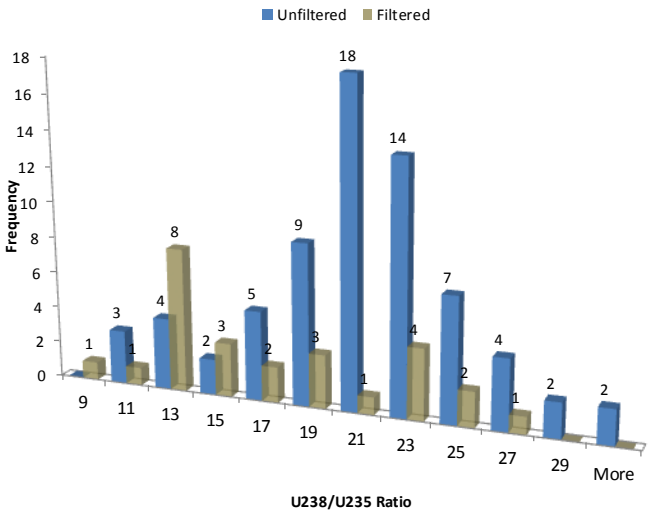

A histogram of the U-238/U-235 ratio for unfiltered and filtered samples was compiled. The results from the unfiltered samples were clustered around the naturally occurring activity ratio of 21, with significant number of ratios below 21, which indicates enriched or mixture of enriched and naturally

occurring uranium (see figure below), expected to be present as a part of the LACW contribution. The ratios from the filtered samples show a different distribution with prevalent low ratio, an indication of enriched uranium.

Figure 50. Type of Uranium in storm water.

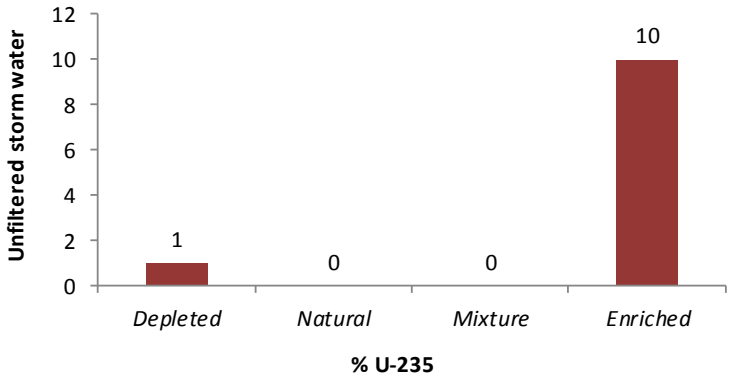

Even though the data was very limited, the percent U-235 was calculated using the total uranium results. The different types of uranium was then categorized based on the percent U-235 in the samples, depleted U for % U-235 of less than 0.45%, natural U for % U-235 of less than 0.86% (large analytical error for U-235 was incorporated in this percent), mixture of U for % U-235 of less than 1%, and enriched U for % U-235 of greater than 1%. The results from the "detects" indicate a prevalent enriched uranium in the storm water samples.

Figure 51. Histogram of U-238/U-235 ratio in storm water, background sediment, and groundwater.

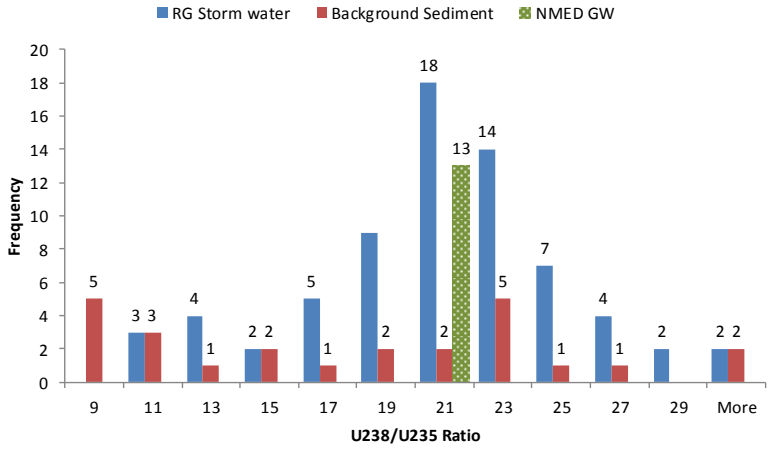

The U-238/U-235 ratio was further compared to the RG sediment background values (from Appendix 5) and to the NMED studies of the groundwater in the Espanola basin from 2012 (LA-UR-13-25923). While the storm water distribution is well defined and bell-shaped, the results from the sediment ratios are not sufficient to exhibit any particular distribution, therefore, conclusion cannot

be made about the storm water and sediment relationship. The groundwater ratios are concentrated in the 21.57 to 21.75 pCi/L range and do not exhibit similarity with the results from the filtered samples.

Figure 52. Time plot for gross alpha and gross beta, unfiltered.

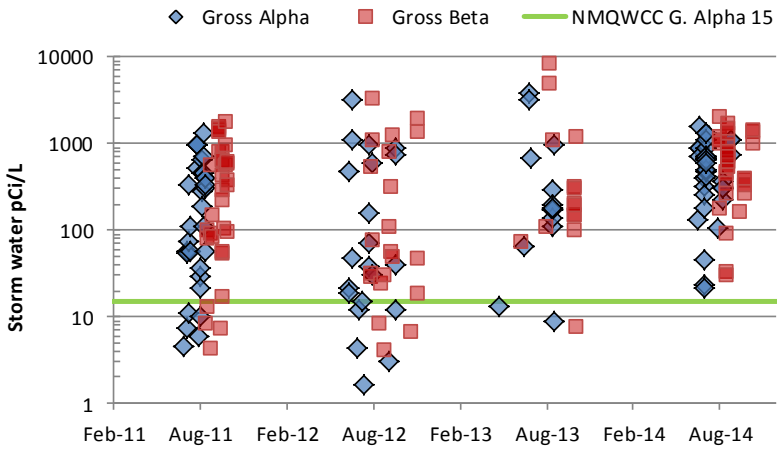

The time plot in Figure 52, presents the annual detects of both, unfiltered gross alpha and beta, time offset for gross beta for presentation purpose. All unfiltered samples were detects, and 50% of the filtered were non-detects. There are no NMWQCC standards for gross beta, but the standard of 15 pCi/L for gross alpha was exceeded on a regular basis. Figure 53 represents the annual distributions of gross alpha and gross beta. Note that identified outliers were not presented on boxplots with log-scale.

Figure 53. Box plots for annual gross alpha and gross beta, unfiltered.

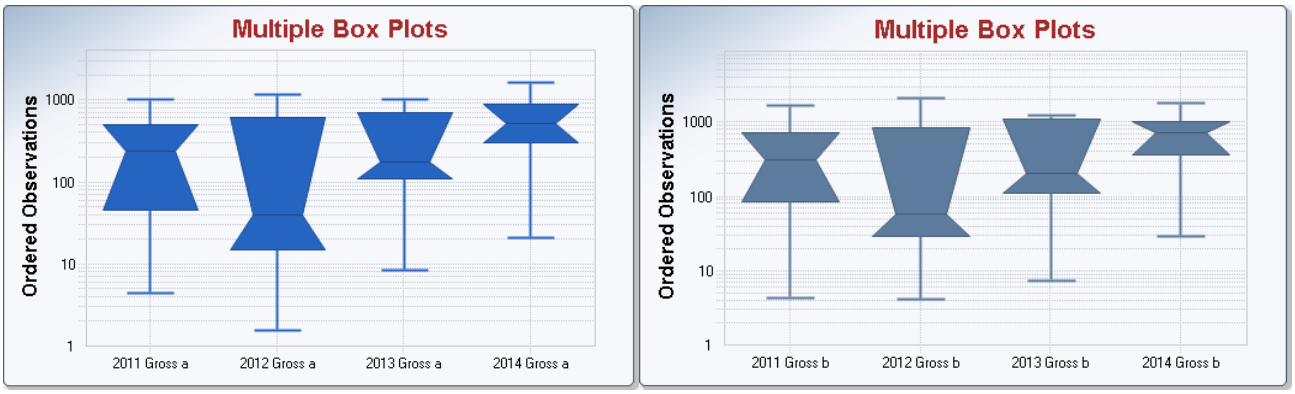

The most interesting fact from the figures is that the shapes of gross alpha and beta were very similar every year, suggesting identical source(s).

Figure 54 and Figure 55 display comparison of the results for the filtered samples of gross alpha and gross beta. The concentrations of the filtered samples were reduced up to two orders of magnitude in comparison to unfiltered, indicative of low solubility constituents, and preferential transport via suspended sediment.

Figure 54. Time plot comparing unfiltered and filtered gross alpha.

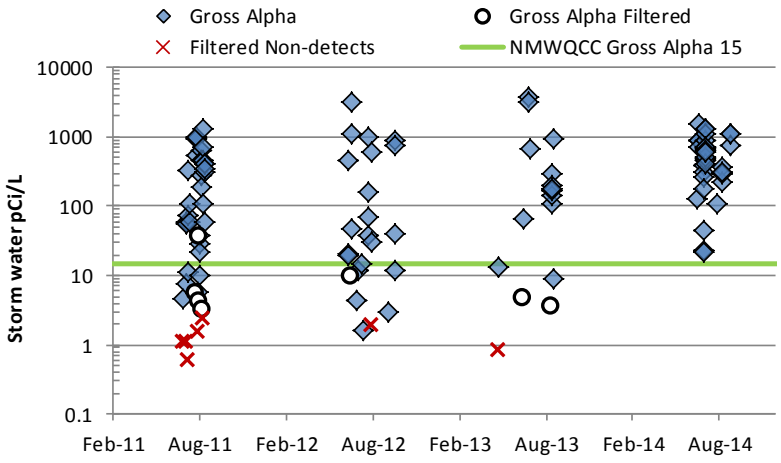

Figure 55. Time plot comparing unfiltered and filtered gross beta.

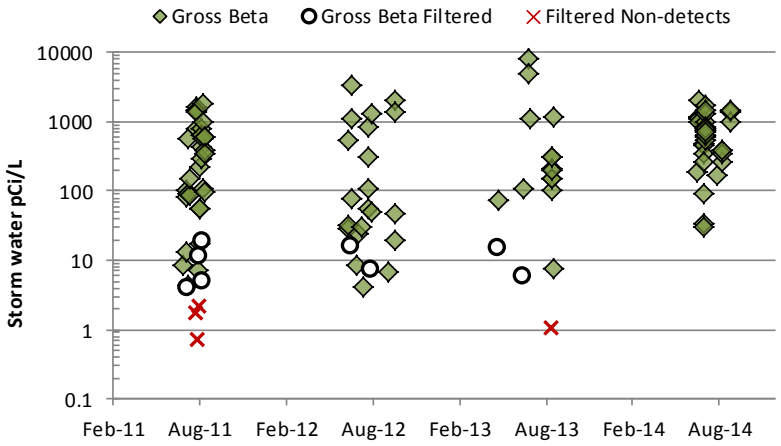

Figure 56. Time plot comparing the unfiltered and filtered gross gamma.

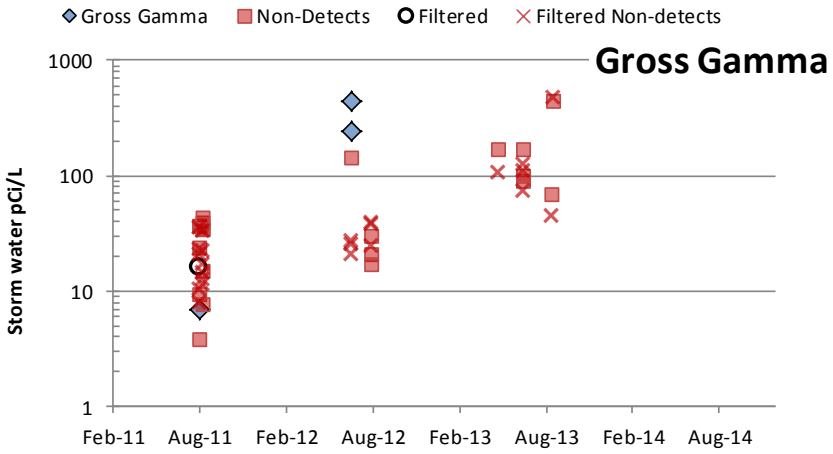

The majority of the gross gamma results presented on Figure 56 were non-detects which demonstrates data of unsatisfactory quality. No conclusions could be drawn from the results.

VII.2.b Sediment Transport of Radionuclides

In this section we present the concentrations of radionuclides vs the suspended sediment as most radionuclides are transported preferentially via suspended sediment. Non-detect values were not included in the plots. Each graph includes also the sediment background with respect to which we will compare the storm water detections. Any results above the "red" line, would indicate detects above the established RG background values that might be expected. In addition, the results were fitted to a straight line in order to determine the contaminants dependence on the suspended sediment carried with storm water.

We calculated the sediment concentration of the contaminants and we presented a time plot of the measured and calculated sediments concentrations. The calculated sediment concentrations are provided in Attachment 5.

Figure 57. Pu 239/240 in sediment transport.

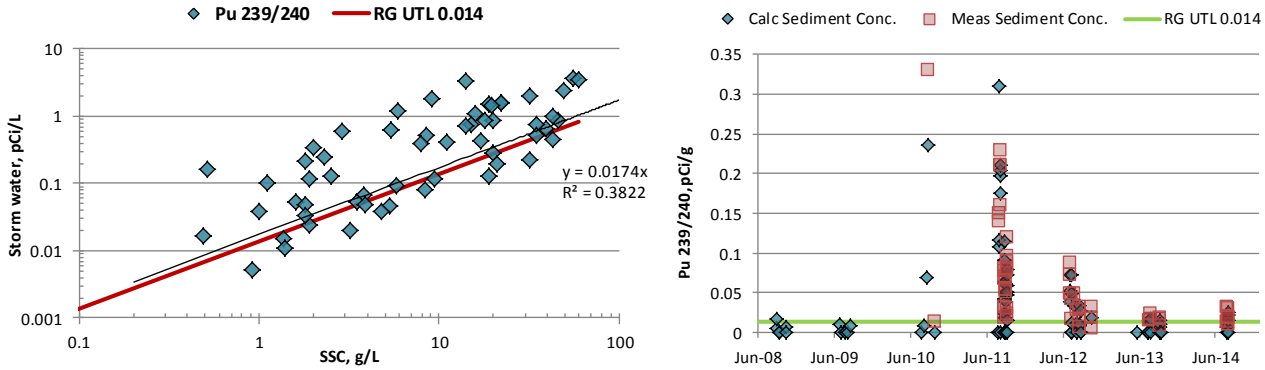

The Pu-239/240 values presented on the graph show more than 50% exceedances of the RG UTL, which is expected considering that LACW is a source of this contaminant and that the PP UTL established by LANL is 0.068 pCi/g. The correlation between the storm water concentrations and SSC is low, which is indicative of anthropological sources of this constituent upgradient from BDD. The plot of sediment concentrations indicates that the exceedances occurred pre- and post-fire, but 2-3 years after the Las Conchas fire the concentrations were the lowest.

Figure 58. Pu 238 in sediment transport.

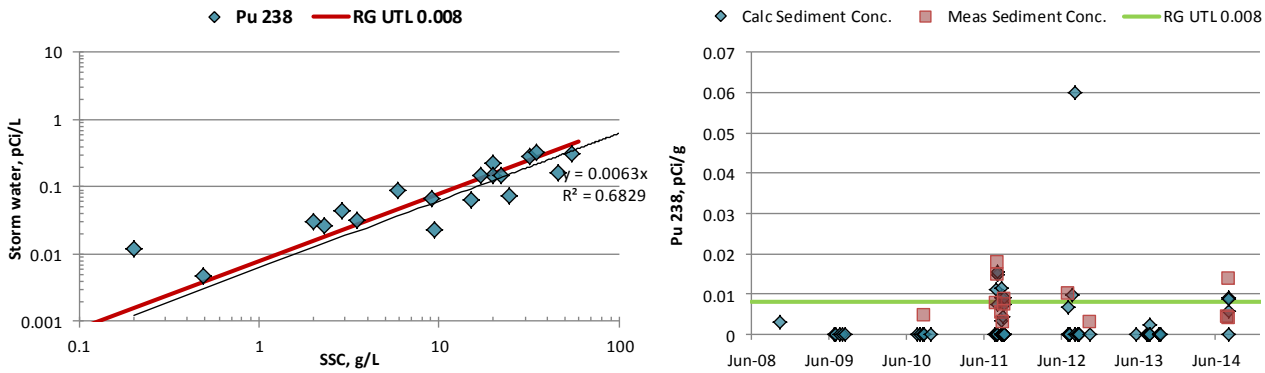

The Pu-238 values presented on the graph show more than 50% exceedances of the RG UTL, which is expected considering that LACW is a source of this contaminant and that the PP UTL established by LANL is 0.008 pCi/g. The correlation between the storm water concentrations and SSC is low, which is indicative of anthropological sources of this constituent upgradient from BDD. The plot of sediment concentrations indicates that the exceedances occurred mostly during and post-fire.

Figure 59. Am 241 in sediment transport.

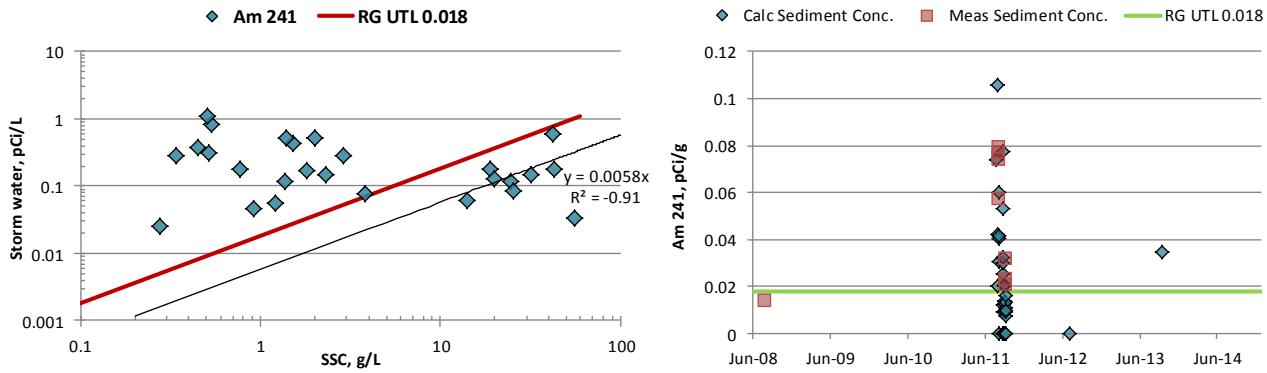

The Am-241 values presented on the graph show large number of exceedances of the RG UTL, which is expected considering that LACW is a source of this contaminant and that the PP UTL established by LANL is 0.040 pCi/g. The correlation between the storm water concentrations and SSC is non-existent, which is indicative of anthropological sources of this constituent upgradient from BDD. The plot of sediment concentrations indicates that the exceedances occurred mostly during the fire, however, we need to note the unsatisfactory quality of the data collected for this contaminant.

Figure 60. Sr 90 in sediment transport.

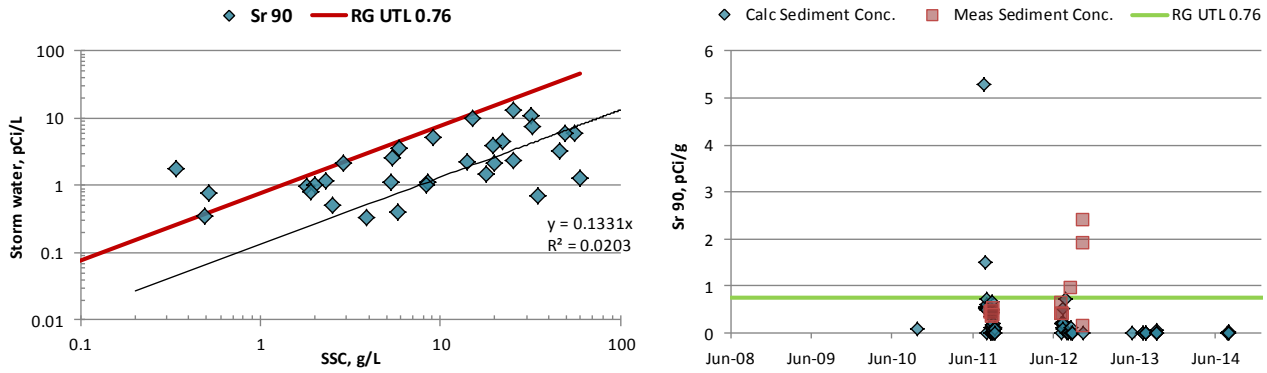

The Sr-90 values presented on the graph show only a couple of exceedances of the RG UTL, which is unexpected considering that LACW is a source of this contaminant and that PP UTL established by LANL is similar to the RG UTL (1.04 pCi/g). The correlation between the storm water concentrations and SSC is non-existent, which is indicative of anthropological sources of this constituent upgradient from BDD. The sediment plot indicates that the exceedances have occurred mostly during the fire and the following year.

Figure 61. Cs 137 storm water vs SSC.

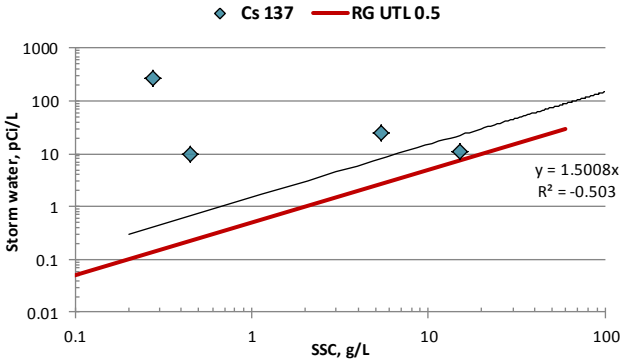

The majority of the results for Cs-137 were non-detects, but of the detected results (4 results) all exceeded the RG UTL, which is expected considering that LACW is a source of this contaminant and that the PP UTL established by LANL is 0.90 pCi/g. The correlation between the storm water concentrations and SSC is non-existent, which is indicative of anthropological sources of this constituent upgradient from BDD.

Figure 62. Ra 226 storm water vs SSC.

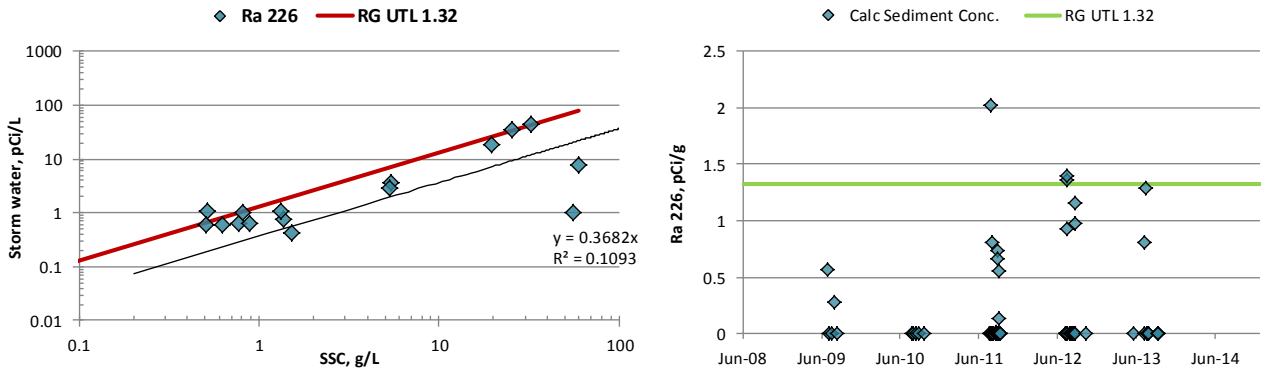

Figure 63. Ra 228 storm water vs SSC.

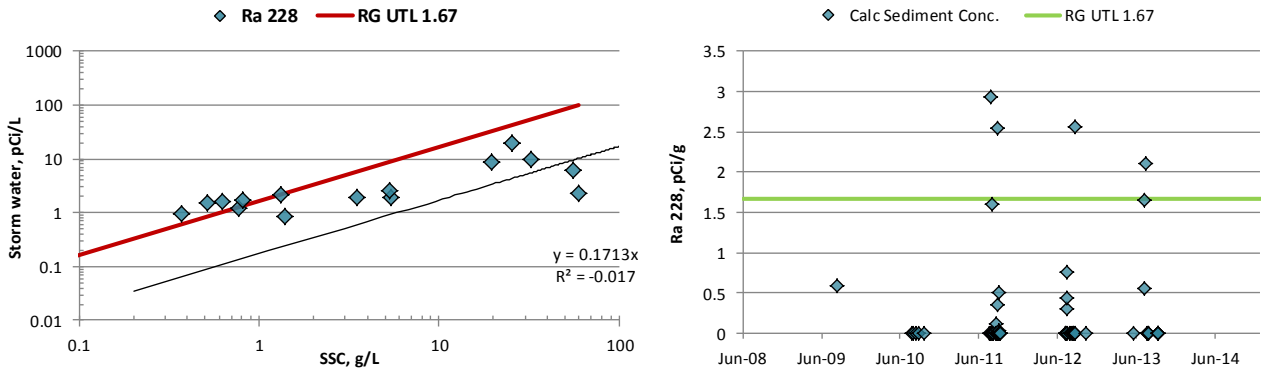

The Ra-226 and Ra-228 values presented on the graphs show only a few exceedances of the RG UTL. The LANL established UTL for these constituents were almost double the RG UTL, 2.59

pCi/g and 2.33 pCi/g, respectively. The correlation between the storm water concentrations and SSC is non-existent, which is indicative of anthropological sources of this constituent upgradient from BDD, which is consistent with the storm water results in Figure 42.

Figure 64. U 234 in sediment transport.

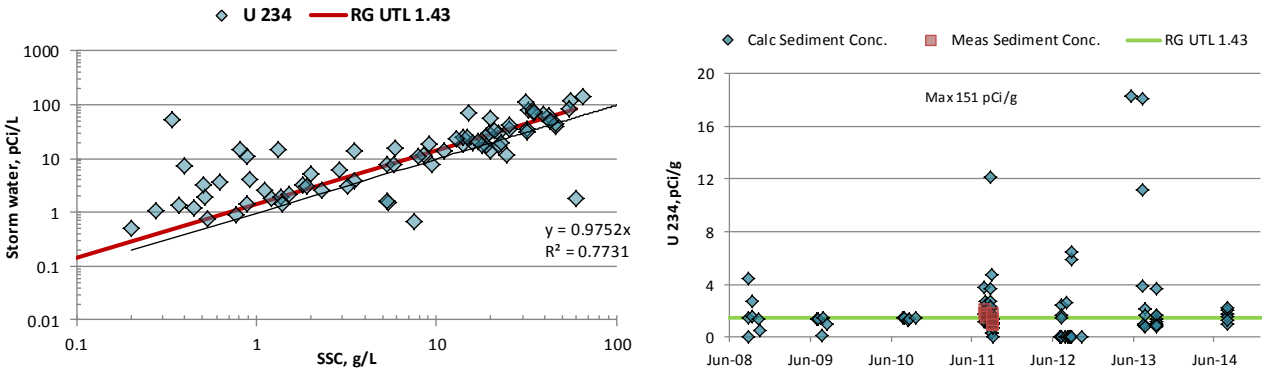

The U-234 values presented on the graph show large number of exceedances of the RG UTL, which is expected considering that LACW is a source of this contaminant (including natural and depleted form of uranium) and that the PP UTL established by LANL is 2.59 pCi/g. The correlation between the storm water concentrations and SSC is very good, which is indicative of naturally occurring tendency of this constituent along the RG. The plot of sediment concentrations indicates that the greatest exceedances have occurred during and post-fire.

Figure 65. U 238 in sediment transport.

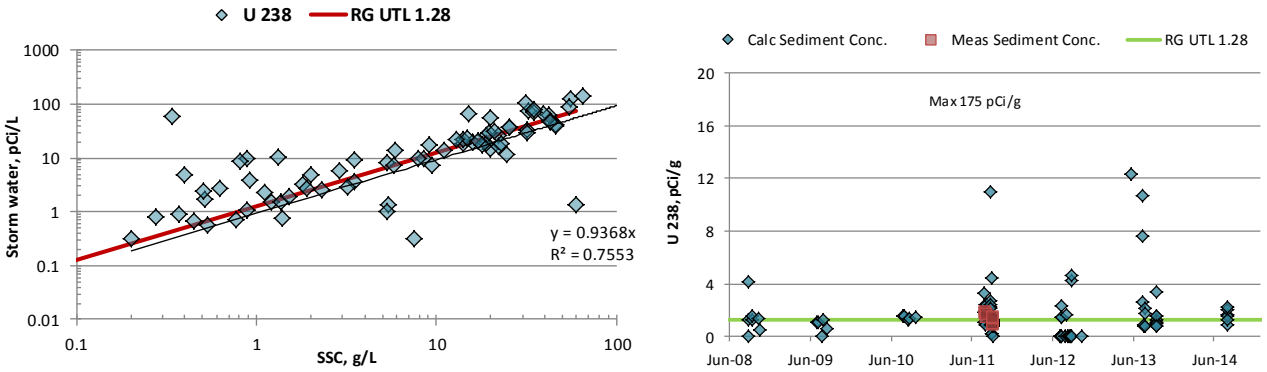

The U-238 values presented on the graph show large number of exceedances of the RG UTL, which is expected considering the fact that LACW is a source of this contaminant (including natural and depleted form of uranium) and that the PP UTL established by LANL is 2.29 pCi/g. The correlation between the storm water concentrations and SSC is very good, which is indicative of naturally occurring tendency of this constituent along the RG. The plot of sediment concentrations indicates that the greatest exceedances have occurred during and post-fire.

Figure 66. U 235 in sediment transport.

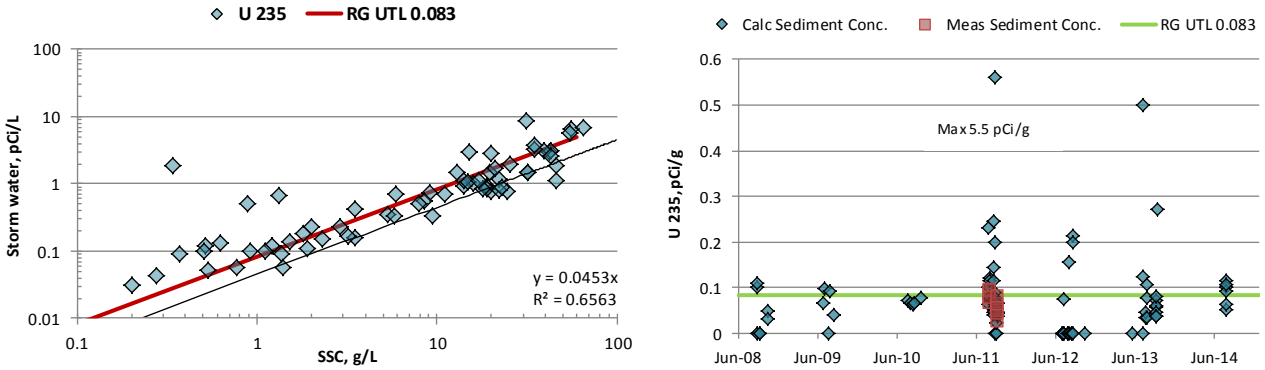

The U-235 values presented on the graph show large number of exceedances of the RG UTL, which is expected considering that LACW is a source of this contaminant (including natural and depleted form of uranium) and that the PP UTL established by LANL is 0.2 pCi/g. The correlation between the storm water concentrations and SSC is not as good as the other uranium isotopes, which is indicative of mixed naturally occurring and anthropogenic sources of this constituent above the BDD. The plot of sediment concentrations indicates that the greatest exceedances have occurred during and post-fire.

VII.2.c Annual Plots and Trends for Inorganics in Storm Water

This section presents the results for inorganic constituents detected in RG at BDD. Two plots were created for each inorganic material when data was available, one that compared the annual mean and 95th percentile for unfiltered samples (detected results only) and another which compared the total unfiltered and filtered samples (detected results only). The applicable NMWQCC standards were plotted for comparison as well. The boxplots compiled in this section used the minimum and maximum concentration for each set as plotted by the low and high whisker, respectively. The body of the boxplot represents the standard 25th, 50th, and 75th percentiles of each set. The descriptive statistics for all inorganics was included in Attachment 4.

One common feature of all inorganic results was the fact that the available data for 2012 and 2013 was very limited, only 2 and 4 (or 5) samples were taken for analyses, respectively. That fact may play a role into the common trend for these two years. The plots in this section depict the detected values for every year, which further limits the amount of data for 2012 and 2013. Therefore, interpreting the trends presented for 2012 and 2013 may not be representative of the inorganics distribution for these two seasons. However, the 2011 and 2014 data contained sufficient number of samples to represent the inorganic occurrences during those years.

Considering the fact that 2011 Las Conchas fire played very important role in the concentrations of contaminants detected at BDD, we expect to see higher concentrations of constituents during 2011 in comparison to 2014 if the constituent is typically occurring (naturally or anthropologically) for

LACW. If the concentrations of a constituent are compatible throughout the monitoring years, then we can conclude that such constituent has sources above Otowi Bridge (natural or anthropological).

Figure 67. Annual trends and box plots for Al.

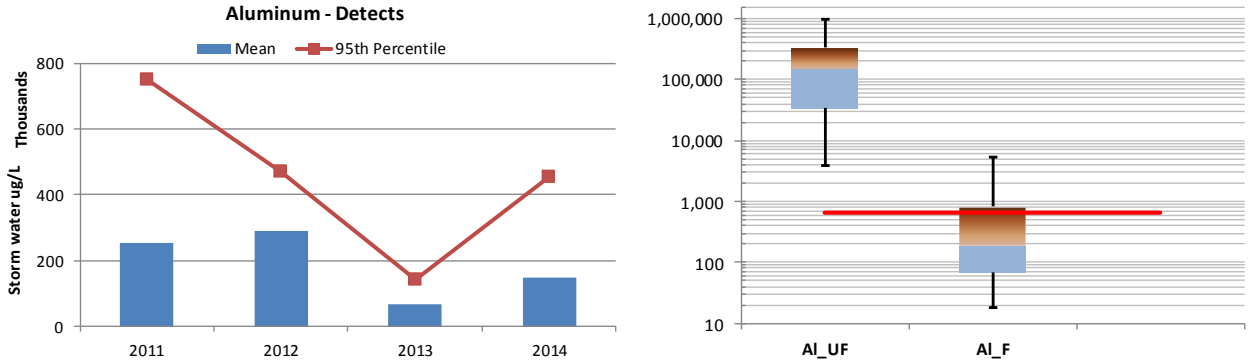

All Al concentrations of unfiltered samples were detects, and 56% of the filtered samples were detects. The concentrations of filtered samples were reduced about two orders of magnitude than the unfiltered indicative of the metal's low solubility and preferential transport via suspended sediment. The concentrations of filtered samples exceeded 11 times the NMQWCC standard for Al (658 ug/L). The mean value and 95th percentile were the highest in 2011, which is expected since Al has been identified as a naturally occurring metal in LACW.

Figure 68. Annual trends for Sb.

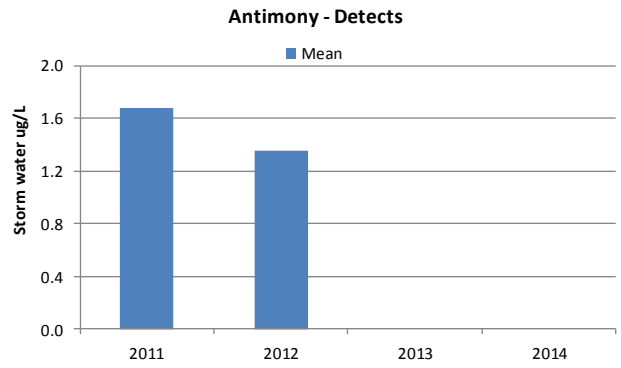

Only 8% of the Sb concentrations of unfiltered samples were detects, and all concentrations of the filtered samples were non-detect. The concentrations of filtered and unfiltered samples could not be compared due to large number of non-detects. There were no exceedances of the NMWQCC standard (Sb 640 ug/L) for filtered samples.

Figure 69. Annual trends and box plots for As.

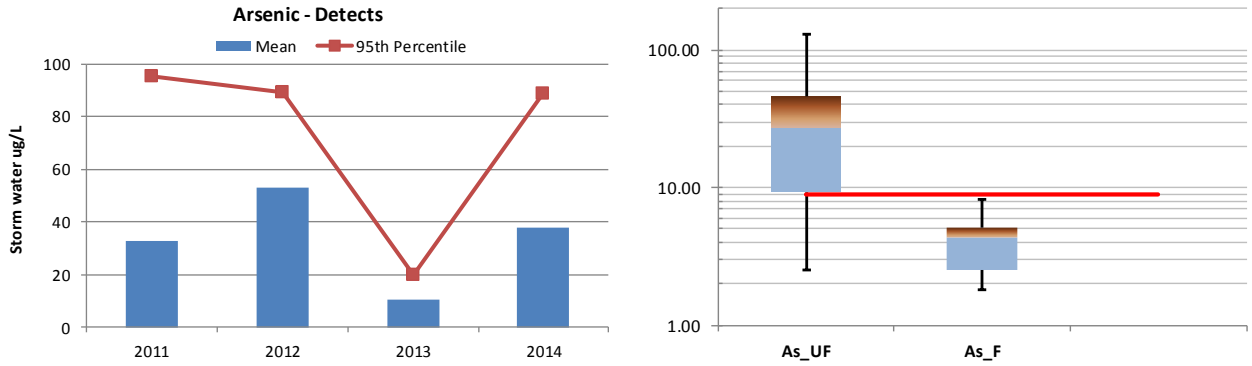

All As concentrations of unfiltered samples for were detects, and 59% of the filtered samples were detects. The concentrations of filtered samples were reduced about one order of magnitude than the unfiltered indicative of metal's some water solubility, but still preferential transport via suspended sediment. There were no exceedances of the NMWQCC standard (As 9 ug/L) for filtered samples. The mean concentration and 95th percentile were compatible in 2011 and 2014, which may indicate naturally occurring sources along the RG.

Figure 70. Annual trends and box plots for Ba.

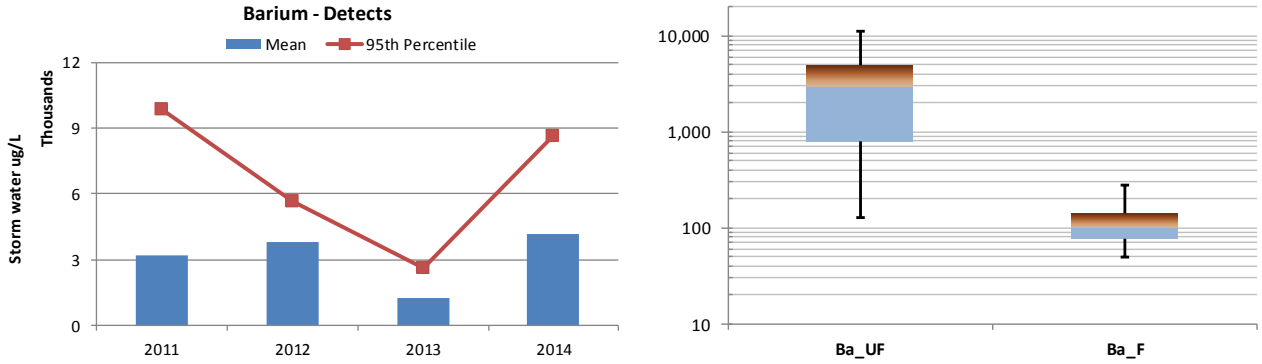

All Ba concentrations of unfiltered and filtered samples were detects. The concentrations of filtered samples were reduced about two orders of magnitude than the unfiltered indicative of the metal's low solubility and preferential transport via suspended sediment. There are no NMQWCC standards for Ba. The mean concentration and 95th percentile were compatible in 2011 and 2014, however the highest values occurred in 2011 which is expected result since Ba concentrations are elevated in ash.

Figure 71. Annual trends and box plots for Be.

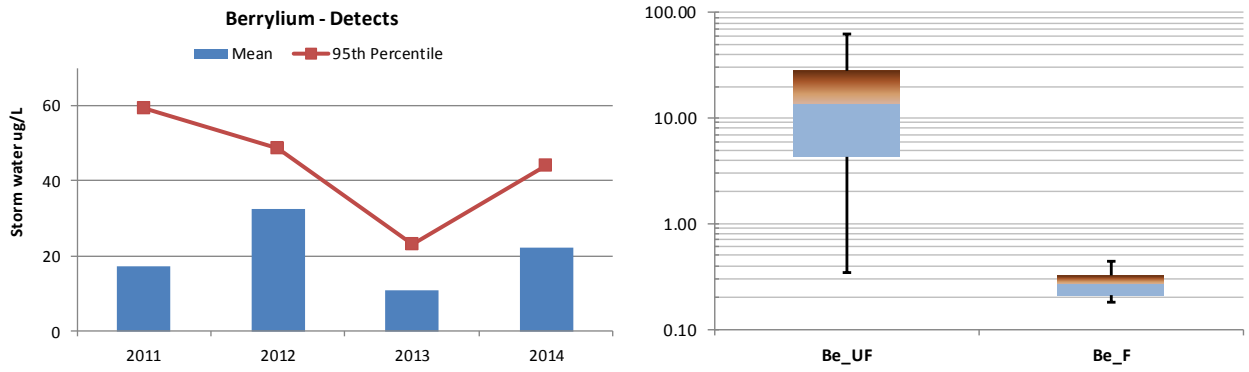

98% of the Be concentrations of unfiltered samples were detects, and 32% of the filtered samples were detects. The concentrations of filtered samples were reduced about two orders of magnitude than the unfiltered, indicative of the metal's low solubility and preferential transport via suspended sediment. There are no NMQWCC standards for Be. The mean concentrations were compatible in 2011 and 2014, however the highest values occurred in 2011 and 2012 which is expected since Be has been identified as a naturally occurring metal in LACW.

Figure 72. Annual trends and box plots for B.

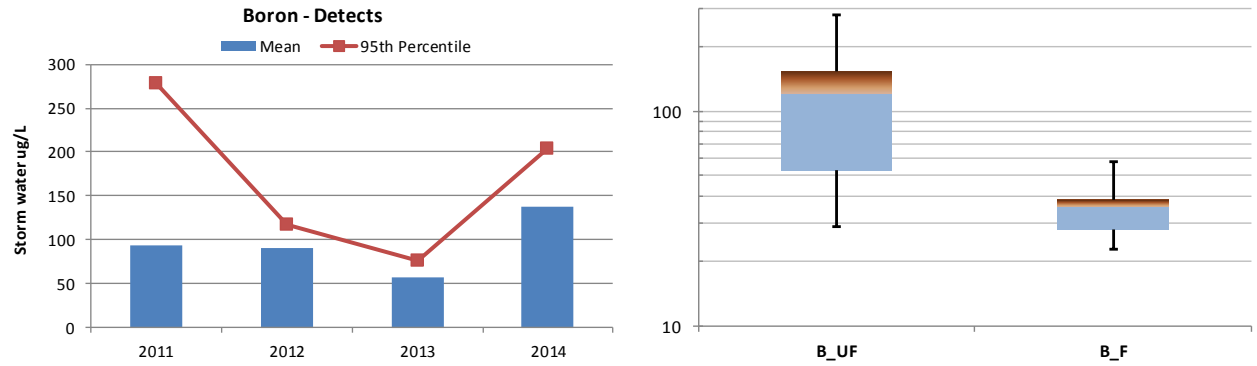

All B concentrations of unfiltered and filtered samples for were detects. The concentrations of filtered samples were reduced less than one order of magnitude than the unfiltered, indicative of metal's some water solubility, but still preferential transport via suspended sediment. There were no exceedances of the NMWQCC standard (B 5,000 ug/L) for filtered samples. The mean concentrations were compatible in 2011 and 2014, but the highest values occurred in 2011 storm events.

Figure 73. Annual trends and box plots for Cd.

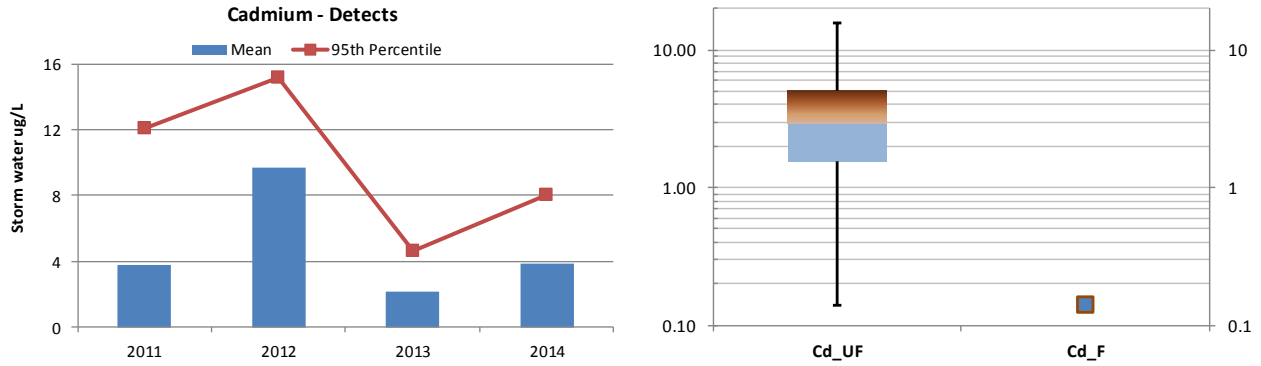

75% of the Cd concentrations of unfiltered samples were detects, and 2% (one result) of the filtered samples were detects. The concentrations of filtered samples were reduced about one order of magnitude than the unfiltered, indicative of metal's some water solubility, but still preferential transport via suspended sediment. There were no exceedances of the NMWQCC standard (Cd 0.59 ug/L) for filtered samples. The mean concentrations were compatible in 2011 and 2014, but the highest values occurred in 2011 and 2012.

Figure 74. Annual trends and box plots for Ca.

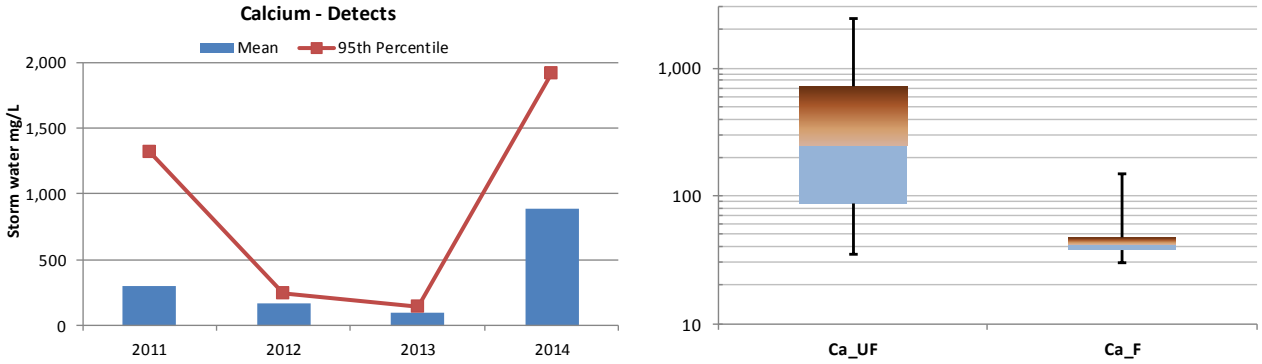

All Ca concentrations of unfiltered and filtered samples were detects. The concentrations of filtered samples were reduced about one order of magnitude than the unfiltered indicative of metal's some water solubility, but still preferential transport via suspended sediment. There are no NMWQCC standards for Ca. The mean concentration and 95th percentile were the highest in 2014.

Figure 75. Annual trends for Cr.

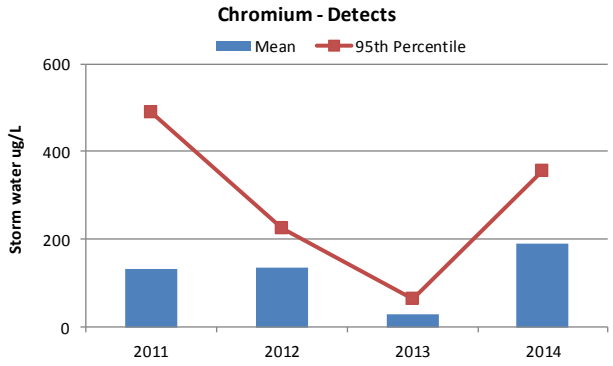

98% of the Cr concentrations of unfiltered samples were detects, and 5% of the filtered samples were detects. The concentrations of filtered samples were reduced with two orders of magnitude than the unfiltered, indicative of metal's low water solubility, and preferential transport via suspended sediment. There were no exceedances of the NMWQCC standard (Cr 1,000 ug/L) for filtered samples. The mean concentration was higher in 2014, but the highest values occurred in 2011.

Figure 76. Annual trends and box plots for Co.

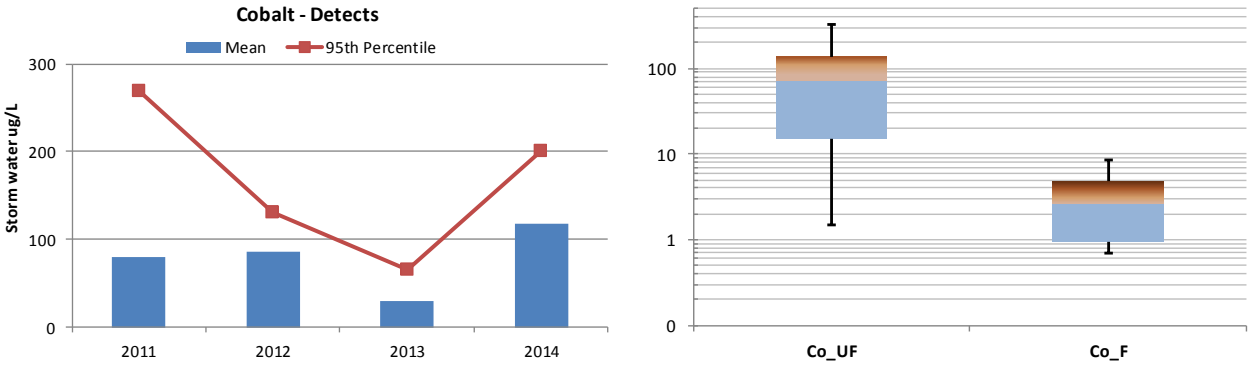

98% of the Co concentrations of unfiltered samples were detects, and 17% of the filtered samples were detects. The concentrations of filtered samples were reduced one order of magnitude than the unfiltered, indicative of metal's some water solubility, but still preferential transport via suspended sediment. There were no exceedances of the NMWQCC standard (Co 1,000 ug/L) for filtered samples. The mean concentration was higher in 2014, but the highest values occurred in 2011.

Figure 77. Annual trends and box plots for Cu.

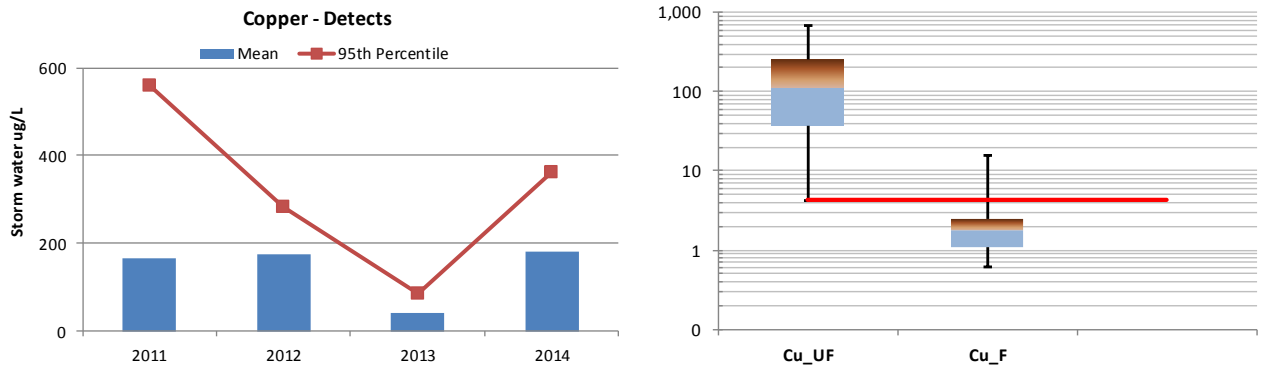

All Cu concentrations of unfiltered samples were detects, and 48% of the filtered samples were detects. The concentrations of filtered samples were reduced with more than one order of magnitude than the unfiltered, indicative of metal's low water solubility and preferential transport via suspended sediment. There were 5 exceedances of the NMWQCC standard (Cu 4.3 ug/L) for filtered samples. The mean concentrations were compatible in 2011 and 2014, but the highest values occurred in 2011.

Total Cyanide. 27% of the concentrations of unfiltered samples for total cyanide were detects, all of them during 2011 when the Las Conchas fire occurred, and all of the filtered samples were non-detects. There were no exceedances of the NMWQCC standard for unfiltered total cyanide (5.2 ug/L), but the detection limit for this constituent was much higher than the standard (DL was 14 ug/L.)

Figure 78. Annual trends and box plots for Fe.

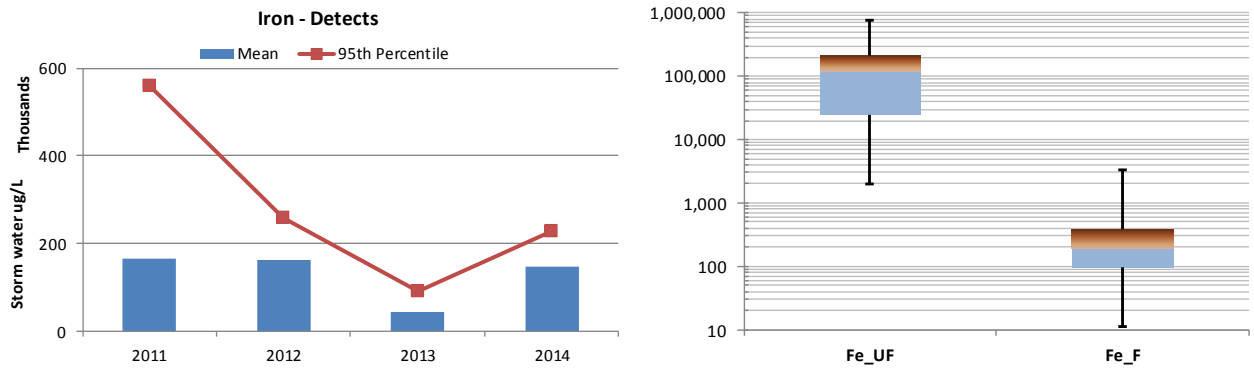

All Fe concentrations of unfiltered samples were detects, and 43% of the filtered samples were detects. The concentrations of filtered samples were reduced three orders of magnitude than the unfiltered, indicative of metal's very low water solubility and preferential transport via suspended sediment. There are no NMWQCC standards for Fe. The mean concentrations were compatible in 2011 and 2014, but the highest values occurred in 2011.

Figure 79. Annual trends and box plots for Pb.

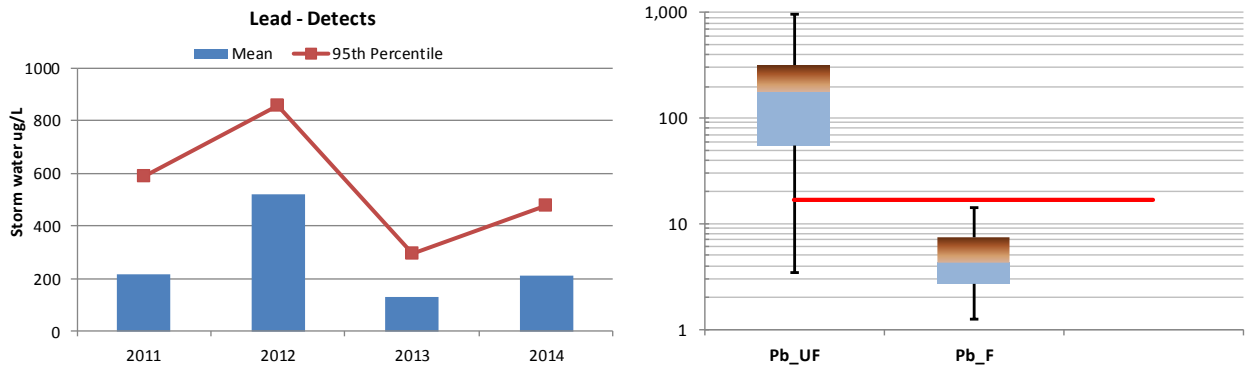

All Pb concentrations of unfiltered samples were detects, and 5% of the filtered samples were detects. The concentrations of filtered samples were reduced with more than one order of magnitude than the unfiltered, indicative of metal's low water solubility and preferential transport via suspended sediment. There were no exceedances of the NMWQCC standard (Pb 17 ug/L) for filtered samples. The mean concentrations in 2011 and 2014 were compatible but the highest results occurred in 2011 and 2012.

Figure 80. Annual trends and box plots for Mg.

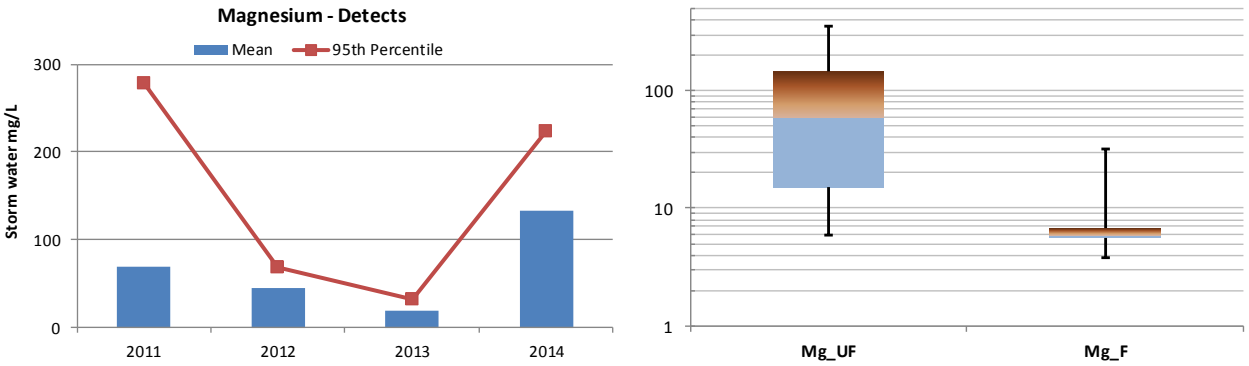

All Mg concentrations of unfiltered and filtered samples were detects. The concentrations of filtered samples were reduced about one order of magnitude than the unfiltered, indicative of metal's some water solubility, but still preferential transport via suspended sediment. An interesting observation is the very tight distribution of the filtered results, while the distribution of unfiltered samples span over an entire order of magnitude. There are no NMWQCC standards for Mg.

Figure 81. Annual trends and box plots for Mn.

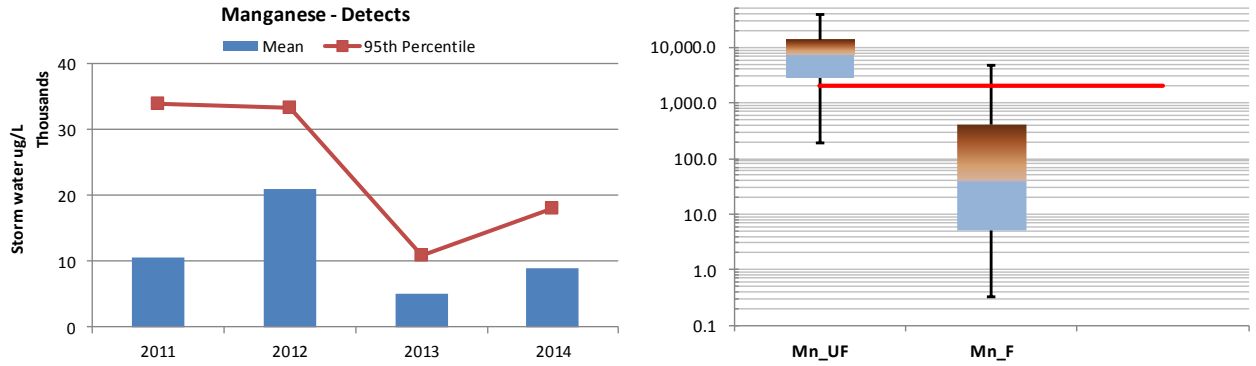

All Mn concentrations of unfiltered samples were detects, and 81% of the filtered samples were detects. The mean concentrations were compatible in 2011 and 2014, but the highest values occurred in 2011. The mean concentration of the filtered samples were reduced about two orders of magnitude than the unfiltered, indicative of metal's low water solubility and preferential transport via suspended sediment. However, the concentrations of filtered samples spanned over large range of values reaching the concentrations of unfiltered samples which indicated that manganese occurs in many different compounds with variable water solubility, poorly soluble (manganese dioxide, manganese tetroxide, manganese carbonate, and manganese sulfide) to soluble (manganese sulfate, manganese chloride, manganese nitrate, permanganate ion). This result suggests anthropogenic sources upgradient from BDD.

The 2011 concentrations of unfiltered samples were elevated in comparison to 2014 which is expected due to the Las Conchas fire. There were 6 exceedances of the NMWQCC standard for filtered Mn (2,000 ug/L) occurring throughout all years of the monitoring period. The distribution of concentrations of filtered samples was plotted below. Except for 2014 (with least number of samples 4), the distributions of the top 25% of the concentrations were very similar from one year to the next, which suggests a constant source of multi-manganese compounds.

Figure 82. Annual distributions for filtered Mn.

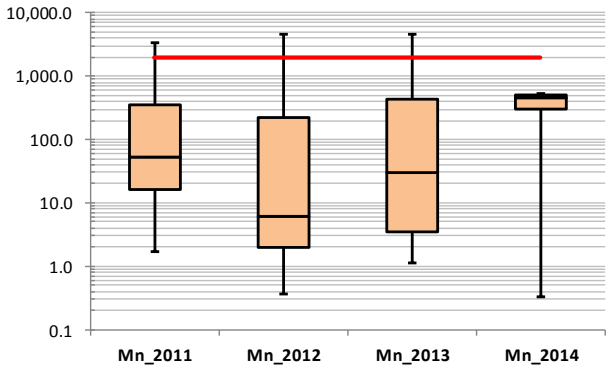

Figure 83. Annual trends for Hg.

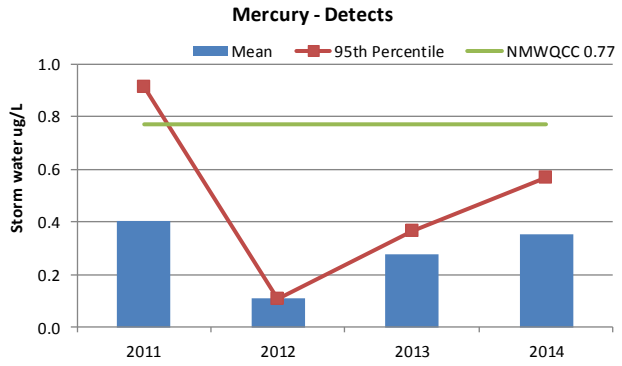

63% of the Hg concentrations of unfiltered samples were detects, and all of the filtered samples were non-detects. The concentrations of filtered samples were reduced about one order of magnitude than the unfiltered, indicative of metal's low water solubility and preferential transport via suspended sediment. There was 1 exceedance of the NMWQCC standard (Hg 0.77 ug/L) for unfiltered samples and no exceedances (Hg 1.4 ug/L) for filtered samples. TA-21 in LACW is a recognized source of Hg, which was confirmed in having higher concentrations in 2011 in comparison to 2014.

Figure 84. Annual trends and box plots for Ni.

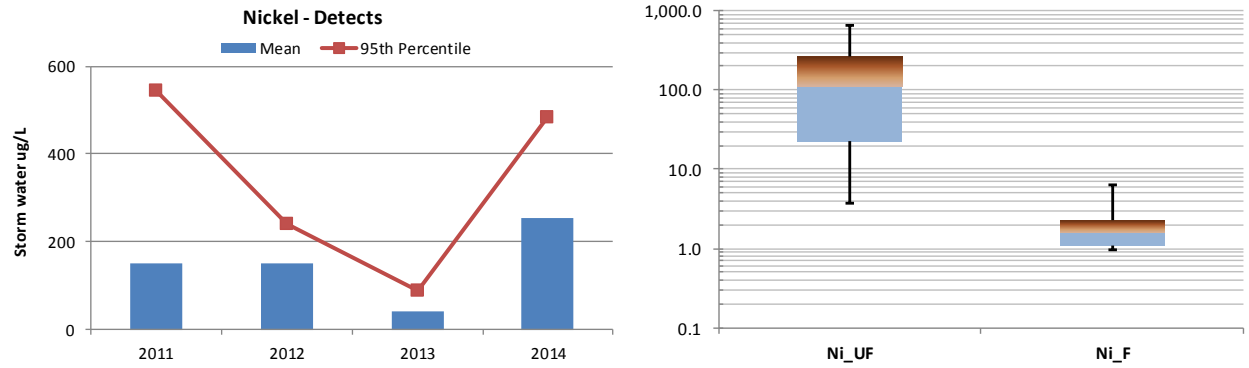

All Ni concentrations of unfiltered samples were detects, and 32% of the filtered samples were detects. The concentrations of filtered samples were reduced about two orders of magnitude than the unfiltered, indicative of metal's low water solubility and preferential transport via suspended sediment. There were no exceedances of the NMWQCC standard (Ni 170 ug/L) for filtered samples. The concentrations in 2011 and 2014 were compatible.

Figure 85. Annual trends and box plots for K.

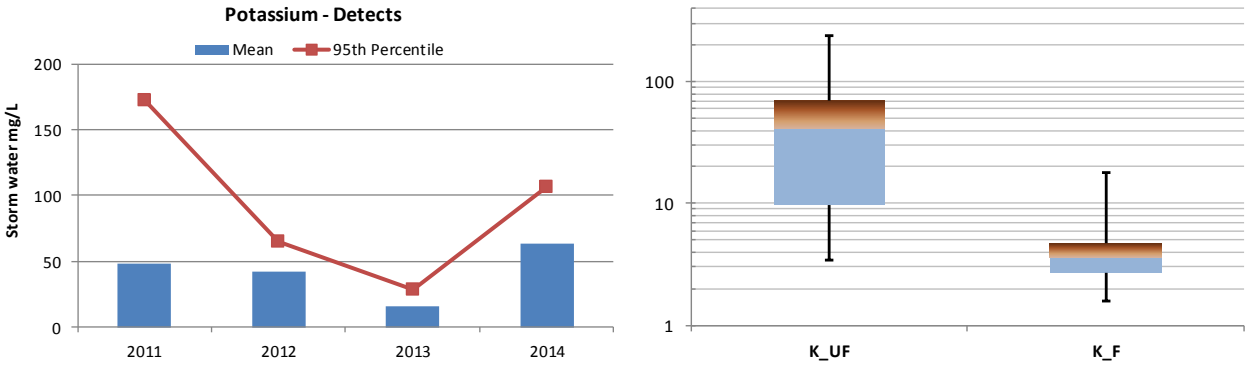

All K concentrations of unfiltered and filtered samples were detects. The concentrations of filtered samples were reduced about one order of magnitude than the unfiltered, indicative of metal's some water solubility, but still preferential transport via suspended sediment. There are no NMWQCC standards for K. The mean concentrations were compatible in 2011 and 2014, but the highest values occurred in 2011.

Figure 86. Annual trends and box plots for Se.

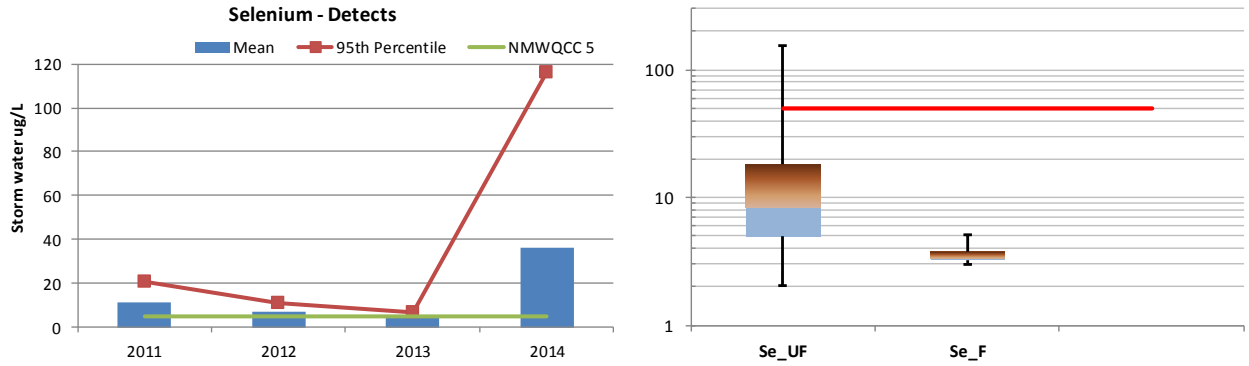

57% of the Se concentrations of unfiltered samples were detects, and 6% of the concentrations of filtered samples were detects. The filtered concentrations had very narrow range of values and its mean value was only 2-3 time less than unfiltered, indicative of metal's good water solubility. There were constant exceedances of the NMWQCC standard (Se 5 ug/L) for unfiltered samples, left graph, and no exceedances (Se 50 ug/L) for filtered samples, right graph. The concentrations in 2014 were a few times higher than in any other monitoring year, for which there is no explanation at this time. This fact does not support LANL statement (LA-UR-12-24822, September 2012) that Las Conchas fire was the source of Se in LACW.

Figure 87. Annual trends for Ag.

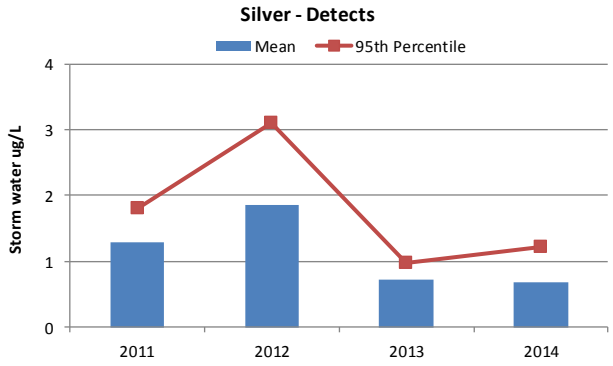

39% of the Ag concentrations of unfiltered samples were detects, and only 2% (one result) of the filtered samples were detects. Since the concentrations of filtered and unfiltered samples, and their detection limits were of the same magnitude, comparison between the filtered and unfiltered samples could not be made. There was 1 exceedance of the NMWQCC standard (Ag 0.41 ug/L) for filtered samples. The highest concentrations occurred in 2011 in comparison to 2014.

Figure 88. Annual trends and box plots for Na.

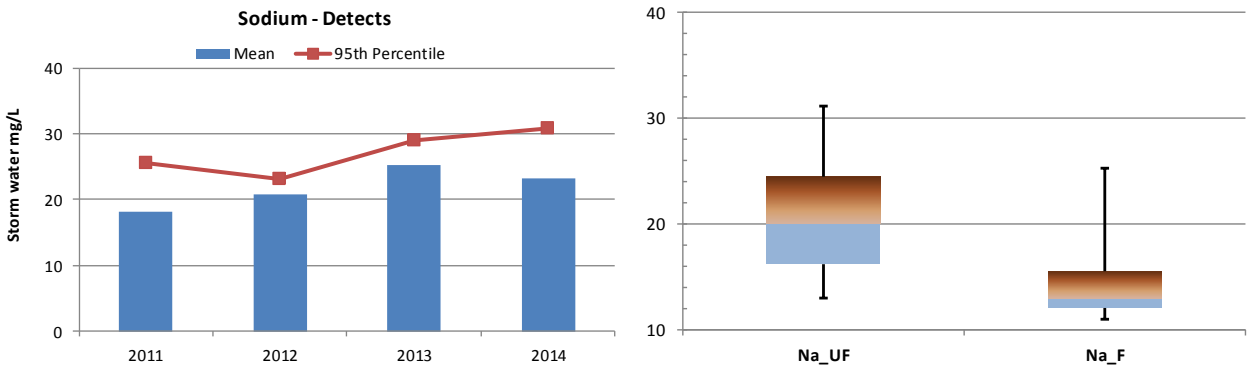

All Na concentrations of unfiltered and filtered samples were detects. The concentrations of filtered samples were only about one half of the unfiltered results, an indication of the high water solubility of this metal. There are no NMWQCC standards for Na. The concentrations of Na throughout the monitoring period were of similar value and thus demonstrate the naturally occurring tendency for this constituent along the RG.

Figure 89. Annual trends and box plots for Tl.

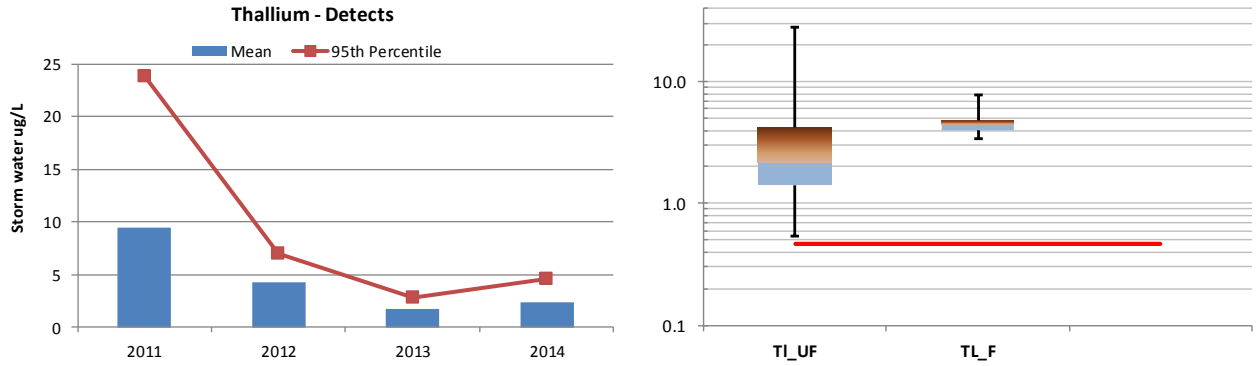

50% of the Tl concentrations of unfiltered samples were detects, and 11% of the filtered samples were detects. The concentrations of filtered samples were higher than its unfiltered counterpart in most occasions, indicative of metal's high water solubility. All concentrations of filtered samples exceeded the NMWQCC standard (Tl 0.47 ug/L) for filtered samples. The concentrations were the highest in 2011 and have progressively declined over the years indicating that LACW might be the potential source of this metal and its high concentrations in 2011.

Figure 90. Annual trends and box plots for U.

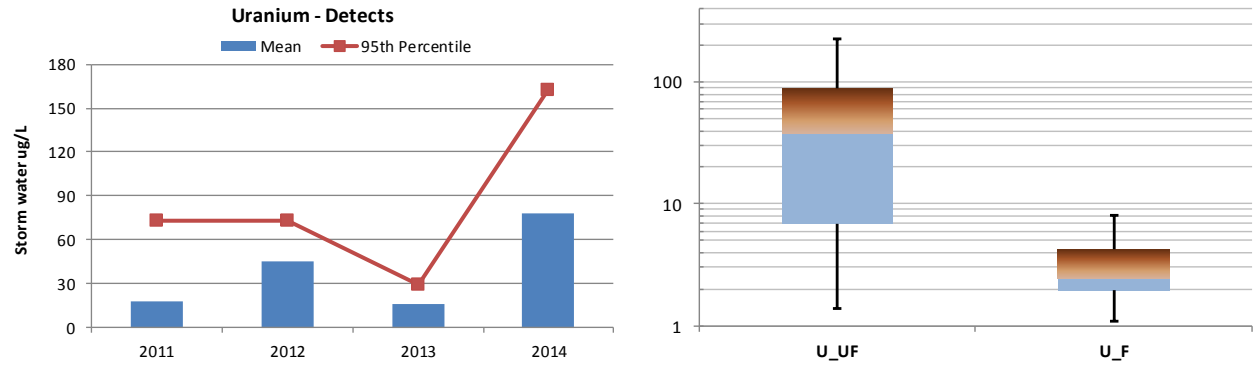

All U concentrations of unfiltered and filtered samples were detects. The concentrations of filtered samples were reduced about one order of magnitude than the unfiltered, indicative of metal's some water solubility, but still preferential transport via suspended sediment. There are no NMWQCC standards for U. The 2014 concentrations of U were much higher than the previous years, probably due to the small sampling size in 2011 (9 samples), 2012 (2 samples), and 2013 (4 samples) which may not be representative of the distribution.

Figure 91. Annual trends and box plots for V.

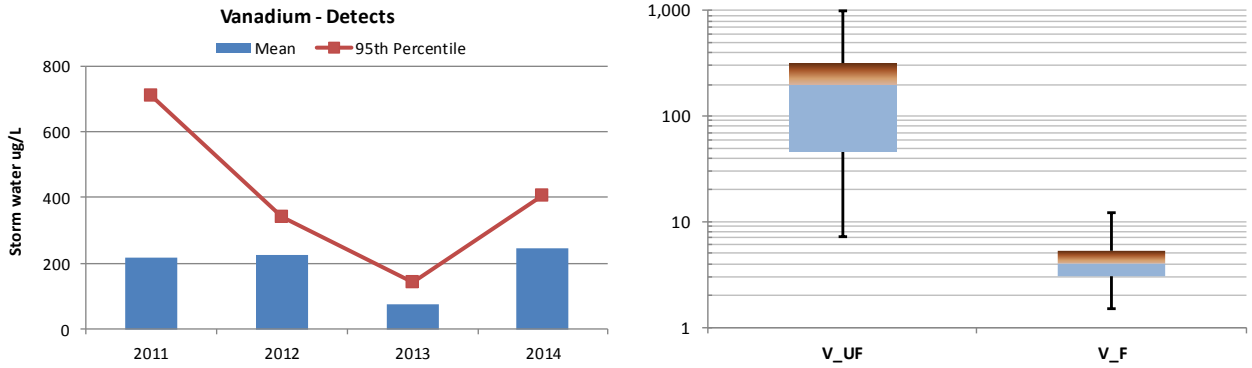

All V concentrations of unfiltered samples were detects, and 97% of the filtered samples were detects. The concentrations of filtered samples were reduced about one order of magnitude than the unfiltered, indicative of metal's some water solubility, but still preferential transport via suspended sediment. There were no exceedances of the NMWQCC standard (V 100 ug/L) for filtered samples. Even though the mean concentrations in 2011 and 2014 were similar, the highest concentrations occurred in 2011.

Figure 92. Annual trends and box plots for Zn.

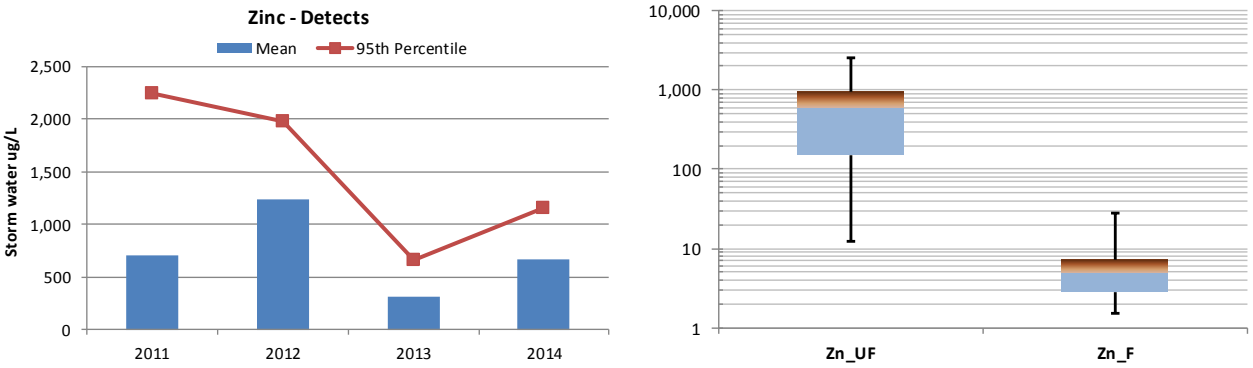

All Zn concentrations of unfiltered samples were detects, and 51% of the filtered samples were detects. The concentrations of filtered samples were reduced about two orders of magnitude than the unfiltered, indicative of metal's low water solubility and preferential transport via suspended sediment. There were no exceedances of the NMWQCC standard (Zn 50 ug/L) for filtered samples. Even though the mean concentrations in 2011 and 2014 were similar, the highest concentrations occurred in 2011.

Figure 93. Time plot of Perchlorate.

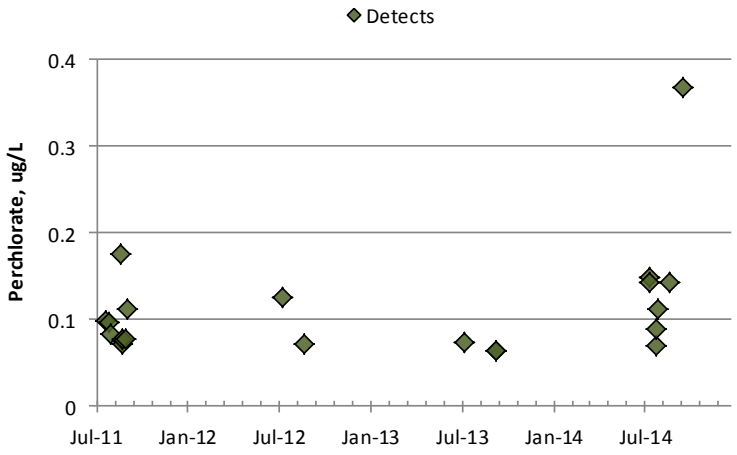

All Perchlorate results were detects. There is no NMWQCC standard for Perchlorate. The values were similar and within the same range throughout the monitoring period, but the highest value of 0.37 ug/L was detected on 9/22/2014.

VII.2.d Significant Storm Events for Inorganics

Each storm event in the RG is unique. At BDD, the concentrations of contaminants, from naturally occurring or anthropological sources, are influenced by sources on the RG above Otowi Bridge, from LACW, or both watersheds. When storm in those two watersheds occurs at a concurrent time, it is hard to distinguish between each watershed contribution. In an attempt to find the predominant contribution (upgradient from Otowi Bridge or LACW), for each sampling event we calculated the relative concentrations in percent (the concentration relative to the maximum concentration) for each inorganic material and plotted them separately by monitoring year. The relative concentrations of 50% or greater (with the exception of Tl and Hg for which results greater than 30% were included) were presented in Table 22. Some inorganics were omitted from the plots. These were Ca, Cu, Fe, Mg, K, and Na.

Figure 94. Relative concentrations of storm water for inorganics 2011.

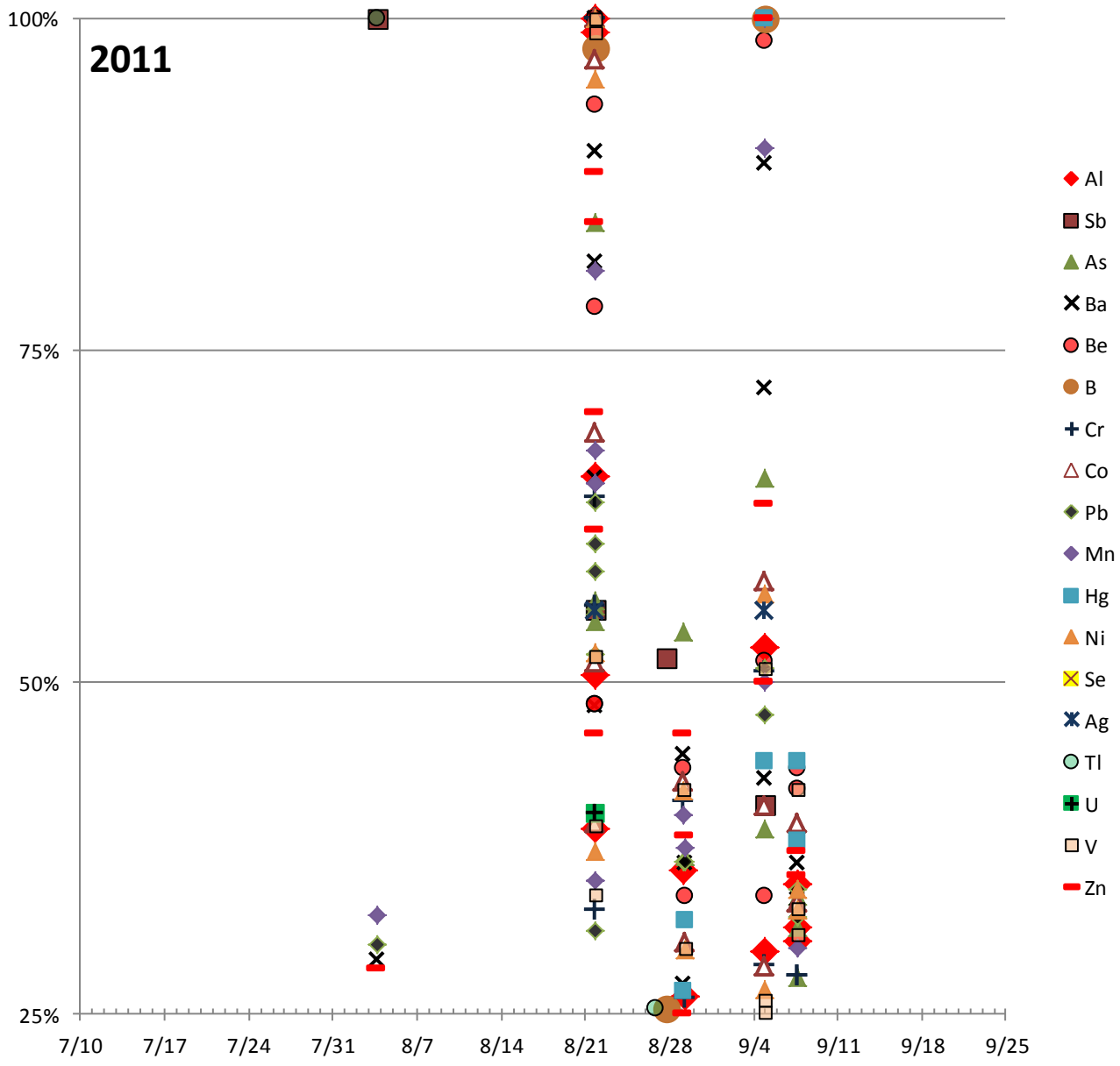

During the sampling event on 8/21/2011 the highest concentrations were detected for most metals. 17 metals achieved their maximum concentrations during this storm. The metals that did not follow this trend were Sb, Ca, Pb, Mn, Na, and Zn. From Table 8 we can see that on this date RG and LACW storm events coincided, with maximum discharges of 2,910 cfs and 610 cfs, respectively. For LACW, such discharge represents very strong event, but for the RG, such event may be characterized as "medium" strength event.

Another significant event with high concentrations of metals occurred on 9/4/2011. The RG and LACW storm events coincided with maximum discharges of 1,140 cfs and 632 cfs, respectively. The metals that achieved their maximum concentrations on that date were Be, B, Pb, Mn, and Zn. On av-

erage, the concentrations during this event were 66% of their maximum values. The difference was that the RG maximum discharge on 9/4/2011 was reduced to almost one half in comparison to 8/21/2011 when the RG discharge was 2,910 cfs.

Figure 95. Relative concentrations of storm water for inorganics 2012.

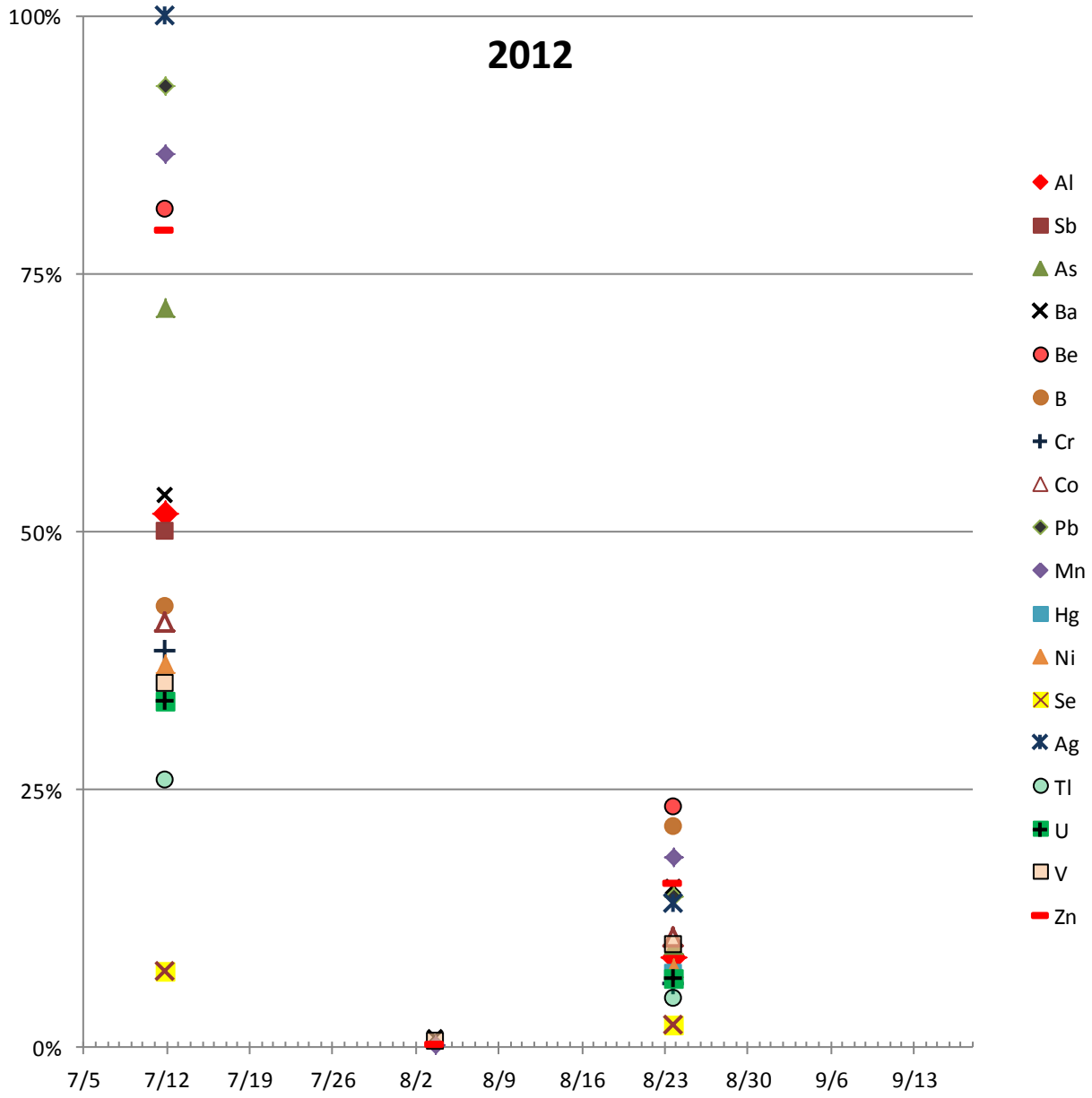

A third date, 7/11/2012, appears to be showing frequently in Table 22 for the metals Al, As, Ba, Be, Cd, Pb, Mn, Ag, Na, and Zn. The storm events in RG and LACW coincided with maximum discharges of 2,210 cfs and 680 cfs, respectively. Even though these conditions were very similar to 8/21/2011 storm event, the concentrations of the inorganics were not as high, but for the 9 metals listed earlier, the average relative concentration was 77%.

Figure 96. Relative concentrations of storm water for inorganics 2013.

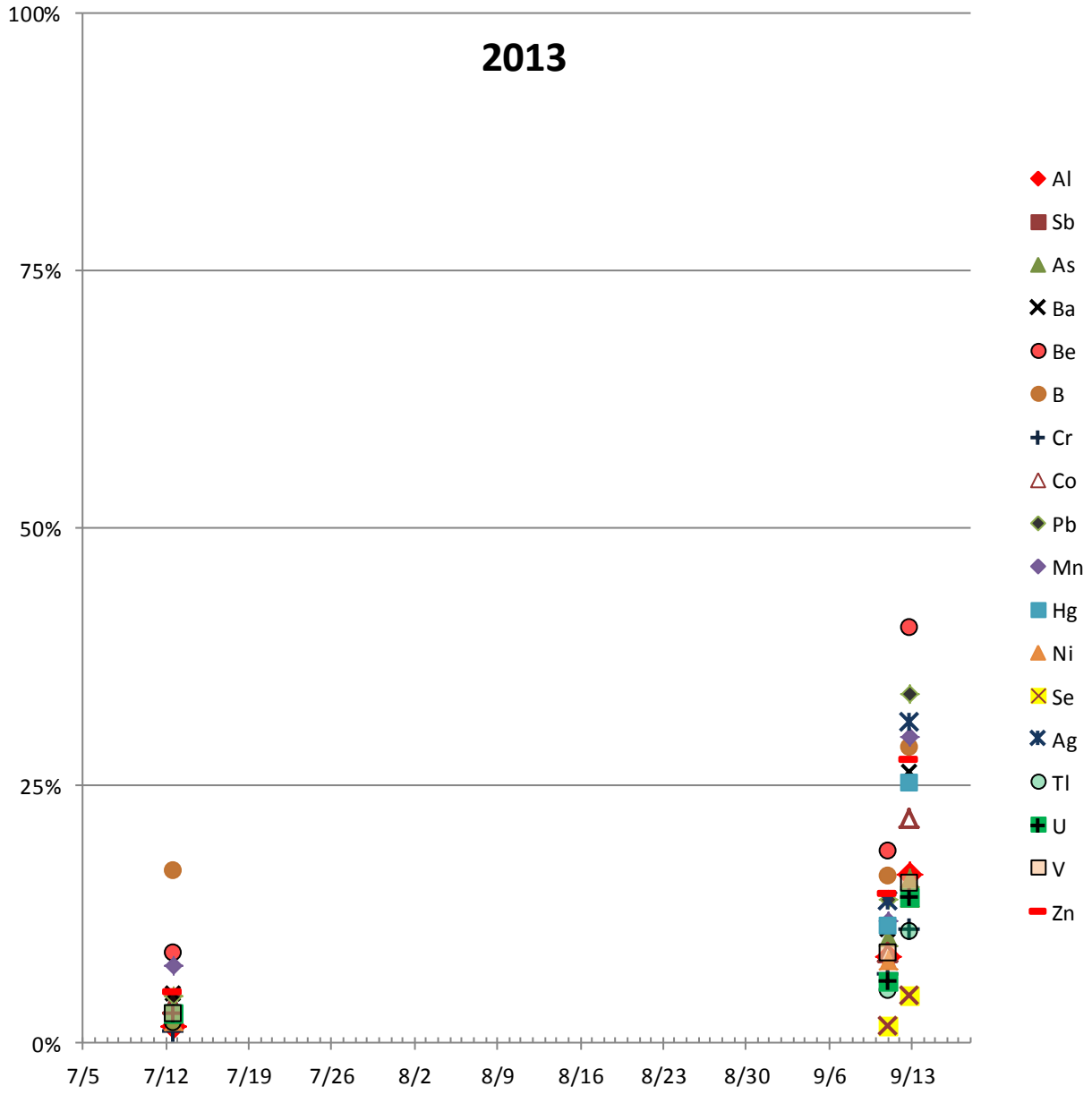

No events with high concentrations of metals occurred in 2013. In 2012 and 2013 the BDD sampling strategy was changed to only keep samples during which discharge in E050 and E060 was 5 cfs or greater. No other events were sampled during these two monitoring years, so the information during 2012 and 2013 was very limited.

Figure 97. Relative concentrations of storm water for inorganics 2014.

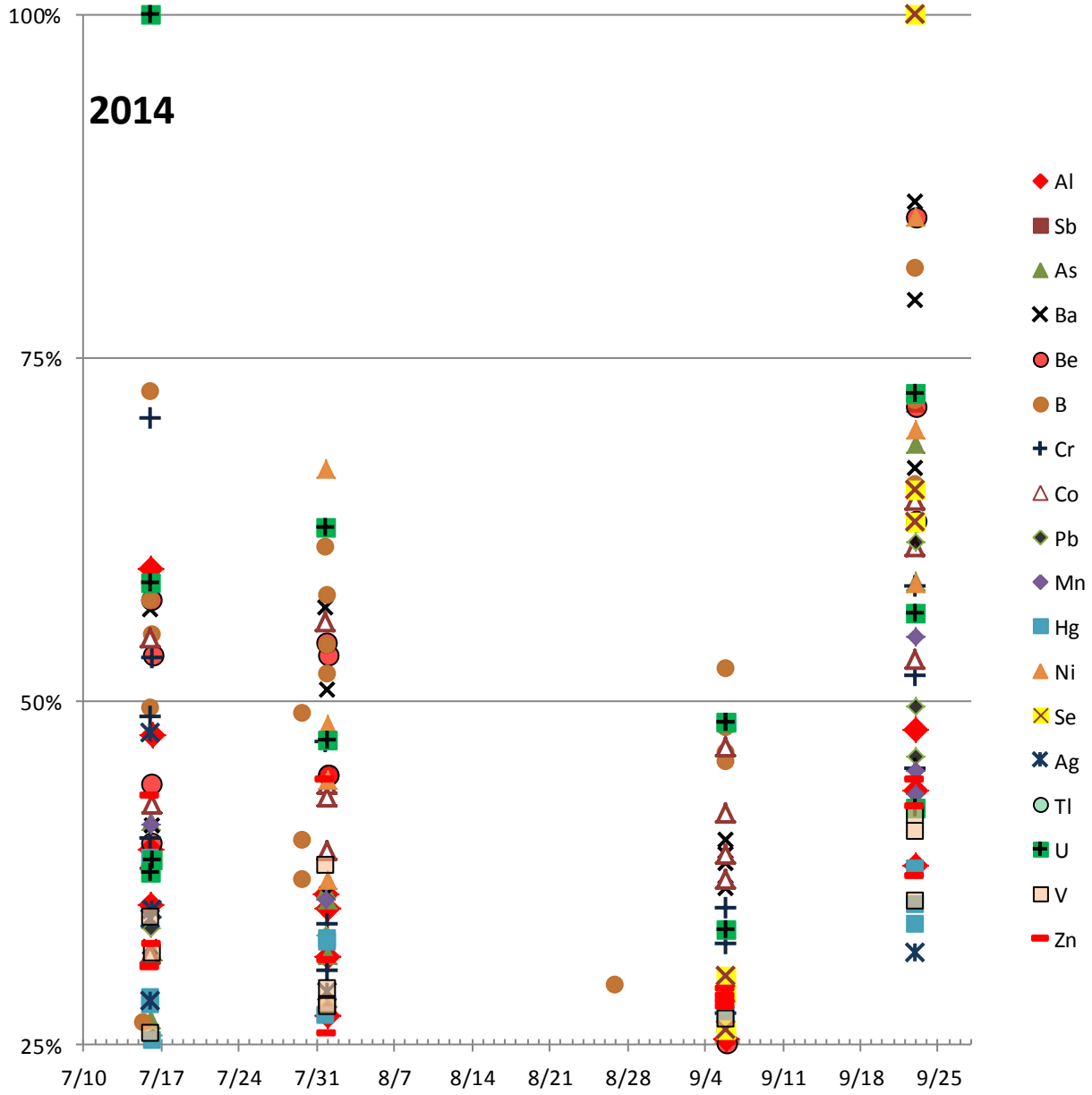

During 2014 summer season, even though large number of events was sampled, most of them were RG storm events because the lower LA Canyon was not monitored any longer. The lower LAC gage station E109.9 was non-operational in 2014. It is possible that certain important storm events originating from LACW were not sampled. It is noteworthy to mention the two dates with the highest relative metal concentrations: 7/16/2014 and 9/22/2014.

Table 22. 2011-2014 Relative metal concentrations in storm water.

08/21/2011	Aluminum	100%	08/21/2011	Calcium	61%	09/04/2011	Manganese	100%	07/12/2013	Sodium	87%
	Aluminum	99%		Calcium	57%		Manganese	90%	09/11/2013	Sodium	69%
	Aluminum	65%		Calcium	52%	07/11/2012	Manganese	87%	09/12/2013	Sodium	74%
	Aluminum	51%	07/16/2014	Calcium	73%	09/22/2014	Manganese	55%	07/16/2014	Sodium	100%
09/04/2011	Aluminum	53%	07/31/2014	Calcium	59%	08/29/2011	Mercury	32%		Sodium	99%
07/11/2012	Aluminum	52%	09/22/2014	Calcium	100%	09/04/2011	Mercury	100%		Sodium	95%
07/16/2014	Aluminum	60%		Calcium	79%	09/04/2011	Mercury	44%		Sodium	83%
08/03/2011	Antimony	100%		Calcium	64%	09/07/2011	Mercury	44%	07/29/2014	Sodium	67%
08/21/2011	Antimony	56%	08/21/2011	Chromium	100%	09/07/2011	Mercury	38%		Sodium	63%
08/27/2011	Antimony	52%		Chromium	100%	07/16/2014	Mercury	39%		Sodium	59%
08/21/2011	Arsenic	100%		Chromium	64%	08/01/2014	Mercury	33%		Sodium	52%
	Arsenic	85%		Chromium	56%	08/01/2014	Mercury	32%		Sodium	51%
	Arsenic	56%	09/04/2011	Chromium	51%	09/22/2014	Mercury	38%	07/31/2014	Sodium	85%
	Arsenic	56%	07/16/2014	Chromium	71%	09/22/2014	Mercury	34%		Sodium	77%
	Arsenic	55%		Chromium	53%	09/23/2014	Mercury	35%		Sodium	80%
08/29/2011	Arsenic	54%	09/22/2014	Chromium	58%	08/21/2011	Nickel	100%		Sodium	64%
09/04/2011	Arsenic	65%		Chromium	52%		Nickel	96%	08/26/2014	Sodium	54%
07/11/2012	Arsenic	72%	08/21/2011	Cobalt	100%		Nickel	52%	09/05/2014	Sodium	85%
09/22/2014	Arsenic	72%		Cobalt	97%	09/04/2011	Nickel	57%		Sodium	81%
	Arsenic	69%		Cobalt	69%	07/31/2014	Nickel	67%		Sodium	74%
	Arsenic	59%		Cobalt	52%	09/22/2014	Nickel	85%		Sodium	67%
08/21/2011	Barium	100%	09/04/2011	Cobalt	58%		Nickel	70%	09/22/2014	Sodium	94%
	Barium	90%	07/16/2014	Cobalt	55%		Nickel	59%		Sodium	86%
	Barium	82%	07/31/2014	Cobalt	56%	08/21/2011	Potassium	100%		Sodium	83%
	Barium	65%	09/22/2014	Cobalt	65%		Potassium	96%	08/03/2011	Thallium	100%
09/04/2011	Barium	89%		Cobalt	61%		Potassium	56%	08/21/2011	Thallium	23%
	Barium	72%		Cobalt	53%		Potassium	54%	08/26/2011	Thallium	25%
07/11/2012	Barium	54%	08/21/2011	Copper	100%	07/16/2014	Potassium	50%	09/04/2011	Thallium	16%
07/16/2014	Barium	57%		Copper	96%	09/22/2014	Selenium	100%	07/11/2012	Thallium	26%
07/31/2014	Barium	57%		Copper	57%		Selenium	65%	09/22/2014	Thallium	18%
	Barium	51%		Copper	54%		Selenium	63%	09/22/2014	Thallium	16%
09/22/2014	Barium	86%	09/04/2011	Copper	71%	08/21/2011	Silver	55%	07/16/2014	Uranium	100%
	Barium	79%	07/16/2014	Copper	53%	09/04/2011	Silver	55%		Uranium	59%
	Barium	67%	09/22/2014	Copper	57%	07/11/2012	Silver	100%	07/31/2014	Uranium	63%
08/21/2011	Beryllium	100%	08/21/2011	Iron	100%	08/03/2011	Sodium	55%	09/22/2014	Uranium	72%
	Beryllium	94%		Iron	100%	08/21/2011	Sodium	93%		Uranium	56%
	Beryllium	78%		Iron	52%		Sodium	87%	08/21/2011	Vanadium	100%
09/04/2011	Beryllium	98%		Iron	51%		Sodium	79%		Vanadium	99%
	Beryllium	52%	09/04/2011	Iron	53%		Sodium	68%		Vanadium	52%
07/11/2012	Beryllium	81%	08/21/2011	Lead	64%		Sodium	58%	09/04/2011	Vanadium	51%
07/16/2014	Beryllium	57%		Lead	60%	08/24/2011	Sodium	64%	08/21/2011	Zinc	88%
	Beryllium	53%		Lead	58%	08/26/2011	Sodium	51%		Zinc	85%
07/31/2014	Beryllium	54%		Lead	52%	08/27/2011	Sodium	58%		Zinc	70%
	Beryllium	53%	09/04/2011	Lead	100%	08/29/2011	Sodium	68%		Zinc	62%
09/22/2014	Beryllium	85%		Lead	51%		Sodium	68%	09/04/2011	Zinc	100%
	Beryllium	71%	07/11/2012	Lead	93%		Sodium	61%		Zinc	63%
	Beryllium	63%	09/22/2014	Lead	62%		Sodium	61%	07/11/2012	Zinc	79%
08/21/2011	Boron	98%	08/21/2011	Magnesium	100%	09/01/2011	Sodium	52%	08/21/2011	Zinc	88%
09/04/2011	Boron	100%		Magnesium	97%	09/04/2011	Sodium	74%		Zinc	85%
07/16/2014	Boron	73%		Magnesium	64%		Sodium	65%		Zinc	70%
	Boron	57%		Magnesium	56%		Sodium	58%		Zinc	62%
	Boron	55%	07/16/2014	Magnesium	67%	09/07/2011	Sodium	74%	09/04/2011	Zinc	100%
07/31/2014	Boron	61%	07/31/2014	Magnesium	61%		Sodium	71%		Zinc	63%
	Boron	58%	09/22/2014	Magnesium	62%		Sodium	61%	07/11/2012	Zinc	79%
	Boron	54%		Magnesium	57%		Sodium	61%	08/21/2011	Cadmium	65%
	Boron	52%	08/21/2011	Manganese	81%		Sodium	55%	09/04/2011	Cadmium	78%
09/05/2014	Boron	52%		Manganese	68%		Sodium	51%		Cadmium	76%
09/22/2014	Boron	81%		Manganese	65%	07/11/2012	Sodium	75%	07/11/2012	Cadmium	100%
	Boron	72%		Manganese	65%	08/23/2012	Sodium	59%	07/16/2014	Cadmium	52%
	Boron	66%				05/21/2013	Sodium	94%	09/22/2014	Cadmium	51%

The dates for which there was no RG storm event but there was significant LACW storm event and detection of metals with high relative concentrations are discussed here. During 8/3/2011, the relative discharge (LACW discharge vs RG discharge) was 10% and two metals, Sb and Tl, had their highest concentrations. In addition, 8/26/2011 (LAC relative discharge of 4%) and 8/27/2011 (LAC relative discharge of 8%) also detected significant concentrations of Sb and Tl. This analysis suggests that potential source of these two metals may be LACW.

Based on the information provided in this section, we can conclude that storm events dated 9/22/2014 and 7/16/2014 had a predominant RG contributions to the concentrations of metals, that storm events dated 8/3/2011 and 8/26-27/2011 had predominant LACW contributions, and that storm events dated 8/21/2011, 9/4/2011, and 7/11/2012 had contributions to the concentrations of metals with unknown ratio from both watersheds: LACW and RG above Otowi Bridge.

VII.2.e Storm Water Concentrations vs SSC - Inorganics

In this section, the concentrations in storm water vs SSC for inorganics were presented. The analysis for each constituent includes the following. The established RG UTL values were plotted on the graph in order to determine exceedances from BDD established background. Any concentration which resides above the "black" line would indicate an exceedance from the RG UTL.

Next, the scatter values were "fitted" to a straight line (passing through zero) in an attempt to determine if there is a correlation between the storm water concentrations and SSC. A good correlation (high coefficient of determination) between these parameters would indicate a preferential transport via suspended sediment. If so, any monitoring of the contaminants may be substituted with simply monitoring for SSC, and any high coefficient of determination may be indicative of naturally occurring constituents rather than an anthropological source upgradient from the BDD. Because the concentrations at BDD are influenced by two watersheds, the RG watershed and the LACW, we will consider a coefficient of determination to be substantial and high if the values are greater than 0.6. Even if the coefficient of determination is high and may indicate a naturally occurring constituent in the RG, the contaminants from the LACW may be observed on the graph as being of higher concentrations and not conforming to the general trend.

When making conclusions about contaminants and their sources, all facts must be taken into consideration, the exceedances from RG UTL, the PP UTL, the naturally occurring constituents in PP or LACW, any potential or known anthropological sources in the LACW or ugradient from the Otowi Bridge, and the chemical and physical properties of the contaminants. This section does not make a complete analysis for each constituent, but presents some of the known information.

For all plots in this section the result of 139 mg/L SSC (7/11/2012) was removed from the data, and results marked with "B" lab qualifier were not included on the graphs.

Figure 98. Al in storm water vs SSC.

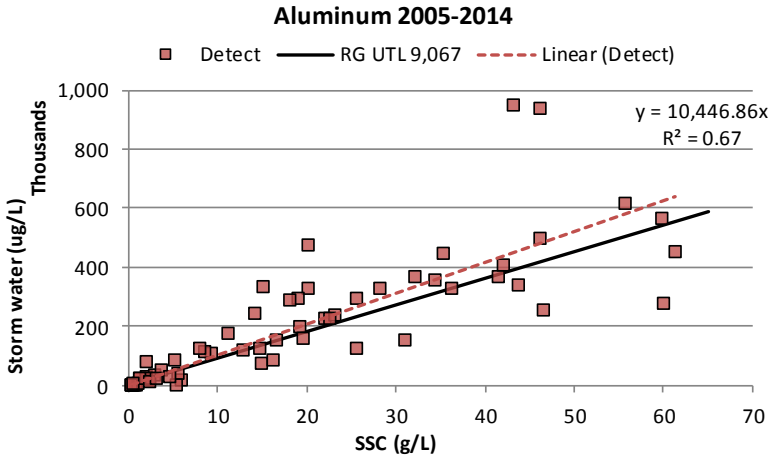

The Al concentrations presented on the graph show exceedances of the RG UTL, which is expected considering Al is known to occur naturally in the LACW (PP UTL 15,400 mg/kg). The correlation between the storm water concentrations and SSC is good, which is indicative of preferential transport via suspended sediment and naturally occurring Al along the RG.

Figure 99. Sb in storm water vs SSC.

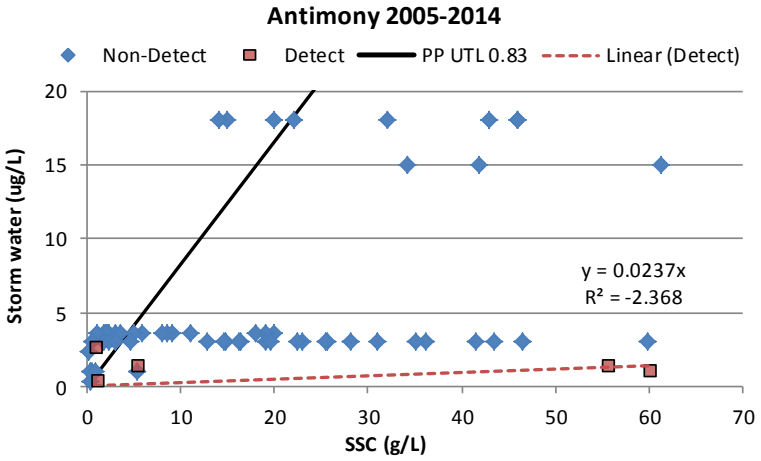

The Sb concentrations show too many non-detects in order to indicate any trend. However, even from the 5 detected concentrations, there was one that exceeded background RG UTL.

Figure 100. As in storm water vs SSC.

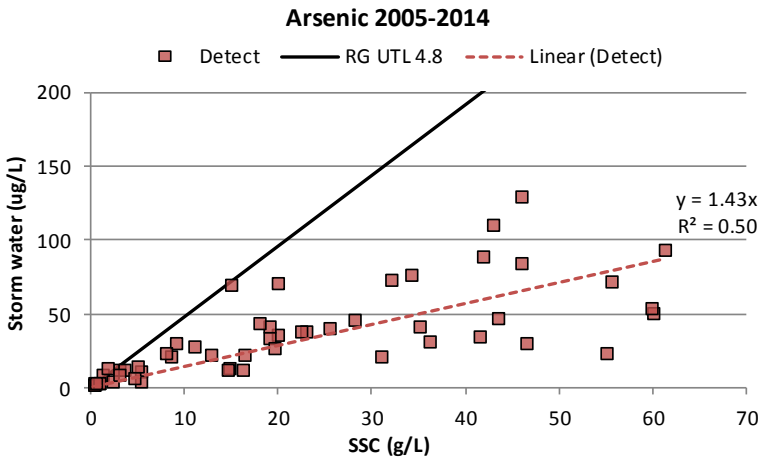

The As concentrations presented on the graph show very few exceedances of the RG UTL. The PP UTL of 3.98 mg/kg is very compatible to the RG UTL. This fact gives us the confidence that the detect values are background values whether from RG watershed or LACW. The correlation between the storm water concentrations and SSC is average but combined with the previous conclusion, it is indicative of naturally occurring As, and somewhat preferential transport via suspended sediments.

Figure 101. Ba in storm water vs SSC.

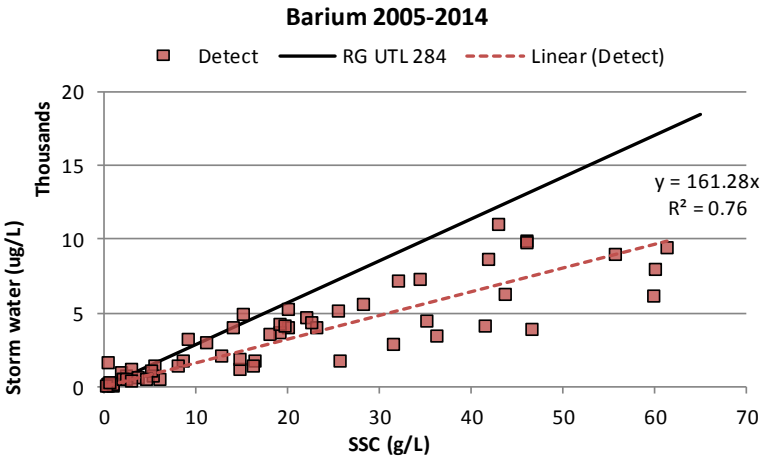

The Ba concentrations presented on the graph show very few exceedances of the RG UTL. The PP UTL of 127 mg/kg is compatible to the RG UTL. This fact gives us the confidence that the detect values are background values whether from RG watershed or LACW. The correlation between the storm water concentrations and SSC is very good, which is indicative of preferential transport via suspended sediment and naturally occurring Ba along the RG. This is surprising result because we expected elevated Ba due to the Las Conchas fire.

Figure 102. Be in storm water vs SSC.

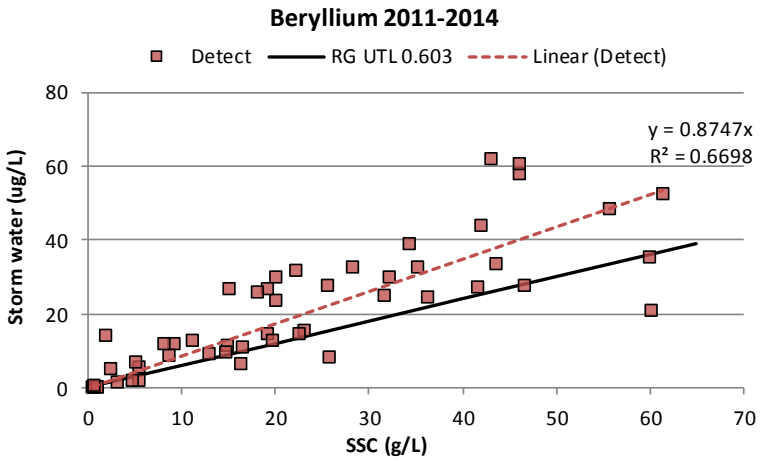

The Be values presented on the graph show many exceedances of the RG UTL, which is expected considering Be is known to occur naturally in the LACW. The PP UTL of 1.31 mg/kg is twice the RG UTL. However, the exceedances are numerous to be attributed solely to LACW. The correlation between the storm water concentrations and SSC is good, which is indicative of preferential transport via suspended sediment and a source of Be along the RG.

Figure 103. B in storm water vs SSC.

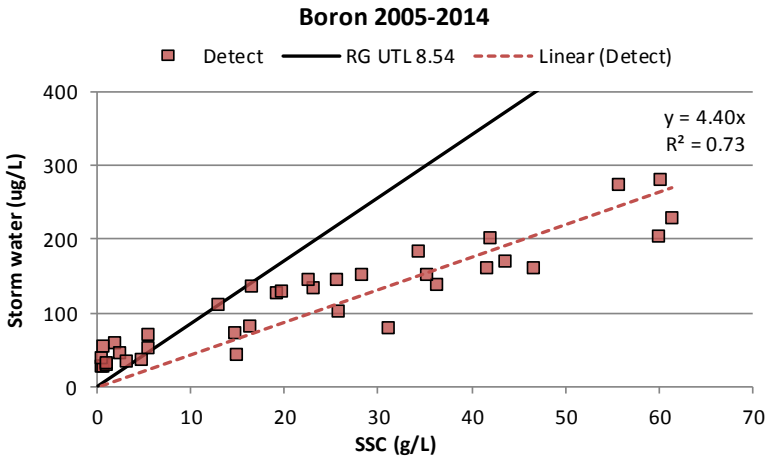

The B values presented on the graph show exceedances of the RG UTL in the low range of SSC. The correlation between the storm water concentrations and SSC is very good, which is indicative of preferential transport via suspended sediment and a source of B along the RG. This is unexpected result since B has higher water solubility than other metals.

Figure 104. Cd in storm water vs SSC.

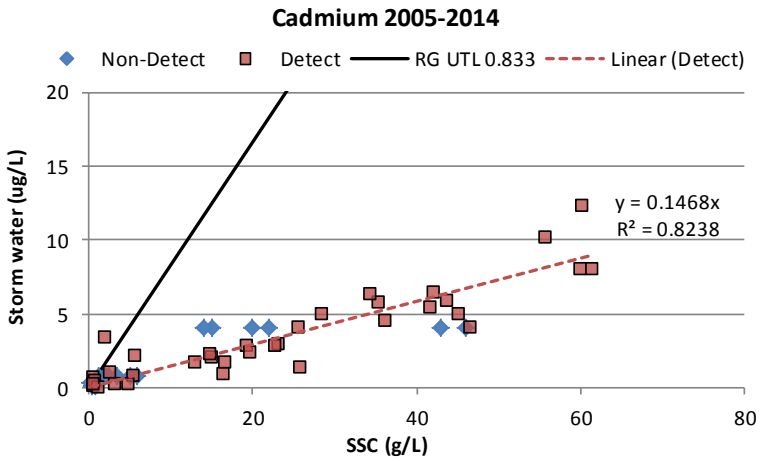

The Cd values presented on the graph show very few exceedances of the RG UTL. The PP UTL of 0.4 mg/kg is lower than the RG UTL. This fact gives us the confidence that the detect values are background values whether from RG watershed or LACW. The correlation between the storm water concentrations and SSC is very good, which is indicative of preferential transport via suspended sediment and naturally occurring Cd along the RG.

Figure 105. Cr in storm water vs SSC.

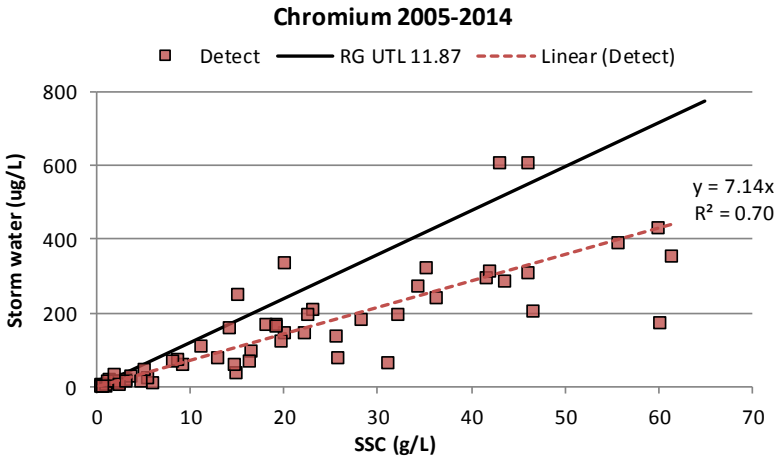

The Cr values presented on the graph show some exceedances of the RG UTL. The PP UTL of 10.5 mg/kg is compatible to the RG UTL. This fact gives us the confidence that the detect values are background values whether from RG watershed or LACW, and that the exceedances are probably due to anthropological contamination from LACW. The correlation between the storm water concentrations and SSC is very good, which is indicative of preferential transport via suspended sediment and naturally occurring Cr along the RG.

Figure 106. Co in storm water vs SSC.

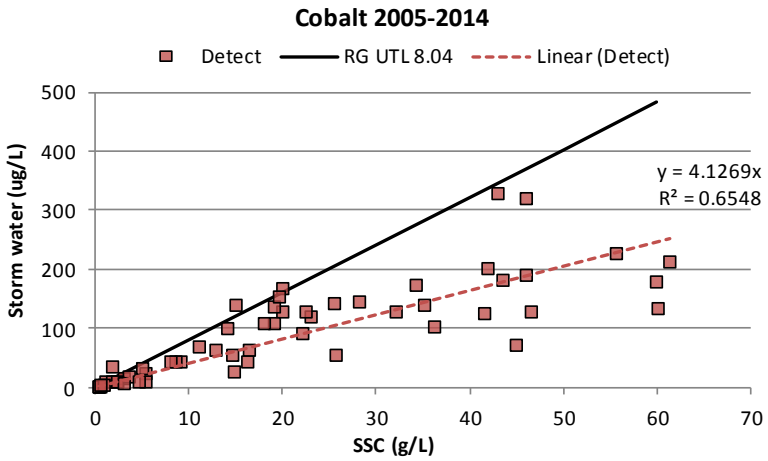

The Co values presented on the graph show some exceedances of the RG UTL. The PP UTL of 4.73 mg/kg is less than the RG UTL. This fact gives us the confidence that the detect values are background values whether from RG watershed or LACW, and that the exceedances are probably due to anthropological contamination from LACW. The correlation between the storm water concentrations and SSC is good, which is indicative of preferential transport via suspended sediment and naturally occurring Co along the RG.

Figure 107. Pb in storm water vs SSC.

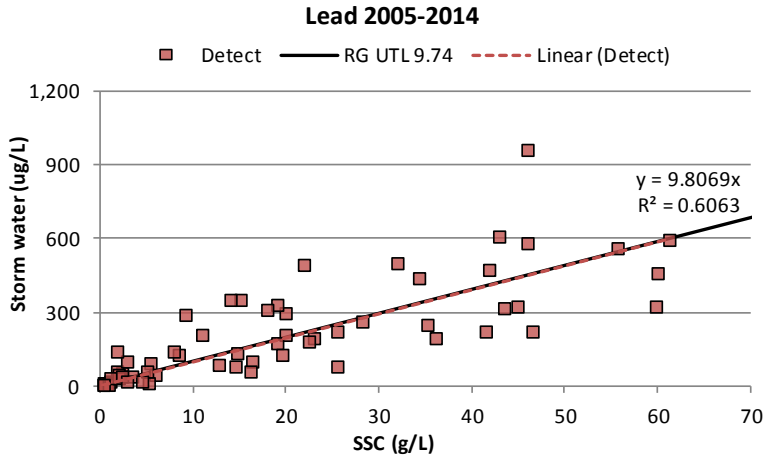

The Pb values presented on the graph show exceedances of the RG UTL. The PP UTL of 19.7 mg/kg is higher than the RG UTL. That fact suggests that the exceedances are probably due to higher PP background or anthropological sources in LACW. The correlation between the storm water concentrations and SSC is good, which is indicative of preferential transport via suspended sediment.

Figure 108. Mn in storm water vs SSC.

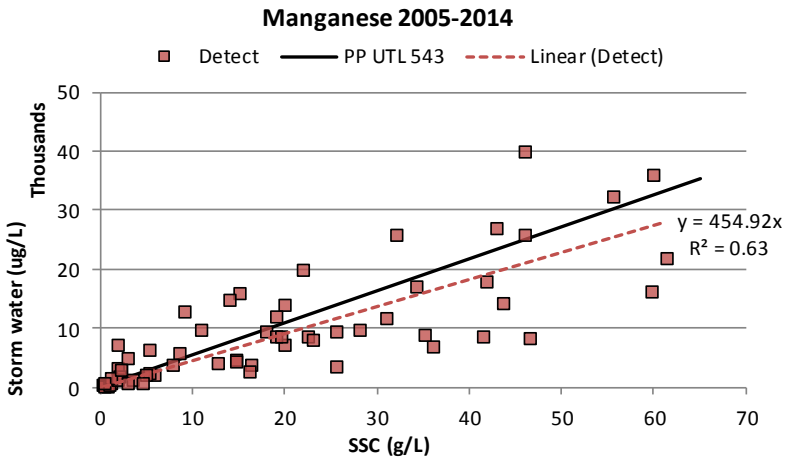

The Mn values presented on the graph show some exceedances of the PP UTL. There is no established RG UTL. Mn concentrations are elevated in ash so this is an expected result. The correlation between the storm water concentrations and SSC is very good, which is indicative of preferential transport via suspended sediment and potential sources of Mn along the RG.

Figure 109. Hg in storm water vs SSC.

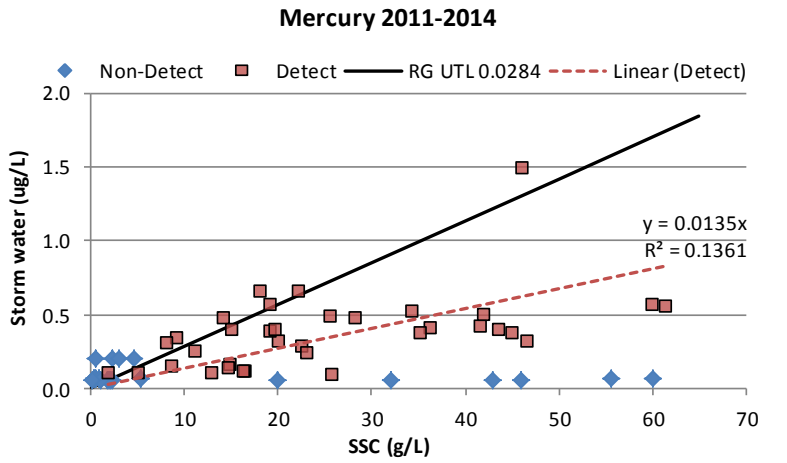

The Hg values presented on the graph show some exceedances of the RG UTL. The PP UTL of 0.1 mg/kg is much higher than the RG UTL. TA-21 in the upper LAC is a known source of Hg, so the exceedances are probably due to contamination from LACW. The correlation between the storm water concentrations and SSC is poor, which confirms that many of the detect values may originate from anthropological sources rather than natural.

Figure 110. Ni in storm water vs SSC.

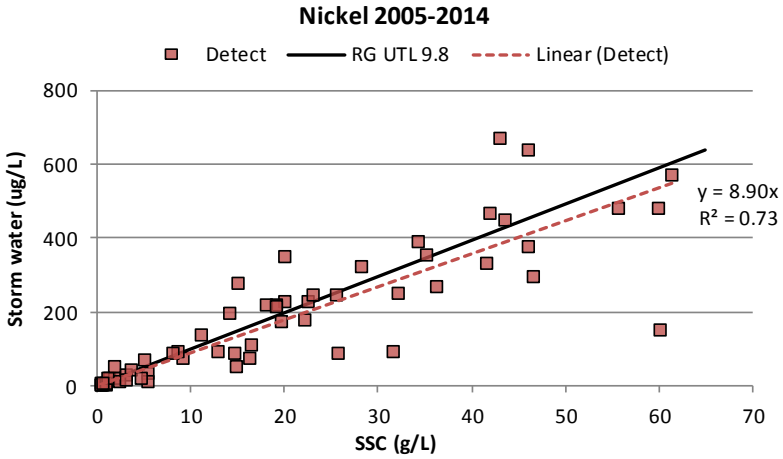

The Ni values presented on the graph show exceedances of the RG UTL. The PP UTL of 9.38 mg/kg is very compatible to the RG UTL. This fact gives us the confidence that the exceedances are probably due to anthropological upgradient sources. The correlation between the storm water concentrations and SSC is very good, which is indicative of preferential transport via suspended sediment and naturally occurring Ni along the RG.

Figure 111. Se in storm water vs SSC.

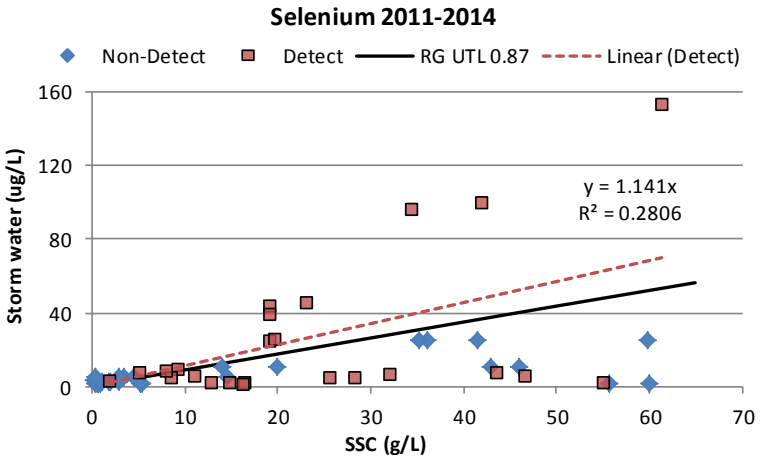

The Se values presented on the graph show some exceedances of the RG UTL. The PP UTL of 0.3 mg/kg is less than the RG UTL. The Se data showed many non-detected values due to very large detection limits.

Figure 112. Ag in storm water vs SSC.

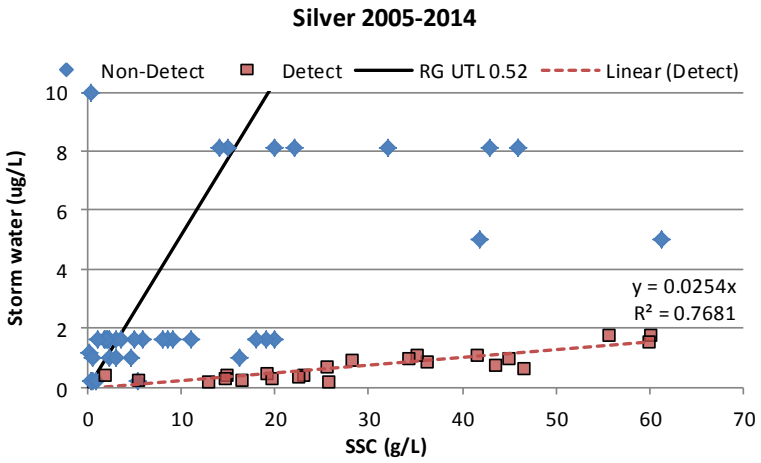

Similar to the Se data, the Ag data showed many non-detected values due to large detection limits. Of the detected values, there were no exceedances of the RG UTL. The correlation between the storm water concentrations of detects and SSC is very good, which is indicative of preferential transport via suspended sediment and naturally occurring Ag along the RG.

Figure 113. Tl in storm water vs SSC.

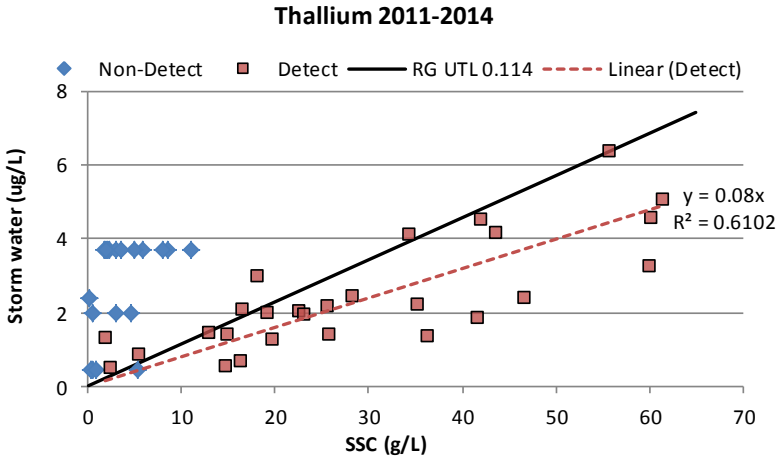

The Tl values presented on the graph show some exceedances of the RG UTL. The PP UTL of 0.73 mg/kg is much higher than the RG UTL. This fact indicates that the exceedances may be due to LACW sources whether natural or anthropological. The correlation between the storm water concentrations and SSC is good, which indicatives preferential transport via suspended sediment and naturally occurring Tl along the RG.

Figure 114. U in storm water vs SSC.

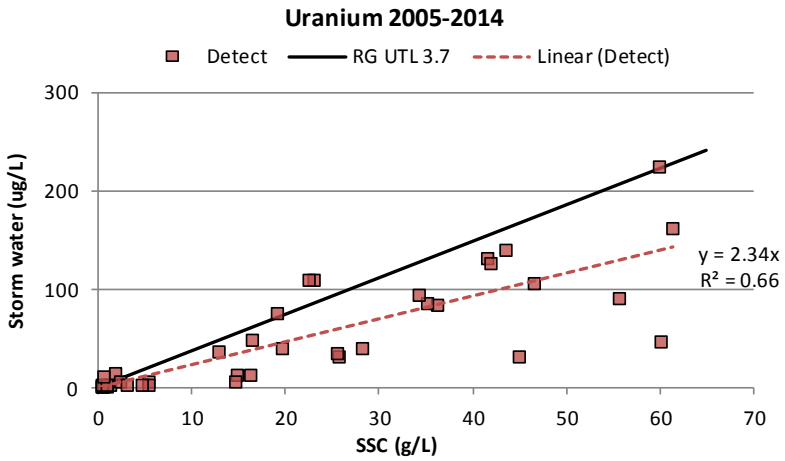

The U values presented on the graph show some exceedances of the RG UTL. The PP UTL of 2.2 mg/kg is less than the RG UTL. This fact gives us the confidence that the few exceedances are probably due to anthropological contamination from LACW. The correlation between the storm water concentrations and SSC is good, which is indicative of preferential transport via suspended sediment and naturally occurring U along the RG.

Figure 115. V in storm water vs SSC.

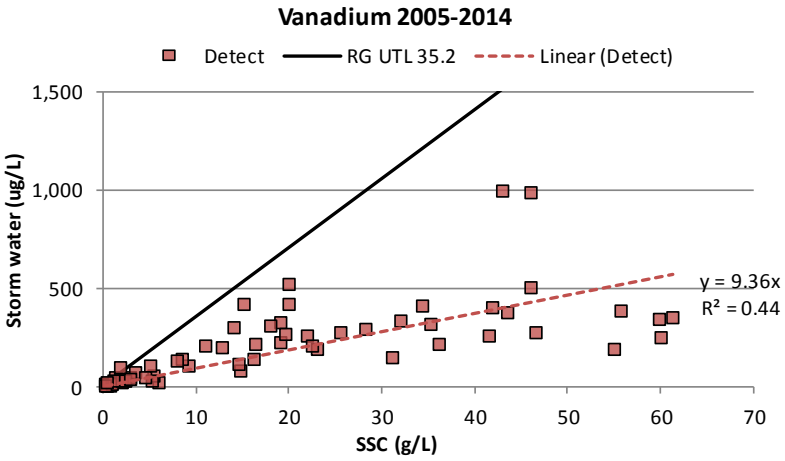

The V values presented on the graph show only a couple of exceedances of the RG UTL. The PP UTL of 19.7 mg/kg is less than the RG UTL. This fact gives us the confidence that the detect values on the plot are background values whether from RG watershed or LACW. The correlation between the storm water concentrations and SSC is not very good, and the scatter plot appears to represent two different populations, perhaps, one from the upper RG watershed and another from LACW with different central tendencies. According to the scientific literature, V is not very soluble in water, so we would expect a transport mostly via suspended sediment although that fact was not supported by our data.

Figure 116. Zn in storm water vs SSC.

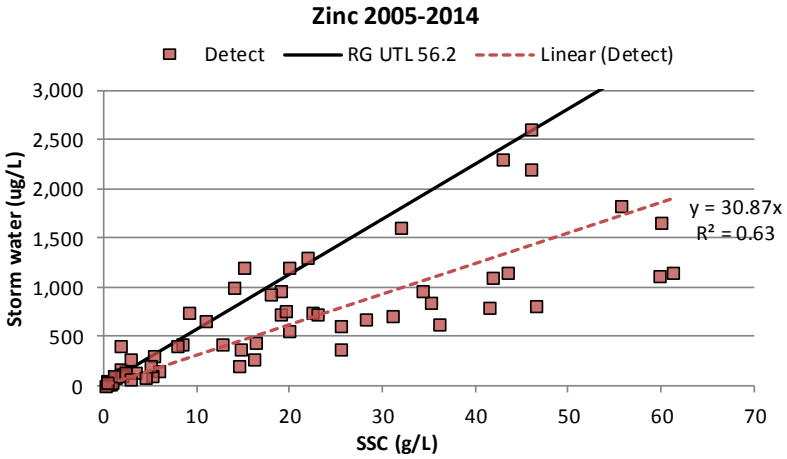

The Zn values presented on the graph show some exceedances of the RG UTL. The PP UTL of 60.2 mg/kg is compatible to the RG UTL. This fact gives us the confidence that the detect values on the plot are background values whether from RG watershed or LACW, and that the exceedances are probably due to anthropological contamination from LACW. The correlation between the storm water concentrations and SSC is good, which is indicative of preferential transport via suspended sediment and naturally occurring Zn along the RG.

Figure 117. Perchlorate in storm water vs SSC.

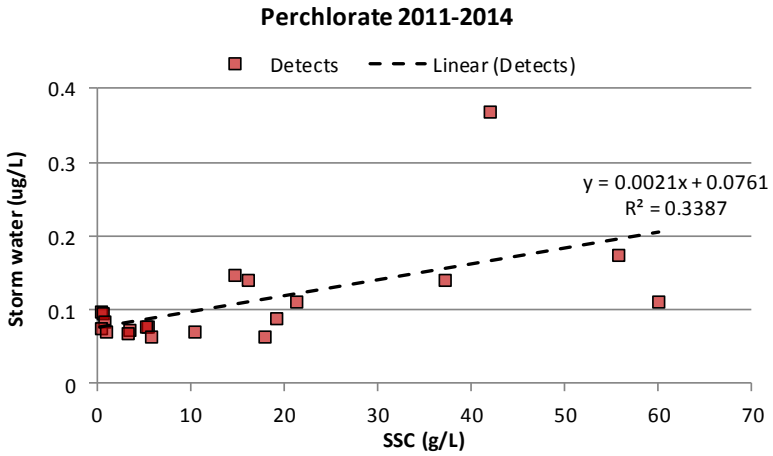

Perchlorate is highly soluble in water with little tendency to absorb to minerals or organic surfaces. Its high water solubility makes it very mobile in water. This expectation is supported by the poor coefficient of determination of the linear fit to the data. The range of the detected concentrations at the BDD was between 0.06 to 0.37 ug/L, which is similar to the range in groundwater wells from 0.07 to 0.45 ppb sampled in the Northern Rio Grande basin (Los Alamos, Santa Fe, and Taos) as studied in (Dale M, Fall Meeting 2007). All values were below the UTL of 0.4 ppb as established in the quoted reference.

If the Rio Grande background is identical to the BDD detects as the data implies and if perchlorate is very soluble in water then we may see good correlation of the concentrations vs the instantaneous discharge in the RG. To investigate that we plotted the perchlorate concentrations vs the instantaneous discharge as measured at Otowi Gage. However, the linear fit in Figure 118 does not indicate good correlation between these parameters.

Figure 118. Perchlorate in storm water vs RG discharge.

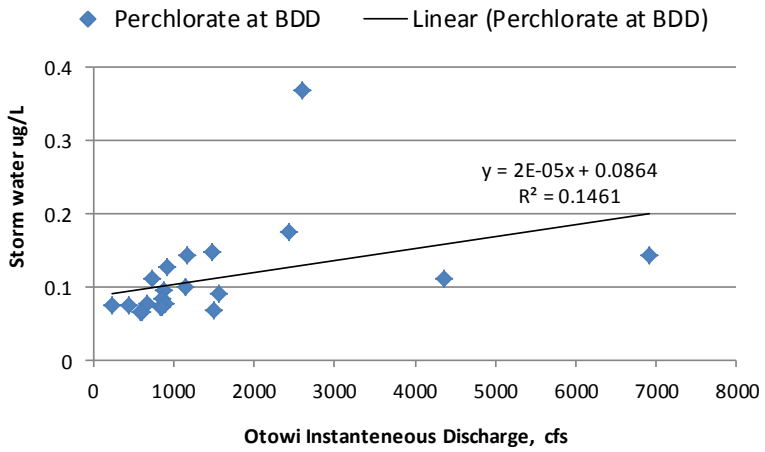

For many hydraulic parameters the properties change as the discharge reaches a critical value. To investigate that we removed data for high discharge values and we discovered that the correlation improves greatly for discharges below 2,600 cfs as it is shown on Figure 119. In order to verify this trend, we would need to collect additional data in our future sampling.

Figure 119. Perchlorate in storm water vs RG discharges below 2,600 cfs.

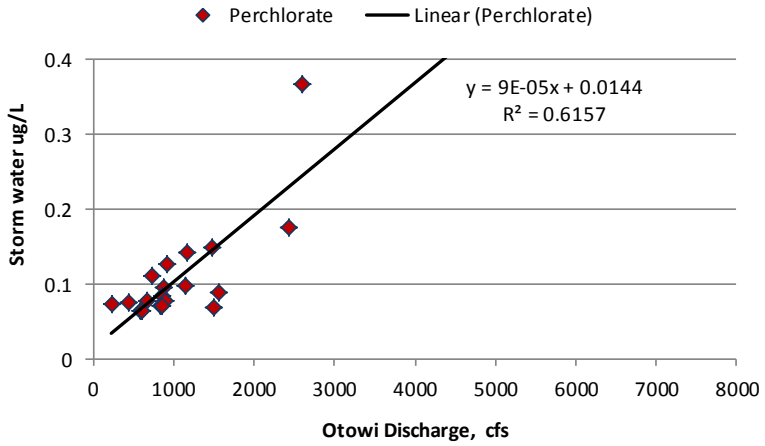

VII.2.f Organics in Storm Water – PCBs and Dioxins/Furans

The figures below display the total PCBs concentrations occurring in the RG at BDD. The time plot indicates that the NMWQCC standard for surface water is exceeded more than 50 percent of the time. The maximum concentrations were detected in 2010 and then in 2011. Exceedances for the northern RG and BDD part of the RG have been documented in many sampling events by NMED, LANL, and other sampling entities, so these results were expected.

Figure 120. Time plot of total PCBs detected values, 2005-2014.

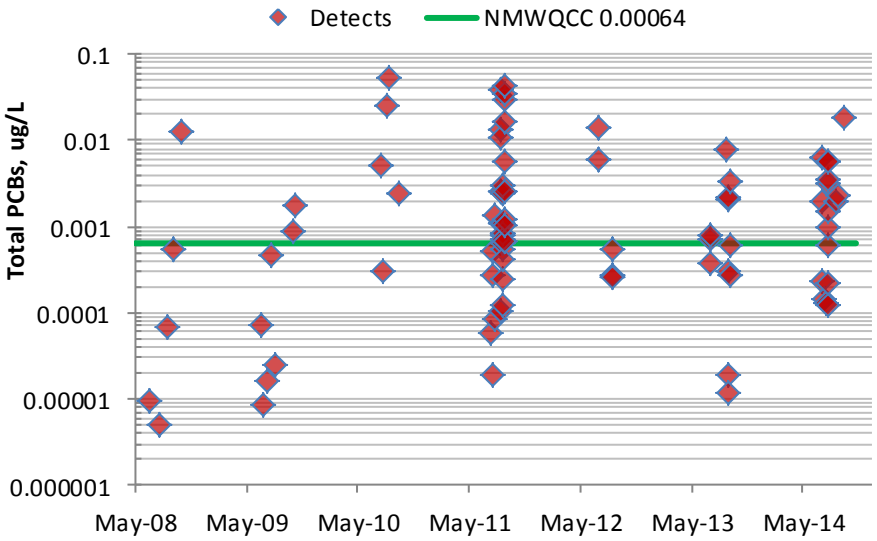

The annual distributions of the concentrations and their shapes are presented in the next two figures.

Figure 121. Annual distribution of total PCBs.

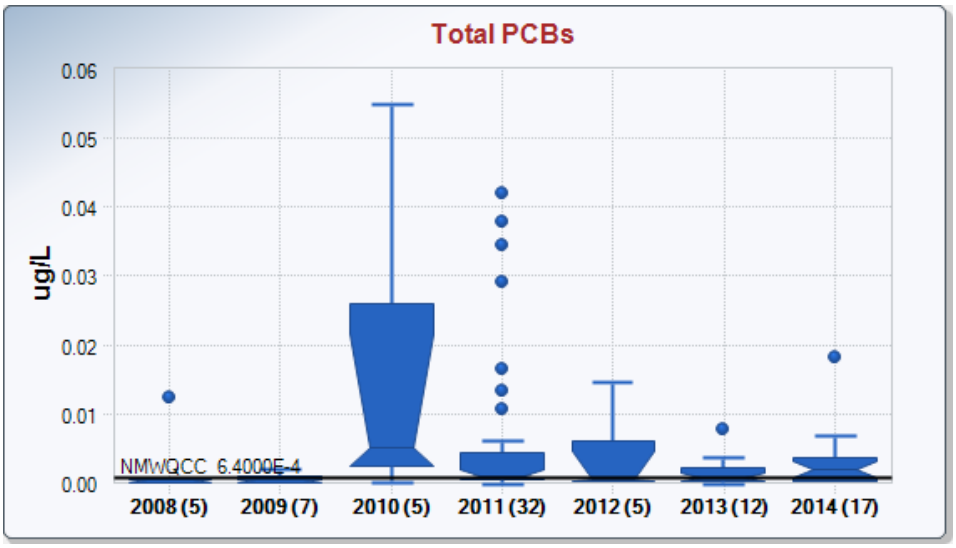

Figure 122. Shape of annual distributions* of total PCBs.

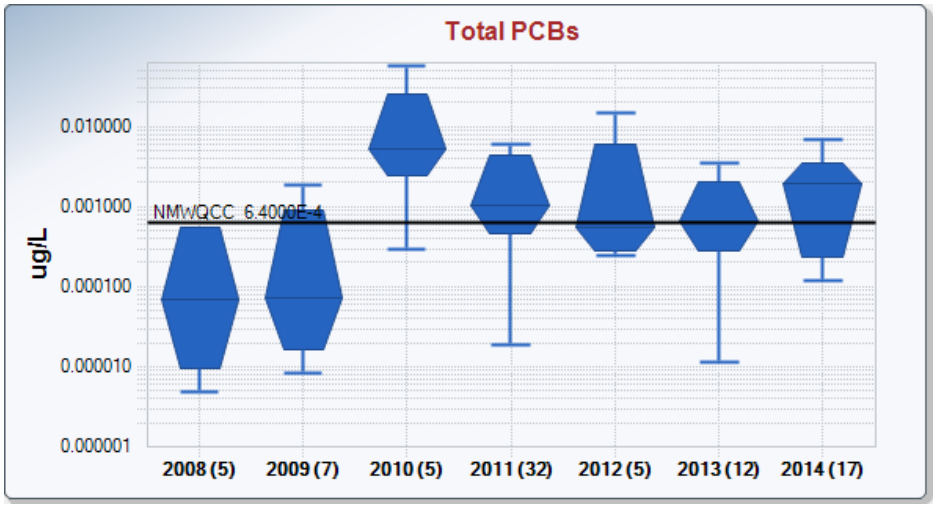

*Note: Outliers are not presented on the graph when on log scale.

The total PCBs concentrations in storm water vs SSC were plotted on Figure 123, and the scatter values were fitted to straight line and power functions. The result for SSC of 138 g/L on 7/11/2012 was not included in the graph. Even though the straight fit did not show good correlation, the power function fit the data with much better coefficient of determination. There were 5 exceedances of the LANL established background UTL for total PCBs.

Figure 123. Total PCBs vs SSC.

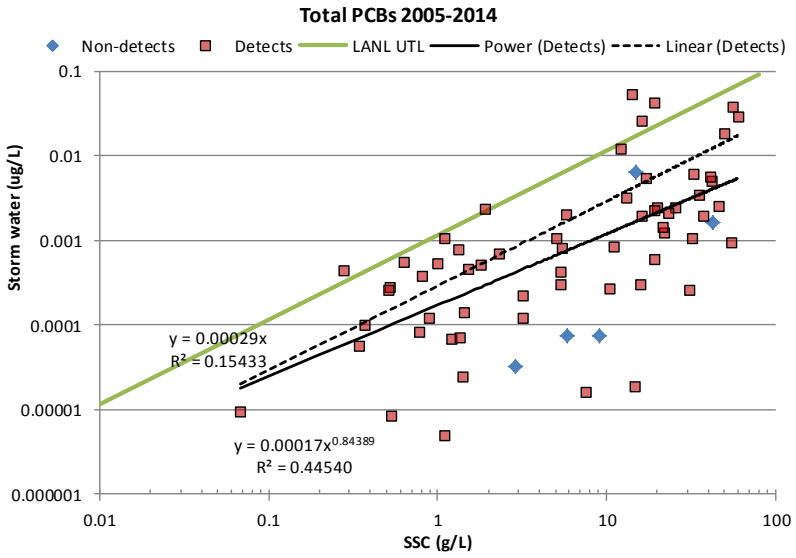

The descriptive statistics of all PCBs detects at the BDD is presented in Table 23, and it was compared with the study described in (LA-UR-12-1081, May 2012). The rows in blue are the BDD data,

the others - from the quoted reference, Section 4.3.1. The highlighted cells in yellow are the exceedances at BDD of the UTL determined by LANL study.

Table 23. Summary statistics of total PCB concentrations at BDD.

Variable	N	Min	Max	Mean	SD	Median	Distribution	UTL*
Total PCB (ng/L)*	29	0.28	29.5	7.5	8.2	4.9	Gamma	24.86
BDD Storm Water Total PCBs (ng/L)	**84**	**0.005**	**54.7**	**4.9**	**10.2**	**0.83**	**Log-Normal**	**6**
Calculated Suspended PCB Concentration(ng/g)*	23	0.03	1.276	0.353	0.329	0.241	Gamma	1.135
BDD Calculated Suspended PCBs (ng/g)	**38**	**0.001**	**3.9**	**0.38**	**0.64**	**0.125**	**Log-Normal**	**5**

We need to note a few important facts from Table 23. The minimum and median values of the data at the BDD were much lower than the sample data in the quoted reference, sometimes more than one order of magnitude. However, the maximum concentrations at BDD were higher, and the standard deviation wider, making them distributions with large range. Since contaminant concentrations at BDD are influenced by the two watersheds, upper Rio Grande (above Otowi Bridge) and LACW, the wide range of the distribution at BDD is an expected result.

The storm water concentration exceedances at BDD from the LANL-established UTL occurred on 8/15/2010, 8/23/2010 (maximum value of 0.054 ug/L), 8/21/2011, 9/4/2011, and 9/7/2011, and the calculated suspended sediment PCB concentrations exceedances occurred on 5/25/2005, 8/15/2010, 8/23/2010, 8/26/2011, and 9/7/2011. For these dates the influence of the LACW flow to the RG flow was significant, and, therefore we could assume that the exceedances at BDD are due to the contaminants arriving from the LACW. For 2011, the data confirms the conclusion in Section VII.2.d that like metals, for total PCBs the contribution of LANL-origin contaminants was predominant on 8/26/2011 and substantial on 8/21/2011 and 9/4/2011.

Table 24 presents all results of samples for dioxins and furans (D/F) in terms of the TEQ 2,3,7,8-TCDD. The most D/F detected concentrations were during the year 2011 when the effect of the Las Conchas fire was the greatest. Except for two sampling events, all results in 2011 exceeded the NMWQCC standard of 5.1×10^{-8} ug/L. There was only one detect value for each of the 2013 and 2014, with no exceedances of the NMWQCC standard in 2013 and very small exceedance in 2014.

Table 24. Dioxins/furans results, 2011-2014.

TEQ 2,3,7,8-TCDD			
Sampling Date	**Time**	**ug/L**	**Sampling Entity**
2011-07-22	23:34	0	BDD
2011-07-28	18:39	0	BDD
2011-07-28	19:06	1.55E-05	NMED
2011-07-28	19:56	1.28E-06	NMED
2011-08-03	17:39	0	BDD
2011-08-03	18:09	1.50E-05	NMED
2011-08-03	18:59	4.65E-07	NMED
2011-08-05	17:54	8.78E-06	NMED
2011-08-05	18:44	2.29E-06	NMED
2011-08-21	18:41	3.30E-08	NMED
2011-08-21	19:29	1.32E-08	NMED
2011-08-21	20:19	1.00E-06	NMED
2011-08-24	15:01	0	BDD
2011-08-26	19:43	0	BDD
2011-08-26	20:14	1.62E-06	NMED
2011-08-27	19:01	0	BDD
2011-08-29	04:21	1.92E-06	NMED
2011-08-29	05:06	2.41E-06	NMED
2011-09-01	19:38	0	BDD
2011-09-04	21:24	4.05E-06	BDD
2011-09-04	21:54	1.58E-06	NMED
2011-09-04	21:55	2.75E-06	NMED
2011-09-04	22:44	1.25E-06	NMED
2011-09-04	22:46	3.09E-06	NMED
2011-09-07	15:11	6.73E-07	NMED
2011-09-07	15:56	5.06E-06	NMED
2012-07-11	20:34	0	BDD
2013-07-12	16:38	0	BDD
2013-09-01	20:14	7.62E-09	NMED
2013-09-11	01:38	0	BDD
2013-09-12	21:16	0	BDD
2014-07-15	11:25	0	BDD
2014-07-29	17:27	0	BDD
2014-07-29	19:27	0	BDD
2014-08-01	00:18	7.38E-08	BDD
2014-08-27	00:50	0	BDD

Figure 124. Dioxins/furans in storm water.

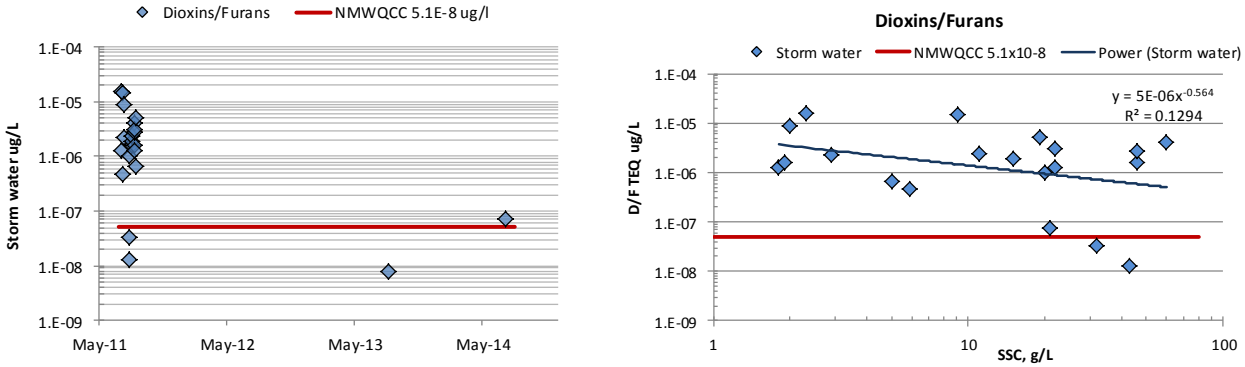

The D/F concentrations vs SSC were plotted in order to determine the manner of transport for these contaminants. Because of the low coefficient of determination, and the small number of detects, such negative slope may be interpreted as no dependence on SSC, and, therefore no preferential transport via suspended sediment.

VII.3 LANL Stations Analytical Data

The LANL stations that were part of the 2010 MOU and outfitted with sampling equipment were E050 (LANL and NMED), E060 (LANL and NMED), and E109.9 (LANL and NMED). The analytical data from NMED/DOE OB (sampler E110), and from other parts of the LAC and the RG (Guaje Canyon and Otowi Bridge) was used in this section to assess the fate and transport of contaminants from LAC to BDD. For detailed description of all sampling stations see Sections III.1 and III.3. The data from sampling stations E050 and E060 was combined in one group called "50/60", the data from all stations around Guaje Canyon was combined and named "Guaje", the data from sampling stations E109.9 and E110 was combined and referred to as "LLAC" (lower LA Canyon), and the data from all sampling stations around Otowi Bridge was combined and named "Otowi".

Usually, analytical data from 2010 to 2014 was used in the analysis of this section. Sometimes, data from 2008 and 2009 was also included but it was clearly marked with the proper year. All available data at BDD was included in the descriptive statistics (2005-2014). The data included in this section was presented in Attachment 6.

The EPA approved program ProUCL was used to obtain the descriptive statistics and to create boxplots. Due to the limitations of this program, log scale boxplot did not display all outliers of the data sets.

In 2010 and 2011, LANL used the method EPA160.2 together with ASTM: D3977-97 in order to analyze the suspended sediment concentrations in LAC. In fact, the preferred analysis for SSC during these two years was EPA160.2 (which is used to analyze total suspended solids, TSS). As discussed previously in Section III.6, USGS does not recommend this analysis for natural waters. Figure 125 plots the difference in results for these two methods, with obvious bias of EPA160.2 toward lower values than the ASTM method. If we assume 20% of precision to be acceptable, then the method EPA160.2 produces results of poor accuracy. However, this section includes all SSC data, from methods EPA 160.2 and ASTM: D3977-97.

Figure 125. Percent difference between EPA160.2 and ASTM: D3977-97.

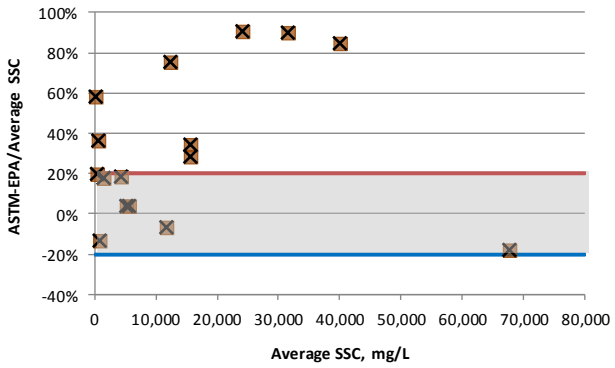

VII.3.a Annual Variations of Radionuclides in Storm Water

Figure 126. Time plot of SSC in LA/PCW.

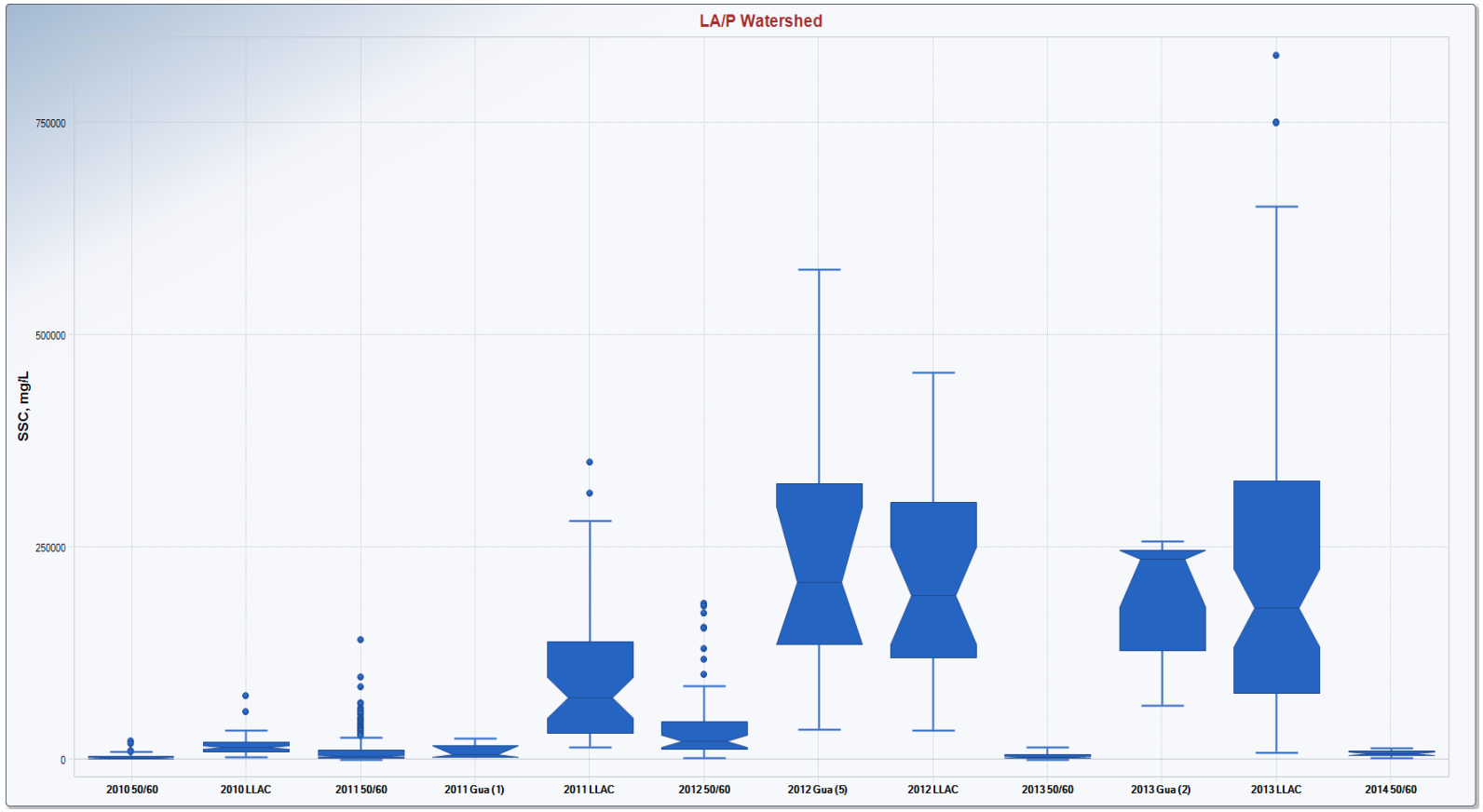

The greatest increase in SSC was observed for Guaje and LLAC locations after the fire in 2012 and 2013. Guaje median concentrations were higher than LLAC for those years. There was an increase in sediment transport for 50/60 in 2012. The plot confirms that the relative difference between 50/60 and LLAC changed dramatically since the fire in 2011.

Figure 127. Time plot of Pu 239/240 in LA/PCW.

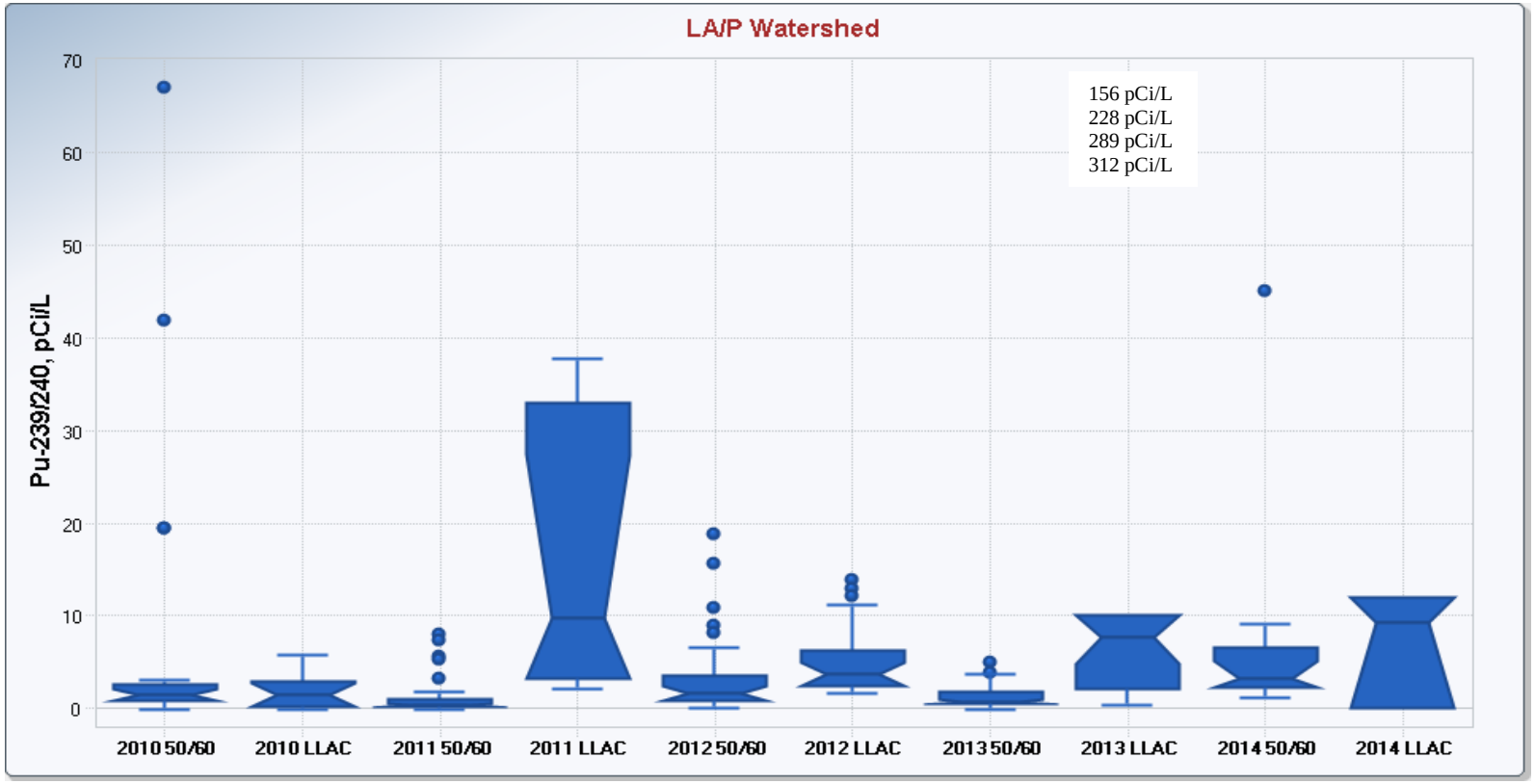

* The results 156 pCi/L, 228 pCi/L, 289 pCi/L, and 312 pCi/L from LLAC (9/12/2013) do not show in the box plot.

The highest Pu-239/240 concentrations in storm water were detected in 2011 at the LLAC even though the greatest SSC discharges for that sampling location occurred in 2012. That fact alone indicates that the fire exposed contaminated sediments and within the same season, mobilized and transported them downstream from their sources to the lower LA Canyon. In the post-fire years, concentrations diminished substantially although the storm water concentrations have not returned to their pre-fire values. Even though the outlier concentrations were quite different, the box concentrations at 50/60 remained similar throughout the years, suggesting lesser fire damage or no additional contaminated sediments exposed by the fire.

Figure 128. Time plot of Pu 238 in LA/PCW.

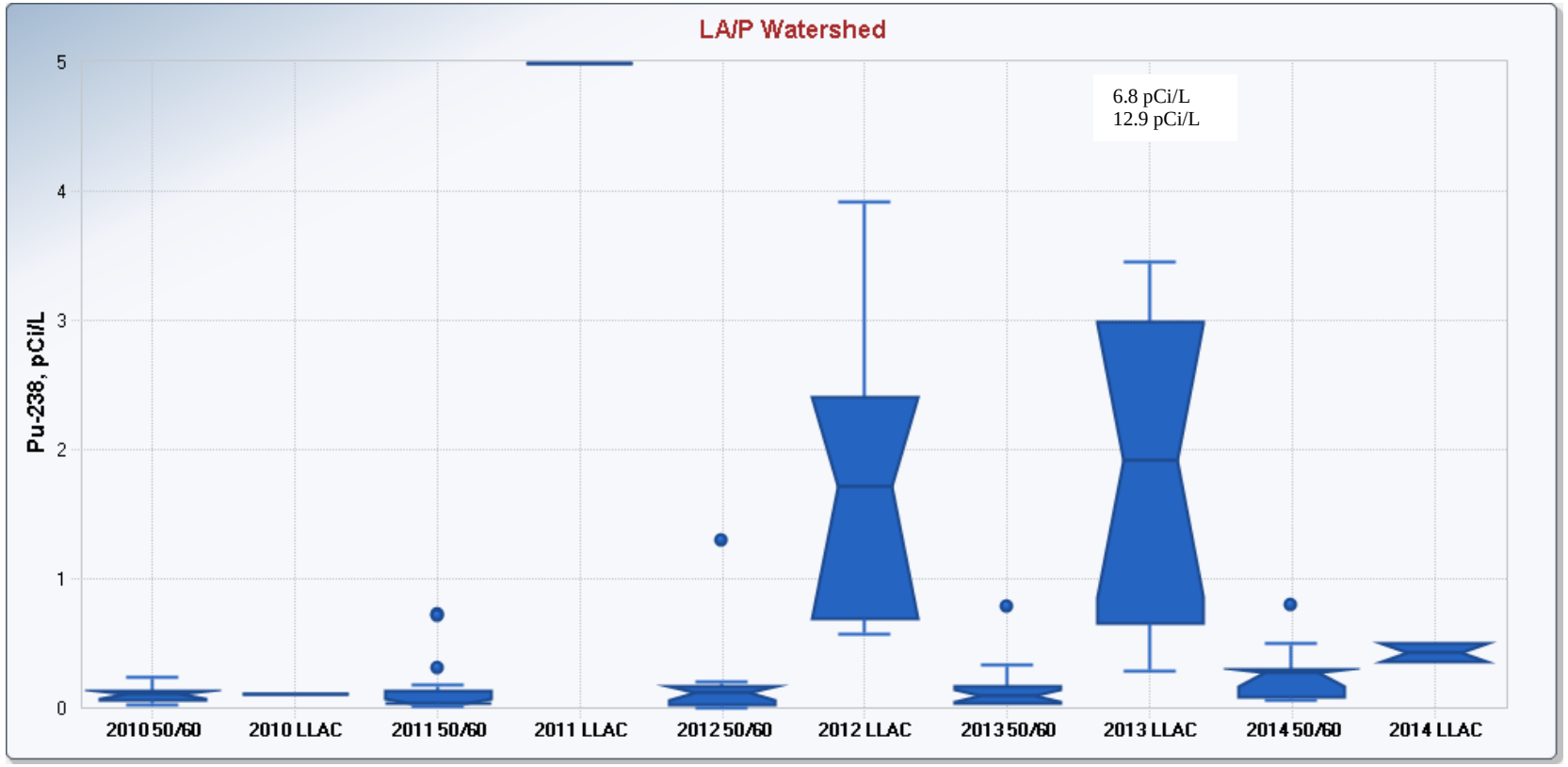

* The results 6.8 pCi/L and 12.9 pCi/L from LLAC (9/12/2013) do not show in the box plot.

The Pu-238 concentrations in storm water follow the SSC trend with maximum in 2012 and 2013 in LLAC, which indicates that the distribution of Pu-239/240 and Pu-238 in the LA/P Canyons watershed is different. The deposits of Pu-238 were not as readily exposed by the fire in 2011 as Pu-239/240 sediment deposits, suggesting different time-frame of release or different source(s) for this contaminant. The 50/60 concentrations remained at similar range for the five monitoring years.

Figure 129. Time plot of Am 241 in LA/PCW.

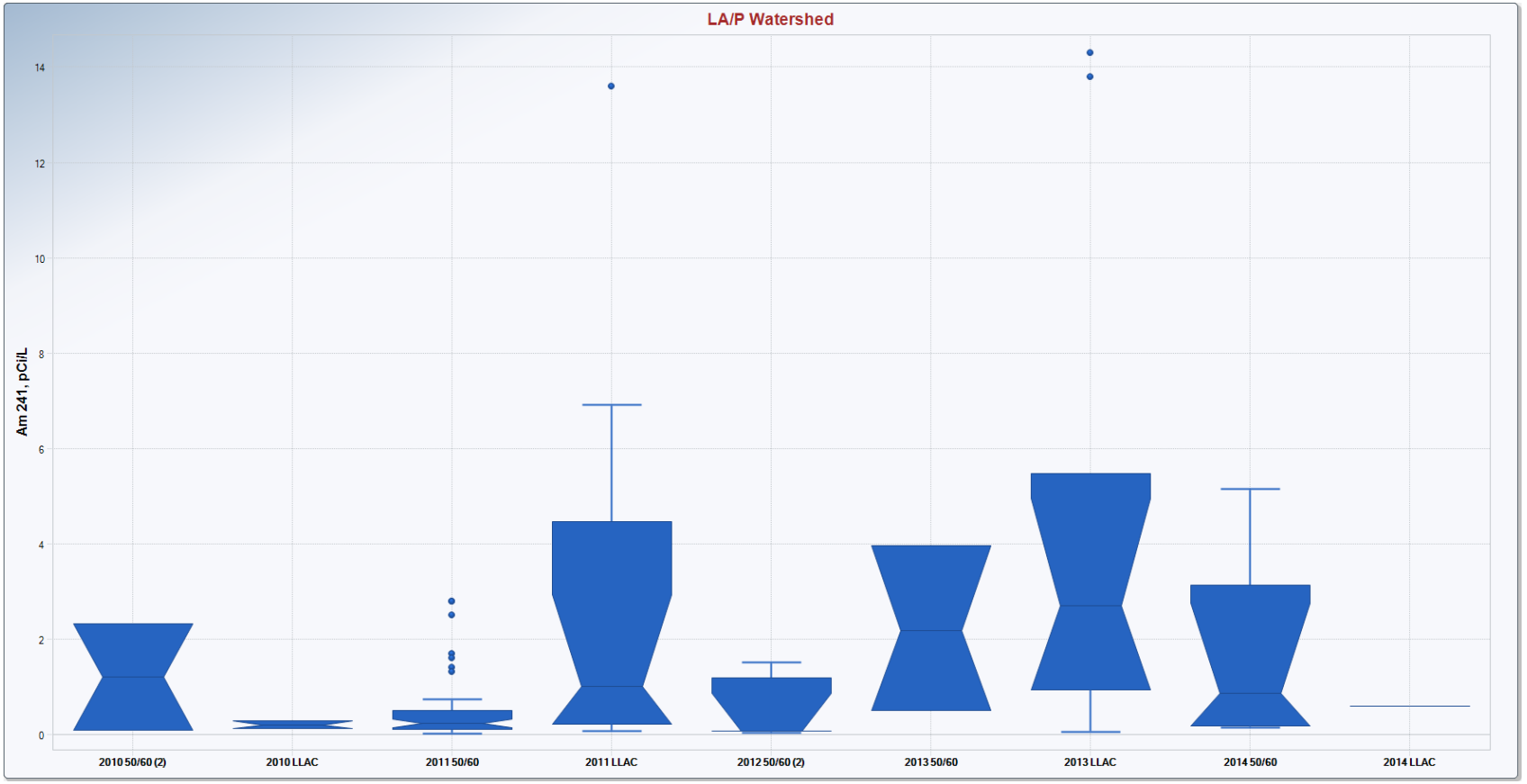

The Am-241 concentrations in storm water were not as abundant in detected values as other radionuclides. Any conclusions on potential trend should be taken with caution. One interesting fact was that in 2013, central tendencies and the 95th percentile at 50/60 and LLAC were twice greater than in 2011.

Figure 130. Time plot of Sr 90 in LA/PCW

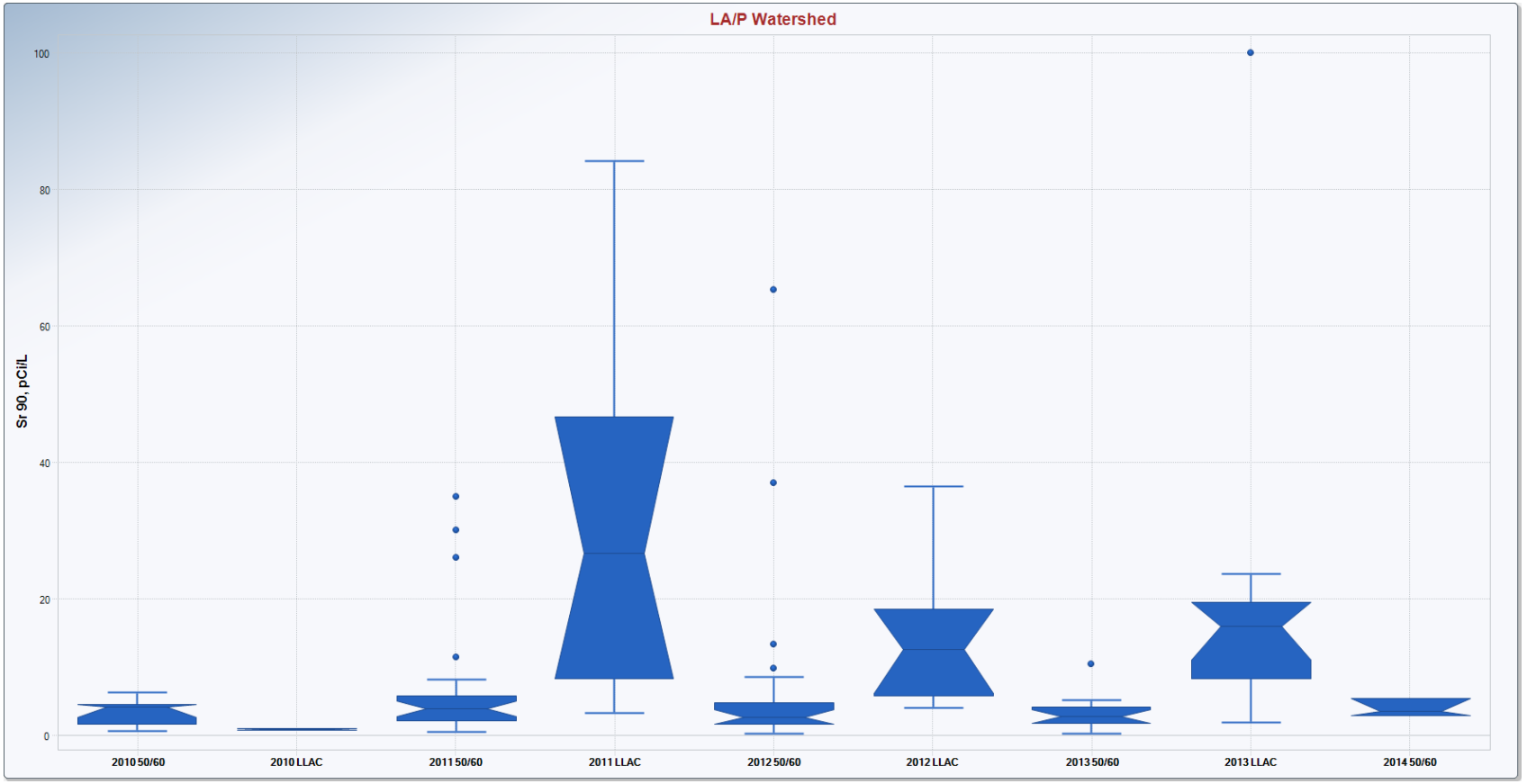

The trend of Sr-90 concentrations in storm water in LLAC was identical to Pu-239/240 with maximum concentrations in 2011, which decreased in post-fire years. That fact indicates that the fire exposed contaminated sediments, and within the same season mobilized and transported them downstream from the sources to the lower LA Canyon. The range of box concentrations at 50/60 was similar with maximum values (the outliers) occurring in 2011 and 2012.

Figure 131. Filtered vs unfiltered Sr 90 in LA/PCW.

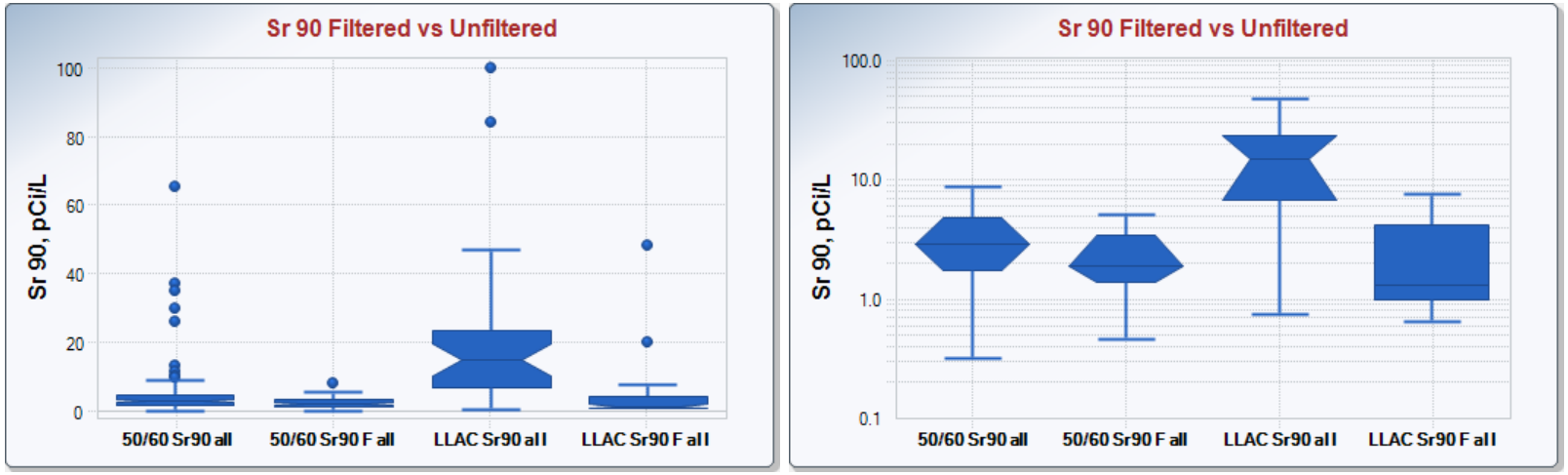

The Sr-90 concentrations of the filtered samples were also presented in Attachment 6. The concentrations of unfiltered samples in 50/60 and LLAC were quite different but the ranges of concentration for filtered samples at the same locations were similar. That fact may indicate that an additional strontium complex/compound, which was not water soluble, was present in LLAC, may be formed during the fire (may be burned particles and debris containing Sr-90.)

Figure 132. Time plot of Cs 137 in LA/PCW.

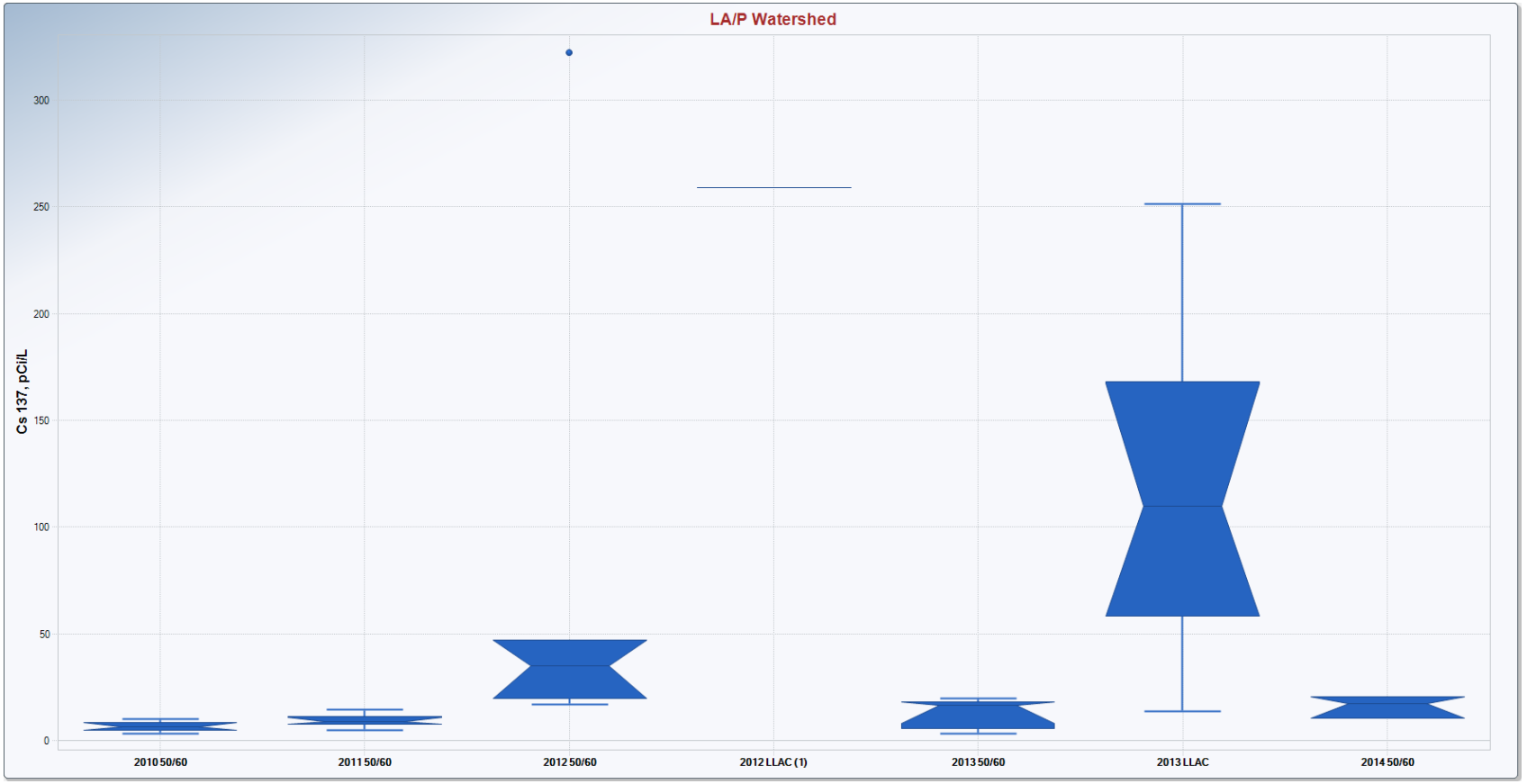

Cs-137 is another contaminant that had only limited detected values. At 50/60 location, the highest concentrations occurred in 2012. Even though they have reduced values in the post-fire years, pre-fire concentrations have not been achieved.

Figure 133. Time plot of U 234 in LA/PCW.

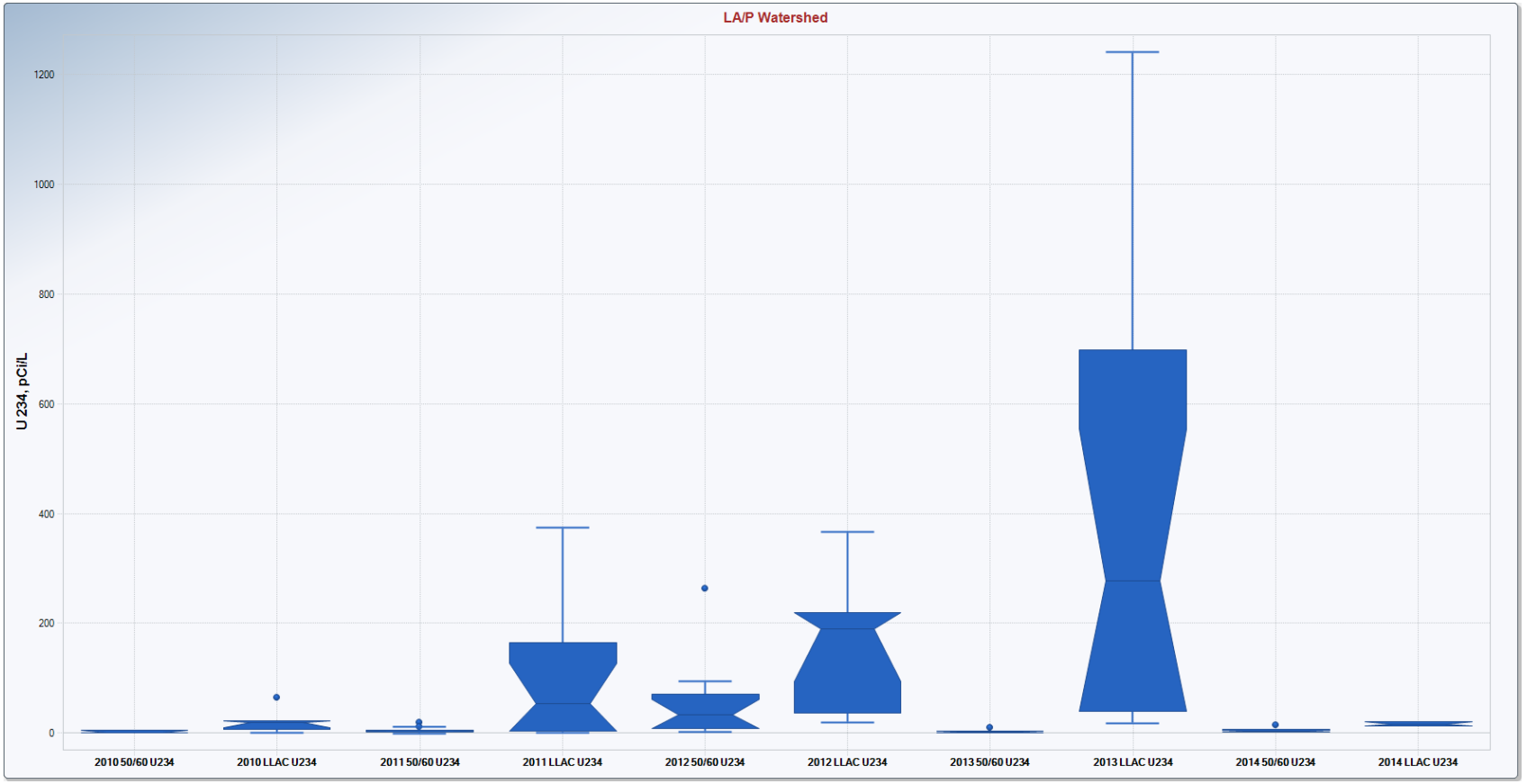

The effect of the fire on U-234 concentrations appears as a delayed response with the highest concentrations occurring at 2013 (LLAC).

Figure 134. Time plot of U 238 in LA/PCW.

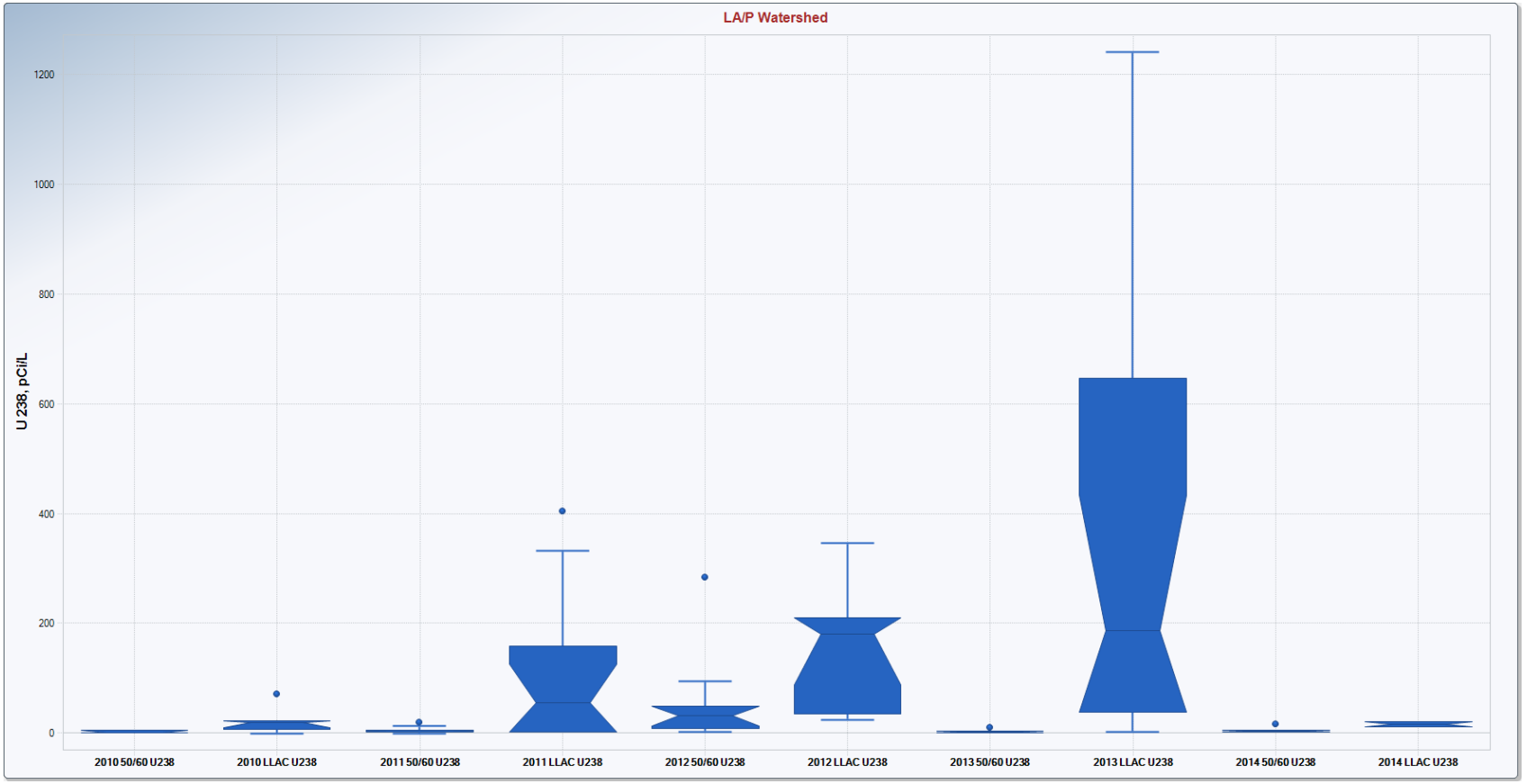

The U-238 trends were almost identical to U-234, with their maximum concentrations detected in 2013.

Figure 135. Time plot of U 235 in LA/PCW.

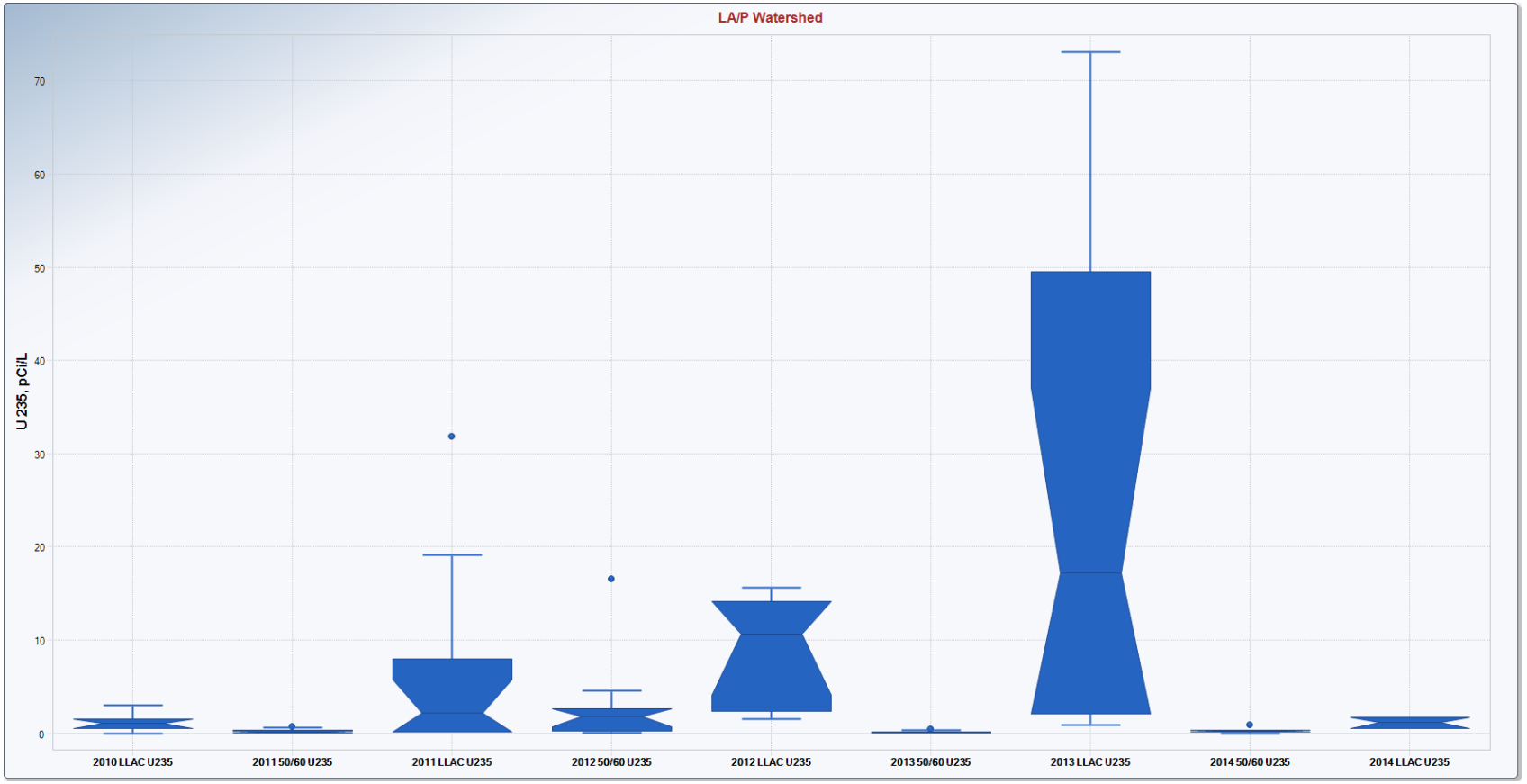

The U-235 trends follow the other uranium isotopes trends which is the expected result in case of the same source.

VII.3.b Annual Variations of Organics

Figure 136. Time plot of total PCBs in LA/PCW.

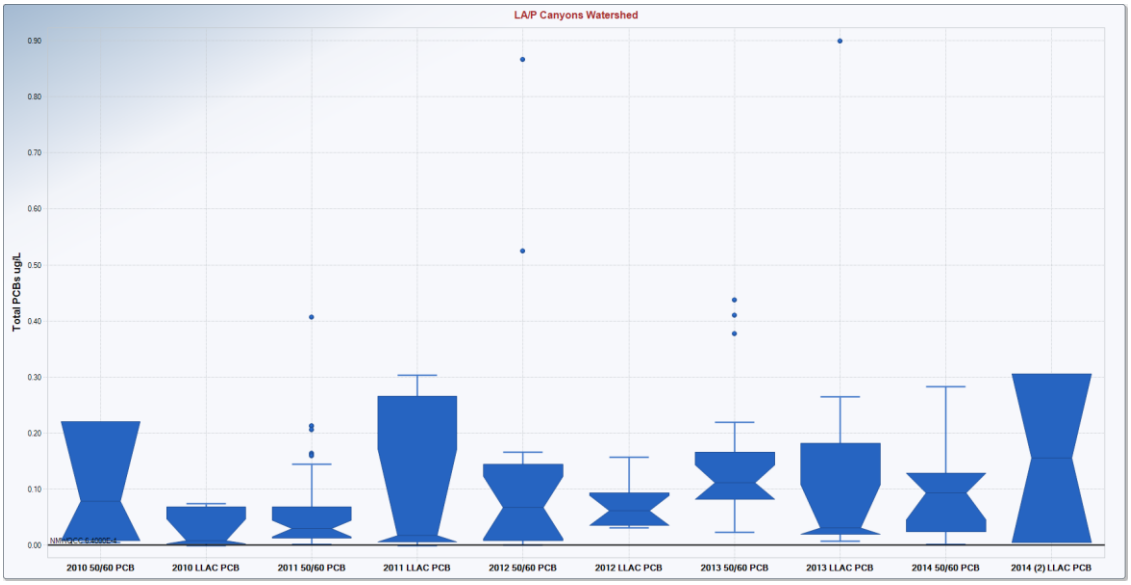

Most results of total PCBs in LA/PCW exceeded the NMWQCC standard for surface water. There was a small change in the outlier values during and post-fire, but the majority of values for total PCBs remained in similar range throughout the monitoring period. This fact suggests that the fire did not influence the contaminant source(s) for PCBs, or that the distribution and transport of these constituents may be different than for radionuclides.

Figure 137. Time plot of Dioxins/furans in LA/PCW.

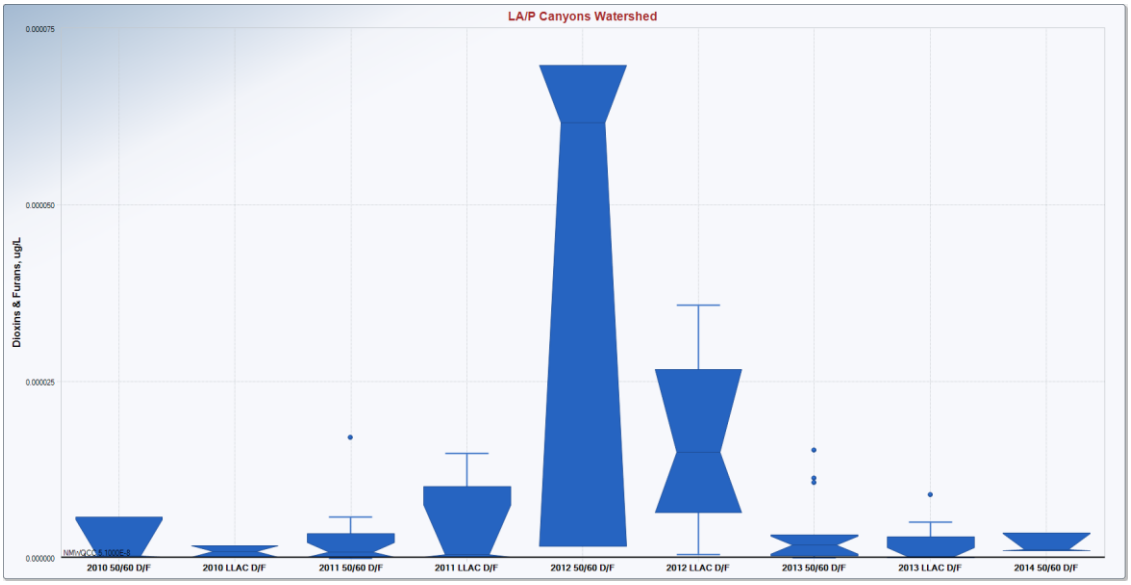

The D/F trends appear similar to some of the radionuclides, with very high concentrations in 50/60 and LLAC in 2012. The 50/60 data indicates that in 2014 the pre-fire concentrations were achieved.

VII.4 Trends from E050/E060 to BDD

VII.4.a Storm Water Trends for Radionuclides

Storm water trends were generated for selected constituents in geographical order from the source "50/60" in middle Los Alamos Canyon, through Guaje and LLAC to the RG (Otowi), and finally to BDD sampling location. The box plots represent the distributions of constituents with their outliers, and the inset – the shape of the boxes on logarithmic scale so that the shapes of the distributions can be compared to each other, with the outliers being omitted automatically by the software. The box plots were created by the EPA program ProUCL, and the boxes represent the 25^{th}, 50^{th}, and 75^{th} percentiles, and the whiskers and outliers were determined using the interquartile range (IQR) method. The sampling locations named on the graph are short for the data from the following sampling stations, listed in Table 2 and Table 3:

- 50/60 location means the combined data from E050 and E060 sampling stations, sampled by LANL and NMED, from 2010 to 2014. The NMED and LANL sampling stations were within 50 feet of each other.
- Guaje location means the combined data from all sampling locations near gage station E099 in Los Alamos Canyon, sampled by LANL and NMED with sampling period specifically marked in Attachment 6. The exact locations for all four sampling stations were presented in Figure 138.
- LLAC location means the combined data from all sampling locations in lower Los Alamos Canyon, LANL and NMED. The locations were presented on Figure 7 and Figure 9.
- Otowi location means the combined data from all NMED sampling locations near Otowi Bridge with sampling period specifically marked in Attachment 6. The approximate locations were presented on Figure 9.
- BDD location means the combined data from all sampling locations at BDD intake from 2005 to 2014, sampled by BDD and NMED.

The storm water distributions represent the concentrations of detected values only as determined by the laboratory qualifiers. BDD staff made an effort to select data for this section as close to the monitoring period as possible (from 2010 until 2014). Whenever samples were not collected or non-detects were a large percent of the data, the selected period was expanded from 2005 until 2014 or even from 2000 until 2014, and for Otowi from 1990 to 2014.

Figure 138. Guaje canyon sampling locations.

Figure 139. SSC in storm water from E050/E060 to BDD.

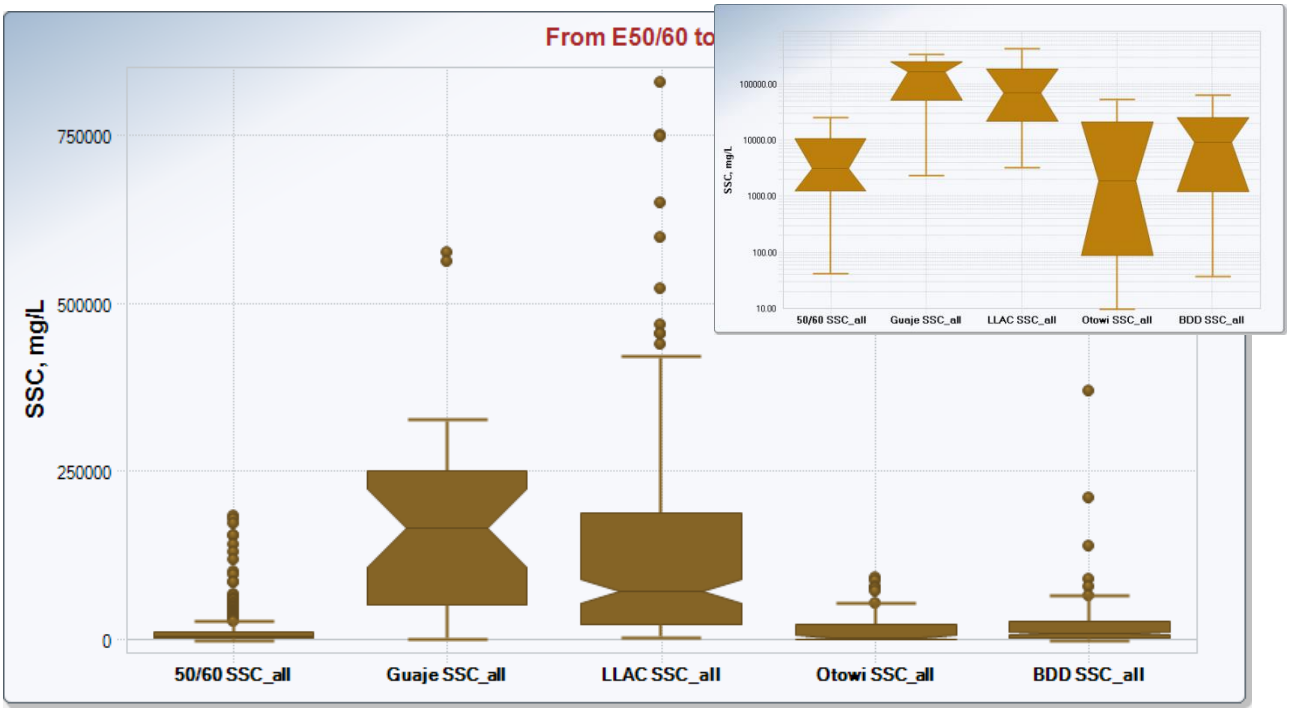

Figure 139 plots the SSC for the different sampling locations. With the exception of the four large outliers at LLAC, the Guaje location had the highest values, which is a confirmed result from Figure 140 (LA-UR-15-21413, May 2015). However, such result is not expected due to the watershed area in Figure 141 developed using the AcrHydro data model and published by LANL in (LA-UR-12-24822, September 2012) and in (LA-UR-15-21413, May 2015).

Figure 140. Box plots for TSS and SSC for all stations in LA/PCW.

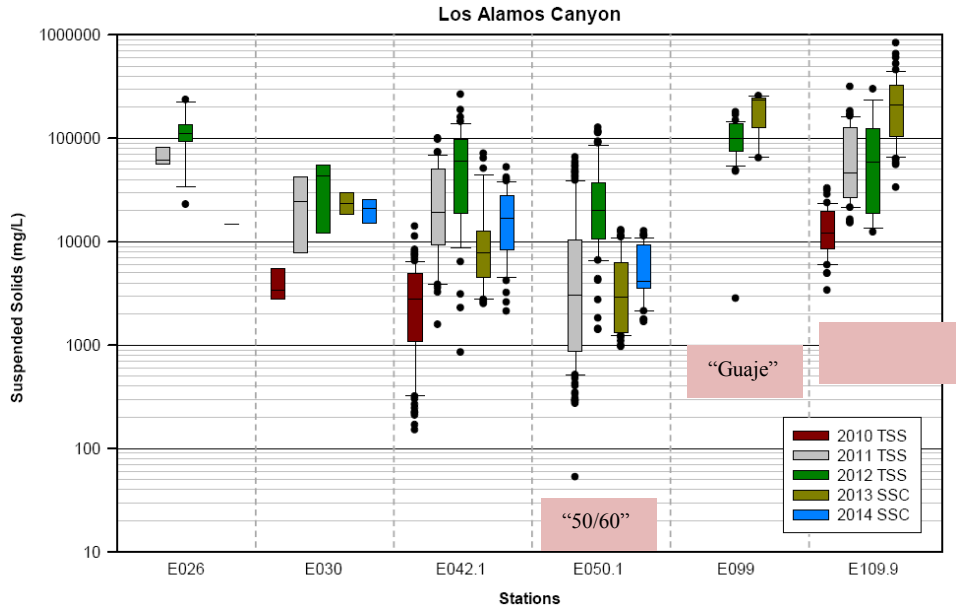

Figure 141. LANL gage station drainage areas in Los Alamos Canyon.

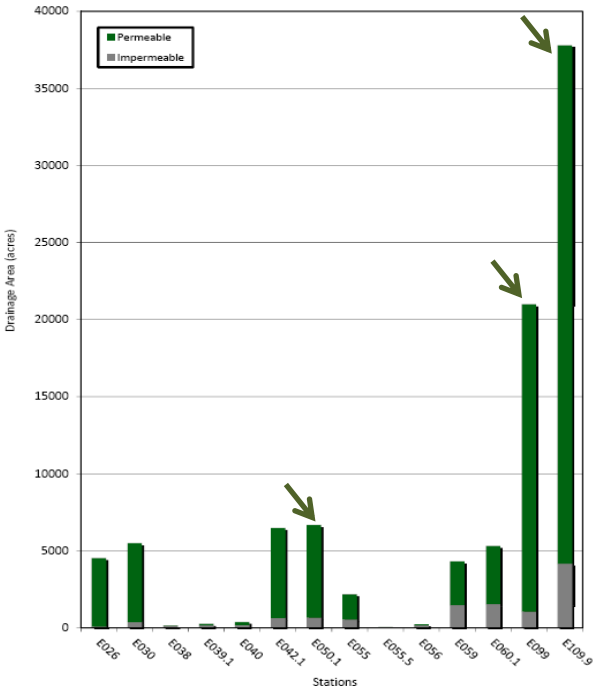

Canyon	Gaging Station	Drainage Area (acres)	Impermeable Surface (%)
Acid	E055.5	53	81
Acid*	E056	237	70
Acid	Acid Canyon above E056	290	72
Pueblo	E055	2191	25
Pueblo*	E059	1827	39
Pueblo*	E060.1	1006	8
Pueblo	Pueblo Canyon above E060.1	5310	29
DP	E038	144	88
DP*	E039.1	112	29
DP*	E040	133	24
DP	DP Canyon above E039.1	256	62
DP	DP Canyon above E040	388	49
LA	E026	4534	2
LA*	E030	960	30
LA*	E042.1	601	12
LA*	E050.1	195	11
LA*	E109.9 (including Guaje Canyon)	25,800	8
LA	Los Alamos Canyon above E050.1	6680	10
LA	Los Alamos, Pueblo, and Guaje Canyons above E109.9	37,800	11
LA*	Los Alamos Canyon between E050.1, E060.1, and E109.9	4761	19
Guaje	E099	21,000	5

* Drainage area marked by an asterisk does not extend to head of watershed above gaging station. The drainage areas without an asterisk extend from the gaging station to the head of the watershed.

The gages of interest are marked with arrows on Figure 141. The drainage areas of E050.1 and E109.9 are different with E109.9 watershed being substantially larger than E050. The collected run off and the corresponding SSC follow the same increasing trend, the higher the drainage area, the higher the SSC. However, while the drainage area of E109.9 is about 70% larger than E099, the collected runoff and SSC at E109.9 were much lower than at E099. With such high values in SSC from Guaje Canyon which is considered to be least contaminated tributary of LACW, we would expect a large dilution of contaminants downgradient from that location.

The SSCs at BDD and Otowi are almost one order of magnitude less than in LA/PCW. When comparing the BDD SSC values with respect to the Otowi values, BDD could be considered a subset of the Otowi distribution, since it is within the range of the Otowi values. However, it is clear that the BDD box percentiles are higher than the Otowi percentiles and this demonstrates the influence of the LA/PCW suspended sediment during the monitoring period. The influence of the LA/PCW is so strong that when we conducted a comparison of the central tendencies (mean/median) of the two distributions (both being non-parametric) using the ProUCL, the result was that these two central tendencies did not represent samples from the same population with very high confidence level (greater than 99%).

Because the LA/PCW contaminants of concern transport mainly via suspended sediment, developing a better understanding of the fluvial processes at the confluence of the Los Alamos Canyon with the RG is of most importance to this project.

Figure 142. Pu-239/240 in storm water* from E050/E060 to BDD.

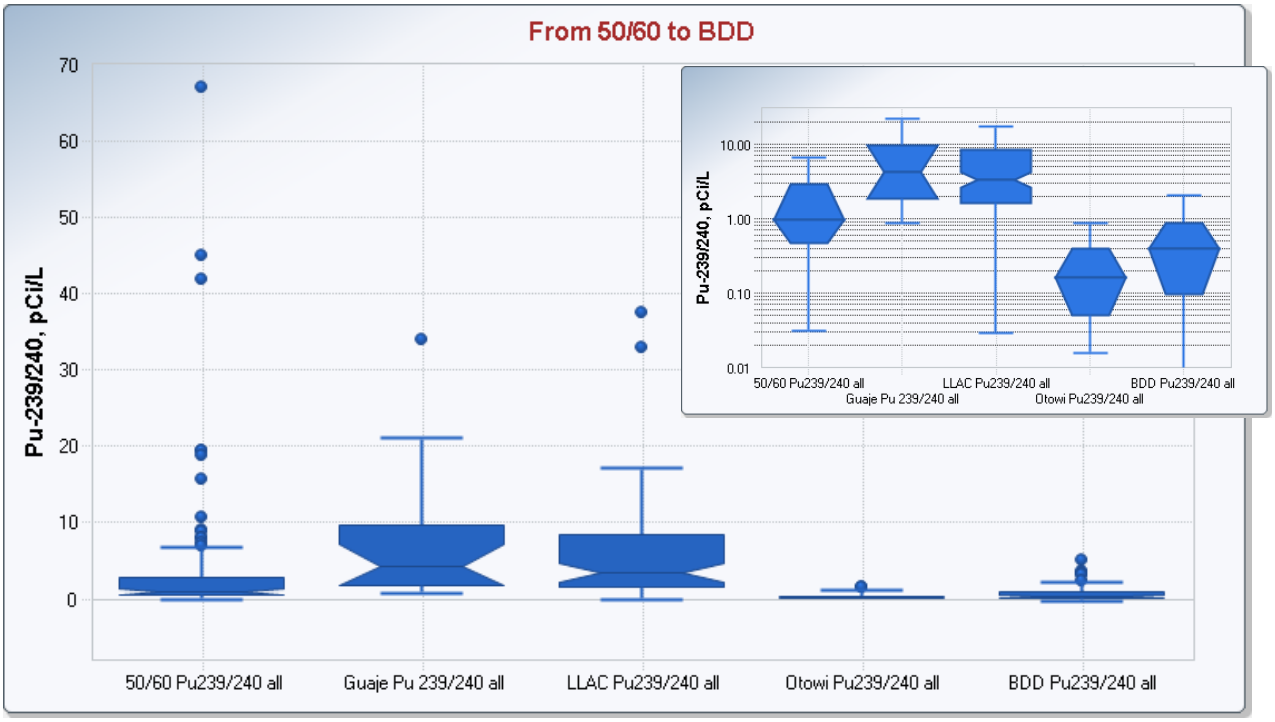

* The outliers 156 pCi/L, 228 pCi/L, 289 pCi/L, and 312 pCi/L from LLAC (9/12/2013) were not shown on the box plot.

Figure 142 indicates that the concentrations of Pu-239/240 downgradient from 50/60 increased as a result of the higher SSC. The trend almost follows the SSC trend with the Guaje concentrations (of the box) being higher than the LLAC's. The relative differences between Guaje and LLAC concentrations are not as high as in SSC suggesting dilution at LLAC, probably due to the less contaminated Guaje storm water contribution. The Pu-239/240 concentrations in sediments (see Figure 153) at those locations also confirm that dilution at LLAC occurred (concentrations of the box percentiles) most probably due to the less contaminated sediment from Guaje.

Similarly to SSC, the Pu-239/240 storm water concentrations at BDD are of one order of magnitude less than in LA/PCW, but all percentiles of the box were higher than at Otowi. As with SSC trend, the difference between these two sites could be attributed to the LA/PCW influence during storm events, and the higher concentrations are most probably due to contamination entering the RG at the confluence. To investigate how substantial the difference between BDD and Otowi was, we ran statistical tests on the central tendencies of these two samples, and for non-parametric distribution of both sets, Gehan test (with non-detects) and Tarone-Ware test (with non-detects) demonstrated that these two samples do not belong to the same population which confirms the strong influence of the LA/PCW to the storm water concentrations at BDD.

Figure 143. Pu-238 in storm water* from E050/E060 to BDD.

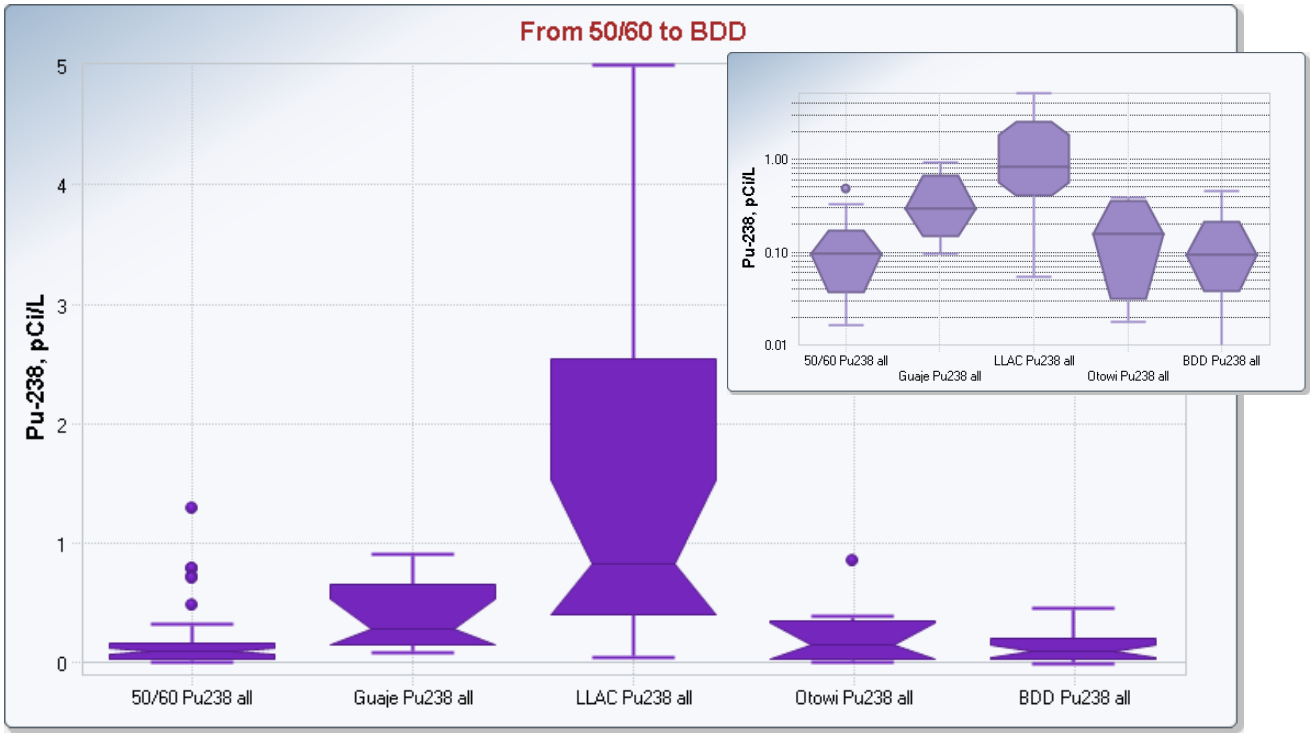

* The outliers 6.8 pCi/L and 12.9 pCi/L from LLAC (9/12/2013) were not shown on the box plot.

The Pu-238 storm water concentration trend and the sediment trend showed similar to the Pu-239/240 trends. The storm water concentrations steadily increased throughout the LA/PCW with their maximum values occurring at LLAC, but the sediment concentrations (Figure 154) indicated a dilution along the Los Alamos Canyon.

At BDD the storm water concentrations of Pu-238 were one order of magnitude lower than in LLAC. With a few exceptions, most storm water concentrations at BDD were lower than the Otowi's. This fact also confirms the fewer exceedances of RG background identified in Figure 58. However, even though the storm water concentrations at BDD were less than at Otowi, the BDD sediment concentrations on Figure 154 were higher than at Otowi for all percentiles of the box and the upper whisker, confirming the influence of the LA/PCW on BDD concentrations.

Figure 144. Am-241 in storm water from E050/E060 to BDD.

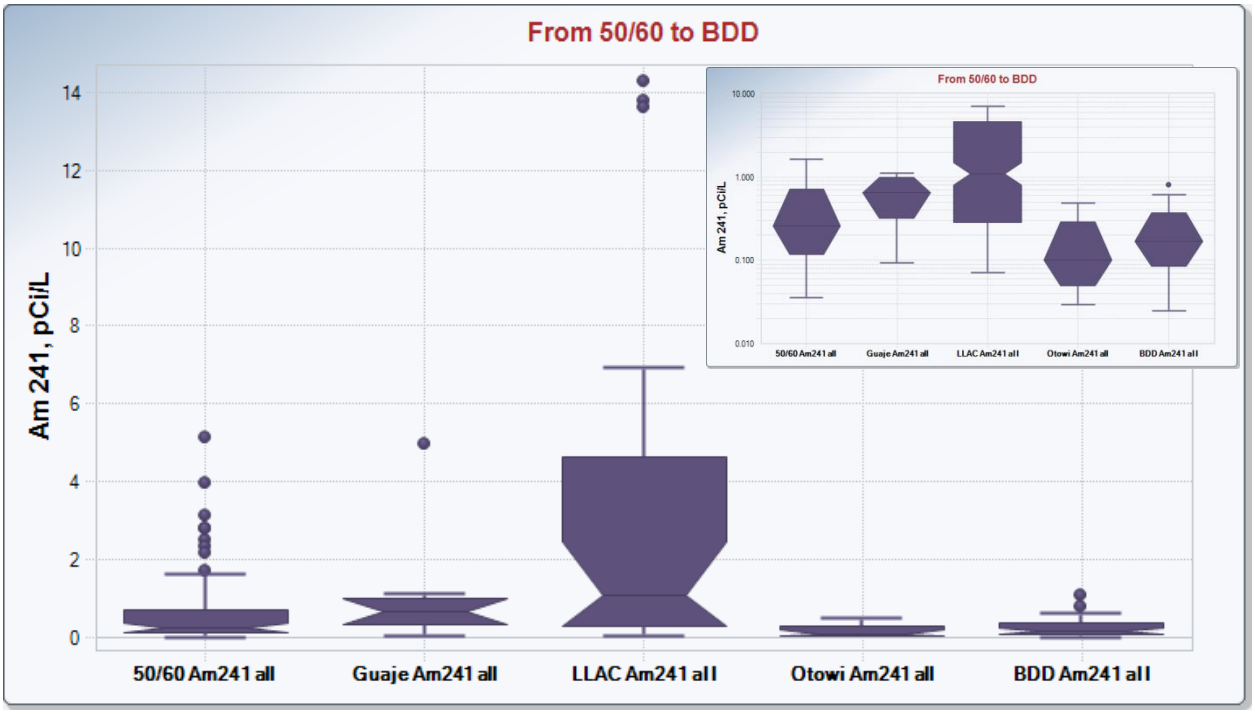

The Am-241 storm water concentrations steadily increased throughout the LA/PCW with their maximum values at LLAC, but the sediment concentrations in Figure 155 decreased substantially in Guaje (probably due to sediment dilution), but increased again in the LLAC, indicating contaminated sediments that might have been "picked up" after the Guaje confluence. This suggests a different source or different fate and transport than the plutonium's sources.

At BDD the storm water concentrations of Am-241 were one order of magnitude lower than in LLAC. All percentiles of the box at BDD were higher than the concentrations at Otowi, confirming the influence of the LA/PCW on BDD concentrations.

Figure 145. Sr-90 in storm water from E050/E060 to BDD.

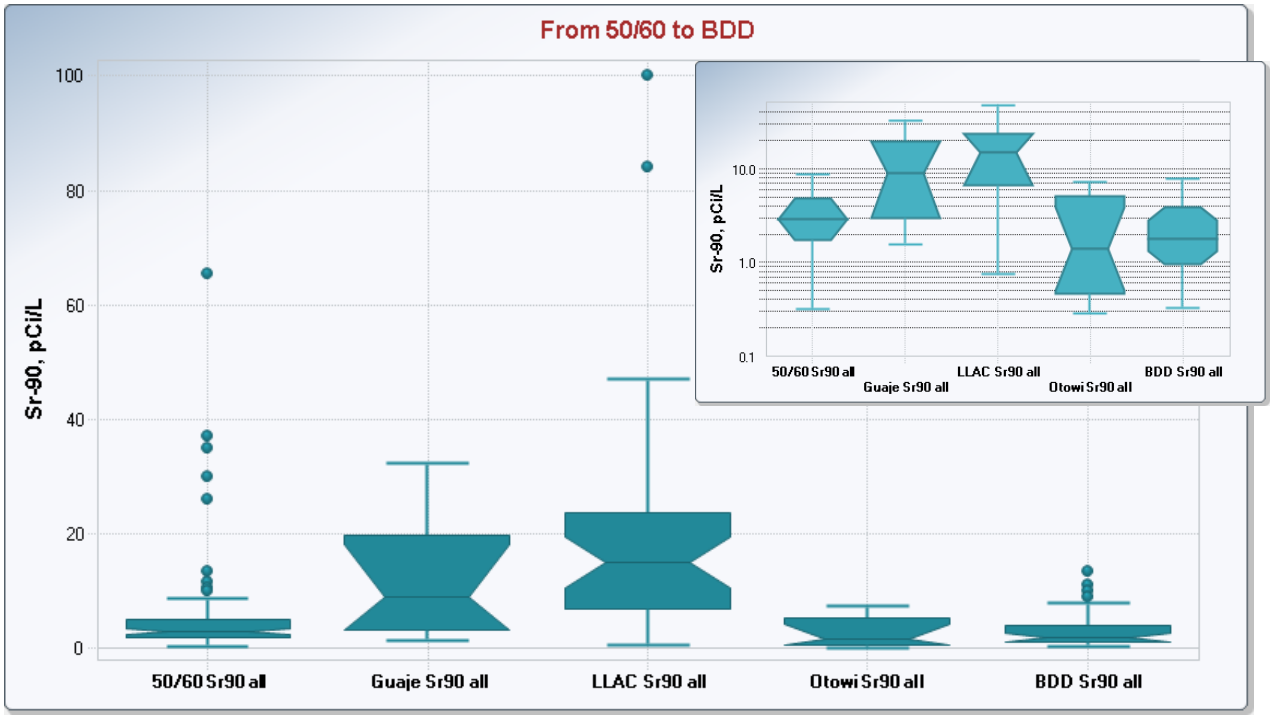

The Sr-90 storm water concentrations steadily increased throughout the LA/PCW with their maximum values occurring at LLAC, but the sediment concentrations in Figure 156 decreased substantially in Guaje (probably due to sediment dilution), but increased in the LLAC, indicating contaminated sediments that might have been "picked up" after the Guaje confluence. The sediment concentrations on Figure 156, show the expected trend of decreased concentrations near Guaje due to dilution by less contaminated sediments, and increasing concentrations at LLAC. The storm water concentrations at BDD were well within the Otowi range, but the outliers were higher than the Otowi concentrations. The boxplot sediment concentrations at BDD (Figure 156) were greater than the same at Otowi confirming the LA/PCW influence on the transport of Sr-90.

The storm water results from the filtered samples of Sr-90 shown on Figure 146 have very different trends than the unfiltered ones. While the Guaje location concentrations were much lower than the 50/60 and in very narrow range, the LLAC concentrations were very similar to the source 50/60 and within the same range. This suggests that the main Sr-90 compounds were the same with the same solubility in water, but the extra Sr-90 concentrations at Guaje and LLAC shown in the unfiltered concentrations may be associated with very different Sr-90 complex most probably generated in the fire.

Figure 146. Sr-90 in storm water, filtered, from E050/E060 to BDD.

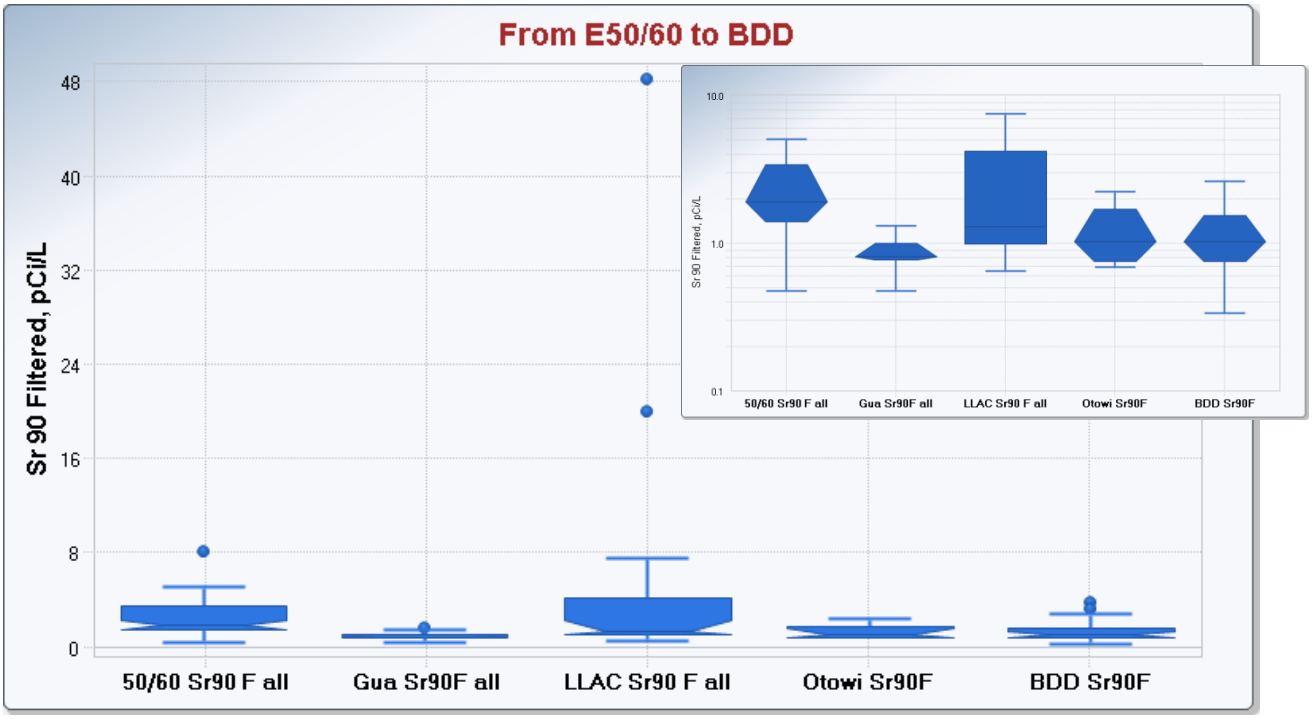

Figure 147. Cs-137 in storm water from E050/E060 to BDD.

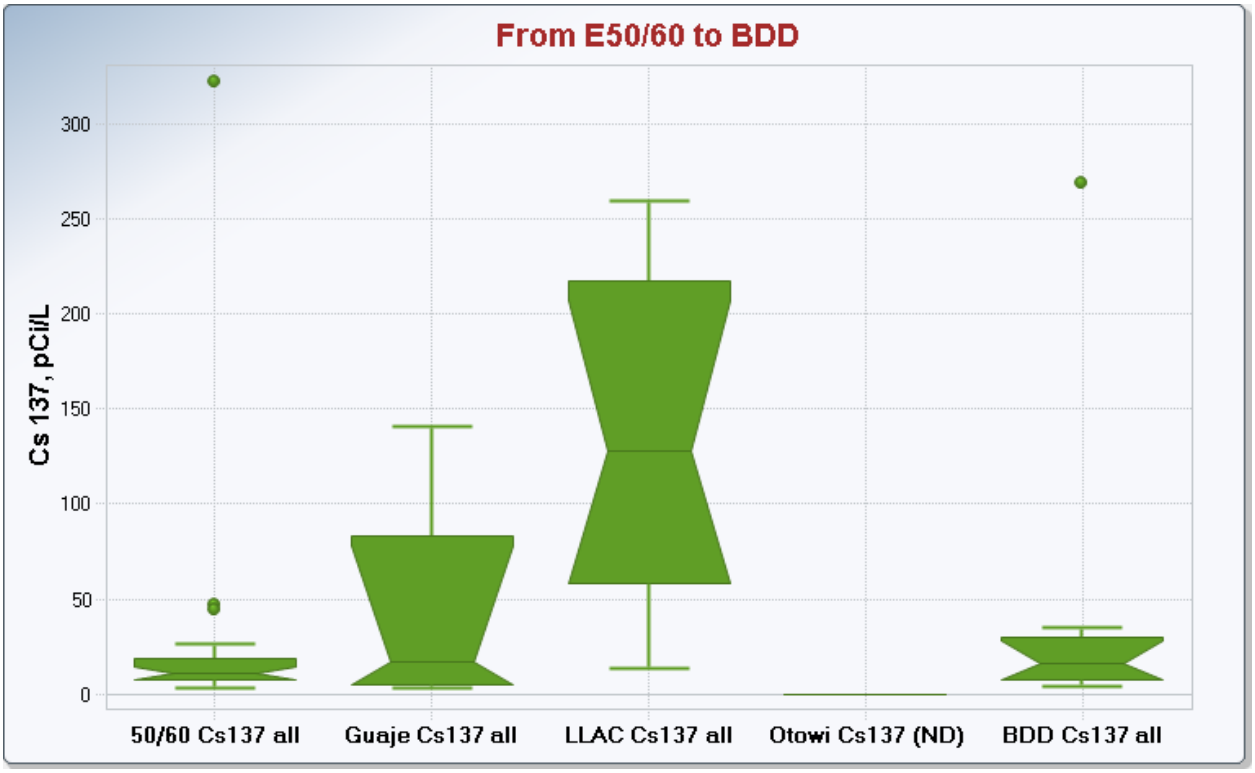

Similarly to other radionuclides, the Cs-137 storm water concentrations steadily increased throughout the LA/PCW with their maximum values occurring at LLAC. The sediment concentrations of Cs-137 on Figure 157 followed an opposite decreasing trend with its lowest concentrations at Guaje. The few storm water concentrations at BDD were higher than the Otowi non-detect results, most probably due to the LA/PCW influence.

Figure 148. Ra-226 in storm water from E050/E060 to BDD.

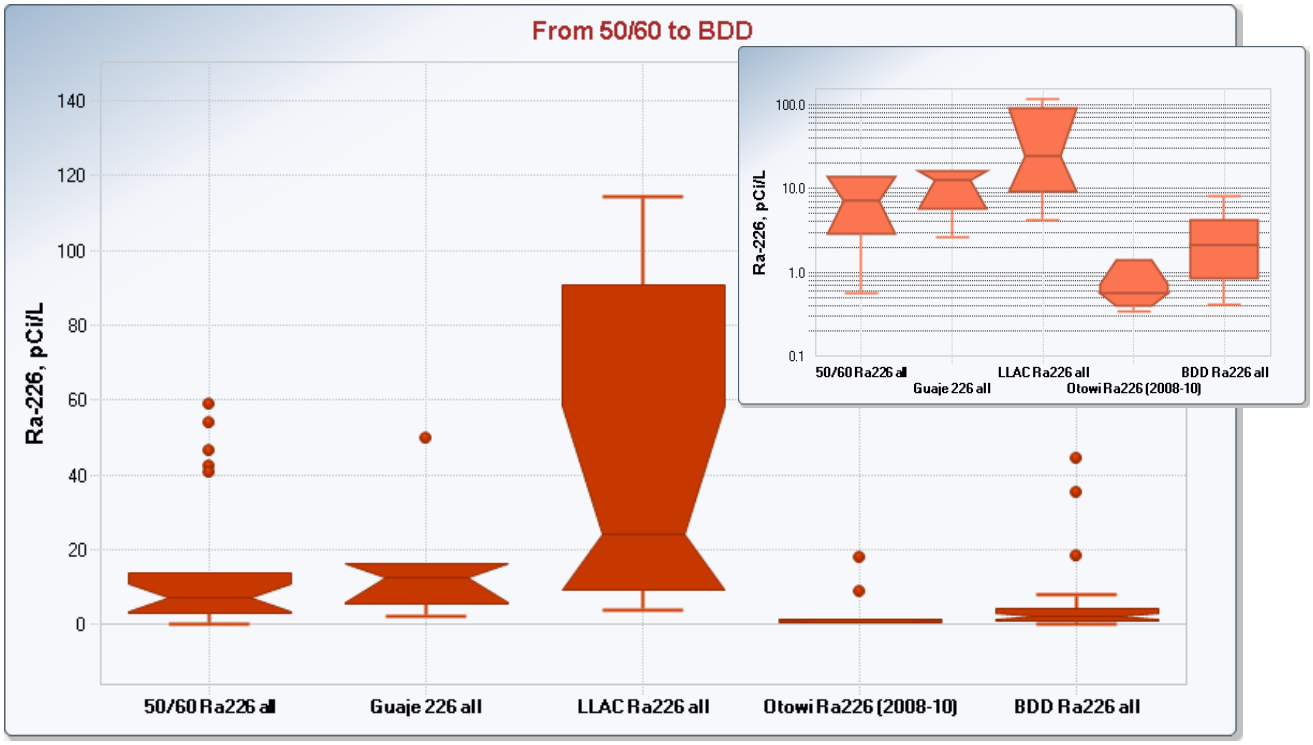

* The outliers 272 pCi/L (8/3/2013) and 672 pCi/L (8/9/2013) from LLAC were not shown on the box plot.

The Ra-226 and Ra-228 storm water concentrations show different trends, which indicate different source(s). The fact that Ra-228 in storm water (Figure 149) at Guaje (only three values in that set) is much higher than in other sampling locations may indicate a potential natural source of this radionuclide since Guaje Canyon is the least contaminated from the tributaries of LACW. The methodical increase of Ra-226 in storm water with its maximum concentrations at LLAC (Figure 148), may indicate that it is wide spread in LACW and that it may be derived from an anthropological source. The Ra-226 and Ra-228 storm water concentrations at BDD were higher than at Otowi, pointing out to LACW as the source. The difference between these two locations was substantial and confirmed by statistical tests comparing their central tendencies.

Figure 149. Ra-228 in storm water* from E050/E060 to BDD.

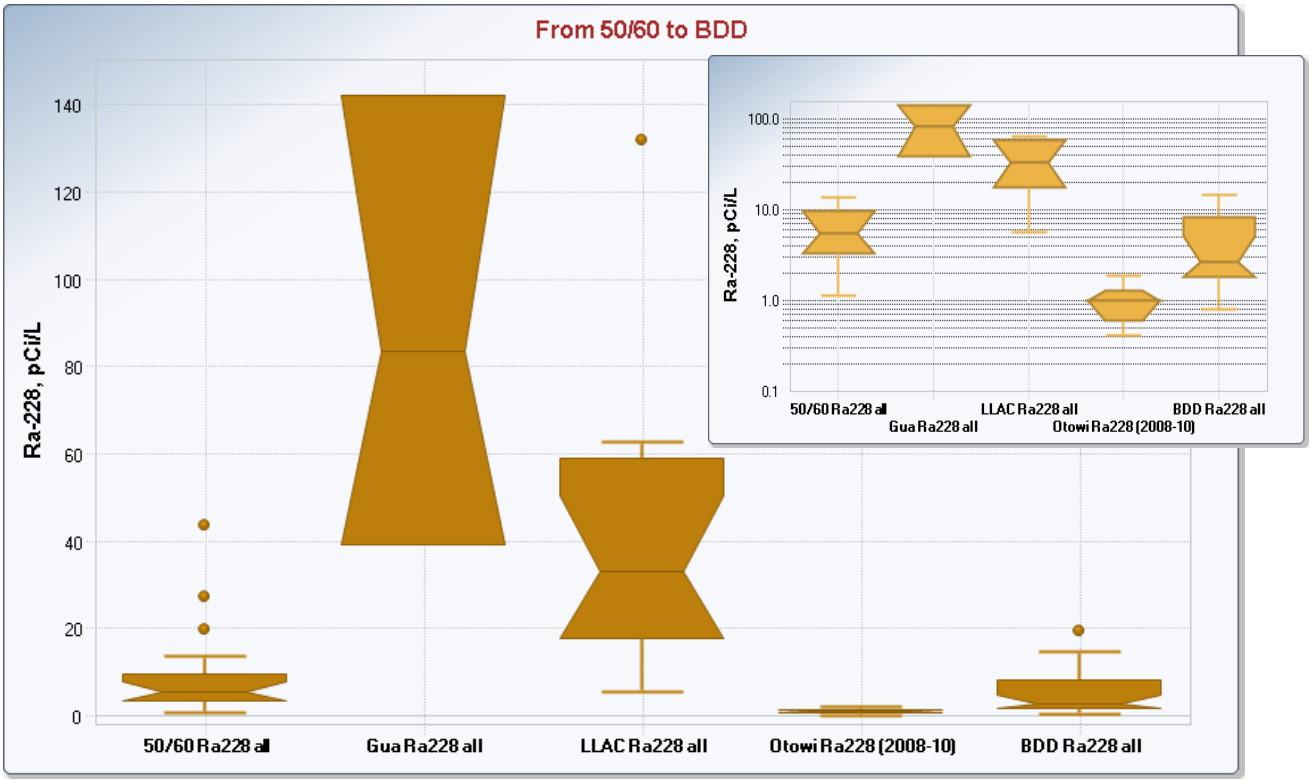

* The outlier 613 pCi/L (8/3/2013) from LLAC was not shown on the box plot.

Figure 150. U-234 & U-238 in storm water from E050/E060 to BDD.

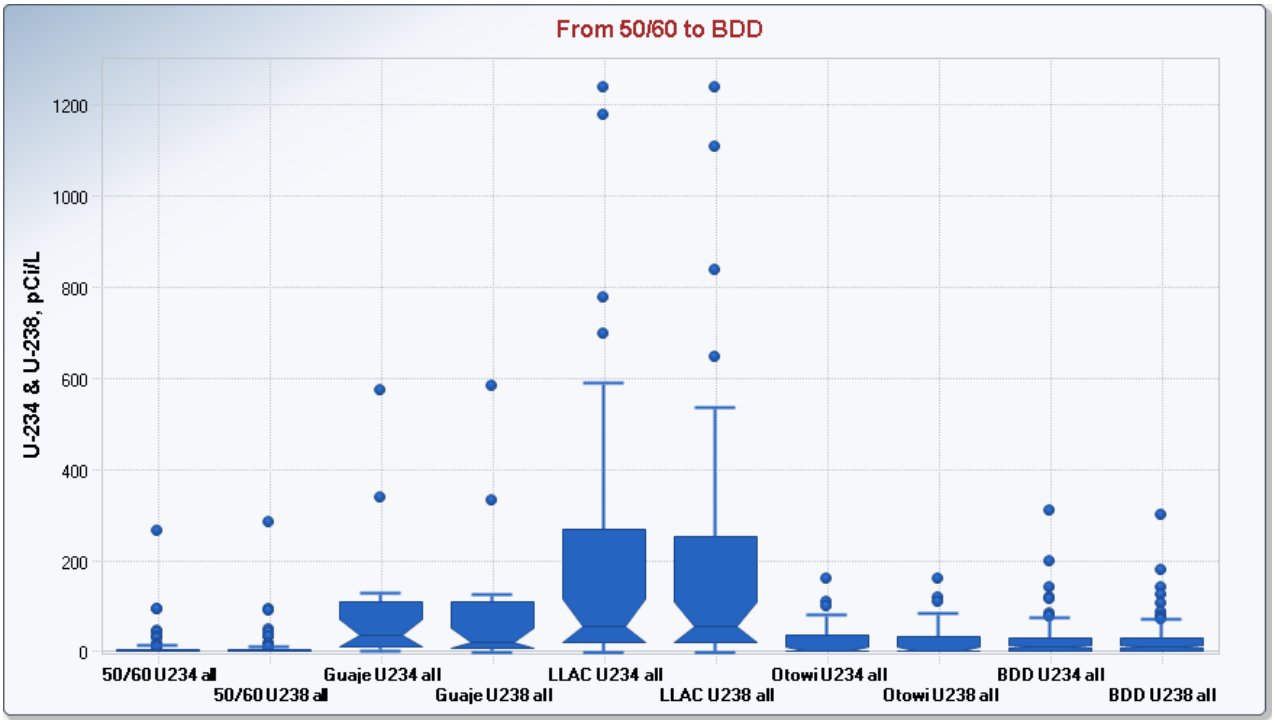

Figure 151. Shape of distribution U-234 & U-238 in storm water from E050/E060 to BDD.

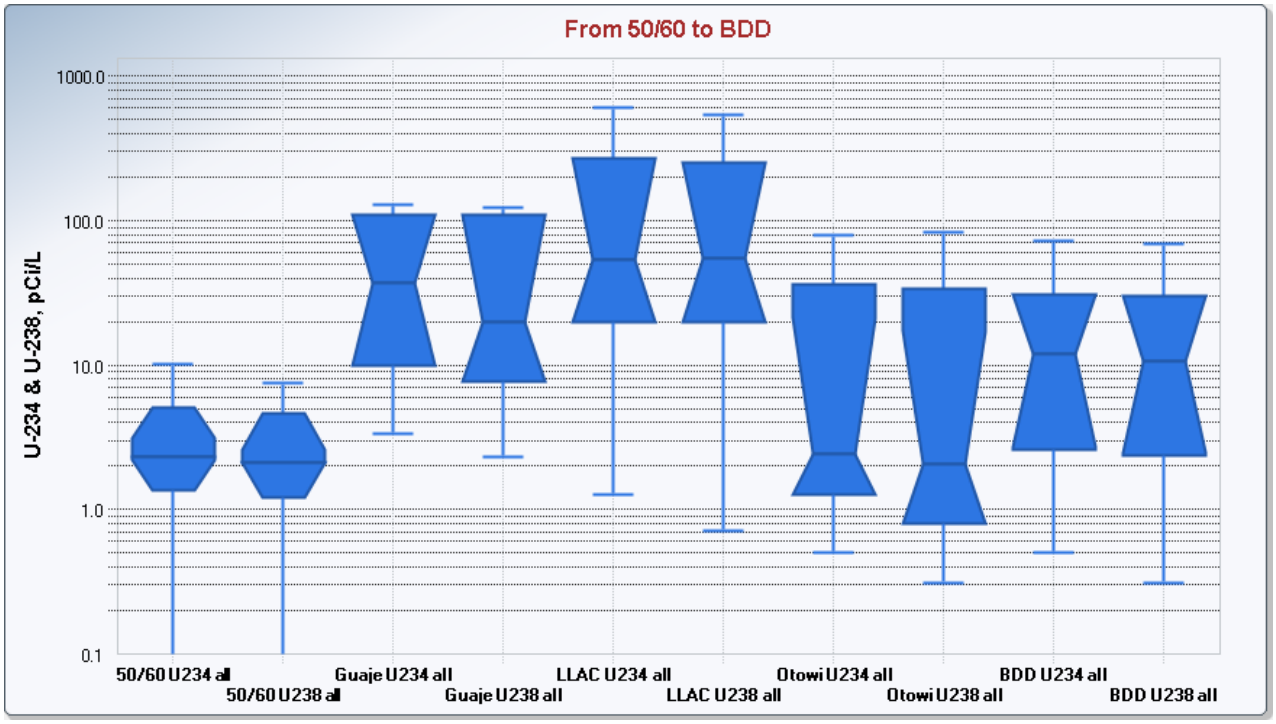

The concentrations of U isotopes in storm water followed the same trend for each isotope, steady increase from 50/60 to LLAC. The sediment concentrations displayed on Figure 158 through Figure 160 also showed the same for each uranium isotope, the "source" 50/60 had the highest concentrations, in Guaje the concentrations were much lower, and in the LLAC concentrations increased but never reach the 50/60 concentrations. The sediment concentrations in LAC were very similar in range for U-234 and U-238 with the maximum concentrations occurring in 50/60, but the concentrations of U-235 were different at the three sampling locations. This suggests different sources of this radionuclide, or potentially a mixture of natural and anthropological uranium.

The boxplots for BDD representing the storm water concentrations appear to be a subset of the Otowi concentrations, but when statistical tests comparing their central tendencies were run, it indicated that U-234 and U-238 concentrations were different at BDD and Otowi at 90% confidence levels, and for U-235, the Tarone-Ware test indicated different central tendencies at BDD and Otowi at 95% confidence level. The difference between these two sites indicates a potential contribution from the LACW on the U isotopes concentrations found at BDD, and that the concentrations might be a result of natural and anthropological sources.

Figure 152. U-235 in storm water from E050/E060 to BDD.

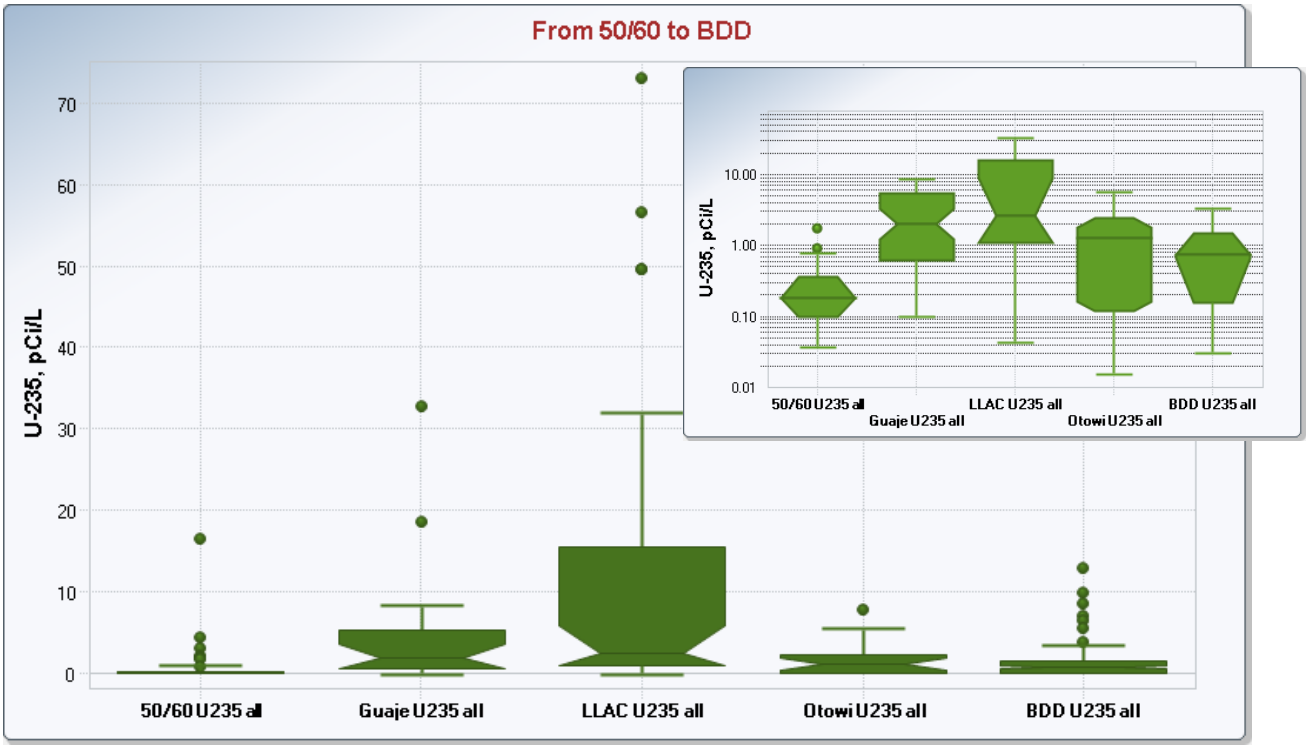

VII.4.b Sediment Trends of Radionuclides

This section describes the available data for radionuclides in sediments from 50/60 to BDD for a specific monitoring period which may be different for each site. The descriptive statistics of the presented data, and the monitoring periods were included in Attachment 6. The sediment data includes the results from the sediments from the Intellus database and all calculated sediments for BDD as presented in Attachment 5, the LACW calculated sediments for 2011 of the sites 50/60 and LLAC as calculated and included in (LA-UR-12-24822, September 2012), and for Cs-137 the calculated sediments from 2011 to 2013 at 50/60. Attachment 6 does not include the very high values detected at BDD on 7/22/2011 (4 hours after LAC storm event) for Cs-137 (791 pCi/g), U-234 (151 pCi/g), U-235 (5.5 pCi/g), and U-238 (175 pCi/g).

Most of the interpretation of the data sets comparing the distributions for all sites was included in the previous section. This section will focus on exceedances from the background values established for the Pajarito Plato (PP UTL) and the Rio Grande (RG UTL).

In addition, the Otowi and BDD sites were compared statistically (two-sample hypothesis) for radionuclides that provided sufficient number of data, to determine whether these two groups were different from each other. For Pu-239/240, Pu-238, Am-241, Sr-90, U-234, U-235, and U-238 the statistical comparison (using ProUCL, NDs included, Gehan, and Tarone-Ware tests) indicated that these two groups were different at 95% confidence level. Since most values at BDD had higher concentrations than at Otowi, the differences in central tendencies must be due to the higher concentrations of

radionuclides being delivered by the LACW storm water into the Rio Grande. Ra-226 and Ra-228 data sets at BDD and Otowi were compared and found to belong to the same populations. Cs-137 was not tested since it contained very few data points.

Legend of color lines in boxplots:
Red line represents the Max ND level for all datasets
Gold line represents the Pajarito Plateau UTL
Green line represents the Rio Grande UTL

Figure 153. Pu-239/240 in sediment from E050/E060 to BDD.

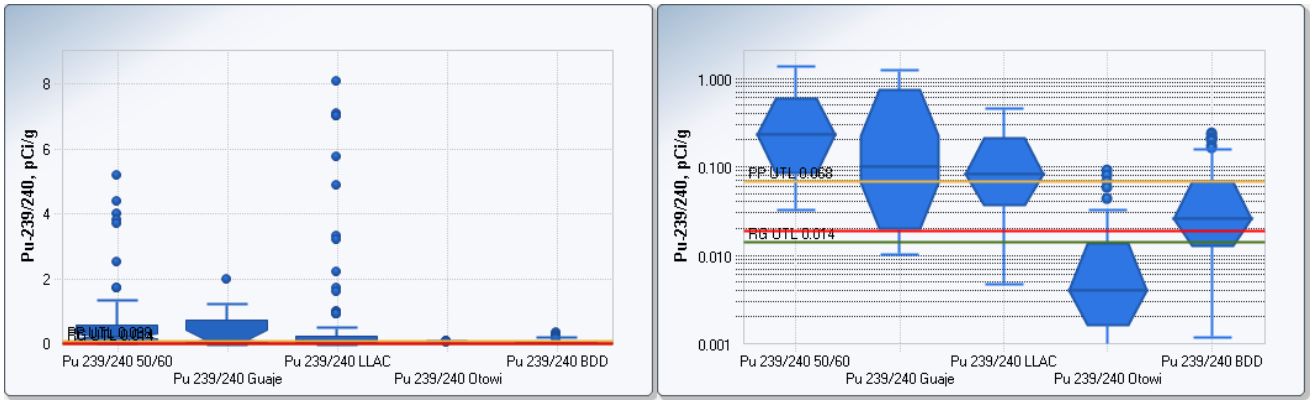

The Pu-239/240 concentrations exceeded PP UTL for all three sites in LACW. Most of the sediments concentrations "diluted" as they were transported down the Canyon, but the LLAC showed the highest concentrations as it can be seen from the identified outliers. The BDD Pu-239/240 concentrations exceeded the RG UTL more than 70 percent of the time, and exceeded the PP UTL 25 percent of the time. All corresponding percentiles of the BDD concentrations exceeded Otowi concentrations.

Figure 154. Pu-238 in sediment from E050/E060 to BDD.

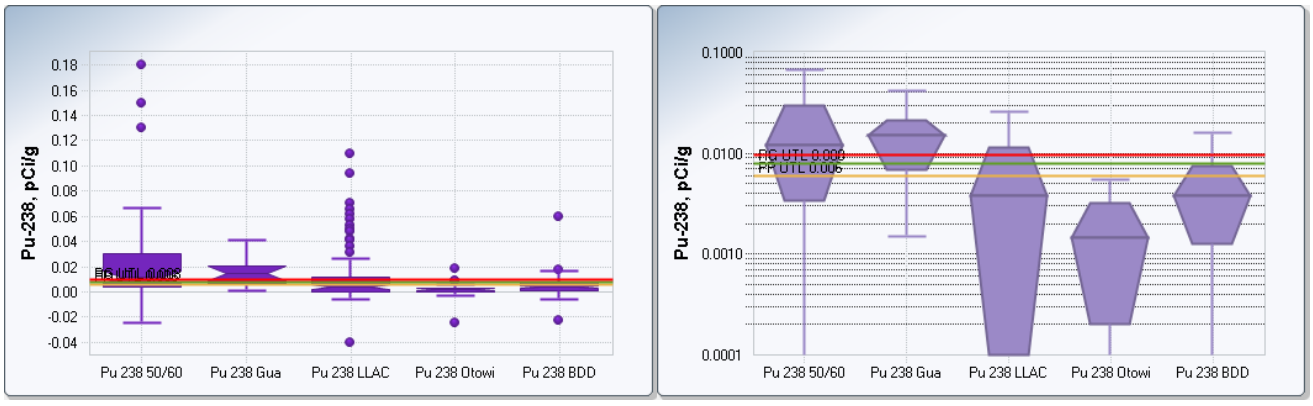

The Pu-238 concentrations were the highest at 50/60 and exceeded PP UTL about 50 percent of the time. The sediments concentrations "diluted" as they were transported down the LAC, although the identified outliers in LLAC were compatible to the 50/60 concentrations. The median value at Guaje was higher than at 50/60. There was also a large number of exceedances of the PP UTL in Guaje and LLAC. Except for the two outliers, all concentrations at Otowi were below both background levels,

and there were only a few exceedances of RG UTL at the BDD. Overall, the concentrations of Pu-238 were almost an order of magnitude less than of the concentrations of Pu-239/240 at all five locations.

Figure 155. Am-241 in sediment from E050/E060 to BDD.

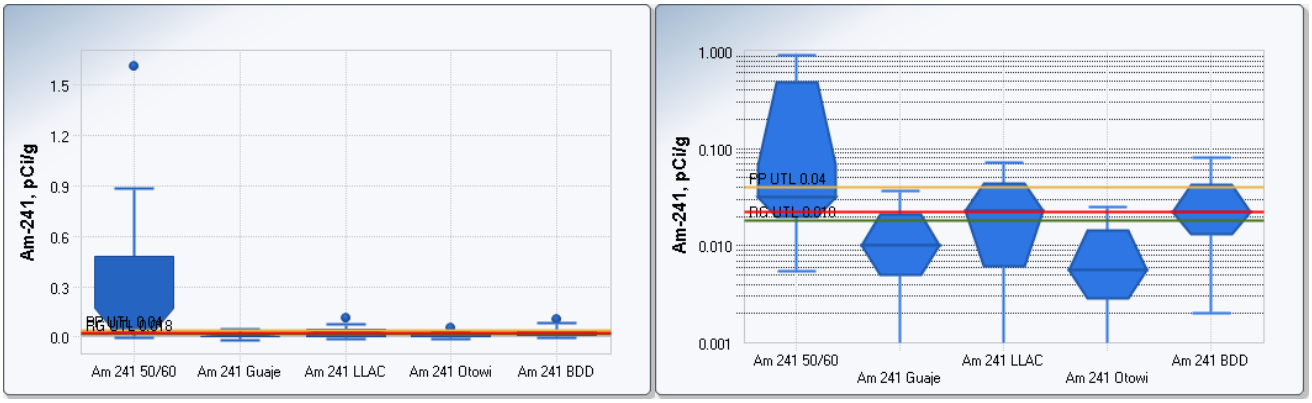

The Am-241 concentrations exhibited similar trend as other radionuclides, the concentrations decreased from the source 50/60. Most exceedances of the PP UTL occurred at 50/60, but more than 25% of the LLAC concentrations exceeded the PP UTL. All percentiles at BDD exceeded the corresponding Otowi percentiles, and more than 50 percent of the concentrations exceeded RG UTL.

Figure 156. Sr-90 in sediment from E050/E060 to BDD.

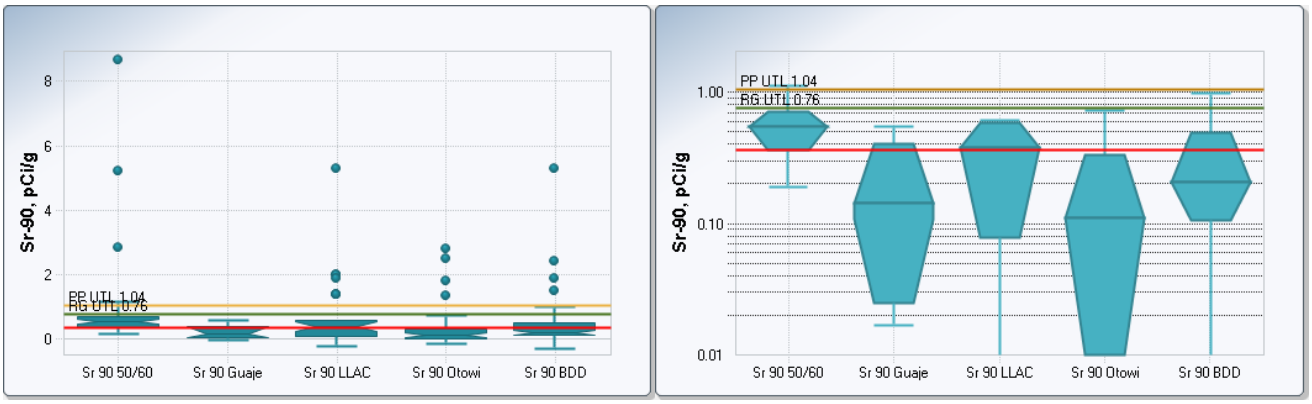

The Sr-90 concentrations exhibited similar trend as other radionuclides, but the relative differences of the concentrations between different sites were not as great. All outliers in LAC exceeded the PP UTL. The highest concentrations occurring in 50/60 and LLAC were similar in values as shown by the outliers. Most percentiles at BDD had higher concentrations than at Otowi but only a few concentrations exceeded the RG UTL.

Figure 157. Cs-137 in sediment* from E050/E060 to BDD.

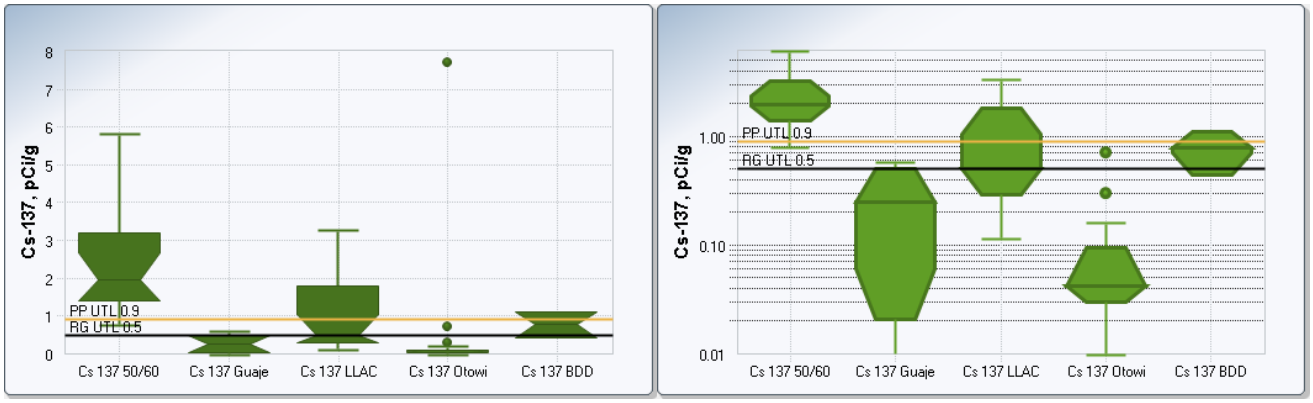

*The largest value of 791 pCi/g detected at BDD on 7/22/2011 23:45 was neither included on the graph nor in the descriptive statistics for that radionuclide.
Note: The RG UTL was marked with black line across the plot for these graphs only.

The Cs-137 concentrations were the highest at 50/60 and decreased with reaching LLAC, with the most sediment dilution occurring at Guaje. There were exceedances of PP UTL throughout the LAC. There were only a few detected values at BDD, so the box plot may not be a good representation of the distribution.

Figure 158. U-234 & U-238 in sediment* from E050/E060 to BDD.

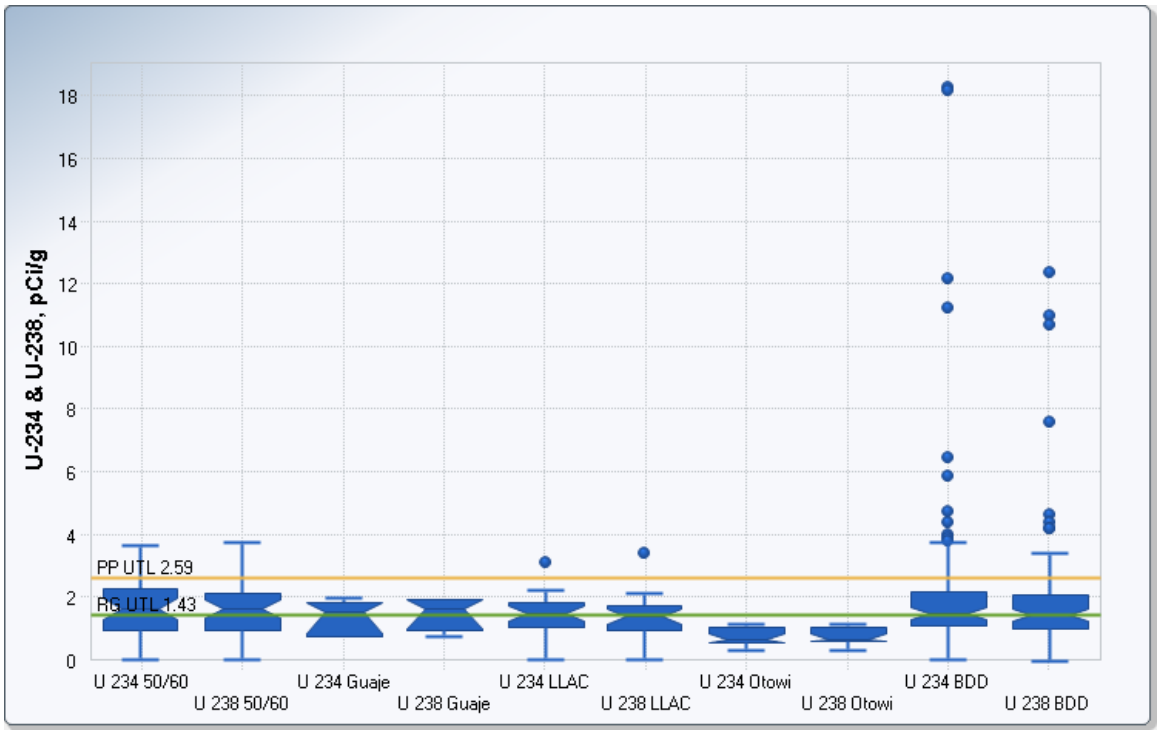

*The largest values of 151 pCi/g and 175 pCi/g for U-234 and U-238 detected at BDD on 7/22/2011 23:45 were neither included on the graph nor in the descriptive statistics for that radionuclide

The trends of U-234 and U-238 were similar so the concentrations of these two radionuclides were presented on the same graph. The uranium isotopes expressed very different behavior than the rest of

the radionuclides. The variations of their median values were not substantial throughout LAC. The upper range of the concentrations was the highest at 50/60 and decreased with distance from that location. There were only a few values that exceeded the PP UTLs at 50/60 only. The shapes of the distributions for U-234 and U-238 were found to be dissimilar, suggesting that different sources might have contributed to these concentrations.

Figure 159. Shape of distribution of U-234 & U-238 from 50/60 to BDD.

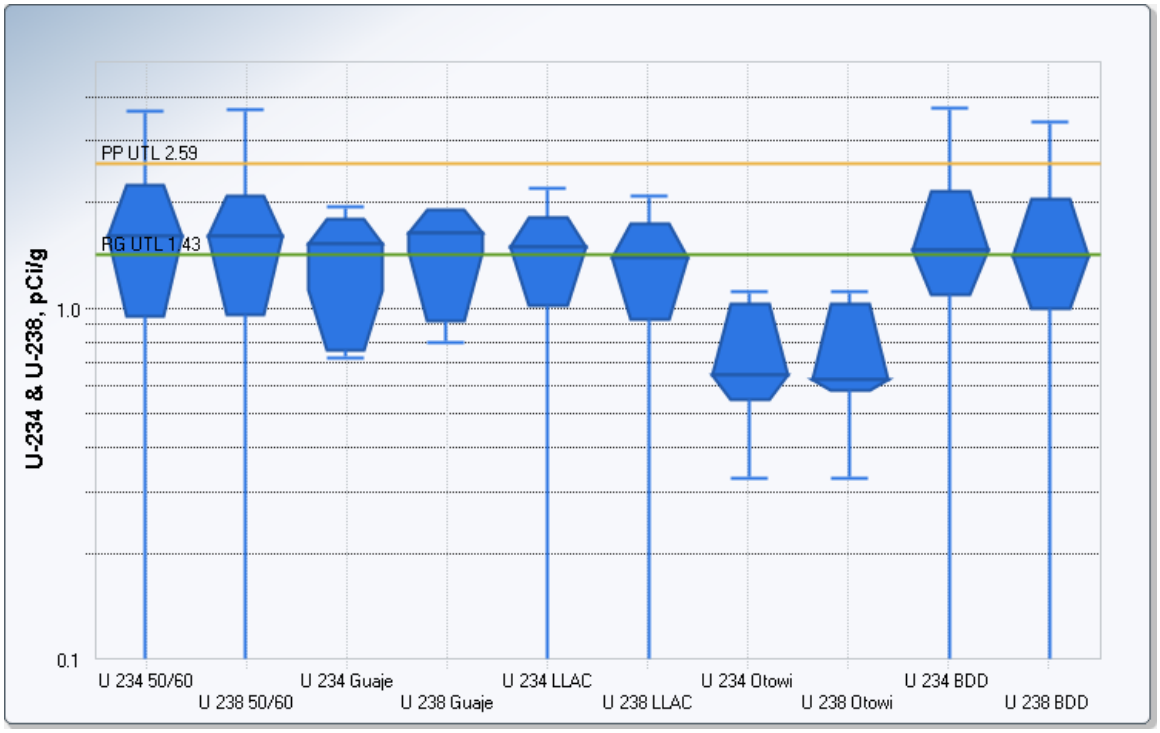

Note: The gold and green lines on the plot represent the PP UTL and RG UTL for U-234 only.

The most interesting results were the outliers at BDD. These were the highest concentrations found throughout the monitoring period of all sites. Figure 64 through Figure 66 indicate that these high values occurred from 2011 to 2013. The specific dates were identified in Attachment 5, and when compared to Table 8 through Table 10, it showed that these concentrations occurred during or after storm events of the LAC and at times during concurrent RG storm event. These facts point out to the LACW as the source of these highest concentrations, since 50/60 was the only sampling location that exceeded the PP UTL. The Otowi concentrations were all below the RG UTLs.

The U-235 trends on Figure 160 follow the earlier mentioned uranium isotopes pattern. There were no exceedances of the PP UTL for U-235 in the LAC, and only a few exceedances were recorded for Otowi and BDD. As an overall conclusion for the uranium isotopes, we can suggest that the data points out to a mixture between naturally occurring uranium and anthropologically changed uranium. However, since LANL has used in their operations naturally occurring uranium as described in (Englert, Dale, Granzow, & Mayer, 2007), then the source(s) for these isotopes cannot be determined.

Figure 160. U-235 in sediment* from E050/E060 to BDD.

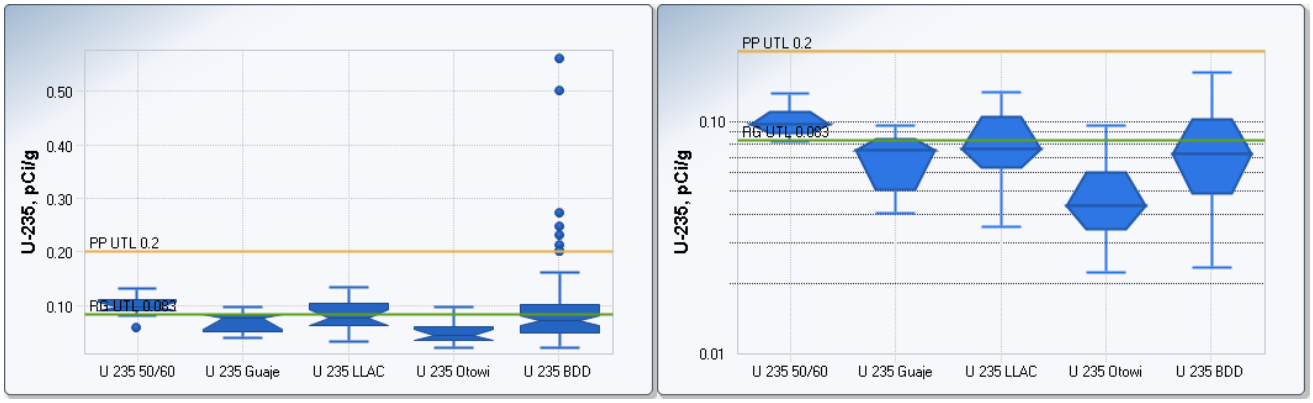

*The largest value of 5.5 pCi/g detected at BDD on 7/22/2011 23:45 was neither included on the graph nor in the descriptive statistics for that radionuclide.

The behavior of both radium isotopes appears similar for the five locations. Guaje and Otowi had concentration below the respective background values, and there were very few exceedances of the corresponding UTLs for all data sets, only one at 50/60, and three concentrations at BDD.

Figure 161. Ra-226 and Ra-228 in sediment from E050/E060 to BDD.

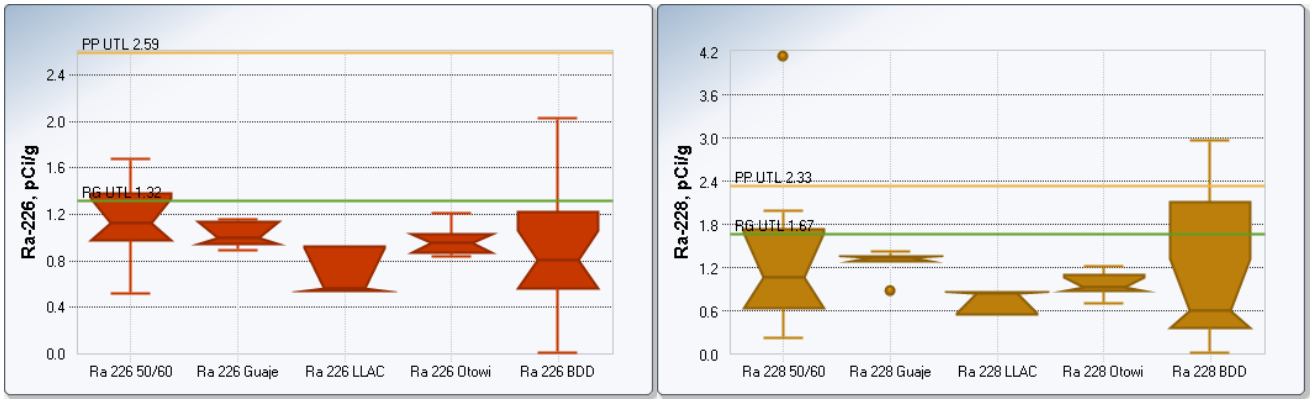

VII.4.c Storm Water Trends of Metals

The available data for metals found in storm water was summarized, and the descriptive statistics for all geographical sites from the middle LAC, gage stations E050/E060, to BDD was presented in Attachment 6. The same data was used to graph boxplots for the 5 sites, 50/60, Guaje, LLAC, Otowi, and BDD, in order to compare them to each other. ProUCL program was used for the descriptive statistics and boxplots. All concentrations were presented in ug/L. Only detected values were used in this section when plotting the boxplots, as determined by the laboratory qualifier.

Except for identified outliers and for Boron, all metal concentrations showed the same trend in LACW for the box and whisker percentiles, the storm concentrations increased from 50/60 to LLAC. The outliers for Al, As, Cd, Cr, and Cu had the highest concentrations at Guaje location, and the outliers for Sb and Ag were the highest at 50/60 location. For Boron, the highest concentrations occurred at Guaje.

The comparison between Otowi and BDD locations indicated that except for As, Be, Co, and Cu, all percentiles of the BDD concentrations were higher than Otowi concentrations at times up to an order of magnitude higher. Even though the median values for As, Be, Co, and Cu at BDD were higher than at Otowi, the 75th percentiles at BDD exhibited lower concentrations than at Otowi. The central tendencies of the results at Otowi and BDD were compared by Wilcoxon-Mann-Whitney test, and for Al, As, Ba, B, Cd, Cr, Co, Cu (90% confidence level), Pb, Mn, Ni, Tl, U, V, and Zn, the differences between these two sets of samples were statistically significant at 95% confidence level. However, for Be, Hg, and Se, the test indicated that these two data sets may belong to the same populations.

Figure 162. Al concentrations (ug/L) in storm water from E050/60 to BDD.

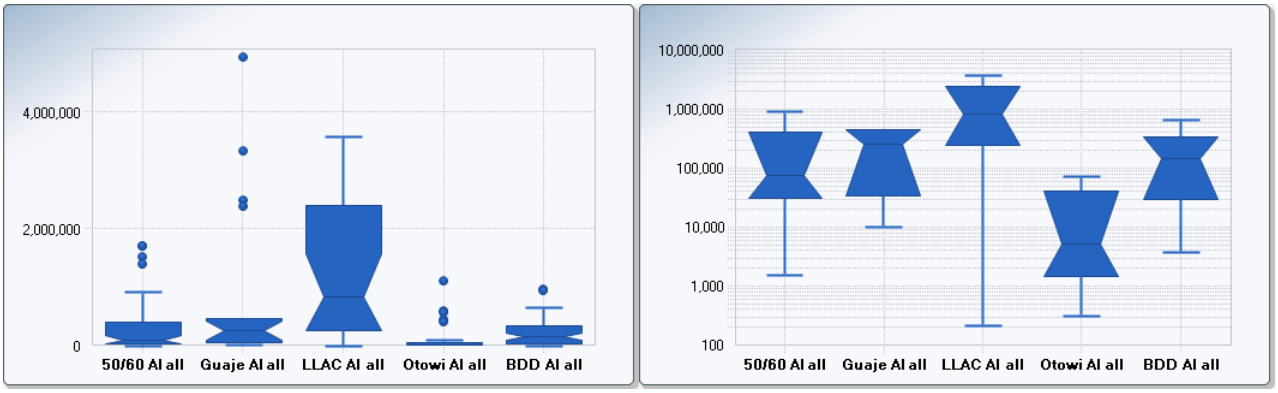

Figure 163. Sb concentrations (ug/L) in storm water from E050/60 to BDD.

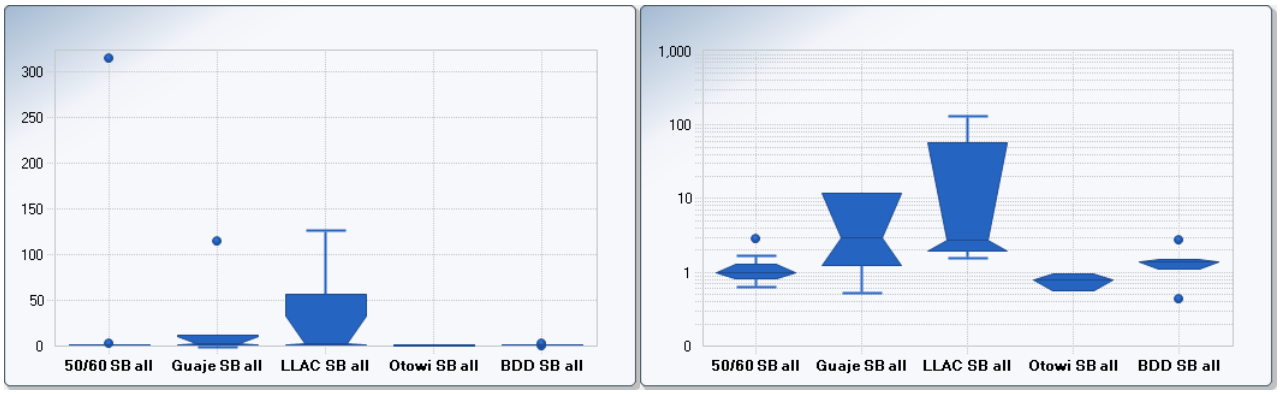

Figure 164. As concentrations (ug/L) in storm water from E050/60 to BDD.

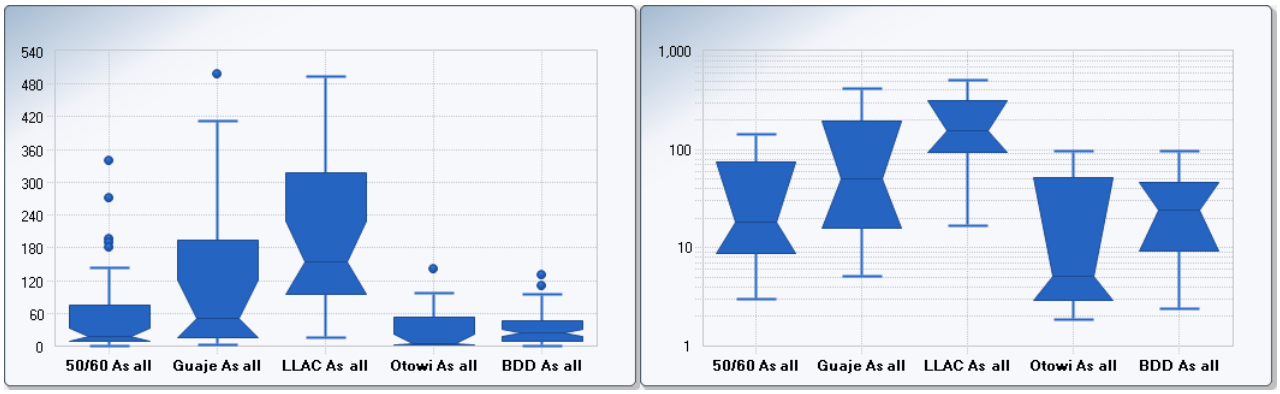

Figure 165. Ba concentrations (ug/L) in storm water from E050/60 to BDD.

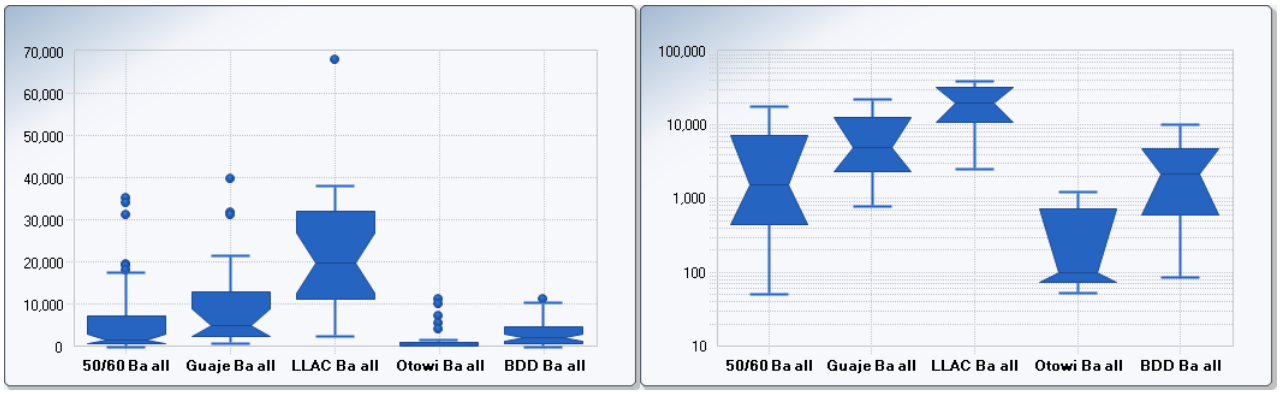

Figure 166. Be concentrations (ug/L) in storm water from E050/60 to BDD.

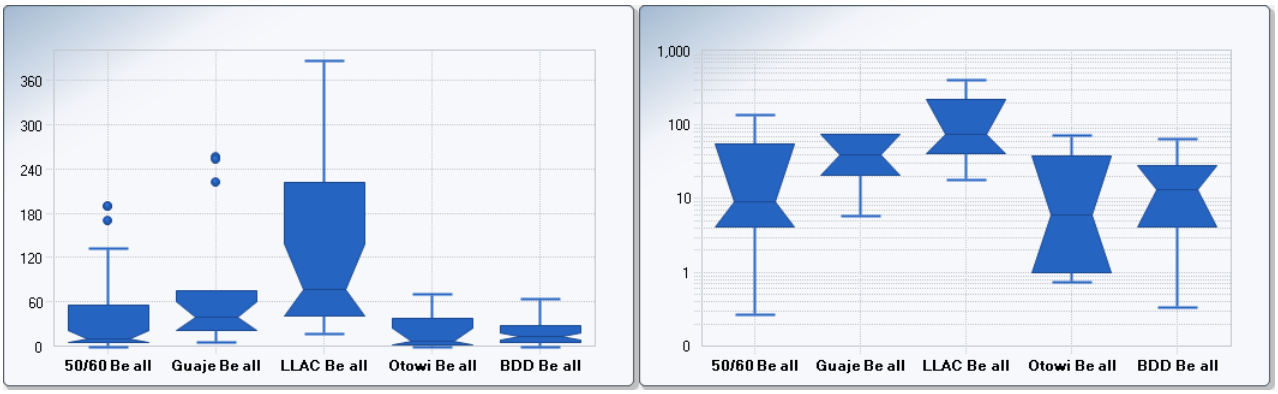

Figure 167. B concentrations (ug/L) in storm water from E050/60 to BDD.

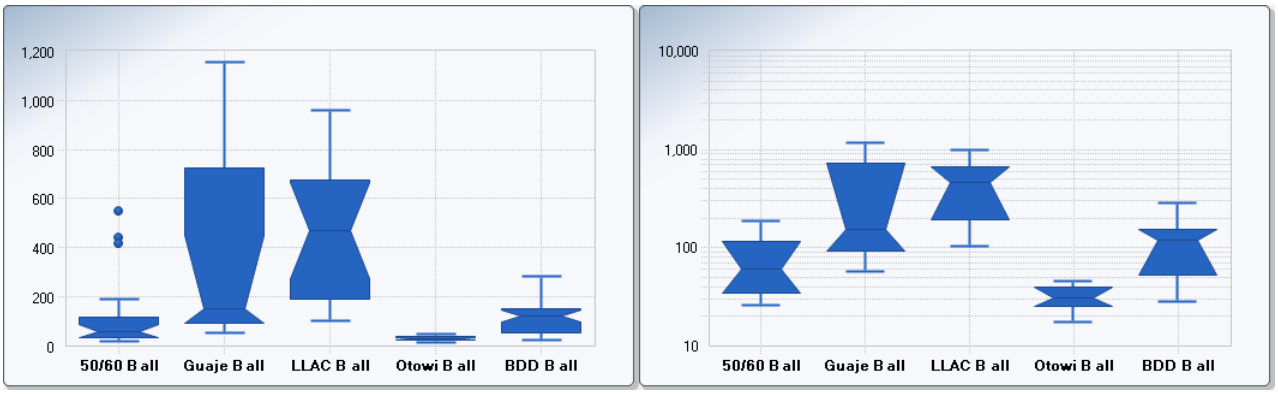

Figure 168. Cd concentrations (ug/L) in storm water from E050/60 to BDD.

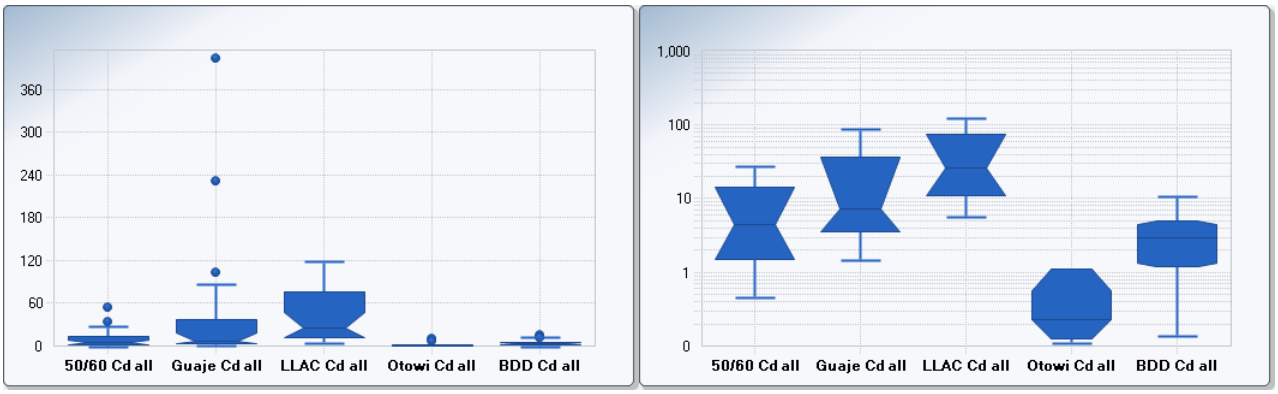

Figure 169. Cr concentrations (ug/L) in storm water from E050/60 to BDD.

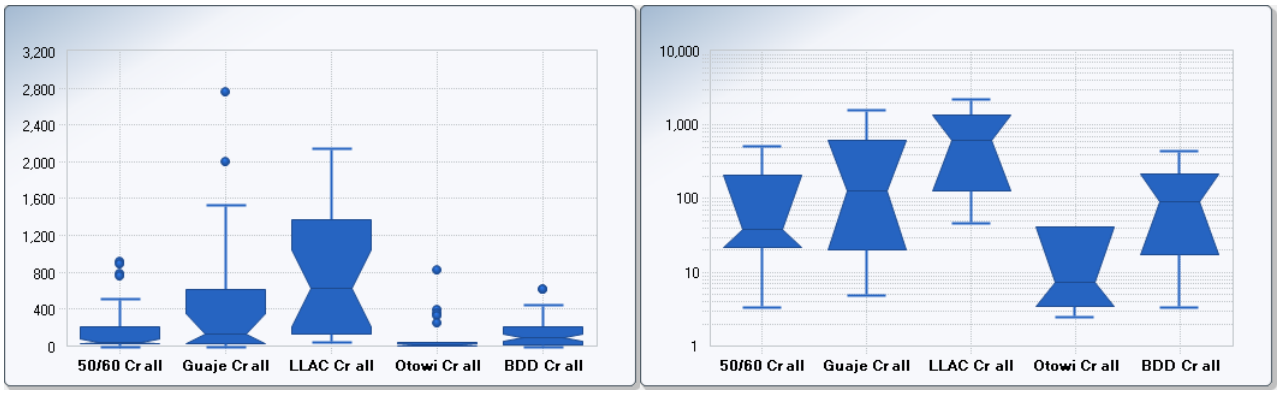

Figure 170. Co concentrations (ug/L) in storm water from E050/60 to BDD.

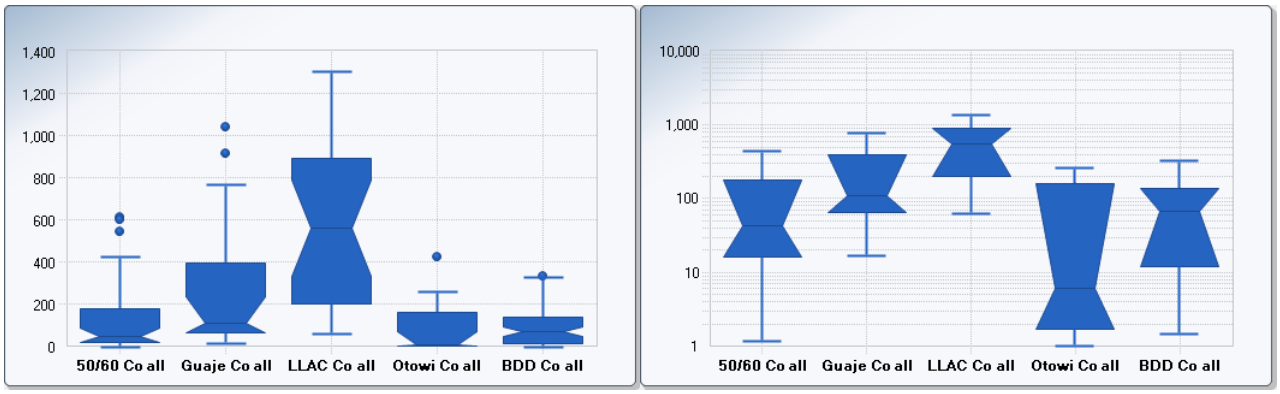

Figure 171. Cu concentrations (ug/L) in storm water from E050/60 to BDD.

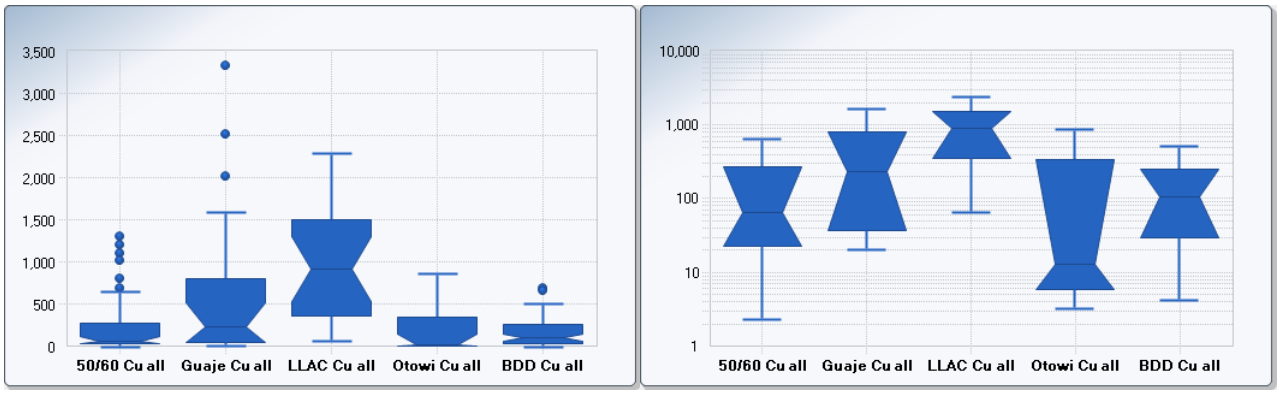

Figure 172. Pb concentrations (ug/L) in storm water from E050/60 to BDD.

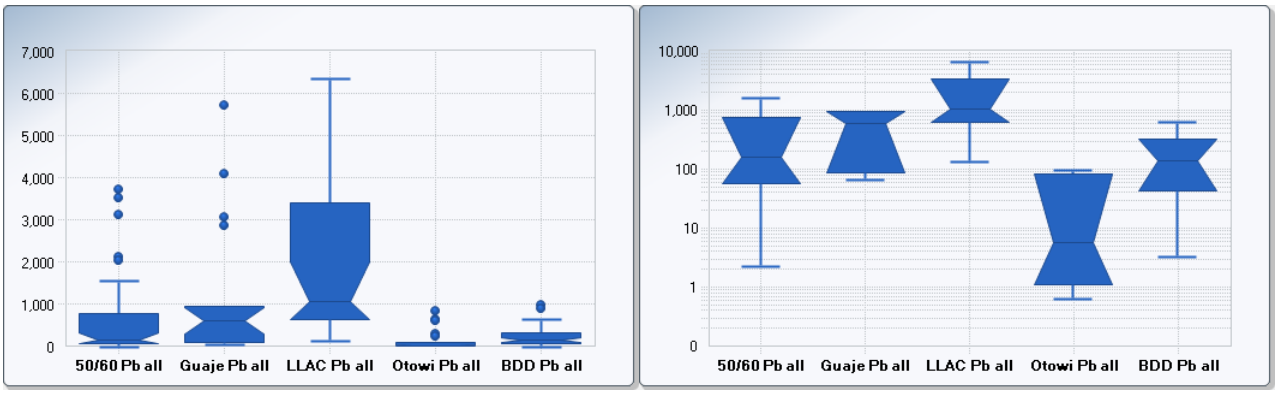

Figure 173. Mn concentrations (ug/L) in storm water from E050/60 to BDD.

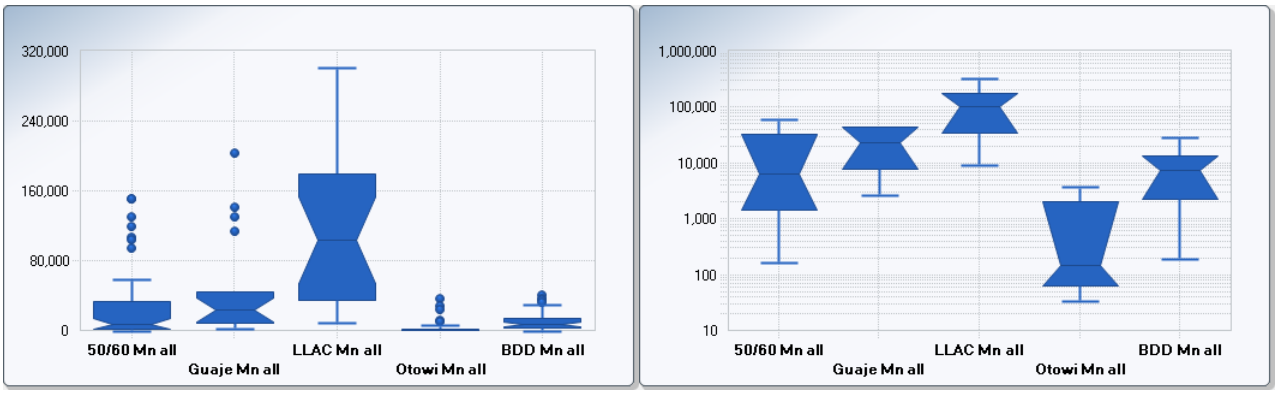

Figure 174. Hg concentrations (ug/L) in storm water from E050/60 to BDD.

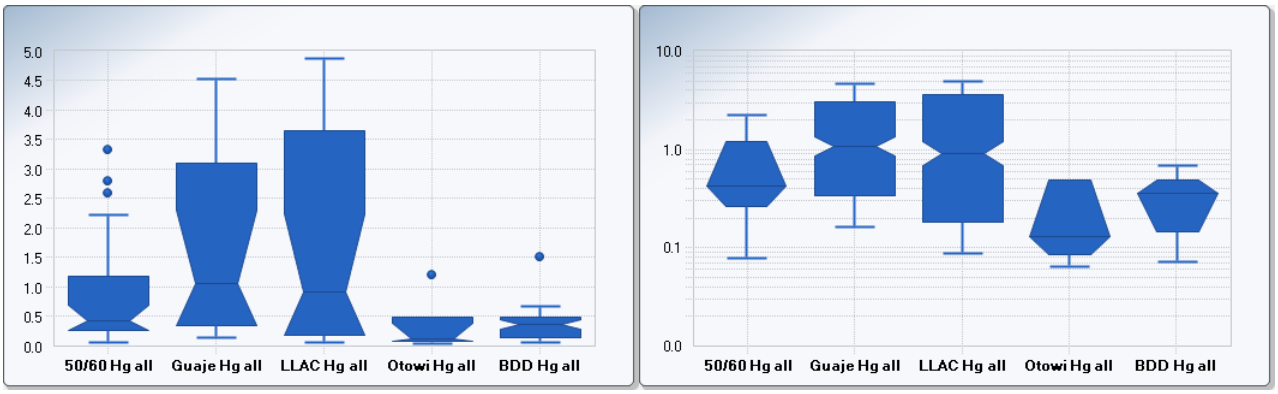

Figure 175. Ni concentrations (ug/L) in storm water from E050/60 to BDD.

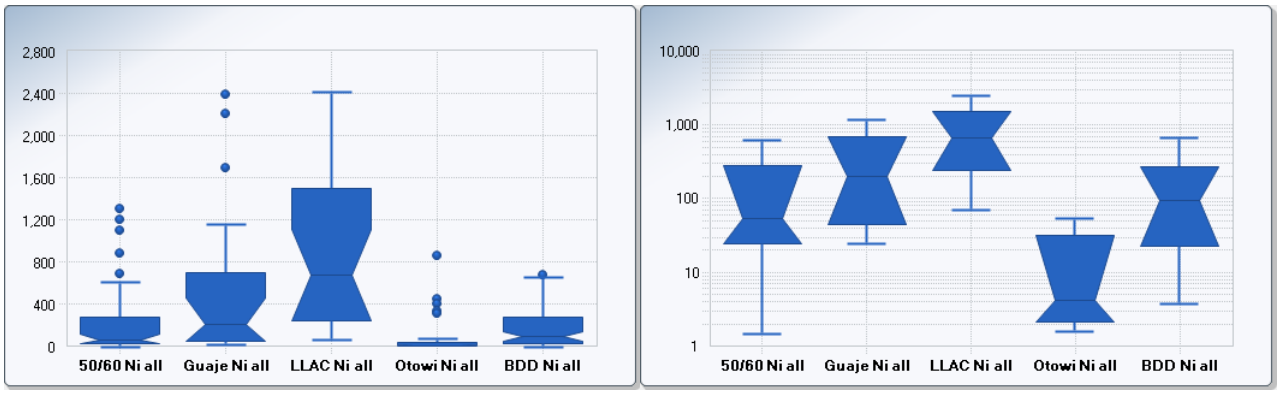

Figure 176. Se concentrations (ug/L) in storm water from E050/60 to BDD.

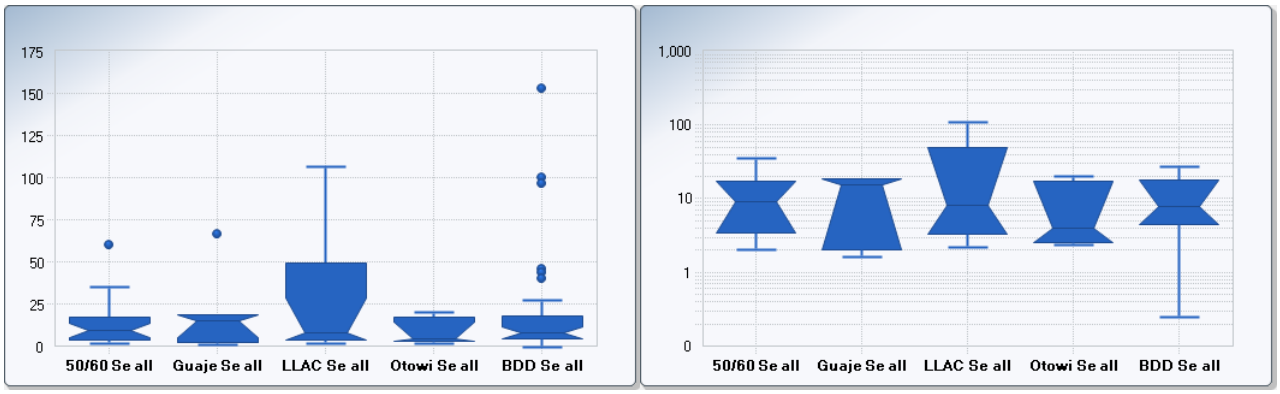

Figure 177. Ag concentrations (ug/L) in storm water from E050/60 to BDD.

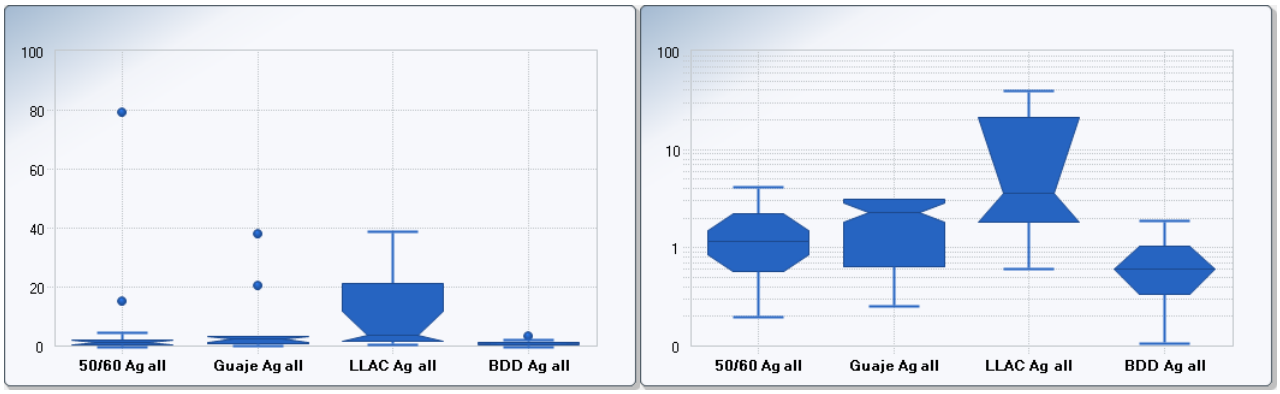

All results of storm water sampling for Ag at Otowi (since 2001) were non-detect, so no distribution for that location was presented on the graph.

Figure 178. Tl concentrations (ug/L) in storm water from E050/60 to BDD.

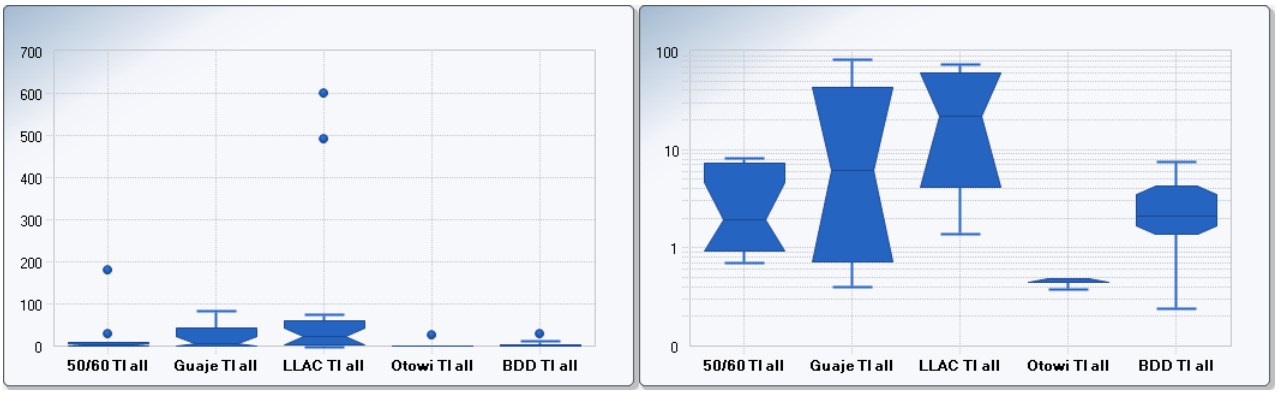

Figure 179. U concentrations (ug/L) in storm water from E050/60 to BDD.

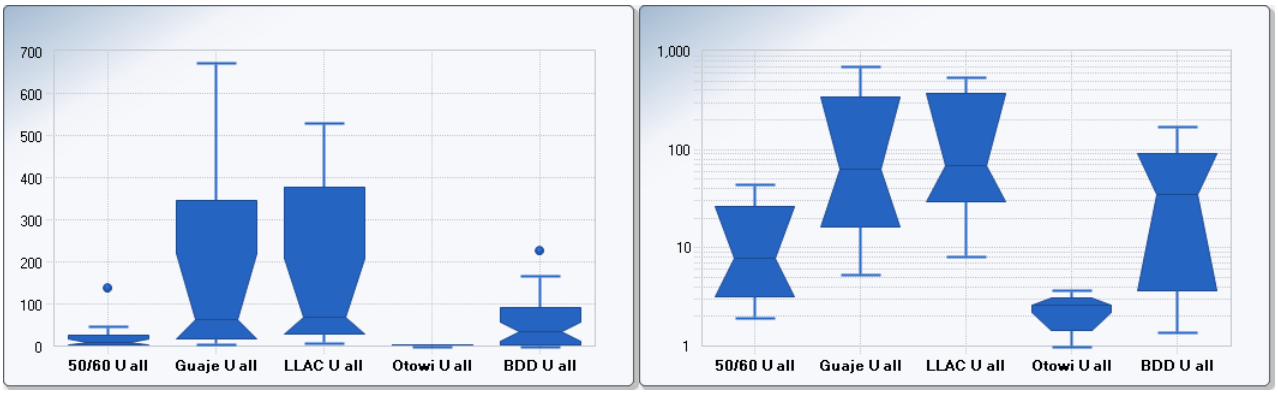

Figure 180. V concentrations (ug/L) in storm water from E050/60 to BDD.

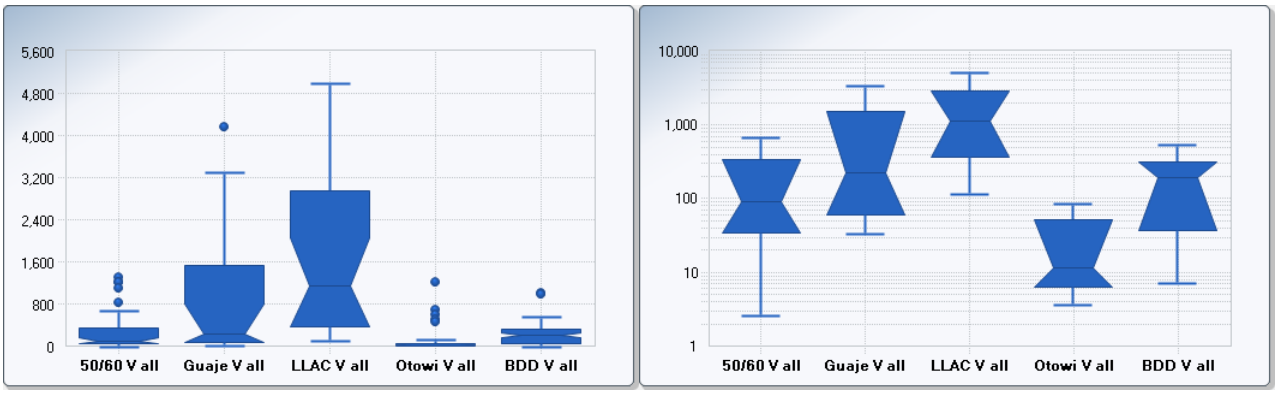

Figure 181. Zn concentrations (ug/L) in storm water from E050/60 to BDD.

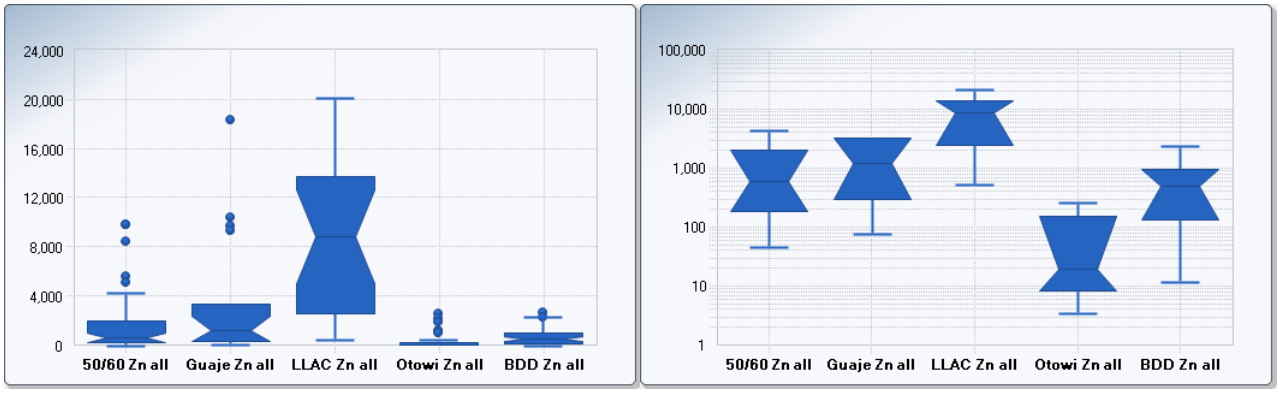

VII.4.d Sediment Trends of Metals

The available data for metals found in sediments was summarized, and the descriptive statistics for all geographical sites from the middle LAC, gage stations E050 and E060, to BDD was presented in Attachment 6. The same data was used to graph boxplots for the 5 sites, 50/60, Guaje, LLAC, Otowi, and BDD, in order to compare them to each other. ProUCL program was used for the descriptive statistics and boxplots. All concentrations were presented in ug/kg. Non-detected values were taken into account when plotting the boxplots if such were present in the data sets. The boxplots would have the maximum non-detect value marked with red line across the graph, if there were non-detects. The boxplots also mark the levels of the RG UTL (green line) and PP UTL (gold line).

Legend of color lines in boxplots:
Red line represents the Max ND level for all datasets
Gold line represents the Pajarito Plateau UTL
Green line represents the Rio Grande UTL

With a few exceptions (Sb, Se, Ag, and V), most metals exhibited a common trend for the box percentiles, which showed their highest concentrations occurring at 50/60, their concentrations decreasing at Guaje, but increasing back at LLAC, however not at the same levels as at 50/60. For these metals, many outliers were the highest at Guaje location, and the values of the upper whisker for some metals were the highest at LLAC, which indicated a large interquartile range for that dataset (large range of the data) at LLAC. This common trend may be suggestive of 50/60 location being a source of these metals, with a dilution of their sediment concentrations occurring at the least contaminated Guaje location, and more metal contaminants being "picked up" in the middle and lower reaches of the LACW because the sediment concentrations increased at LLAC.

The comparison between Otowi and BDD locations indicated that except for Cd and Se, all box percentiles and upper whisker of the BDD concentrations for Al, Sb, As, Be, Ba, Be, Cr, Co, Cu, Pb, Mn, Hg, Ni, Tl, V, and Zn were higher than Otowi concentrations. The central tendencies of the results at Otowi and BDD were compared by Gehan test (includes non-detects), and for Al, Sb, As, Ba, Cr (90% confidence level), Co, Cu, Pb, Mn, Hg, Ni, Tl, V, and Zn, the differences between these two

sets of samples were statistically significant at 95% confidence level. For Cd, Se, and Ag, the test indicated that these two data sets may belong to the same populations. However, the data sets for Sb (6 concentrations for Otowi and 4 concentrations for BDD) and Ag (3 concentrations for Otowi and 0 concentrations for BDD) contained only a few detects as indicated in the parenthesis, so statistically the tests do not give a good confidence in the conclusions.

Figure 182. Al concentrations (ug/kg) in sediment from 50/60 to BDD.

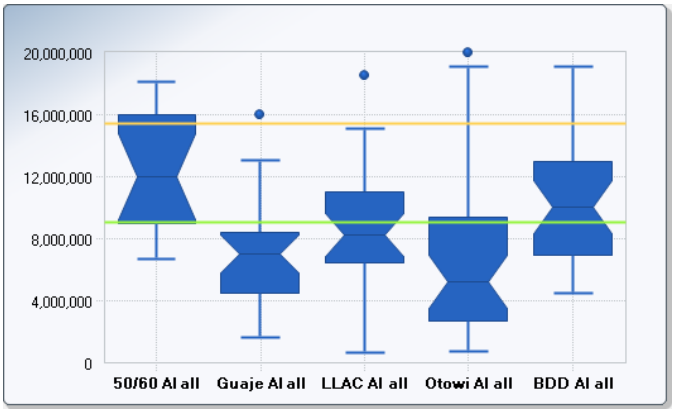

Both background UTLs for Al, PP UTL and RG UTL, were exceeded in LAC and on the RG. Only a few exceedances of the PP UTL were documented in LAC, but more than 50 percent of the results at BDD exceeded the RG UTL.

Figure 183. Sb concentrations (ug/kg) in sediment from 50/60 to BDD.

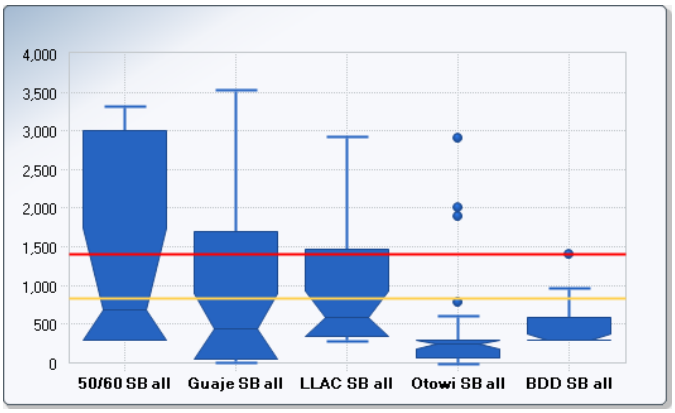

Most percentiles of the boxes for Sb and V, except for the upper whisker and outlier concentrations, showed decreasing trend throughout the LACW. However, the detect results for Sb were small number for all locations, and, therefore the trend cannot be statistically reliable. There were exceedances of the PP UTL for Sb at all LAC sampling locations. No RG UTL was established for Sb.

Figure 184. As concentrations (ug/kg) in sediment from 50/60 to BDD.

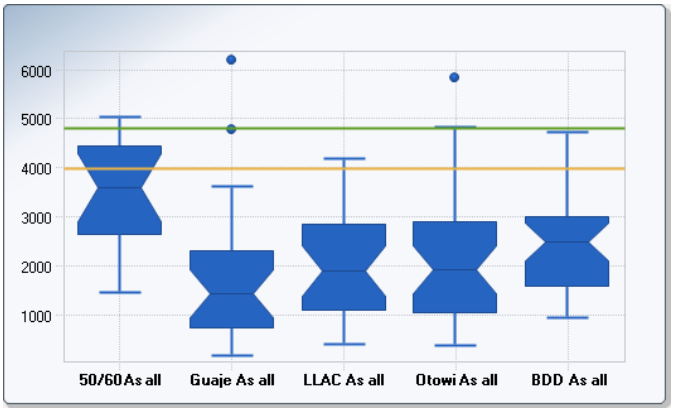

There were very few exceedances of As PP UTL, mainly at 50/60, and except for the outlier, there were no exceedances of the RG UTL for As at Otowi and BDD.

Figure 185. Ba concentrations (ug/kg) in sediment from 50/60 to BDD.

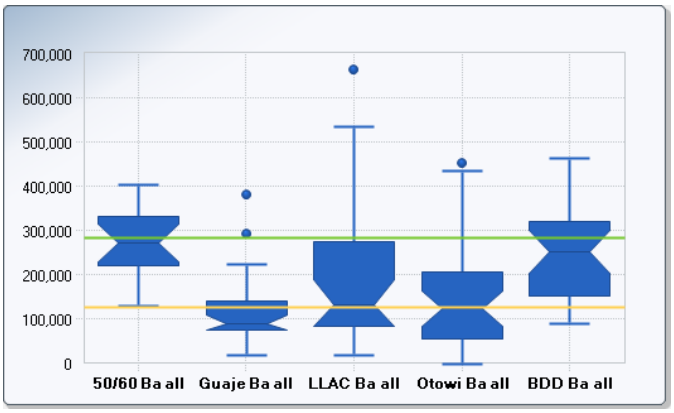

There were a large number of exceedances of Ba PP UTL throughout the LACW, but only a few exceedance of RG UTL at BDD and Otowi.

Figure 186. Be concentrations (ug/kg) in sediment from 50/60 to BDD.

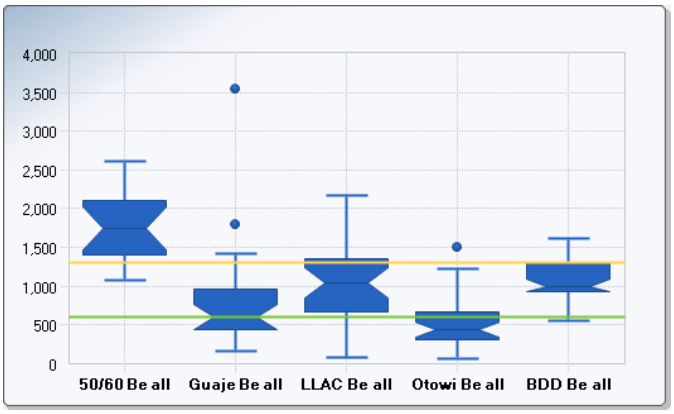

Most results at 50/60 exceeded the Be PP UTL, and most results at BDD exceeded the RG UTL.

Figure 187. B concentrations (ug/kg) in sediment from 50/60 to BDD.

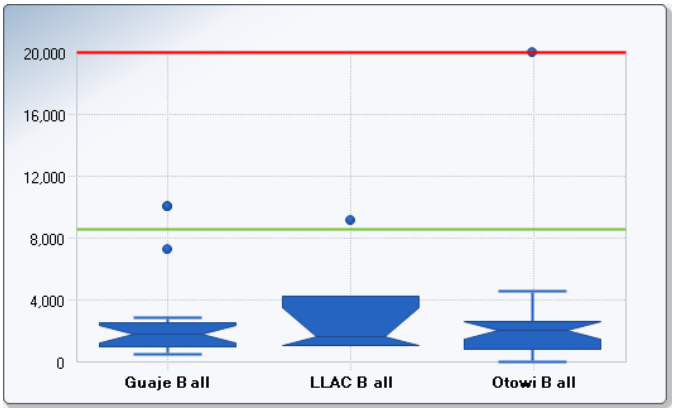

Boron was not included in the sediment analysis at the 50/60 and BDD locations, and, therefore not plotted on the figure.

Figure 188. Cd concentrations (ug/kg) in sediment from 50/60 to BDD.

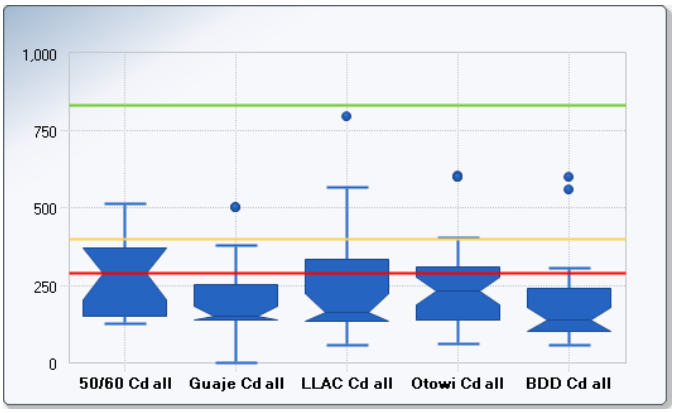

There were only a few exceedances of the Cd PP UTL in the LACW, and no exceedances of the RG UTL at BDD.

Figure 189. Cr concentrations (ug/kg) in sediment from 50/60 to BDD.

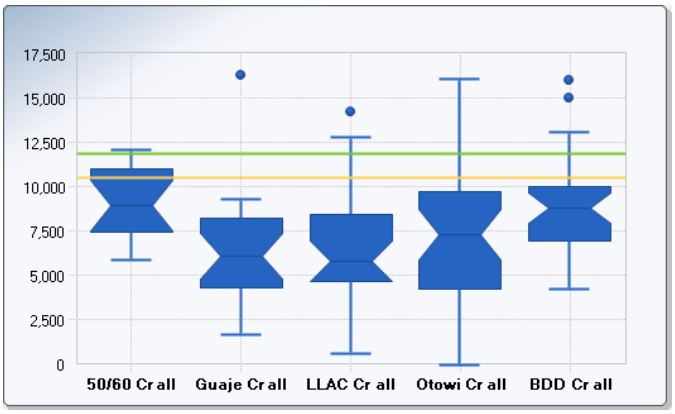

There were only a few exceedances of the Cr PP UTL in the LACW, and a few exceedances of the RG UTL at BDD.

Figure 190. Co concentrations (ug/kg) in sediment from 50/60 to BDD.

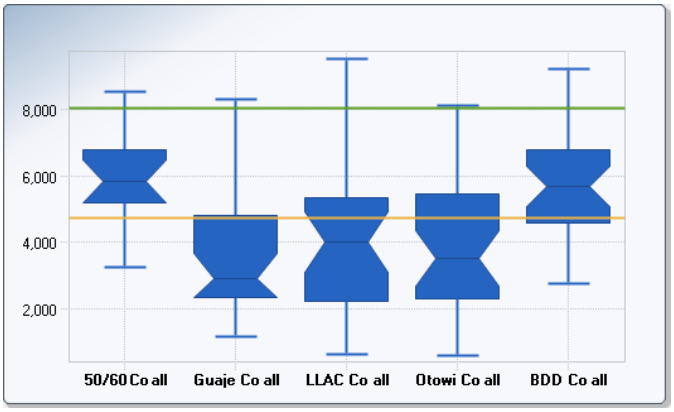

Most results at 50/60 exceeded the Co PP UTL, and only few results at BDD exceeded the RG UTL.

Figure 191. Cu concentrations (ug/kg) in sediment from 50/60 to BDD.

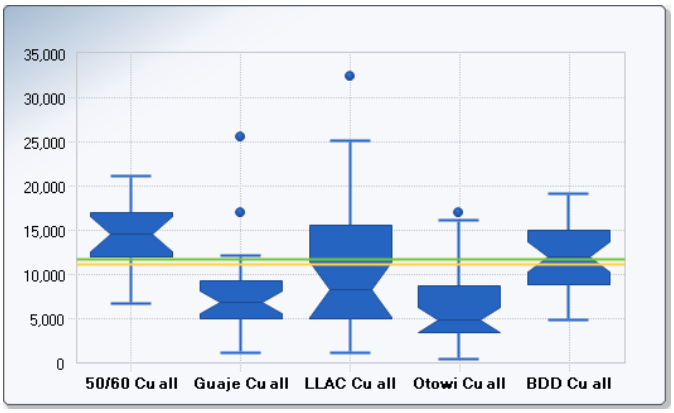

Most results at 50/60 exceeded the Cu PP UTL, and about 50 percent of the results at BDD exceeded the RG UTL.

Figure 192. Pb concentrations (ug/kg) in sediment from 50/60 to BDD.

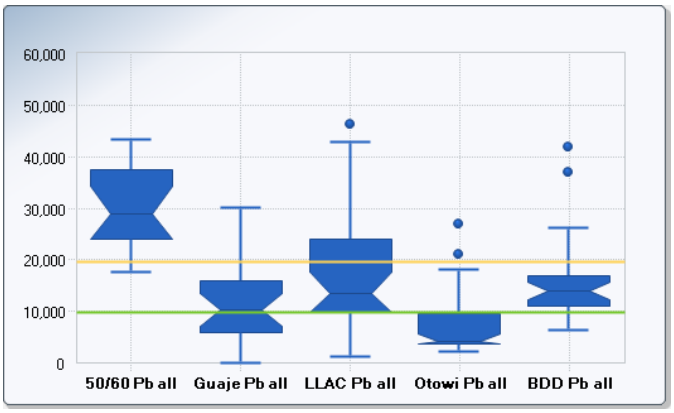

Most results at 50/60 exceeded the Pb PP UTL, and most results at BDD exceeded the RG UTL.

Figure 193. Mn concentrations (ug/kg) in sediment from 50/60 to BDD.

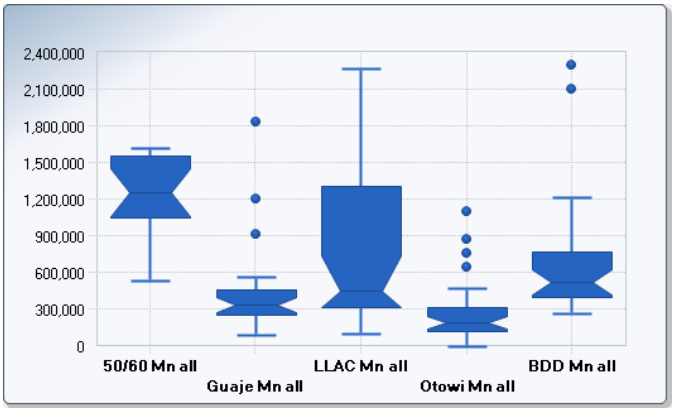

No Mn UTLs were established.

Figure 194. Hg concentrations (ug/kg) in sediment from 50/60 to BDD.

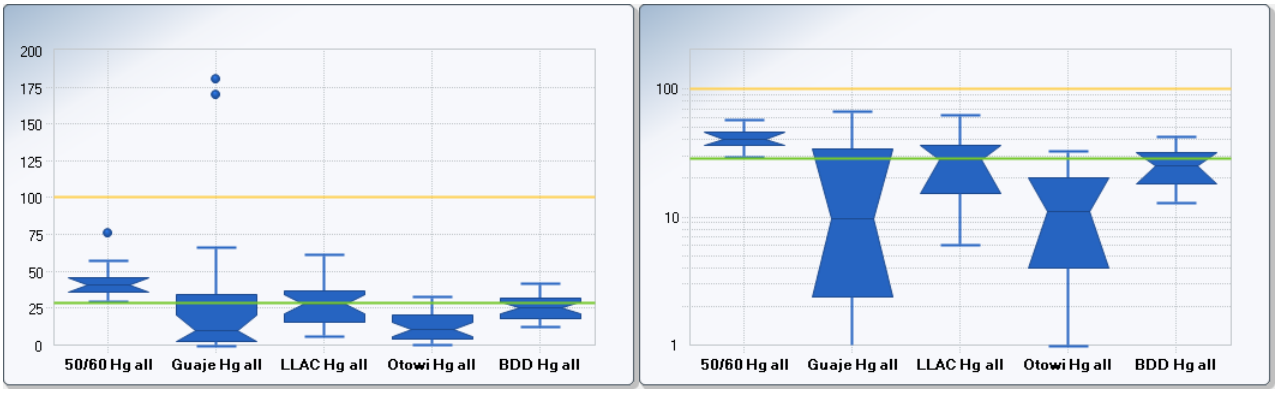

Except for a couple of outliers, most results in LACW were within the Hg PP UTL, but a few data points at BDD exceeded the RG UTL.

Figure 195. Ni concentrations (ug/kg) in sediment from 50/60 to BDD.

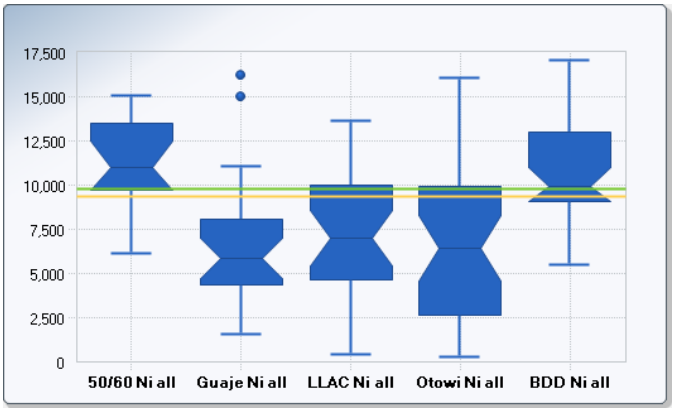

Most results at 50/60 exceeded the Ni PP UTL, and about 50 percent of the results at BDD exceeded the RG UTL.

Figure 196. Se concentrations (ug/kg) in sediment from 50/60 to BDD.

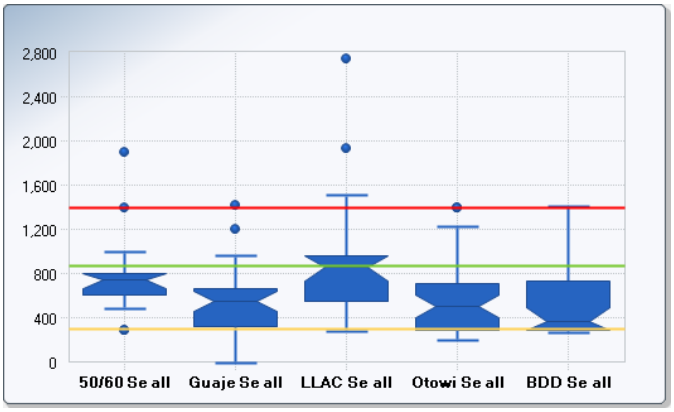

Most concentrations at LLAC location were the highest in LACW, which was the only such occurrence of all metals. This suggests a different source of contamination for Selenium (Se) than for the rest of the metals. Most results exceeded the Se PP UTL in all sampling locations of LAC, but only a few concentrations exceeded the RG UTL at BDD. This result is due to the large difference between the UTLs in both watersheds.

Figure 197. Ag concentrations (ug/kg) in sediment from 50/60 to BDD.

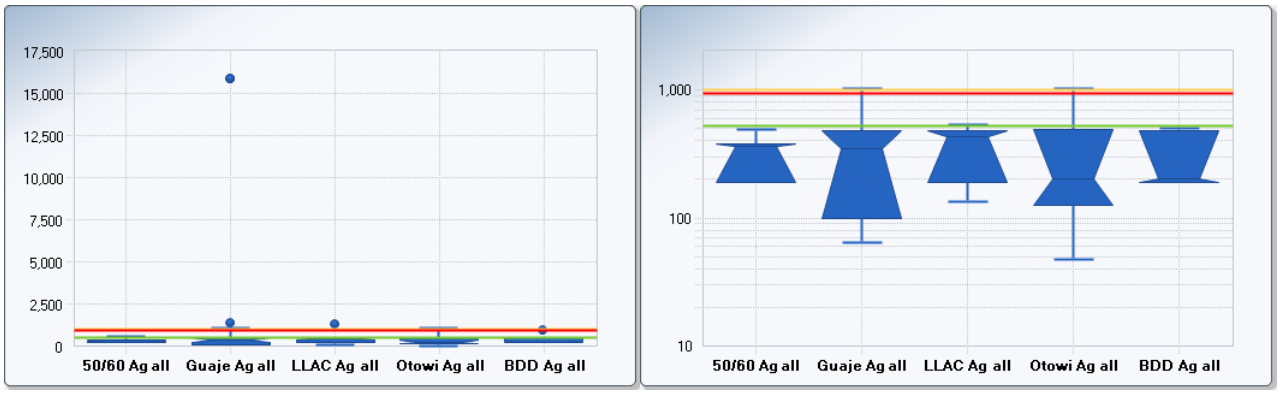

All results for 50/60 and BDD were non-detect, so the displayed trend should not be interpreted as significant for the fate and transport of this metal. The rest of the locations had only 3 to 5 detected concentrations.

Figure 198. Tl concentrations (ug/kg) in sediment from 50/60 to BDD.

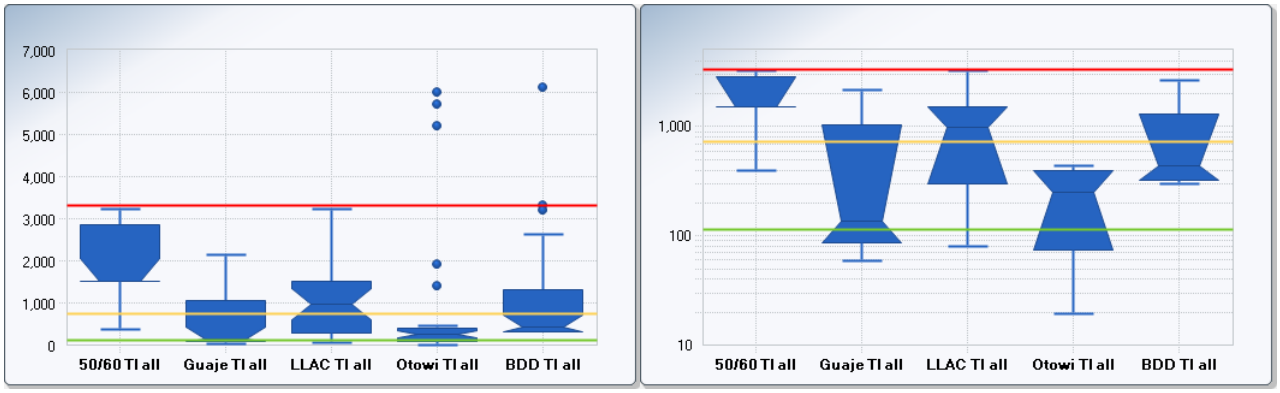

Most results at 50/60 exceeded the Tl PP UTL, and all results at BDD exceeded the RG UTL.

Figure 199. U concentrations (ug/kg) in sediment from 50/60 to BDD.

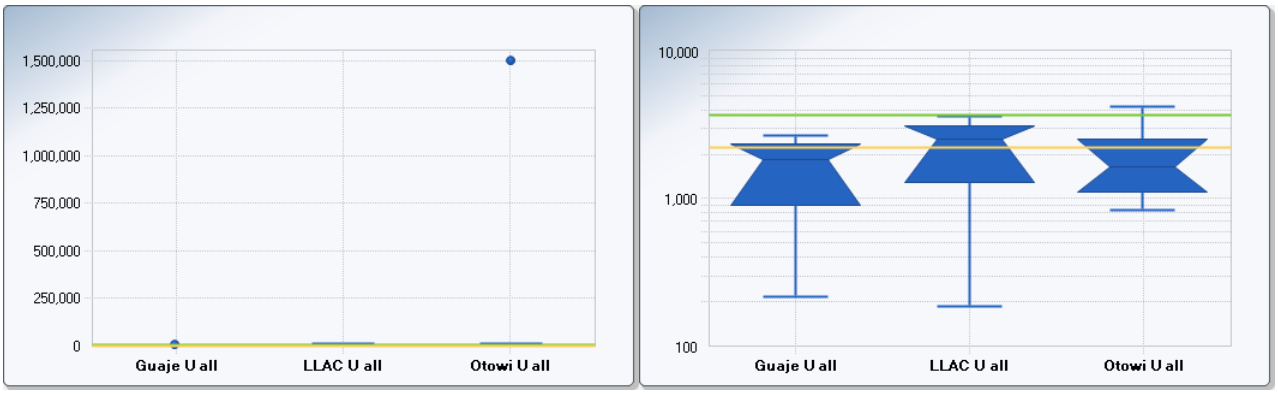

Uranium was not included in the sediment analysis at the 50/60 and BDD locations, and, therefore not plotted on the figure.

Figure 200. V concentrations (ug/kg) in sediment from 50/60 to BDD.

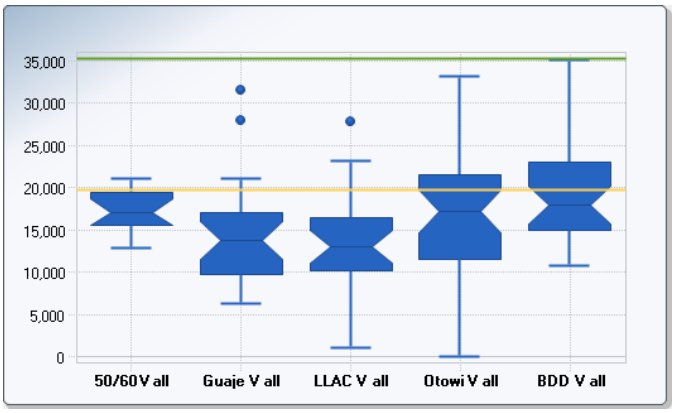

The Vanadium results also showed slightly decreasing trend throughout the LACW, and the outliers at Guaje were the maximum concentrations of all sites. Only a few results exceeded the V PP UTL, and none exceeded the RG UTL at BDD.

Figure 201. Zn concentrations (ug/kg) in sediment from 50/60 to BDD.

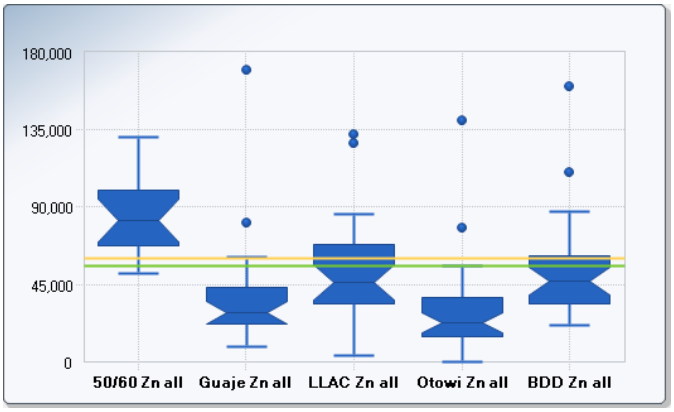

Most results at 50/60 exceeded the Zn PP UTL, and about 25 percent of the results at BDD exceeded the RG UTL.

VII.4.e Storm Water Trends of Organics

Figure 202. Total PCBs in storm water from E050/E060 to BDD.

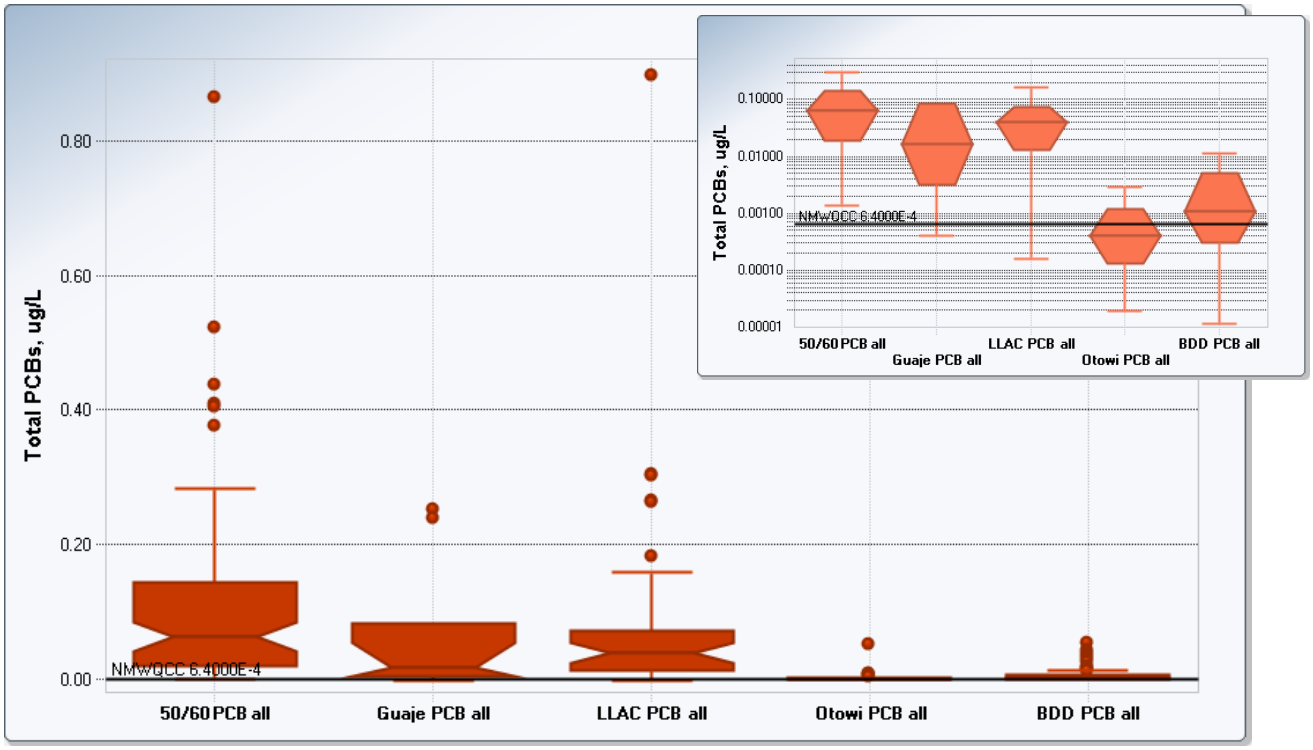

The total PCBs concentrations fit very well the trend that was observed for metals, the highest concentrations occurred at 50/60, lowest concentrations occurred at Guaje, and then concentrations increased at LLAC but not at as high as at 50/60. Such behavior points out to 50/60 as one potential source of total PCBs. Almost all results at LAC exceeded the NMWQCC standard of $6.4x10^{-4}$ ug/L. All percentiles of the BDD distribution showed higher concentrations than Otowi's concentrations. The difference in concentrations for these two sites is substantial and supported by

the t-test and Wilcoxon-Mann-Whitney test (log-normal distribution for both sets of data) comparing their central tendencies at 95 percent confidence level. There were more exceedances of the NM WQCC standard at BDD than at Otowi, suggesting the LACW as the source for additional contaminant's source. However, the occasional exceedance of the NMWQCC standard at Otowi points out to total PCBs being wide-spread along the RG upgradient from Otowi Bridge.

Figure 203. Dioxins/furans in storm water from E050/060 to BDD.

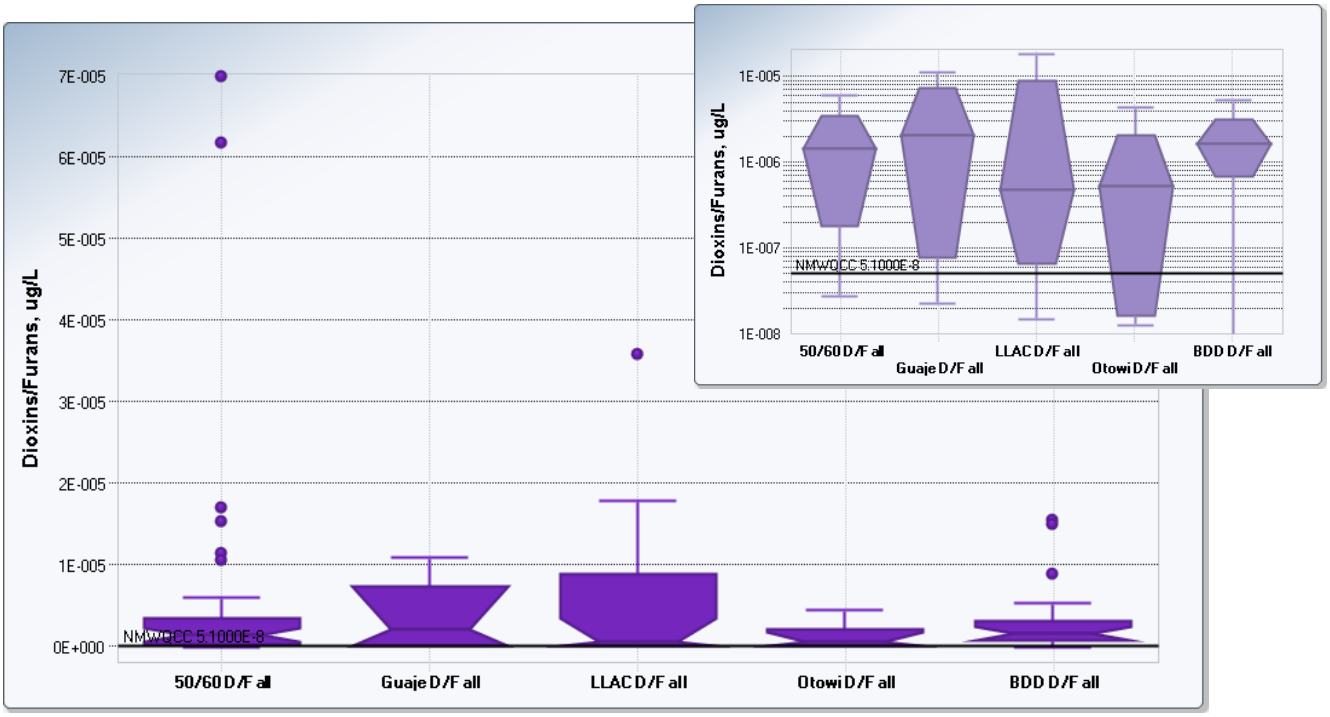

The highest concentrations of D/F occurred at 50/60, although the median concentration at that location was lower than at Guaje. Guaje data set contained only four results which is insufficient amount of data. The D/F median concentration at LLAC were the lowest in the LAC, but the distribution had a very wide range, and at times exceeded the 50/60 concentrations. Most results in LAC exceeded the NMWQCC standard of 5.1×10^{-8} ug/L.

Most box plot percentiles and the outliers of the D/F concentrations at BDD were higher than Otowi's concentrations. However, the difference between these two sets of data was not statistically significant. Even though the range of BDD concentrations was within the Otowi range, the highest concentrations might be due to the D/F occurrences at LAC during strong LAC storm events.

VII.5 Conclusions of Data Analysis

The contaminants concentrations for radionuclides, inorganic and organic constituents at BDD exceeded RG UTL levels. There were also exceedances of the NMWQCC standards for all contaminants as well. Most exceedances occurred during 2011 sampling when Las Conchas fire changed some parts of the LACW and mobilized contaminants. The BDD data analysis pointed out that for certain constituents, the Los Alamos Canyon was the source for the exceedances, and for other constituents there was no clear indication of the source(s).

These results were confirmed by the LA/PCW results collected at locations E050/E060, Guaje, LLAC, and Otowi. Through the data analysis, the E050/E060 was easily identified as the source of most radionuclides, many metals, PCBs and D/F. As the contaminated sediments were transported down the LAC, their concentrations were diluted by less contaminated run off from Guaje Canyon. However, the data demonstrated that the entire LAC contained contaminated sediments which could be mobilized at any storm event, because the concentrations at LLAC were higher than at Guaje location, and therefore contaminants were being "picked up" between Guaje and LLAC sampling locations. The graphs clearly demonstrated that the higher concentrations at BDD were due to the LACW because most sampling sets showed higher concentrations at BDD than Otowi location at significant statistical level.

The influence of the LACW is quite significant even though it has small storm water contribution from that watershed to the Rio Grande flow. Higher concentrations of contaminants are evident during and post- fire, and demonstrate the need for more permanent surface water monitoring along the Rio Grande between LACW confluence and BDD.

VII.6 Special Study of Plutonium-239/240

The obtained data during this program was vast. Plutonium-239/240 has been of special interest to most entities that monitor LA/P watershed and its confluence with Rio Grande, and downgradient from this confluence. The objective of this Section is to analyze in detail the results obtained at the BDD and make an attempt to explain them and connect them with results in the LA/P watershed on a small scale such as during each storm event.

VII.6.a Storm Water Concentrations at BDD

As an initial step of the analysis, we plotted graphically the detected values for storm water during the monitoring program at the BDD, including the results from the years before the MOU (Figure 204). As mentioned earlier the NMED DOE OB has conducted storm water monitoring at the BDD since 2005, and those results were included in this section. The plot below did not include non-detects. The RG Screening Criteria of 1.5 pCi/L was also plotted on the graph. There were exceedances of the screening criteria including during 2010, before the Las Conchas fire. The maximum value of 5 pCi/L was detected on 7/21/2013.

Figure 204. Annual storm water detects of Pu-239/240 at BDD Intake 2009-2014.

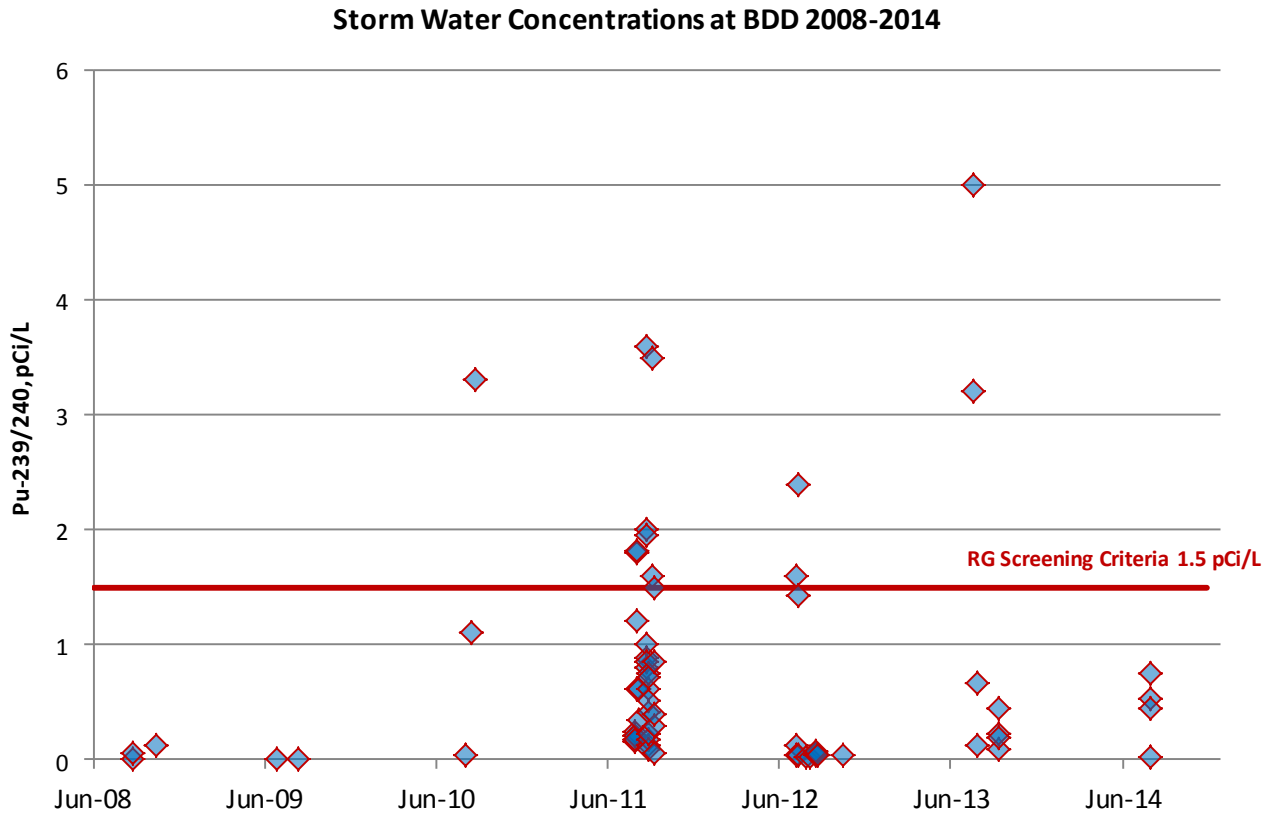

As part of the analysis of storm water we included an analysis of the storm water results vs. SSC (Figure 205) in an attempt to determine whether there is any correlation between these constituents. As it is presented below the correlation is weak, which indicates the presence of contaminants neither from naturally occurring sources nor from global fall out. In addition, the linear fit slope of 0.0175 is close to the RG UTL value of 0.014 which would be expected because the RG flow is most often the predominant flow if storm events from both watersheds coincided.

Similarly to Sections V.3 and V.4, we need to note that we have two types of sampled events, one when only RG events occurred and the other when LA Canyon event and RG event occurred within a close time frame. When a RG event coincided with a LA Canyon storm event, if the predominant flow was a RG flow then the contaminants emanating from the LA Canyon would be diluted by the RG flow and RG SSC, and the resulting flow would be representative of the RG contaminants rather than the LA Canyon.

Figure 205. Pu-239/240 in storm water vs SSC.

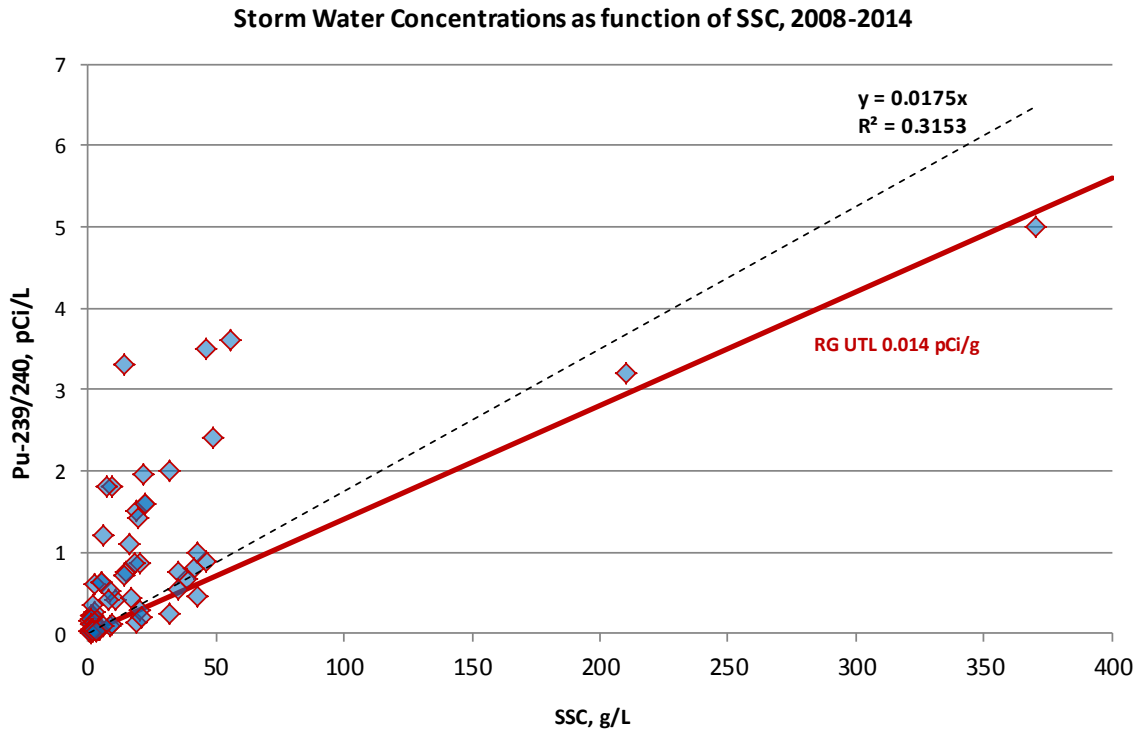

In order to explore whether there is a correlation between the Pu-239/240 and SSC, we need to separate the two types of storm events. The events with strong LA Canyon influence would be considered events for which the relative flow of the LA Canyon is 10% or greater than the RG flow.

After examining the flow parameters for each event, the results were filtered and only storm events with strong LA Canyon flow were retained for analysis. The storm events that met this condition are listed in Table 25.

Table 25. Storm events with strong LA Canyon influence.

Sampling Date	LA flow/RG flow %
08/15/2010	13
08/23/2010	39
08/03/2011	10
08/27/2011	10
08/29/2011	11
09/04/2011	45
09/07/2011	12
07/11/2012	42
08/23/2012	21
10/12/2012	18
Weighted Average	20

The LA flow/RG flow was calculated by taking the maximum lower LA Canyon flow at E109.9 and the RG flow at the time of sampling. Thus, the percent listed in the table are *biased high*, because the maximum LA flow does not last for the entire storm event.

For the selected events the storm water results vs. SSC was plotted and presented on Figure 206. The error bars for the storm water results were 30% and for the SSC – 10%.

Figure 206. "Strong" LA Canyon events Pu-239/240 vs SSC.

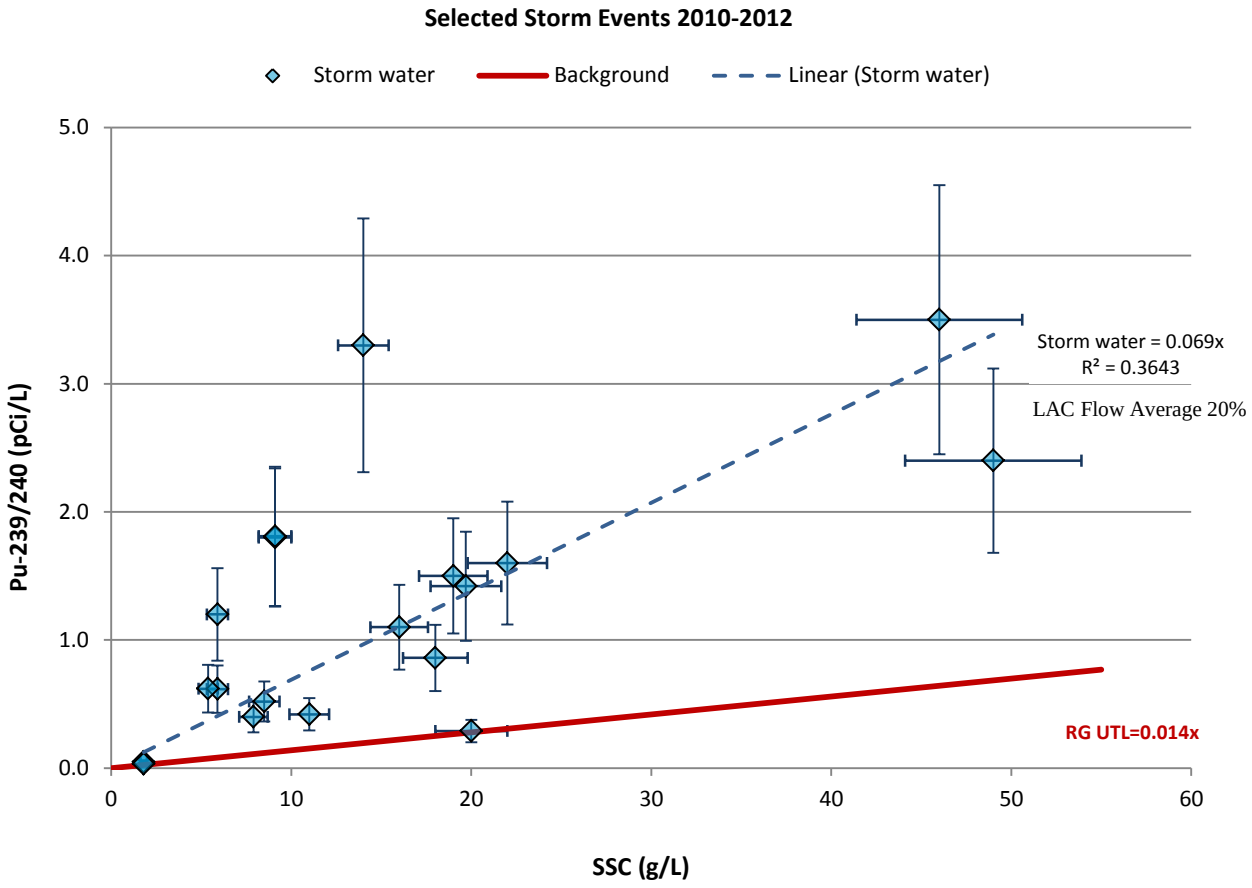

As a result of the selection process, the correlation improves only slightly, but the slope of the calculated best fit is 4 times steeper (0.069 pCi/g), which is expected since during strong LA Canyon events higher Pu-239/240 concentrations would be delivered to the RG and transported downstream to BDD. Therefore, this methodology of selection of these storm events is quite appropriate at an "average behavior" level.

We compared the BDD "average concentrations" to the LA Canyon "average concentrations" in terms of the slope of the linear fit (Pu-239/240 storm water concentrations vs. SSC), as published in the LANL annual reports referenced in the previous sections.

Table 26. E109.9 linear fit of Pu-239/240 vs. SSC.

Year	Slope of Linear Fit (pCi/g)	R^2	R^2/LA Canyon station
2010	1.2	neg	0.296 (E042)
2011	0.3	0.16	0.351 (E050)
2012	0.09*	<0.13	Not plotted
2013	Not fitted	-	-
Average	0.53 (2010, 2011, 2012)		
* different linear fit applied to 2012 data.			

There are a few observations that need mentioning. (1) The "average concentrations" (slope of linear fit) in the lower LA Canyon were the highest in 2010 (slope of 1.2) and 4 times or more higher than the following years. This is an unexpected result since it is believed that the Las Conchas fire "produced" higher concentrations in the LA Canyon than pre- or post-fire years; and (2) Although, the data for the entire LA Canyon displays negative and poor correlation, the correlation at single LA station is improved and similar to that of the BDD intake (R^2=0.364). One explanation of this fact is that the Pu detections at the BDD are influenced by the strongest and most contributing events from the lower LA Canyon, superimposed on a consistent low concentration river "background". So, the behavior at the BDD is similar to a single LA Canyon gage station.

One of the main conclusions from the analysis in this subsection that could be applied to future assessments of contaminant concentrations at the BDD is that fact that the contribution of the lower LA Canyon flow is critical and the main source for the concentrations detected at the BDD intake. As long as the percent LA flow is above 10% with respect to the RG flow, the Pu-239/240 detections at BDD Intake would be higher than at lower percent ratio of the LA flow. If lower LA Canyon events coincide with stronger RG storm events (higher discharges), the river flow and river suspended sediment would dilute the LA Canyon concentrations and obscure their differences as observed at the BDD. This is an important observation because it demonstrates the need to know the flows of the LAC before it drains into the RG if any predictions of the Pu 239/240 concentrations at the BDD are to be made.

VII.6.b Conclusions from Storm Water Analysis

The most important storm events to monitor in the future would be events for which the lower LA Canyon flow is substantial in comparison to RG flow. Higher flows can carry higher SSC than the RG even if those might be time delayed. As shown in the previous section, RG transport rates of suspended sediment are also influenced by this relative flow ratio. As such, a flow meter at the lower LA Canyon is critical for future work and sampling strategies at the BDD Intake.

VII.6.c Pu-239/240 Sediments Concentrations at BDD

BDD calculated the Pu-239/240 concentrations in suspended sediments for each event during which the storm water was sampled. This was done by identifying Pu-239/240 and SSC for the same date

and time. Data which used the analytical method EPA 160.2 was not excluded from the analysis but marked with a star in Table 27. This process was conducted for all monitoring years, 2008-2014. The table below includes the results for the calculated sediment results by BDD and the calculated or measured sediment results by NMED/DOE OB. Only detected results were included in this analysis. Results marked non-detect by the laboratory were not included. The highlighted cells are all results that exceeded the RG UTL, which for Pu-239/240 was calculated to be 0.014 pCi/g (Appendix 5.)

Table 27. Pu-239/240 sediment concentrations at BDD intake 2008-2014.

Date & Time	Detected Result pCi/g	Sampling Entity†	Date & Time	Detected Result pCi/g	Sampling Entity
8/24/08 20:57	0.00560	NMED	8/21/11 19:27	0.01913	NMED
8/24/08 21:57	0.01737	NMED	8/21/11 19:27	0.03200	NMED sed
10/11/08 19:47	0.00684	NMED	8/21/11 19:29	0.02326	NMED
6/27/09 0:32	0.01102	NMED	8/21/11 19:29	0.01800	NMED sed
8/13/09 19:08	0.00790	NMED	8/21/11 19:44	0.01939*	BDD
8/1/10 3:56	0.00868	NMED	8/21/11 20:19	0.04300	NMED
8/15/10 18:27	0.06875	NMED	8/21/11 20:19	0.03200	NMED sed
8/23/10 17:59	0.23571	NMED	8/21/11 20:28	0.09007**	BDD
8/23/10 17:59	0.33000	NMED sed	8/26/11 20:14	0.06316	NMED
			8/26/11 20:14	0.06800	NMED sed
7/28/11 18:39	0.30962	BDD	8/26/11 20:32	0.11554*	BDD
7/28/11 19:06	0.10870	NMED	8/26/11 21:04	0.09090	NMED
7/28/11 19:06	0.15000	NMED sed	8/26/11 21:04	0.08100	NMED sed
7/28/11 19:24	0.18460*	BDD	8/26/11 21:17	0.11518*	BDD
7/28/11 19:56	0.11670	NMED	8/27/11 19:07	0.11520	BDD
7/28/11 19:56	0.14000	NMED sed	8/29/11 4:21	0.05067	NMED
7/28/11 20:09	0.14285*	BDD	8/29/11 4:21	0.05100	NMED sed
8/3/11 18:09	0.19780	NMED	8/29/11 5:06	0.03818	NMED
8/3/11 18:09	0.23000	NMED sed	8/29/11 5:06	0.07100	NMED sed
8/3/11 18:27	0.24133**	BDD	8/29/11 5:51	0.06118	NMED
8/3/11 18:59	0.20339	NMED	8/29/11 5:51	0.05400	NMED sed
8/3/11 18:59	0.21000	NMED sed	8/29/11 6:36	0.05143	NMED
8/3/11 19:12	0.1116*	BDD	8/29/11 6:36	0.05400	NMED sed
8/5/11 17:54	0.17500	NMED	9/4/11 21:54	0.07608	NMED
8/5/11 17:54	0.16000	NMED sed	9/4/11 21:54	0.09600	NMED sed
8/5/11 18:44	0.21035	NMED	9/4/11 22:44	0.07272	NMED
8/5/11 18:44	0.21000	NMED sed	9/4/11 22:44	0.08100	NMED sed
8/21/11 18:42	0.06250	NMED	9/7/11 14:41	0.01450	NMED
8/21/11 18:42	0.07800	NMED sed	9/7/11 14:41	0.02000	NMED sed
8/21/11 18:58	0.06469	BDD	9/7/11 15:11	0.03000	NMED sed
9/7/11 15:26	0.01543	NMED	10/12/12 17:31	0.01800	NMED sed

Date & Time	Detected Result pCi/g	Sampling Entity†	Date & Time	Detected Result pCi/g	Sampling Entity
9/7/11 15:26	0.02400	NMED sed	10/12/12 17:56	0.01830	NMED
9/7/11 15:56	0.07895	NMED	10/12/12 17:56	0.03200	NMED sed
9/7/11 15:56	0.08900	NMED sed	10/12/12 19:56	0.00520	NMED sed
9/7/11 15:56	0.08900	NMED sed	7/21/13 1:43	0.01351	NMED
9/7/11 16:11	0.04780	NMED	7/21/13 2:43	0.01524	NMED
9/7/11 16:11	0.12000	NMED sed	7/21/13 2:43	0.01500	NMED sed
9/7/11 16:56	0.05063	NMED	7/26/13 4:26	0.01263	NMED
9/7/11 16:56	0.08000	NMED sed	7/26/13 4:26	0.01700	NMED sed
7/5/12 22:52	0.05200	NMED	7/26/13 6:26	0.01692	NMED
7/5/12 22:52	0.04900	NMED sed	7/26/13 5:26	0.02400	NMED sed
7/5/12 23:42	0.03900	NMED	9/11/13 2:33	0.01569	NMED
7/5/12 23:42	0.07300	NMED sed	9/11/13 2:33	0.01700	NMED sed
7/6/12 0:32	0.07273	NMED	9/11/13 4:33	0.01047	NMED
7/6/12 0:32	0.08800	NMED sed	9/11/13 4:33	0.00910	NMED sed
7/11/12 20:58	0.04898	NMED	9/11/13 5:33	0.00719	NMED
7/11/12 20:58	0.04300	NMED sed	9/11/13 5:33	0.01900	NMED sed
7/11/12 22:52	0.07208	BDD	9/11/13 6:33	0.00952	NMED
7/12/12 12:28	0.01230	NMED	7/29/14 17:26	0.00625	NMED
7/12/12 12:28	0.01700	NMED sed	7/29/14 17:26	0.01400	NMED sed
7/26/12 21:57	0.03470	NMED	7/29/14 17:28	0.03200	NMED sed
7/26/12 21:57	0.04900	NMED sed	7/31/14 20:26	0.00970	NMED sed
8/6/12 3:20	0.01263	NMED	7/31/14 22:18	0.02143	NMED
8/6/12 3:20	0.02800	NMED sed	7/31/14 22:18	0.01800	NMED sed
8/16/12 19:41	0.00792	NMED	7/31/14 22:20	0.01514	NMED
8/16/12 19:41	0.00740	NMED sed	7/31/14 23:18	0.03000	NMED sed
8/17/12 23:04	0.03375	NMED	7/31/14 23:50	0.02588	NMED
8/17/12 23:04	0.03300	NMED sed	7/31/14 23:50	0.01100	NMED sed
8/17/12 23:25	0.00964	NMED	8/1/14 0:18	0.02100	NMED sed
8/17/12 23:25	0.01500	NMED sed	8/1/14 1:18	0.01800	NMED sed
8/23/12 17:52	0.02670	NMED	8/1/14 2:18	0.01900	NMED sed

* The results of method EPA 160.2 was used to calculate the sediment for this sampling event.

** The SSC result was interpolated from before and after sampling times in order to calculate the sediment for this sampling event.

† When "sed" is added to the sampling entity, it indicates that a sediment sample was analyzed, when no "sed" exists then the sediment results was obtain by dividing pCi/L (from storm water data) by g/L (from SSC for the same sampling time).

The presented results were time plotted together with the RG UTL on Figure 207 in order to visualize them throughout the years.

Figure 207. Annual sediment detects of Pu-239/240 at BDD intake 2008-2014.

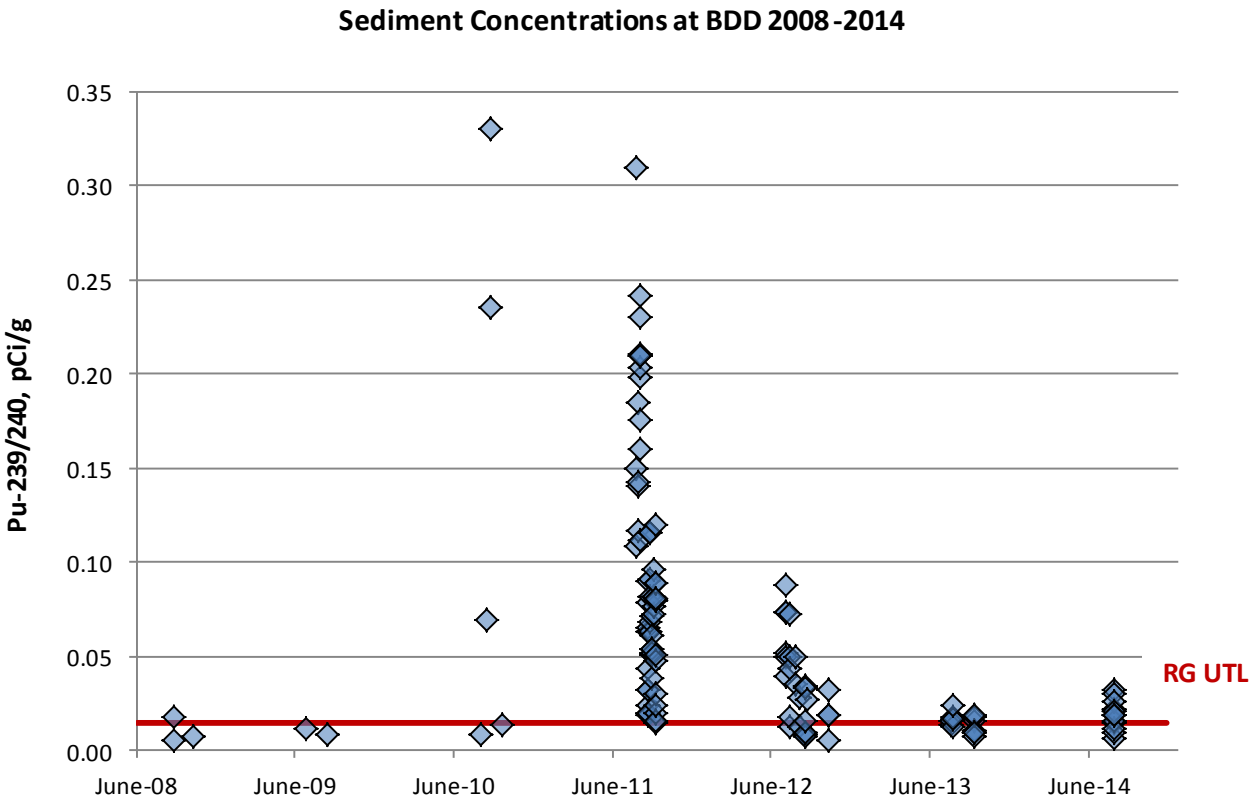

Observations for the presented data.

- All 2011 calculated sediment results and sediment data for Pu-239/240 exceeded RG UTL, and 76% of all detect values for the last 7 years exceeded the RG UTL as well.
- The amount of data collected at the BDD with the launching of the ENS in 2011 increased by an order to magnitude. In part, a large amount of data might be a result of an active storm season, which 2011 was. In addition, two entities (BDD and NMED) were collecting surface water samples at the BDD which increased the visibility of trends and Pu-239/240 detected occurrences. As a third factor of the 2011 season, the Las Conchas fire could have played a role in the Pu-239/240 detections above the background.
- The highest Pu-239/240 concentrations occurred in 2010 and 2011, 0.33 and 0.31 pCi/g respectively. The concentrations exceeded 20 times the background values for Rio Grande. The range of detections in 2010 was an unexpected result because there was an agreement in the environmental community that the Las Conchas fire in 2011 was the main source of increased Pu-239/240 concentrations within the LA/P watershed. When compared with other monitoring years, concentrations one order of magnitude higher were detected in 2011 rela-

tive to 2014 (max 0.032 pCi/g) and more than 18 times higher concentrations were detected in 2011 than in 2008 and 2009, pre-fire. The table and the graph indicated that the impact of the Las Conchas fire to storm water Pu-239/240 transport was *substantial*.

- As quoted in the environmental literature, the Pu-239/240 detections decreased greatly within 2 years of the Las Conchas fire, and currently they appear to be at pre-fire levels.

VII.6.d Conceptual Model of Contaminant Fate and Transport

As part of the analysis of Pu-239/240, a detailed analysis of each storm event throughout the project was conducted. The timing of the storm events in the LA/P Canyons in relation to local/river storms is critical in understanding the collected data as explained earlier. Relating contaminant transport in terms of detected stormwater concentrations at the BDD to the concentrations in the LA/P Canyons, the major source of LANL legacy contaminants, would give an insight whether we have the correct understanding of the fluvial processes between LA/P watershed and the Rio Grande.

The system that this project is investigating is a complex one. There is the contaminants source, LA/PCW, which is ephemeral stream with its own watershed, sedimentary, and hydrologic characteristics (different background concentrations, special geologic units, contaminated and uncontaminated tributaries, positioned partly in LANL property and partly in San Ildefonso tribal land), and the permanent water body, the Rio Grande, with its own unique watershed, sedimentary and hydrological characteristics. The mixing of the water and sediments from these two systems can obscure the differences between both systems and the influence of the LA/P watershed would tend to be diluted with distances from the LA/PC confluence near the Otowi Bridge. To further complicate matters, the summer weather patterns for both systems do not coincide, the LA/PC stream responds to local storm events in the Jemez Mountains while Rio Grande responds to larger-scale conditions in the San Juan Mountains. Therefore, any contaminants from the LA/PC system would enter the Rio Grande sporadically and will be diluted by the main stream suspended sediment for that particular day. This part of the study would investigate each single event during the study monitoring period and attempt to connect the contaminants' fate and transport for each system in order to prove the understanding of the conceptual model for the entire system.

Conceptual Model. As a first step in putting together a conceptual model of the system described in the previous paragraph, we would discuss the pertinent variables of the study and the assumptions made. One of the most important variables is the *date and time* (D/T) of storm events in the LA/P and RG. The D/T for LA/PC does not coincide with the D/T for RG. Using the tables in Chapter IV, we can estimate the average frequency when D/T for LA/PC coincided with D/T for RG, 39%, 53%, 65%, and 70%, for 2011, 2012, 2013, and 2014 respectively. In our analysis we took into consideration this fact. Conceptually, it matters whether LA/PC flow is mixed with a RG baseflow (low SSC) or with RG storm water (high SSC); such fact will determine the amount of dilution occurring at the confluence and therefore the concentrations of LA/PC contaminants measured at the BDD.

Another variable that influences the interpretation of results is the *relative discharge* (RQ) of LA/PC with respect to RG at the time of mixing. Flows in the LA/PC watershed vary from a few cfs to thousands cfs, with most events occurring in the 50-500 cfs range. Similarly, RG flows during the summer season may vary from 400 to 8,000 cfs, with baseflow of 400 to 1,000 cfs. Conceptually, the higher the relative flow (RQ) of LA/PC flow, the higher the concentrations that might be measured at BDD with respect to the concentrations in the LA/P Canyons. It was already established in the previous sections that the average behavior of the SSC and discharge (Q) is similar, with increased flow in the LAC watershed, the SSC increases as well. In this section, we will document the RQ because we will be comparing instantaneous concentrations at the lower LA Canyon (E109.9/110) with the measured concentrations at BDD at a later time.

The last variable in the study, and the only one that is not dependent on the environmental conditions, is *the coordinated sampling* of the LA/P flow just before it enters the RG, and the sampling at the BDD Intake. The fact that different entities sample LA Canyon and BDD, under different programs, with different goals and foci, makes coordination difficult and during most events it is not coordinated. Conceptually, concentrations detected at the lower LA Canyon during storm events could be detected at the BDD intake within 1.5 to 3 hrs taking into account a dilution factor as determined by the previous mentioned variables D/T and RQ. Based on this conceptual model, we will attempt to find storm events for which storm water was sampled at gage station E109.9/110 and then sampled at BDD Intake within 15 min to 3 hours. The goal is to calculate expected concentration at the BDD based on the results at E109.9/110 and the dilution factor, and then to compare those expected calculated values with the measured BDD concentrations as sampled within reasonable time delay. Such analysis would test the validity of our conceptual model. The flow chart of this analysis is presented in Figure 208.

To summarize, the conceptual model that we will be testing with our assessment is as follows: we assume that the concentrations detected at the BDD should be associated with the concentrations found at the lower LA Canyon during LAC storm events. The concentrations at the BDD would be related to the lower LA Canyon by a dilution factor determined by the RQ and the D/T of the LAC storm event and the RG storm event.

Figure 208. Flow chart of contaminant analysis.

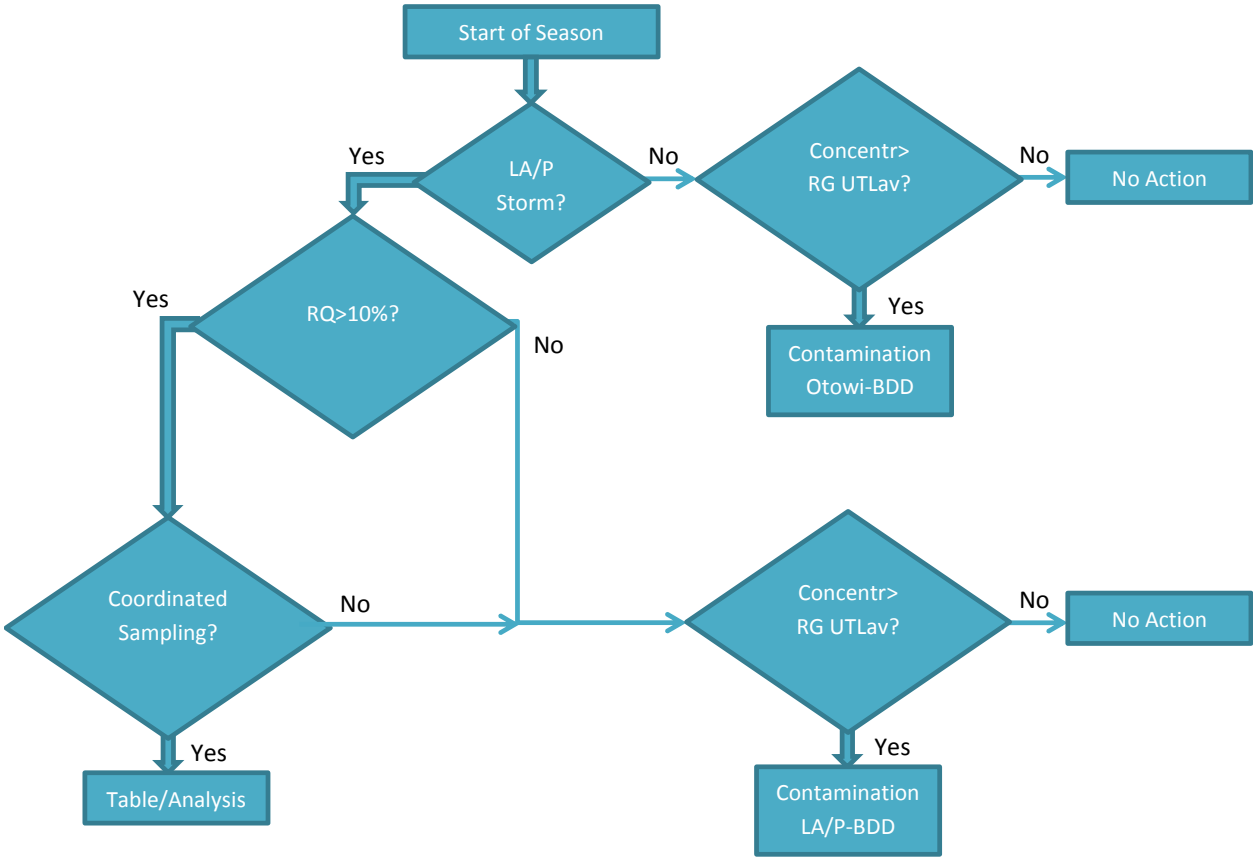

Assumptions of the Conceptual Model:

- The discharge from the lower LA Canyon at the confluence with the RG is as measured by the gage station E109.9. In reality, the flow might be much lower. Gage station E109.9 was located at the most narrow location of the lower LA Canyon, approximately 0.7 miles from the confluence. After that location, the lower LA Canyon bed widens and it is expected that the energy and strength of the flow would diminish greatly. As a result, the calculated RQ would be biased high due to this assumption.
- All suspended sediment as measured at E109.9 is transported to BDD. In reality, most of the coarse fraction measured at the E109.9 SSC would not make it to the RG and BDD, since the energy of the flow to carry the coarse fraction would diminish with entering the last 0.7 miles of the LA Canyon before its confluence with the RG as explained in the previous assumption. As a result any calculation using the SSC from E109.9 would be biased high due to this assumption.
- In most cases, we would assume the average time of travel for a flow from the lower LA Canyon to BDD Intake is approximately 60-90 minutes, depending on LAC and RG discharges. We would be looking for a coordinated sampling from 15 min to 2-3 hours between E109.9 and BDD sampling station.

- For the calculated predictions of Pu-239/240 at the BDD, we would assume that the RG carries Pu-239/240 at levels of the RG UTL of 0.014 pCi/g. Such assumption would bias the results high since the median concentration of Pu 239/240 in the RG is 0.0026 pCi/g as calculated by the RG background study in Appendix 5.

VII.6.e Analysis of Pu-239/240 Sediment Concentrations at BDD

All sampled events from 2010 through 2014 were analyzed and the events that fit the selection criteria were presented in Table 28, 14 sampling events only. Of the 2014 sampling, no events could be selected because the lower LA Canyon was not monitored or sampled, and LANL contract laboratory had filtered samples for Pu analysis. Each column in the table would be explained as follows:

Column 1: the date and time of BDD sampling. Not all sampling times for a specific date were presented. Only those times that might have happened within 15 minutes to 2-3 hours after the E109.9/110 sampling were selected. For events that met this condition, we continued with quantitative analysis (see column 12). Those were only 3-4 events. There were a lot of exceptions to this intended time frame because there was no coordination in sampling. For most events qualitative analysis was conducted and included in the table as well. The exceptions would be explained later as part of column 12.

Column 2: the Pu-239/240 storm water concentration as measured at BDD at the D/T listed in column 1.

Column 3: the Pu-239/240 storm water concentration at specified time in parenthesis as measured at location E109.9/110. When "starred" (*), the measurements were calculated from the sediment results by using the formula: C_t (pCi/L)=C_t (pCi/g) * SSC_t (g/L) and/or from Otowi SSC (as reported by USGS) when the contribution from LA flow was determined to be insignificantly low.

Column 4: Otowi discharge (cfs) at D/T listed in column 1, time adjusted (30-45 min) for its arrival at BDD Intake. The cells in blue indicate the dates when RG storm event occurred.

Column 5: lower LA Canyon discharge (cfs) at D/T listed in column 1 at the time of arrival at the RG confluence. The flows were calculated from the plots of the annual LANL reports.

Column 6: RQ, relative discharge, the ratio of the discharges of lower LA Canyon (from column 5) and RG (from column 4) at the time of arrival of the LAC flow at the confluence with RG.

Column 7: the SSC as measured at the diversion at the D/T listed in column 1.

Column 8: the SSC as measured at E109.9/110 at the specified time in parenthesis.

Column 9: the calculated or measured (marked with "sed") sediment concentration of Pu-239/240 at E109.9/110 using the data in previous columns.

Column 10: the calculated sediment concentration of Pu-239/240 at BDD using columns 2 and 7 at the D/T specified in column 1.

Column 11: the maximum sediment concentration of Pu-239/240 calculated or measured at BDD for that specific date or event. These values were included in the table because the selected time of sampling did not always result in the maximum concentration.

Column 12: the expected sediment concentration at BDD calculated by using the concentration measured at E109.9/110, dilution factor based on RQ, and the RG UTL av. Example of the calculation is shown below:

Date 8/23/2010

By substituting the data from the table in the equation RG SSC*(1-RQ) + LA SSC*RQ=BDD SSC, we can find that the RG SSC for that D/T was 10,292 mg/L.

Substituting the known parameters in the equation: BDD expected (pCi/L)=(1-RQ)*RG SSC*RG Pu-239/240 UTL + RQ*LA Pu-239/240(pCi/L), the storm water concentration (pCi/L) expected to be measured at BDD could be found. The result was 0.755 pCi/L.

Then, we can calculate the BDD expected sediment concentration in pCi/g by using the equation, BDD Con. (pCi/g)= BDD expected (pCi/L)/BDD SSC (g/L), and compare with column 10. The result for the expected BDD concentration was 0.054 pCi/g. We can compare that result with what was actually measured at BDD, which was 0.24 pCi/g. The measured Pu-239/240 was more than 4 times greater than the expected Pu-239/240 value.

As discussed earlier there were only a few events that met the time frames for quantitative comparison between BDD expected (column 12) concentration and BDD measured (column 10) concentration. The dates were, 8/15/2010, 8/23/2010, 7/28/2011 (3 hrs later), 8/3/2011 (3 hrs later), 8/29/2011 (8 hrs later), 9/7/2011, 7/11/2012, 10/12/2012, and 7/26/2013. As it can be seen certain concentrations were calculated 3 hrs to 8 hrs later, and certain concentrations were marked as less than a number (i.e. <0.007 pCi/g). However, for all dates listed above, the expected concentrations at BDD were less than what was actually measured at the BDD. For certain D/T, it was determined that at the BDD sampling time, the event should have been “over”, and therefore no detectable Pu-239/240 should have been found at BDD. Those D/Ts were marked with “low (over)” in column12, indicating that the expected concentration should be very low because the event was “over” at the time of BDD sampling. For those D/T as well, the measured Pu-239/240 concentration at BDD was much greater than the “expected” concentration, which should have been “non-detect.”

Table 28. Conceptual model predictions of Pu-239/240 concentrations.

Column 1	Col. 2	Column 3	Column 4	Col. 5	Col. 6	Col. 7	Column 8	Column 9	Col. 10	Col. 11	Col. 12	Col. 13	Col. 14
BDD Sampling Date& Time	**BDD pCi/L**	**109.9/110 pCi/L(Time)**	**Otowi Flow cfs**	**LA Flow cfs**	**RQ %**	**BDD SSC mg/L**	**109.9/110 SSC mg/L**	**109.9/110 pCi/g**	**BDD pCi/g**	**BDD max**	**Expected pCi/g**	**E050.1 Max Flow, %**	**Max RQ %**
8/15/10 18:27	1.1	0.16 (18:00)	3000	100	3.2	16,000	11,300 (18:00)	0.014 (18:00)	0.06875	0.069	0.014	31	13
8/23/10 17:59	3.3	5.7 (16:49)	1200	150	11	14,000	44,000 (16:49)	0.13 (16:49)	0.24	0.330	0.054	no	39
7/28/11 18:39	0.161	13.4*	870	6	0.68	520 (1030*)	103,000 (16:23)	0.130 sed(16:23)	0.31	0.310	0.096*/3hr	no	1.5
7/28/11 19:06	0.25	ns	870	2.5	0.3	2,300	na	ns	0.109		low (over)		
8/3/11 18:09	1.8	31.2*	850	<<81	insign[2]	9,100	242,000 (15:18)	0.129 sed (15:18)	0.198	0.210	0.127*/3hr	no	10
8/3/11 18:27	1.81	ns	850	<<81	insign[2]	9,100	ns	ns	0.199		low (over)		
8/3/11 18:59	1.2	ns	850	<<81		5,900	ns	ns	0.203		low (over)		
8/3/11 19:12	0.617	ns	850	<<81		5,900	ns	ns	0.105		low (over)		
8/5/11 17:54	0.35	16.9 (15:34)	880	<<70	insign[2]	2,000	136,000 (15:34)	0.124 (15:34)	0.175	0.210	low (over)	no	5.4
8/5/11 18:44	0.61	ns	880	<<70		2,900	ns	ns	0.2103		low (over)		
8/26/11 20:14	0.12	0.103 (17:14)	780	11	1.44	1,900	75,000 (17:14)	0.0014 (17:14)	0.063	0.200	0.016	no	4.3
8/26/11 20:32	0.171	ns	780	<<35	insign[2]	1,900	ns	ns	0.090		low (over)		
8/27/11 19:07	0.62	ns	611	58	9	5,380	ns	ns	0.115	0.115		poss no[1]	9
8/29/11 5:06	0.42	19*	586 (20:41)	<<69	insign[2]	11,000	220,000 (20:41)	0.087 sed (20:41)	0.0382	0.071	0.071*/8hr	poss no[1]	11
8/29/11 5:51	0.52	ns	947	<<69		8,500	ns	ns	0.0612		low (over)		
9/4/11 21:54	3.5	ns	758	200	21	46,000	ns	ns	0.0761	0.081		188	45
9/4/11 22:44	1.6	ns	758	50	6.2	22,000	ns	ns	0.0727				
9/7/11 14:41	0.29	3.3/5.76* (14:27)	565	100	15	20,000	120,000 (14:27)	0.0275/0.048sed (14:27)	0.0145	0.120	0.025/ 0.046*sed	11	12
9/7/11 15:56	1.5		565	100		19,000			0.0789				
9/7/11 16:11	0.86	ns	565	100		18,000	ns	ns	0.0478				
9/7/11 16:56	0.4	0.0208 ND	565	5	0.9	7,900	16,000 (16:35)	0.0014 (16:35)	0.0506		<<0.014		
7/11/12 20:58	2.4	ns	927	200	18	49,000	ns	0.064sed (20:40)	0.0490	0.072		130	42
7/11/12 22:52	1.42	7*	1850	100	5	19,700	109,000 (21:50)	0.064 sed (20:40)	0.0721		0.028*sed		
8/6/12 3:20	0.024	2.1 (14:57)	1050	86	7.5	1,900	35,000 (14:57)	0.060 (14:57)	0.0126	0.028		insign[2]	7.5
10/12/12 17:56	0.033	2.9 (18:00)	2000	50	2.4	1,800	110,000 (18:00)	0.026 (18:00)	0.0183	0.018	<0.007	30	18
7/26/13 6:26	0.66	1.37 (3:50)	1120	<5	insign[2]	39,000	37,000 (3:50)	0.037sed (3:50)	0.0169	0.017	<0.014	no	8.2
Comments			RG event blue	Biased high	Biased high							Time av. 31%	

[1] possibly no flow. There is no information about this specific date but conclusion was drawn based on preceding or following day or both.

[2] insignificantly low

* estimated from sediment measurement and/or using USGS SSC data at Otowi

Results of Analysis. The comparison of columns 10 and 12 represents the essence of the Pu-239/240 analysis because it tested our conceptual model described earlier. On average, the measured Pu-239/240 concentrations were 3.4 times greater than what we calculated using data from E109.9. To explore this subject matter further, we plotted on Figure 209 the maximum concentrations for Pu-239/240 at BDD (column 11) vs the maximum concentrations at E109.9 for the same date. We did not consider the time factor in this case. We wanted to gain an overall picture of the peak concentrations at both locations.

The linear fit was modified to express the median concentration of 0.0026 pCi/g (from the background study the median concentration was 0.0026 pCi/g) when there is no contribution from E109.9/110. The coefficient of determination was surprisingly high, indication of good correlation between the two sets of data. The slope of the linear fit indicates that for any 1 pCi/g increase in concentration at the lower LA Canyon, the BDD increase in concentration is 1.65 pCi/g. This result is not plausible and one explanation of this fact could be that the measured concentrations of Pu-239/240 in the lower LA Canyon were not representative of the concentrations being discharged in the Rio Grande by the LA Canyon flow. There was an additional contamination being "picked up" by the LA flow in the stretch of 0.7 mi between the E109.9 sampling station and the confluence with the RG.

Figure 209. Pu-239/240 sediment concentrations at BDD vs LLAC.

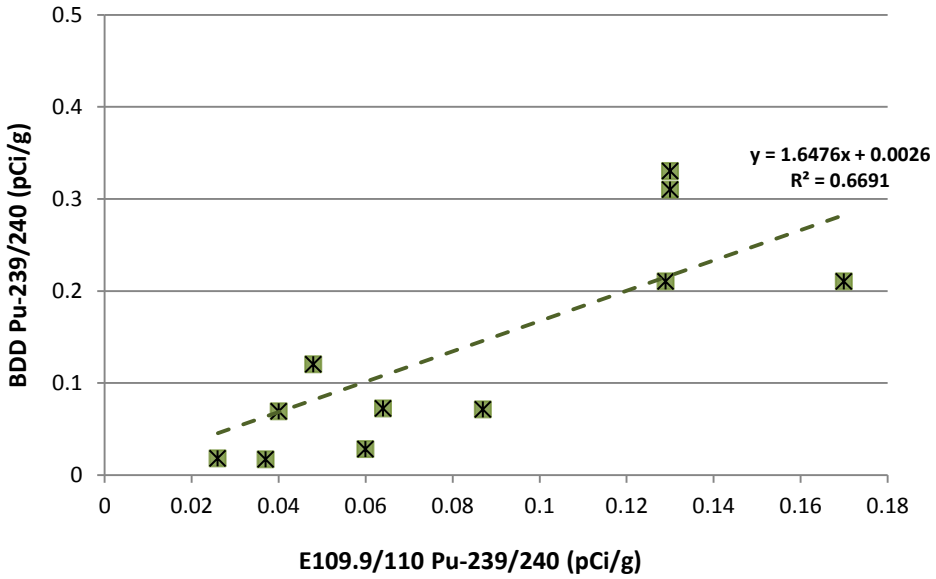

The conclusion from the analysis in this section is that our model does not represent realistic picture of the fate and transport of Pu-239/240 from E109.9 to BDD Intake. All measured concentrations at BDD were much greater than what was expected to arrive at the BDD based on the parameters/concentrations measured at the lower LA Canyon. We need to modify our conceptual model or at least list the incorrect assumptions that might be responsible for the amiss picture. There are a couple of assumptions that might need to be modified:

- The location of E109.9 gage station was 0.7 miles from the RG. We assumed that the LA/PC flow was as measured at the E109.9. Considering the size of the lower LACW, it is very possible that the flow after E109.9 does not lose strength and energy but it increases as more surface runoff is collected from that part of the watershed. So, we need to assume higher RQ and most probably higher SSC with respect to the measured ones at E109.9 location.
- Only revised RQ and SSC cannot not account for the concentrations measured at the BDD because an additional surface runoff may increase the RQ, but it also would dilute the concentrations measured at E109.9 if only non-contaminated sediments were "picked up" by the flow. There must be sufficient contamination of Pu-239/240 being stored in the sediments of the lower LA Canyon below E109.9 and transported during storm events. This result confirms the finding of the NMED DOE OB in (Englert & Ford-Schmid, April 2011) that up to 82% of Pu-239/240 transported beyond the LANL boundaries remains in the lower LA Canyon readily available for transport when conditions allow.

  This result is also supported by the dates when concentrations of Pu-239/240 were detected at BDD hours after the lower LA Canyon storm event has ended or its flow was insignificant as measured at E109.9, and, therefore, no contribution from LA Canyon was expected at the confluence with the RG.

  In order to understand how long after a LA Canyon event Pu-239/240 might be detected above background values, we selected detects during RG events when there was no LA/P Canyons storm event. Table 29 lists all dates when Pu-239/240 was found above background values, and the time of the preceding LA Canyon event.

Table 29. Pu-239/240 detections after LAC storm events.

Date & Time	Result pCi/g	Sampling Entity	Occurred when?
8/27/11 19:07	0.1152	BDD	24 hrs after LAC storm event
7/12/12 12:28	0.0170	NMED sed	13 hrs after LAC storm event
7/26/12 21:57	0.0390	NMED	2 days after LAC storm event
7/26/12 21:57	0.0490	NMED sed	2 days after LAC storm event
8/17/12 23:04	0.0338	NMED	4 days after LAC storm event
8/17/12 23:04	0.0330	NMED sed	4 days after LAC storm event
8/17/12 23:25	0.0150	NMED sed	4 days after LAC storm event
RG UTL 0.014 pCi/g			

The table gives us the idea that after a LA event, Pu-239/240 continues to be transported downstream the RG hours and even days after a LA/P Canyons storm event has ended. This result further modifies our conceptual model. To account for this fact, we need to assume that certain lower LA Canyon flows "deposit" sufficient amount of sediment along the RG at locations or "pockets" which might not be immediately accessible to the RG flow, but which re-

main in storage for later transport during RG storm events. This idea was suggested by Graf (Graf, Plutonium and the Rio Grande, 1994) on page 62:

> *When water spills out of the channel, it loses velocity and energy, and suspended materials settle out of the flow. Hence the flood plains along the Rio Grande contains mixture of sand, silt and clay, depending on the type of materials carried and energy available to perform the hydraulic work of transport.*

Considering the wide LA Canyon delta at the confluence with the RG, most probably large amount of sediments is deposited on the right bank of the river, just below Otowi Bridge. During LA Canyon storm event, the sediments with most energy would be mixed with the main flow of RG and transported downstream to BDD, but certain amount may be stored at the delta, readily available for a stronger RG flow to "pick up" the deposits. At higher RG flows, the width of the river channel increases and "sweeps" sediments deposited days earlier at or near the LA Canyon delta. The most unexpected result is the concentrations of those deposits. Their concentration must be sufficiently high to compensate for the dilution by the RG sediments which during RG storm events are dominant. Such scenario is possible if the "temporary" deposits at the delta are large and the concentration of Pu-239/240 is high enough to compensate for the dilution.

Column 13: the maximum discharge at gage station E050.1 was entered in this column. This data was selected in order to confirm whether the maximum concentrations at BDD were associated with the highest flows (and potential highest concentrations) measured at that station. The data did not confirm such fact. For the 2014 monitoring season, gage stations E050.1 and E060 were selected as the sole triggers to the ENS because station E109.9 was not restored. The trigger gage stations were selected based on LANL studies of the LA/PC Canyons watershed sediments and storm water concentrations implying that the flows with highest Pu-239/240 (and other COCs) concentrations were transported when these two gage stations were flowing. The data from the table does not support this assumption with respect to transport to the BDD intake. On the contrary, it appears that the highest concentrations of Pu-239/240 detected at BDD were at dates and events when these stations did not flow. In addition, the average time when E050.1 flowed for these significant RQ events (RQ greater than 10%) was only 36 percent of the time when evaluated as a "percent events." Table 30 summarizes the results for all storm events from 2003 through 2013 when E050.1 flowed with respect to lower LA Canyon flows.

When evaluated as a percent daily discharges (see Section III.4.b), the frequency of flow of E050.1 was 26% for three consecutive years and the average was 30%.

Table 30. Frequency of 5 cfs flows of E050 and E109.9.

Year	E109.9 Frequency of Flow	E050.1 Frequency of Flow	Percent E050.1/E109.9
2003-2008*	32	13	41%
2010	5	2	40%
2011	20	8	40%
2012	15	5	33%
2013**	19	5	26%
* from reference (Englert & Ford-Schmid, April 2011)			
** events after 9/13/13 were not taken into consideration			

Based on this data if the BDD ENS system continues to use the E050.1 as a trigger then the potential of obtaining representative data for Pu-239/240 would be diminished, and the number of lower LA Canyon events being monitored would be less than one half of the time. If BDD and LANL do not improve the ENS trigger, the monitoring results would be incomplete to make future determinations.

Column 14: the maximum RQ for each storm event was listed in this column. The data was included for reference purposes only.

Using Table 28, we plotted the maximum sediment concentration for each event and the maximum LAC RQ for the same event, column 11 vs column 14. We also added the event dated 8/23/2012 with maximum concentration of 0.0267 pCi/g and RQ of 21%. The maximum concentrations detected at BDD did not correlate to the maximum RQ of the LA Canyon flow.

Figure 210. Maximum Pu-239/240 sediment concentration vs LLAC RQ.

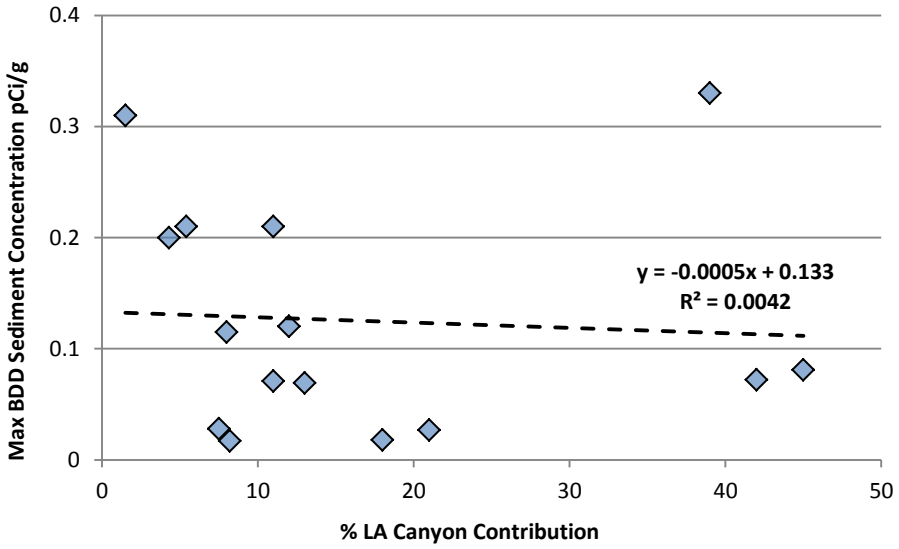

One explanation for that fact is that the BDD sampling is not well coordinated with the arrival of maximum flow from the LA Canyon. Another explanation is the result that we found earlier, the measured flow at the lower LA Canyon does not represent the actual flow arriving at the confluence

with the Rio Grande. And lastly, the Pu-239/240 is bound to the sediment carried by the flow, and considering the fact that in the LA Canyon there is no positive correlation between the flow and instantaneous SSC, we should not expect any relation between the concentration and LACW RQ.

Thus the RQ may not be a good indicator to consider in predicting concentrations at the BDD due to the uncertainty in its measured value. So, the plot on Figure 206 was modified to include all events listed in Table 28 even the ones with RQ less than 10%, but excluded Pu detections when RG event coincided with LA Canyon event. The error bars for storm water were 30% and for SSC – 10%. The result is presented in Figure 211.

Figure 211. Revised Pu-239/240 storm water vs SSC.

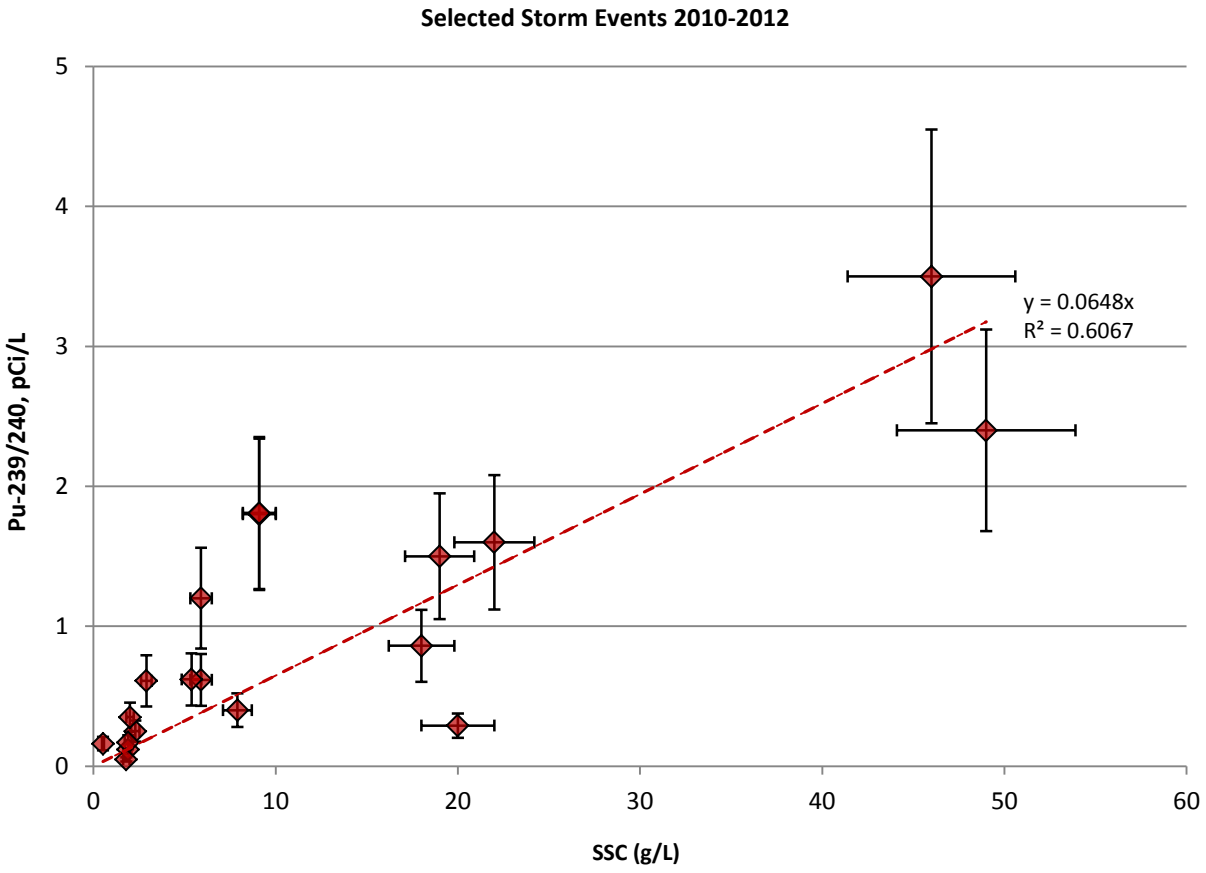

When Figure 206 and Figure 211 were compared, it was noted that the correlation factors (the slope of the linear fit) were very similar, but the coefficient of determination in the latter case was improved. This suggests that Pu-239/240 concentrations behave in a predictable manner during storm events of LA Canyon flows when RG is at base flow conditions, and Pu-239/240 concentrations are well correlated to the measured SSC, at least 61% of the time in such occasions.

VII.6.f Conclusions of Pu-239/240 Analysis

The analysis of the Pu-239/240 concentrations at the BDD attempted to connect those concentrations with the LA Canyon concentrations as measured at the LANL former gage station E109.9. Conceptual model was developed according to which BDD concentrations during storm events could be predicted based on the measured flow and concentrations at E109.9. The results from the analysis were summarized below:

- The conceptual model underestimates the Pu-239/240 concentrations that would be expected to arrive at BDD. Two explanations were suggested: there were much higher flows from LACW being delivered to the Rio Grande, and there were higher concentrations of Pu 239/240 at the lower parts of LA Canyon than as measured at former gage station E109.9. Even though the former E109.9 station was placed in a convenient location in the lower LAC, it is insufficient in describing the conditions in the lower part of the LAC in term of fate and transport of contaminants, and in terms of its hydrological characteristics.

- The highest concentrations of Pu-239/240 at BDD occurred when flow from LACW (during storm events in LAC) were mixed with RG *base flow*, meaning when the LAC relative discharge was high. During such events minimum dilution of LAC flows occurred and the LACW sediment transported to the RG had its maximum impact in terms of measured contaminant concentrations.

- Fires in the region of LANL play important role in the fate and transport of Pu-239/240. The last stand replacing fire, the Las Conchas fire, indicated that in LACW not only the frequency of storms and the amount of transported sediment increased, but the amount of contaminated sediment transported to the Rio Grande and to the BDD was significant in comparison to pre- or post-fire years. Monitoring at the BDD Intake during stand replacing fires affecting Los Alamos watersheds is highly recommended, including a few years following such fires.

- In the absence of direct measurement, the correlation between Pu-239/240 concentrations and the suspended sediment concentrations may be used to predict the concentrations of this contaminant, given that the RG is under base flow conditions and the discharge at the lower LA Canyon was measured in real time. However, when storm events from the two watersheds coincide, there are no practical means of estimating those concentrations in addition to the fact that they become insignificant due to the dilution of the RG flow.

- One approach to the sediment transport (and, therefore contaminant transport for chemicals bound to sediment) has been that it occurs in a wavelike or pulsed fashion. Such sediment movement would make modeling of contaminants even harder to describe with predictions being grossly erroneous, thus making monitoring and obtaining empirical data even more important.

VIII. CONTAMINANT FATE ANALYSIS PROGRAM

VIII.1 Sampling and Analysis Plan

The Contaminant Fate Analysis (CFA) was a series of sampling and testing of water samples undertaken pursuant to the *2010 MOU*. The purpose of the CFA was to determine the fate of certain radionuclides when water was diverted from the Rio Grande and treated to produce drinking water by the Buckman Direct Diversion (BDD) Project.

Samples were taken by BDD personnel at three locations from March 3, 2012 to February 28, 2013. These locations were: (1) the Rio Grande approximately 7 feet upstream from the BDD diversion structure, (2) the Sediment Return Line located in the BDD Sediment Removal Facility, and (3) the BDD Finished Water Tank. Samples were taken following the BDD Laboratory Standard Operating Procedure (SOP) Number 2003, *Contaminant Fate Analysis Samples*.

Once each day, a 1-Liter sample was taken from each of the three sample locations. No samples were taken from the Sediment Return Line on days the Sediment Removal Facility was not in operation and no samples were taken from the Finished Water Tank when it was empty. After the end of each calendar month, a flow-weighted composite sample for the preceding calendar month was produced for each of the three sampling locations. The flow-weighted volumes for the Rio Grande samples were based on the flows reported at the USGS gauging station at Otowi Bridge. The flow-weighted volumes for the Sediment Return Line samples were based on the daily volumes of discharges back to the Rio Grande by the Sediment Removal Facility. The flow-weighted volumes for the Finished Water Tank were based on the daily combined flows of drinking water through Booster Station 4A and Booster Station 5A. The composite samples were then divided into individual 1-Liter samples for analysis according to an analysis plan supplied by LANL. Half of the samples remained unfiltered and half of the samples were filtered through a 0.43 μm filter. All samples were preserved with approximately 3 mL nitric acid. Samples were shipped directly from the BDD to General Engineering Laboratories (GEL) in Charleston, South Carolina for analysis. All sampling containers, sample labels, compositing and filtering equipment, processing logs, and shipping materials were supplied by LANL. The nitric acid was supplied by the BDD.

The results of the analyses by GEL were reviewed by LANL and BDD and after review were posted on the Intellus New Mexico website (Intellusnmdata.com). All of the results may be retrieved by searching for the following three sample locations: "Rio Grande at BDD intake CFA", "BDD Sediment Removal Facility", and "BDD Finished Water Facility".

The analytes to be tested were described in the 2010 MOU: Gross alpha, Gross beta, Gross gamma, Sr-90, Am-241, Cs-137, Co-60, Na-22, Np-237, K-40, Pu (isotopic), U (isotopic), Ra-226, and Ra-228. In addition to these analytes, some samples were also analyzed for Ac-228, Be-7, Bi-212, Bi-214, Cs-134, I-131, Pb-212, Pb-214, Pa-234m, Tl-208, and Th-234. Due to limited volumes of some

composite samples, not every composite sample was analyzed for all of the analytes described in the 2010 MOU and presented below.

Table 31. Analytes/Methods for CFA sampling.

Analytes	Method	Detection Limit	Field Prep Code
Gross alpha	EPA:900	3 pCi/L	F, UF
Gross beta	EPA:900	3 pCi/L	F, UF
Sr-90	EPA:905.0	0.5 pCi/L	F, UF
Am-241	HASL-300:AM-241	0.05 pCi/L	F, UF
Gross gamma	EPA:901.1	15 pCi/L	F, UF
Cs-137	EPA:901.1	5 pCi/L	F, UF
Co-60	EPA:901.1	5 pCi/L	F, UF
Na-22	EPA:901.1	10 pCi/L	F, UF
Np-237	EPA:901.1	40 pCi/L	F, UF
K-40	EPA:901.1	75 pCi/L	F, UF
Pu (isotopic)	HASL-300:ISOPU	0.05 pCi/L	F, UF
U (isotopic)	HASL-300:ISOU	0.05 pCi/L	F, UF
Ra-226, -228	903.1, 904	1 pCi/L	F, UF

In addition to the composite samples, a several sets of both filtered and unfiltered deionized water samples were submitted as equipment blanks. These equipment blanks were subjected to all of the sample preparation steps as the ordinary composite samples. Although a few of the blank samples were shown to have some of the analytes present above the detection limits, none were detected at levels considered significant.

VIII.2 Analytical Results from CFA Sampling

The table below summarizes the results from the samples collected pursuant to the 2012/2013 CFA. The results for detected constituents were presented only. If a constituent was not detected in any of the samples, then it was not included in this table. Plutonium-238, which measured at 0.272 pCi/L, was not included in the table. This was the only detection of the contaminant and it was detected in the monthly river sample for July 2012.

Table 32. Summary table of detected values from CFA sampling.

Sample source	Analyte	No. Detects	Range (min-max)	MCL/Standard
Rio Grande at BDD Intake	Bismuth-214	1 of 12	ND - 14.3	NA
BDD Sediment Removal Facility	Bismuth-214	2 of 12	ND – 10.0	NA
BDD Finished Water Facility	Bismuth-214	3 of 12	ND - 24.3	NA

Sample source	Analyte	No. Detects	Range (min-max)	MCL/Standard
Rio Grande at BDD Intake	Gross alpha	9 of 12	ND - 44.7	15 pCi/L
BDD Sediment Removal Facility	Gross alpha	8 of 12	ND - 38.8	NA
BDD Finished Water Facility	Gross alpha	5 of 12	ND - 7.4	15 pCi/L
Rio Grande at BDD Intake	Gross beta	12 of 12	ND - 76.8	NA
BDD Sediment Removal Facility	Gross beta	12 of 12	3.4 - 114.0	NA
BDD Finished Water Facility	Gross beta	8 of 12	ND – 603.0	Dose 4 mrem/yr
Rio Grande at BDD Intake	Potassium-40	4 of 12	ND – 104.0	None
BDD Sediment Removal Facility	Potassium-40	3 of 12	ND - 74.9	None
BDD Finished Water Facility	Potassium-40	1 of 12	ND - 45.9	None
Rio Grande at BDD Intake	Lead-212	1 of 12	ND - 11.3	None
BDD Sediment Removal Facility	Lead-212	2 of 12	ND - 10.9	None
BDD Finished Water Facility	Lead-212	1 of 12	ND - 10.3	None
Rio Grande at BDD Intake	Lead-214	3 of 12	ND - 21.7	None
BDD Sediment Removal Facility	Lead-214	0 of 12	ND	None
BDD Finished Water Facility	Lead-214	0 of 12	ND	None
Rio Grande at BDD Intake	Radium-226	6 of 12	ND - 1.4	None
BDD Sediment Removal Facility	Radium-226	10 of 12	ND - 1.1	None
BDD Finished Water Facility	Radium-226	5 of 12	ND - 1.2	None
Rio Grande at BDD Intake	Radium-226 & Radium-228	7 of 12	ND - 5.9	30 pCi/L
BDD Sediment Removal Facility	Radium-226 & Radium-228	9 of 12	ND - 2.2	None
BDD Finished Water Facility	Radium-226 & Radium-228	6 of 12	ND - 1.2	5 pCi/L
Rio Grande at BDD Intake	Radium-228	4 of 12	ND - 4.5	None
BDD Sediment Removal Facility	Radium-228	6 of 12	ND - 1.5	None
BDD Finished Water Facility	Radium-228	4 of 12	ND - 0.9	None
Rio Grande at BDD Intake	Thallium-208	1 of 12	ND - 4.31	None
BDD Sediment Removal Facility	Thallium-208	1 of 12	ND - 6.95	None
BDD Finished Water Facility	Thallium-208	3 of 12	ND - 5.80	None
Rio Grande at BDD Intake	Uranium-234	12 of 12	0.61 - 2.07	None
BDD Sediment Removal Facility	Uranium-234	12 of 12	0.52 - 2.67	None
BDD Finished Water Facility	Uranium-234	12 of 12	0.08 - 1.78	None
Rio Grande at BDD Intake	Uranium-235	6 of 12	ND - 0.10	None
BDD Sediment Removal Facility	Uranium-235	7 of 12	ND - 0.10	None
BDD Finished Water Facility	Uranium-235	3 of 12	ND - 0.08	None

Sample source	Analyte	No. Detects	Range (min-max)	MCL/Standard
Rio Grande at BDD Intake	Uranium-238	12 of 12	0.37 - 1.84	None
BDD Sediment Removal Facility	Uranium-238	12 of 12	0.31 - 2.38	None
BDD Finished Water Facility	Uranium-238	12 of 12	0.05 - 1.06	None

IX. WORKS CITED

Dale M, L. P. (Fall Meeting 2007). *Trace Perchlorate in Background Groundwater and Local Precipitation, Northern Rio Grande basin, New Mexico.* American Geophysical Union.

Englert, D., & Ford-Schmid, R. (April 2011). *Los Alamos Canyon Watershed Stormwater Monitoring from 2003 through 2008: Contaminant Transport Assessment.* Santa Fe: NMED DOE OB.

Englert, D., Dale, M., Granzow, K., & Mayer, R. (2007). *Distribution of radionuclides in Northern Rio Grande Fluvial Deposits near Los Alamos National Laboratory, New Mexico.* Santa Fe: NMED DOE OB.

Graf, W. L. (1994). *Plutonium and the Rio Grande.* Oxford University Press, Inc.

Graf, W. L. (1996). *Transport and deposition of plutonium contaminated sediments by fluvial processes, Los Alamos Canyon, New Mexico.* Los Alamos: Los Alamos National Laboratory.

Gray, J. R. (2000). *Comparability of Suspended-Sediment Concentration and Total Suspended Solids Data.* Reston, VA 2000: USGS, Water-Resources Investigations Report 00-4191.

LA-UR-11-0941. (February 2011). *Stormwater Performance Monitoring in the Los Alamos/Pueblo Watershed During 2010.* LANL.

LA-UR-11-5459. (2010). *Stormwater Performance Monitoring in the Los Alamos/Pueblo Watershed During 2010, Revision 1.* Los Alamos: LANL.

LA-UR-12-1081. (May 2012). *Polychlorinated Biphenyls in Precipitation and Stormwater within the Upper Rio Grande Watershed.* LANL.

LA-UR-12-24822. (September 2012). *Stormwater Performance Monitoring in the Los Alamos/Pueblo Watershed during 2011, Revision 1.* LANL.

LA-UR-13-22113. (March 2013). *Storm Water Performance Monitoring in the Los Alamos/Pueblo Watershed during 2012.* LANL.

LA-UR-14-21169. (2014). *MOU, Technical Meeting, February 18, 2014.* Los Alamos: LANL.

LA-UR-14-22549. (May 2015). *2014 Monitoring Plan for Los Alamos and Pueblo Canyons Sediment Transport Mitigation Project.* LANL.

LA-UR-14-24516. (June 2014). *Storm Water Performance Monitoring in the Los Alamos/Pueblo Watershed during 2013.* LANL.

LA-UR-14-25041. (2014). *July 2014 Public Meeting Presentation, Individual Permit for Storm water, NPDES Permit No. NM0030759.* LANL.

LA-UR-15-21413. (May 2015). *2014 Monitoring Report for Los Alamos/Pueblo Watershed Sediment Transport Mitigation Project.* Los Alamos: Los Alamos National Laboratory.

NMED, D. O. (2014). Correspondence between D. Bowman and C. Perkins.

NMED/DOE/OB. (2012). *Summary of Rio Grande Water Sampling Efforts by the NMED, prepared for BDDB, October 6, 2012.* Santa Fe: NMED DOE OB.

Nordin, C. (1965). Sediment Transport in the Rio Grande New Mexico. *US Geological Survey Professional Paper 462-F*.

Reale, J. (2012, May 1). Using GIS and the Revised Universal Soil Loss Equation (RUSLE) to Determine Sediment Loading after Las Conchas Fire. Albuquerque, NM: UNM.

Ryti, R. L. (September 22, 1998). *Inorganic and radionuclide Background Data for Soils, Canyon Sediments, and Bandelier Tuff at Los Alamos National Laboratory.* Los Alamos National Laboratory.

Szabo Z, R. D. (1997). *Relation of distribution of radium, nitrate, and pesticides to agricultural land use and depth, Kirkwood-Cohansey aquifer system, New Jersey Costal Plain, 1990-91*. USGS Water-Resources Investigations Report 96-4165A, 107 p.

Yanicak, S. (2012, June 20). Submittal 2011 and 2012 Post Las Conchas Fire Sampling Results for Stormwater, Farm Soils, Post-flood Muck and Precipitation. Los Alamos: NMED .